

Hayabusa 2021 Symposium Schedule (Online Meeting)
(8th ISAS Symposium of the Solar System Materials)

version. 20211111

16th(Tue)-17th(Wed) of November 2021

Oral : Zoom Meeting (10+5 min for Invited and normal talks, 7+3 min for 10 min short talks)

Poster : Zoom Meeting Breakout Rooms

Non-real time discussion : Slack

Day-1 (Nov 16th) : Oral Session

JST	GMT	EST	PST	No.	Title	Author/Presenter	Invited
		(-1day)	(-1day)		Session-0 : Opening session: T. Okada		
09:45	00:45	19:45	16:45	S0-1	Opening and Logistics	Tatsuaki Okada	
09:50	00:50	19:50	16:50	S0-2	Status of JAXA Curation activity and future plan	Tomohiro Usui	
					Session-1: Ryugu sample : S. Tachibana, T. Usui		
10:00	01:00	20:00	17:00	S1-1	An overview of initial descriptions for samples returned from C-type asteroid Ryugu	Toru Yada	Invited
10:15	01:15	20:15	17:15	S1-2	First NIR hyperspectral imaging of Hayabusa2 returned samples by the MicroOmega microscope within the ISAS Curation Facility	Cedric Pilorget	Invited
10:30	01:30	20:30	17:30	S1-3	Initial analysis of Hayabusa2 returned samples from asteroid (162173) Ryugu	Shogo Tachibana	
10:45	01:45	20:45	17:45	S1-4	Progress of chemical characterization of asteroid Ryugu samples	Hisayoshi Yurimoto	Invited
11:00	02:00	21:00	18:00	S1-5	Initial analysis of "stone" size Ryugu samples: current status	Tomoki Nakamura	Invited
11:15	02:15	21:15	18:15	S1-6	Mineralogy and surface modification of small grains recovered from the asteroid 162173 Ryugu	Takaaki Noguchi	Invited
11:30	02:30	21:30	18:30	S1-7	Initial Analysis of Volatile Components in the Hayabusa2 Samples	Ryuji Okazaki	Invited
11:45	02:45	21:45	18:45	S1-8	An initial look at the distributions and compositions of organic macromolecules in the asteroid Ryugu samples	Hikaru Yabuta	Invited
12:00	03:00	22:00	19:00	S1-9	Soluble Organic Matter (SOM) analysis of the Hayabusa2 samples: The first results	Hiroshi Naraoka	Invited
12:15	03:15	22:15	19:15		<Lunch break> [Group Photo-1]	All	
					Sessions-2 : Ryugu Sample (Cont.) : R. Brunetto, A. Nakato		
13:30	04:30	23:30	20:30	S2-1	A first look at the interior and exterior of Ryugu preserved in samples collected by Hayabusa2	Eizo Nakamura	Invited
13:45	04:45	23:45	20:45	S2-2	The C-type asteroid Ryugu: A first detailed look by Phase2 Curation Kochi (Ph2K)	Motoo Ito	Invited
14:00	05:00	00:00	21:00	S2-3	JAXA Detailed Description -Variation of surface characteristics of Ryugu returned samples-	Aiko Nakato	
14:15	05:15	00:15	21:15	S2-4	Overview of the features of returned samples from the C-type asteroid 162173 Ryugu based on optical microscope observations and their weights	Akiko Miyazaki	10 min
14:25	05:25	00:25	21:25	S2-5	Initial description of Ryugu returned samples: characteristics of individual grains by FT-IR analysis	Kentaro Hatakeda	10 min
14:35	05:35	00:35	21:35	S2-6	MicroOmega detections of C-rich phases in Ryugu returned samples within the Hayabusa2 JAXA Extraterrestrial Curation Center	Jean-Pierre Bibring	
14:50	05:50	00:50	21:50	S2-7	MicroOmega detections of carbonates in Ryugu returned samples within the Hayabusa 2 JAXA Extraterrestrial Curation Center	Damien Loizeau	10 min
15:00	06:00	01:00	22:00	S2-8	The 2.7µm OH band in different grains of Ryugu from the two collection sites, as seen by MicroOmega in the Hayabusa2 Curation Facility	Tania Le Pivert-Jolivet	10 min
15:10	06:10	01:10	22:10	S2-9	Microscale diversity of H, C, and N isotopes in asteroid Ryugu	Larry R. Nittler	
15:25	06:25	01:25	22:25	S2-10	Diversity of Insoluble Organic Matter at the Nanoscale in Asteroid Ryugu	Rhonda Stroud	
15:40	06:40	01:40	22:40	S2-11	Infrared transmission spectra of Ryugu particles and their unique adsorption behavior	Yoko Kebukawa	
15:55	06:55	01:55	22:55	S2-12	Thermal history of Ryugu based on Raman characterization of Hayabusa2 samples	Lydie Bonal	
16:10	07:10	02:10	23:10	S2-13	Elemental and isotopic compositions of organic grains from asteroid Ryugu	Laurent Remusat	
16:25	07:25	02:25	23:25		<Coffee Break>		
					Sessions-3 : Ryugu Sample (Cont.) : H. Sugahara, D. Yamamoto		
16:40	07:40	02:40	23:40	S3-1	Exposure Conditions of Samples Collected on Ryugu's Two Touchdown Sites Determined by Cosmogenic Nuclides	Kunihiko Nishiizumi	
16:55	07:55	02:55	23:55	S3-2	Small grains from Ryugu: handling and analysis pipeline for Infrared Synchrotron Microspectroscopy	Stefano Rubino	
17:10	08:10	03:10	00:10	S3-3	Preliminary results from FTIR hyper-spectral imaging campaign on Ryugu small grains and fragments.	Zelia Dionnet	
17:25	08:25	03:25	00:25	S3-4	Iron valence state and mineralogy in particles from asteroid Ryugu	Mathieu Roskosz	
17:40	08:40	03:40	00:40	S3-5	Three-dimensional analysis of Ryugu sample particles using X-ray nanotomography.	Akira Tsuchiyama	
17:55	08:55	03:55	00:55	S3-6	Surface morphologies and space weathering features of Ryugu samples	Toru Matsumoto	
18:10	09:10	04:10	01:10	S3-7	CNHOS contents with their isotopic compositions and preliminary organic profiles from the Hayabusa2 samples	Yoshinori Takano	
18:25	09:25	04:25	01:25	S3-8	Compound distribution determined by nanoLC-Orbitrap MS	François-Régis Orthous-Daunay	
18:40	09:40	04:40	01:40	S3-9	Highest molecular diversity and structural complexity revealed with ultrahigh resolution mass spectrometry and nuclear magnetic resonance spectroscopy of Ryugu's samples	Philippe Schmitt-Kopplin	
18:55	09:55	04:55	01:55		Discussion on Ryugu sample	S. Tachibana (Lead)	
					[Group Photo-2]	All	

Hayabusa 2021 Symposium Schedule (Online Meeting)
(8th ISAS Symposium of the Solar System Materials)

version. 20211111

16th(Tue)-17th(Wed) of November 2021

Oral : Zoom Meeting (10+5 min for Invited and normal talks, 7+3 min for 10 min short talks)

Poster : Zoom Meeting Breakout Rooms

Non-real time discussion : Slack

Day-2 (Nov 17th) : Oral Session

JST	GMT	EST	PST	No.	Title	Author/Presenter	Invited
		(-1day)	(-1day)		Session-4 : Asteroid - Meteorite Connection : K. Righter, T. Okada		
09:30	00:30	19:30	16:30	S4-1	The Winchcombe Meteorite: A Pristine Sample of the Outer Asteroid Belt	Ashley J King	Invited
09:45	00:45	19:45	16:45	S4-2	Thermal History of Dehydrated CY Chondrites Reconstructed from their Fe-sulfide Grains	Catherine Harrison	
10:00	01:00	20:00	17:00	S4-3	Hydrothermal history of (162173) Ryugu's parent body inferred from remote-sensing data	Eri Tatsumi	Invited
10:15	01:15	20:15	17:15	S4-4	Multiband thermal radiometry and related laboratory studies, indicating possible origin and evolution of Ryugu.	Maximilian Hamm	Invited
10:30	01:30	20:30	17:30	S4-5	Color Mapping of Asteroid Bennu	Daniella DellaGiustina	Invited
10:45	01:45	20:45	17:45	S4-6	The Mineralogy and Organic Composition of Bennu as Observed by VNIR and TIR Spectroscopy	Victoria E. Hamilton	Invited
11:00	02:00	21:00	18:00	S4-7	The Nature of Extraterrestrial Amino Acids in Carbonaceous Chondrites and Links to Their Parent Bodies	Daniel Patrick Glavin	Invited
11:15	02:15	21:15	18:15	S4-8	Oxygen isotopes and water in bulk matrix of CM2 Murchison as an analog for Ryugu matrix	Aditya Patkar	
11:30	02:30	21:30	18:30	S4-9	Anomalous and ungrouped carbonaceous chondrites in the US Antarctic meteorite collection and their potential relevance to Ryugu and Bennu	Kevin Righter	
11:45	02:45	21:45	18:45		<Lunch break> [Group Photo-3]	All	
					Session-5 : Itokawa Sample and Meteorites : T. Ireland, T. Yada		
13:00	04:00	23:00	20:00	S5-1	Volatiles in Chondrites and Achondrites	Maitrayee Bose	Invited
13:15	04:15	23:15	20:15	S5-2	Space weathering of sulfides and silicate minerals from asteroid Itokawa	Laura Camila Chaves	
13:30	04:30	23:30	20:30	S5-3	Space weathering of iron sulfides on airless bodies	Toru Matsumoto	Invited
13:45	04:45	23:45	20:45	S5-4	Extraterrestrial Non-Protein Amino Acids Identified in Carbon-Rich Particles Returned from Asteroid Itokawa	Eric Thomas Parker	
14:00	05:00	00:00	21:00	S5-5	NaCl in an Itokawa Particle: Terrestrial or Asteroidal?	Shaofan Che	
14:15	05:15	00:15	21:15	S5-6	Northwest Africa 5401 CV chondrite: Not oxidized, not reduced, maybe in between?	Timothy J. Fagan	
14:30	05:30	00:30	21:30	S5-7	Organics and iron speciation in CI chondrites : a combined STXM and TEM study	Corentin Le Guillou	
14:45	05:45	00:45	21:45	S5-8	Shocked regolith in asteroid 25143 Itokawa surface	Josep M. Trigo-Rodriguez	
15:00	06:00	01:00	22:00	S5-9	Organic matter in Itokawa particles	Queenie Hoi Shan Chan	Invited
15:15	06:15	01:15	22:15		<Coffee Break>		
					Session-6 : Sample Return & Space Missions: M. Abe, J. Helbert		
15:30	06:30	01:30	22:30	S6-1	Hayabusa2 curation: from concept, design, development, to operations	Masanao Abe	
15:45	06:45	01:45	22:45	S6-2	Sample Analysis Plan for NASA's OSIRIS-REx Mission	Harold C. Connolly Jr.	Invited
16:00	07:00	02:00	23:00	S6-3	Scientific importance of the sample analyses of Phobos regolith and the analytical protocols of returned samples by the MMX mission	Wataru Fujiya	Invited
16:15	07:15	02:15	23:15	S6-4	What should we do with these Martian rocks? A tale of MSR Sample Science and Curation	Aurora Hutzler	Invited
16:30	07:30	02:30	23:30	S6-5	A New Laboratory Facility in the Era of Sample Return: the Sample Analysis Laboratory (SAL) at DLR Berlin	Enrica Bonato	
16:45	07:45	02:45	23:45	S6-6	Milani CubeSat for ESA Hera mission	Tomas Kohout	
17:00	08:00	03:00	00:00	S6-7	The young basalts on the Moon: Pb-Pb isochron dating in Chang'e-5 Basalt CE5C000YJYX03501GP	Dunyi Liu	Invited
17:15					<Coffee break>		
					Session-7 : Summary and Ending : T. Usui		
17:30	08:30	03:30	00:30	S7-1	Wrap-up and Summary	Tomohiro Usui (Lead)	
18:00	09:00	04:00	01:00		Adjourn [Group Photo-4]	All	

Hayabusa 2021 Symposium Schedule (Online Meeting)
(8th ISAS Symposium of the Solar System Materials)

version. 20211111

16th(Tue)-17th(Wed) of November 2021

Oral : Zoom Meeting (10+5 min for Invited and normal talks, 7+3 min for 10 min short talks)

Poster : Zoom Meeting Breakout Rooms

Non-real time discussion : Slack

Day-1 (Nov 16th) : Poster Session

JST	GMT	EST	PST	No.	Title	Author/Presenter	Invited
					Poster Session and chat (2 hours) : R. Fukai, T. Hayashi		
19:15	10:15	05:15	02:15	P-1	The fundamental deformation of cosmic bodies not depending of their sizes and compositions(from asteroids to Universe)	Gennady Gregory Kochemasov	
				P-2	Exogenous copper sulfide in a returned grain from asteroid Itokawa	Katherine D Burgess	
				P-3	A Series of Recent Falls of Carbonaceous Chondrites - Perfect Analogues for Returned Hayabusa 2 and Osiris Rex Asteroidal Materials	Viktor H Hoffmann	
				P-4	Heated Synthetic Murchison Reflectance Spectra	Sahejpal Sidhu	
				P-5	Status of the Curatorial Database System for the Ryugu Samples	Masahiro Nishimura	
				P-6	Methodology of MicrOmega data acquisition/processing in initial description of Ryugu returned samples	Kasumi Yogata	
				P-7	Comparison of ion- and laser-weathered spectra of olivines and pyroxenes	Kateřina Chrbolková	
				P-8	Solid Materials of Mineral and Rock on the Solar System: X-ray Unit and Mixed Status	Yasunori Miura	
				P-9	Model of Material Characteristics of Carbonaceous Meteorites from Texture of Carbon-Bearing Grains	Yasunori Miura	
				P-10	Neural network for classification of asteroid spectra	David Korda	
				P-11	Assessment of organic, inorganic, and microbial contamination in the facilities of the Extraterrestrial Sample Curation Center of JAXA	Yuya Hitomi	

An overview of initial descriptions for samples returned from C-type asteroid Ryugu.

T. Yada¹, M. Abe¹, A. Nakato¹, K. Yogata¹, A. Miyazaki¹, K. Kumagai², K. Hatakeda², T. Okada¹, M. Nishimura¹, S. Furuya^{1,3}, M. Yoshitake^{1,4}, A. Iwamae^{2,5}, Y. Hitomi², H. Soejima², K. Nagashima¹, R. Sawada², L. Riu^{1,6}, L. Lourt⁶, C. Pilorget⁶, V. Hamm⁶, D. Loizeau⁶, R. Brunetto⁶, J.-P. Bibring⁶, Y. Cho³, K. Yumoto³, Y. Yabe³, S. Mori³, S. Sugita³, S. Tachibana^{1,3}, H. Sawada¹, K. Sakamoto¹, T. Hayashi¹, D. Yamamoto¹, R. Fukai¹, H. Sugahara¹, H. Yurimoto⁷, T. Usui¹, S. Watanabe⁸, Y. Tsuda¹

¹Inst. Space Astronaut. Sci., Japan Aerosp. Explor. Agency (JAXA), Kanagawa 252-5210, Japan (yada@planeta.sci.isas.jaxa.jp), ²Marine Works Japan Ltd., Yokosuka 237-0063, Japan, ³UTOPS, Grad. Sch. Sci., Univ. Tokyo, Tokyo 113-0033, Japan, ⁴Japan Patent Office, Chiyoda-ku, Tokyo 100-8915, Japan, ⁵Toyo Univ., Bunkyo-ku, Tokyo 112-8606, Japan, ⁶Institut d'Astrophysique Spatiale, Université Paris-Saclay, CNRS, 91400 Orsay, France, ⁷Dept. Earth Planet. Sci., Grad. Sch. Sci., Hokkaido Univ., Hokkaido 060-0808, Japan, ⁸Dept Earth Planet. Sci., Grad. Sch. Sci., Nagoya Univ., Nagoya 464-8601, Japan.

Introduction: Hayabusa2 spacecraft operated by JAXA explored a near-Earth asteroid 162173 Ryugu from Jun 2017 to Nov 2019 [1]. During the exploration, the spacecraft accomplished touchdown sampling on the asteroid's surface in Feb and Jul of 2019 [2]. The samples recovered by the first touchdown were stored in the Chamber A of a sample catcher and those by the second one were in the Chamber C [2]. The sample catcher was sealed in a sample container, which was set in a reentry capsule of the spacecraft, and the capsule was returned to the Earth, the Woomera Prohibited Area in South Australia, on 6 Dec 2020 [2, 3].

Extraction Procedures for Ryugu samples: As the container was transported from Australia to Japan by air and arrived at cleanrooms of the Extraterrestrial Sample Curation Center (ESCuC), it was disassembled to remove unnecessary parts and cleaned on its surface in the cleanrooms and introduced into the clean chamber (CC) 3-1 to be evacuated to high vacuum [2, 3]. In the static vacuum condition, the container was opened and the sample catcher was extracted from the container. The catcher was transported to the next chamber, CC3-2, and a lid of the Chamber A of the catcher was removed from the catcher and a few mm-size particles were recovered from the Chamber A to a quartz glass container in vacuo. Then the catcher with rest of samples was transported to the next chamber, CC3-3, then the catcher handling environment have changed from vacuum to purified nitrogen condition. Hereafter, all the extraction works and initial descriptions have been done in this purified nitrogen condition in the clean chambers. The catcher was firstly measured with a balance equipped in the chamber CC4-2 to confirm the bulk samples' weight in it, to be 5.4 grams [3]. Then it was dismantled with catcher handling tools in the chamber CC4-1 to recover samples from each chamber of the catcher to sapphire dishes of 23mm in diameter.

Initial descriptions for bulk and individual Ryugu samples: Each of the bulk samples in the dishes were observed and photographed with a stereomicroscope equipped above the chamber CC4-2. Then they were also measured with the balance for their bulk weights to be 3.2 grams and 2.0 grams from the from the Chamber A and C, respectively [4]. They were then analyzed with a Fourier Transmission Infrared spectrometer (FT-IR) for their near infrared reflectance spectra in wavelength ranging from 2.0 to 4.0 μm [4]. They were also analyzed with a MicrOmega, infrared imager comparable to that onboard instrument of MASCOT lander released from Hayabusa2 spacecraft, for obtaining overall and local infrared spectra in the bulk Ryugu samples [1, 5-7]. Finally, they were analyzed with an optical microscopic imaging through six filters (ul: 0.39 μm , b: 0.48 μm , v: 0.55 μm , Na: 0.59 μm , w: 0.70 μm , x: 0.85 μm), compatible with the ONC-T camera of Hayabusa2, onboard instrument of Hayabusa2 [8]. After the series of initial descriptions for bulk Ryugu samples, individual particles have been handpicked from the bulk samples to sapphire dishes for individual samples with a vacuum tweezer, and described in the same manner as the bulk samples experienced [9-11]. The results of initial descriptions for bulk Ryugu samples are presented in [4]. Their small bulk densities and dark visible and infrared spectral features indicates that obtained samples are representative of surface materials of Ryugu. Together with absence of high temperature components like a chondrule and a Calcium-Aluminum rich Inclusion (CAI) and presence of 2.7 μm absorption band in infrared spectra, which corresponds to hydroxyls (-OH) absorption implying abundant phyllosilicate, they are most similar to CI chondrites among known planetary materials.

Data archive and sample distributions: All the obtained data by the initial descriptions have been archived in Hayabusa2 sample data catalog [12]. This catalog will be in public soon as a reference of Announcement of Opportunity (AO) for Ryugu samples, which will start in early 2022. Any researcher can apply for the AO, and Ryugu samples will be distributed to Principle Investigators (PIs) of selected proposals in the middle of 2022.

References: [1] Tsuda Y. et al. (2020) *Acta Astron.* 171, 42-54. [2] Tachibana S. et al. (2021) *LPS*, XXXXXII, Abstract #1289. [3] Yada T. et al. (2021) *LPS*, XXXXXII, Abstract #2008. [4] Yada T. et al., *submitted to Nature Astron.* [5] Pilorget C. et al., *submitted to Nature Astron.* [6] Bibring J.-P. et al., *this meeting*. [7] Yogata K. et al., *this meeting*. [8] Sugita S. et al. (2020) *Science* 364, eaaw0422. [9] Miyazaki A. et al., *this meeting*. [10] Hatakeda K. et al., *this meeting*. [11] Cho Y. et al., *this meeting*. [12] Nishimura M. et al., *this meeting*.

First NIR hyperspectral imaging of Hayabusa2 returned samples by the MicrOmega microscope within the ISAS Curation Facility

¹Pilorget, C.; ^{2,3}Okada, T.; ¹Hamm, V.; ¹Brunetto, R.; ²Yada, T.; ¹Loizeau, D.; ²Riu, L.; ^{2,3}Usui, T.; ⁴Moussi-Soffys, A.; ^{2,5}Hatakeda, K.; ²Nakato, A.; ²Yogata, K.; ^{2,6}Abe, M.; ¹Aléon-Toppani, A.; ¹Carter, J.; ¹Chaigneau, M.; ¹Crane, B.; ¹Gondet, B.; ^{2,5}Kumagai, K.; ¹Langevin, Y.; ¹Lantz, C.; ¹Le Pivert-Jolivet, T.; ¹Lequertier, G.; ¹Lourit, L.; ²Miyazaki, A.; ²Nishimura, M.; ¹Poulet, F.; ⁷Arakawa, M.; ⁸Hirata, N.; ⁸Kitazato, K.; ²Nakazawa, S.; ⁹Namiki, N.; ²Saiki, T.; ³Sugita, S.; ^{2,3}Tachibana, S.; ^{2,6,10}Tanaka, S.; ^{2,6}Yoshikawa, M.; ^{2,6}Tsuda, Y.; ¹¹Watanabe, S.; ¹Bibring, J.-P.

[1] Institut d'Astrophysique Spatiale, Université Paris-Saclay, CNRS, 91400 Orsay, France, [2] Institute of Space and Astronautical Science, Japan Aerospace Exploration Agency, Sagami-hara 252-5210, Japan, [3] University of Tokyo, Bunkyo, Tokyo 113-0033, Japan, [4] Centre National d'Etudes Spatiales, 18 Avenue E. Belin, 31401 Toulouse, France, [5] Marine Works Japan, Ltd., Yokosuka 237-0063, Japan, [6] The Graduate University for Advanced Studies (SOKENDAI), Hayama 240-0193, Japan, [7] Kobe University, Kobe 657-8501, Japan, [8] The University of Aizu, Aizu-Wakamatsu 965-8580, Japan, [9] National Astronomical Observatory of Japan, Mitaka 181-8588, Japan, [10] University of Tokyo, Kashiwa 277-8561, Japan, [11] Nagoya University, Nagoya 464-8601, Japan.

Introduction: On December 6, 2020, the Hayabusa2 mission successfully returned to Earth ~ 5.4 g of samples collected at the surface of the C-type asteroid Ryugu [1,2]. Its surface was first sampled on February 22, 2019, then on July 11, 2019, close to a 15-meter large artificial crater, so as to possibly access sub-surface material [3]. The collected samples are now kept at the Extraterrestrial Samples Curation Center of JAXA at ISAS in Sagami-hara, Japan, for a first round of preliminary analyses, with the objective of characterizing in a non-destructive manner both the bulk samples and a few hundreds of grains extracted from them [4]. In particular, the goal is 1) to support their further detailed characterization by the international Initial Analysis Teams, and 2) to build a catalogue of the grains, accessible to the international community through AO selection, starting mid-2022.

Methods: The preliminary characterization of these samples is being conducted with a visible microscope with five color filters, a FTIR spectrometer operating in the 1-4 μm range, and MicrOmega, a hyperspectral NIR microscope developed at Institut d'Astrophysique Spatiale (Université Paris-Saclay/CNRS, Orsay, France), operating in the near-infrared range (0.99-3.65 μm) [5]. This is the first time that preliminary analyses of returned extraterrestrial samples include a characterization by a NIR hyperspectral microscope.

Results: Preliminary outcomes of the analyses performed with MicrOmega will be presented. In particular, the representativity of the samples collected by the Hayabusa2 spacecraft will be addressed through the comparison of the spectra obtained by MicrOmega and of the NIRS3 remote sensing IR spectrometer [6] which performed a spectral characterization (1.8-3.2 μm) of Ryugu's surface, including the sites of the samples' collection [7,8].

At a global scale, all bulks exhibit similar features, with a dominant OH- 2.7 μm component and a 3.3 – 3.5 μm band centered around 3.4 μm . Their variation at different spatial scales and significance will be presented. Specific signatures, detected in grains typically present in <1% of the pixels, but of high relevance regarding the processes determining Ryugu formation and evolution, will also be presented and discussed.

References: [1] Binzel R. P. et al. (2002), *Physical Properties of Near-Earth Objects*. pp. 255-271, [2] Vilas F. (2008) *The Astronomical Journal* 135 (4), 1101-1105, [3] Morota et al. (2020) *Science* 368, Issue 6491, pp. 654-659, [4] Yada T. et al., *Nature Astronomy*, *submitted*, [5] Bibring J.-P. et al. (2017) *Astrobiology* 17, Issue 6-7, pp.621-626, [6] Iwata T. et al. (2017) *Space Science Reviews* 208 (1-4), 317-337, [7] Kitazato K. et al. (2019) *Science* 364 (6437), 272-275, [8] Kitazato K. et al. (2020) *Nature Astronomy*, Volume 5, p. 246-250.

Initial analysis of Hayabusa2 returned samples from asteroid (162173) Ryugu

Shogo Tachibana^{1,2}, Hisayoshi Yurimoto³, Tomoki Nakamura⁴, Takaaki Noguchi^{5,6}, Ryuji Okazaki⁶, Hikaru Yabuta⁷, Hiroshi Naraoka⁶, Kanako Sakamoto², Sei-ichiro Watanabe⁸, Yuichi Tsuda², and the Hayabusa2 Initial Analysis team

¹Univ. Tokyo, ²ISAS, JAXA, ³Hokkaido Univ., ⁴Tohoku Univ., ⁵Kyushu Univ., ⁶Kyoto Univ., ⁷Hiroshima Univ., ⁸Nagoya Univ.

The JAXA's Hayabusa2 spacecraft explored C-type near-Earth asteroid (162173) Ryugu from June 2018 to November 2019, during which two touchdown operations were made to collect surface and subsurface samples. The Hayabusa2 delivered its reentry capsule on December 6, 2020 to Woomera, South Australia [1]. The sample container inside the reentry capsule was opened in the clean chamber system dedicated to Ryugu samples at ISAS, JAXA. Dark particles were found in both chambers A and C, which were used for the storage of the samples collected at the first and second touchdown, respectively. The total amount of the samples exceeds 5 g, which is much larger than the minimum requirement of 0.1 g [2]. Many millimeter-sized particles were present with fine powdery materials, and centimeter-sized grains, close to the maximum obtainable size [3], were found in the chamber C. The color, morphology, and spectroscopic features of the grains indicates that they well represent the surface materials of Ryugu.

The initial analysis of a fraction of returned samples, led by the Hayabusa2 project, has begun in June 2021 after the 6-month sample description at the ISAS curation facility without exposure to the air. The initial analysis aims at maximizing the scientific achievement of the project with answering important fundamental questions such as what materials Ryugu consists of, how Ryugu evolved from its formation to the present, and how similar or different Ryugu samples are to the known meteorites. The findings from Ryugu samples are expected to invoke cosmochemical discussion on the origin and evolution of the Solar System architecture such as the isotopic dichotomy in the early Solar System, the delivery of water and organics to the inner Solar System, and the asteroid-comet continuum. The initial analysis also aims at providing the ground truth for the remote sensing data obtained by the Hayabusa2 spacecraft.

The initial analysis team consists of six sub-teams for 1) chemistry (elements and isotopes) (Lead: Hisayoshi Yurimoto, Hokkaido University), 2) petrology and mineralogy of coarse grains (mm-sized grains [stone]) (Lead: Tomoki Nakamura, Tohoku University), 3) petrology and mineralogy of fine grains (<100 μm -sized grains [sand]) (Lead: Takaaki Noguchi, Kyoto University/Kyushu University), 4) volatiles (Lead: Ryuji Okazaki, Kyushu University), 5) insoluble organic matter (macromolecular organics) (Lead: Hikaru Yabuta, Hiroshima University), and 6) soluble organic matter (organic molecules) (Lead: Hiroshi Naraoka, Kyushu University). The total number of teams members is nearly 300 from fourteen countries. The initial analysis will continue for 12 months. The data obtained during the initial analysis will be archived in the JAXA curatorial sample database to prove the potential of the samples to the community.

Three hundred milligrams of Ryugu samples (6 % of the total samples by mass) have been allocated from JAXA to the initial analysis team; Twenty two grains, which were individually photographed, weighed, and spectroscopically examined in the clean chamber system, and ten aggregate samples that mainly consist of particles smaller than 1 mm in diameter (Table 1).

Table 1. Samples allocated to the Hayabusa2 initial analysis team.

Individual grains (Chamber A)	Individual grains (Chamber C)	Aggregates (Chamber A)	Aggregates (Chamber C)
A0026 3.9 mg	C0002 93.5 mg	A0104 0.3 mg	C0105 0.4 mg
A0040 3.0 mg	C0023 5.0 mg	A0105 4.0 mg	C0106 4.0 mg
A0055 5.9 mg	C0025 5.6 mg	A0106 38.4 mg	C0107 38.8 mg
A0058 3.3 mg	C0033 2.4 mg	A0107 31.0 mg	C0108 33.0 mg
A0063 3.8 mg	C0040 4.9 mg	A0108 3.5 mg	C0109 3.7 mg
A0064 6.7 mg	C0046 2.6 mg		
A0067 3.6 mg	C0055 0.8 mg		
A0080 1.4 mg	C0057 0.9 mg		
A0086 0.9 mg	C0061 1.3 mg		
A0089 1.0 mg	C0076 4.7 mg		
A0094 1.8 mg	C0103 1.5 mg		

The allocated samples have been individually investigated by each sub-team or by collaboration of multiple sub-teams. The C0002 grain from the chamber C is the third largest particle (~9 x 5 x 4 mm) among all the returned particles (Table 1). This grain has been analyzed by all six sub-teams.

In this presentation we discuss the goals and overall activities of the initial analysis of Ryugu samples. Preliminary results of elemental and isotopic analyses, mineralogical and petrological observation, and analyses of volatiles and organic components will be presented from each sub team at the meeting [e.g., 4–22].

References

- [1] Tachibana S. et al. (2021) *51st LPSC*, Abstract #1289.
- [2] Tachibana S. et al. (2014) *Geochem. J.* **48**, 571–587.
- [3] Sawada H. et al. (2017) *Space Sci. Rev.* **208**, 81–106.
- [4] The Hayabusa2-initial-analysis chemistry team et al. (2021) *this meeting*.
- [5] Nakamura T. et al. (2021) *this meeting*.
- [6] Noguchi T. et al. (2021) *this meeting*.
- [7] Okazaki R. et al. (2021) *this meeting*.
- [8] Yabuta H. et al. (2021) *this meeting*.
- [9] Naraoka H. et al. (2021) *this meeting*.
- [10] Tsuchiyama A. et al. (2021) *this meeting*.
- [11] Dionnet Z. et al. (2021) *this meeting*.
- [12] Rubino S. et al. (2021) *this meeting*.
- [13] Viennet J.-C. et al. (2021) *this meeting*.
- [14] Matsumoto T. et al. (2021) *this meeting*.
- [15] Nishiizumi K. et al. (2021) *this meeting*.
- [16] Kebukawa Y. et al. (2021) *this meeting*.
- [17] Bonal L. et al. (2021) *this meeting*.
- [18] Stroud R. M. et al. (2021) *this meeting*.
- [19] Nittler L. R. et al. (2021) *this meeting*.
- [20] Takano Y. et al. (2021) *this meeting*.
- [21] Orthous-Daunay F.-R. et al. (2021) *this meeting*.
- [22] Schmitt-Kopplin P. et al. (2021) *this meeting*.

Progress of chemical characterization of asteroid Ryugu samples

The Hayabusa2-initial-analysis chemistry team¹,

T. Nakamura², T. Noguchi², R. Okazaki², H. Yabuta², H. Naraoka², K. Sakamoto², S. Tachibana², S. Watanabe² and Y. Tsuda²

¹*See end of this abstract*

²*Tohoku Univ., Kyoto Univ., Kyushu Univ., Hiroshima Univ., Kyushu Univ., JAXA, Tokyo Univ., Nagoya Univ. and JAXA*

It is believed that meteorites come from asteroids. Samples of asteroid (25143) Itokawa returned by the JAXA Hayabusa mission revealed that S-type asteroids are composed of materials consistent with the ordinary chondrite class [1, 2]. The JAXA Hayabusa2 [3] spacecraft launched on December 3rd, 2014 towards an asteroid (162173) Ryugu to clarify relationships between C-type asteroids and the carbonaceous chondrite class. Remote sensing observations from Hayabusa2 show that (1) the albedo of Ryugu is darker than those of every known meteorite class [4, 5], (2) an absorption band at 2.72 μm indicates that phyllosilicates are ubiquitous on Ryugu [5], (3) the strength and shape of the absorption band feature suggests that Ryugu materials experienced heating above 300 $^{\circ}\text{C}$ [6], and (4) thermal inertia suggests that Ryugu materials are more porous than every known carbonaceous chondrite [7]. These results suggest that carbonaceous chondrite class materials are plausible for Ryugu materials, but no known carbonaceous chondrite completely matches the results obtained from Ryugu.

The Hayabusa2 spacecraft made two successful landings operations onto Ryugu to collect asteroidal materials in 2019 and delivered the collected samples to the Earth on December 6th, 2020. The returned samples are detritus from pebbles to clay, exceeding 5 grams in total. Their colors, shapes and macro-structures are consistent with those of the remote sensing observations, indicating that the returned samples are representative of the asteroid Ryugu [8]. The initial analysis of the Ryugu samples began in June 2021. At that time, samples totaling ~ 125 mg, containing powder and particles from the 1st and 2nd touchdown sites, were allocated to the Initial Analysis Chemistry Team.

The goals of the Initial Analysis Chemistry Team analyses are to provide fundamental answers to questions relating to the provenance of Ryugu samples for in-depth research by international scientists in the future: (i) What are the elemental abundances of Ryugu? (ii) What are the isotopic compositions of Ryugu? (iii) Does Ryugu consist of primary materials formed in the protosolar disk or secondary materials altered on the parent body? (iv) When were Ryugu materials formed? and (v) What are the relations to known meteoritic samples?

Hydrogen, C and S are analyzed by combination of thermogravimetric analysis coupled with mass spectrometry (TG-MS) and by pyrolysis and combustion analyses (EMIA-Step). Major and minor elements are analyzed by X-ray fluorescence analysis (XRF) using laboratory X-rays and synchrotron radiation. Trace elements are analyzed by inductively coupled plasma mass spectrometry (ICP-MS) using calibration curve and isotope dilution methods after acid digestion. We quantify the abundance of 66 elements in Ryugu samples: H, Li, Be, C, O, Na, Mg, Al, Si, P, S, Cl, K, Ca, Sc, Ti, V, Cr, Mn, Fe, Co, Ni, Cu, Zn, Ga, Ge, As, Se, Rb, Sr, Y, Zr, Nb, Mo, Ru, Rh, Pd, Ag, Cd, In, Sn, Te, Cs, Ba, La, Ce, Pr, Nd, Sm, Eu, Gd, Tb, Dy, Ho, Er, Tm, Yb, Lu, Hf, Ta, W, Tl, Pb, Bi, Th, and U. Inorganic and organic element concentrations are also analyzed for H and C.

For isotope analyses, the Ryugu samples are digested with acids, and the target elements are successively separated by ion-exchange column chromatography. We use thermal ionization mass spectrometry (TIMS) and ICP-MS with multi-collectors to measure isotope ratios. We determine isotope ratios for chronological systems of Rb-Sr, Sm-Nd, U-Th-Pb, Lu-Hf, Hf-W, Re-Os, Al-Mg, and Mn-Cr. We also determine stable isotope systematics of Ca, Ti, Cr, Fe, Ni, Sr, Ba, Zr, Mo, Ce, Gd, Ru and Nd to test isotopic dichotomy in the solar system. Oxygen isotope systematics of Ryugu are measured by laser-fluorination isotope-ratio mass-spectrometry (LF-IRMS) for bulk samples and by secondary ion mass spectrometry (SIMS) for individual components in the samples. The SIMS technique is also applied to the Mn-Cr chronological systematics to determine ages of aqueous alteration. Surveying for circumstellar and molecular cloud matter is conducted by isotope microscope and NanoSIMS.

References

- [1] Yurimoto H. et al. 2011. *Science* 333: 1116. [2] Nakamura T. et al. 2011. *Science* 333: 1113. [3] Tachibana S. et al. 2014. *Geochem. J.* 48: 571. [4] Kitazato K. et al. 2019. *Science* 364: 272. [5] Sugita S. 2019. *Science* 364, eaaw0422. [6] Kitazato K. et al. 2021. *Nature Astronomy* 5: 246. [7] Okada T. et al. 2020. *Nature* 579: 518. [8] Tachibana S. et al. 2021. in review.

The Hayabusa2-initial-analysis chemistry team:

H. Yurimoto¹, T. Yokoyama², K. Nagashima³, I. Nakai⁴, Y. Abe⁵, Y. Terada⁶, S. Komatani⁷, M. Morita⁷, K. Ichida⁷, H. Homma⁸, K. Motomura⁸, K. Yui⁴, T. Usui⁹, M. K. Haba², T. Iizuka¹⁰, S. Yoneda¹¹, H. Hidaka¹², K. Yamashita¹³, M. Bizzarro¹⁴, F. Moynier¹⁵, M. Schöenbächler¹⁶, T. Kleine¹⁷, N. Dauphas¹⁸, Q-Z. Yin¹⁹, M. Wadhwa²⁰, R. J. Walker²¹, R. W. Carlson²², A. Bouvier²³, Y. Amelin²⁴, L. Qin²⁵, I. Gautam², R. Fukai⁹, Y. Masuda², Y. Hibiya¹⁰, A. Ishikawa², A. Pack²⁶, E. D. Young²⁷, C. Park²⁸, N. Sakamoto¹, W. Fujiya²⁹, N. Kawasaki¹, S. Itoh³⁰, K. Terada³¹, M. Ito³², M. Chaussidon¹⁵, J. Aleon³³, L. Piani³⁴, S. Russell³⁵, P. Hoppe³⁶, S. Amari³⁷, K. D. McKeegan²⁷, M-C. Liu²⁷, G. R. Huss³, A. N. Krot³, C. M. O'D. Alexander²², L. R. Nittler²², A. M. Davis¹⁸, A. Nguyen³⁸, N. Kita³⁹, K. Kitajima³⁹, T. R. Ireland⁴⁰, B-G. Choi⁴¹, A-C. Zhang⁴², K. Bajo¹

¹Hokkaido Univ., ²Tokyo Tech., ³Univ. Hawaii 'i, ⁴Tokyo Univ. Sci. ⁵Tokyo Denki Univ., ⁶SPRING-8, ⁷HORIBA TECHINO SERVICE Co., Ltd., ⁸Rigaku Co., ⁹JAXA, ¹⁰Univ. Tokyo, ¹¹National Museum Nature Sci. Tokyo, ¹²Nagoya Univ. ¹³Okayama Univ., ¹⁴Natural History Museum Denmark, ¹⁵Inst. Phys. Globe Paris, ¹⁶ETH, ¹⁷Univ. Münster, ¹⁸Univ. Chicago, ¹⁹UC Davis, ²⁰ASU, ²¹Univ. Maryland, ²²Carnegie Inst. Sci., ²³Univ. Bayreuth, ²⁴ANU, ²⁵China Univ. Geosci., ²⁶Univ. Göttingen, ²⁷UCLA, ²⁸KOPRI, ²⁹Ibaraki Univ., ³⁰Kyoto Univ., ³¹Osaka Univ., ³²JAMSTEC, ³³MNHN, ³⁴CRPG, ³⁵NHM, ³⁶MPI Chemistry, ³⁷Washington Univ. St. Louis, ³⁸NASA, ³⁹Univ. Wisconsin, ⁴⁰Univ. Queensland, ⁴¹SNU, ⁴²Nanjing Univ.

Initial analysis of “stone” size Ryugu samples: current status

Tomoki Nakamura¹, Megumi Matsumoto¹, Kana Amano¹, Yuma Enokido¹, Mike Zolensky², Takashi Mikouchi³, Yuri Fujioka¹, Mizuha Kikui¹, Eiichi Kagawa¹, Daisuke Nakashima¹, Adrian Brearley⁴, Mikhail Zolotov⁵, Akira Tsuchiyama⁶, Masayuki Uesugi⁷, Yoshio Takahashi³, Moe Matsuoka⁸, Ralph Milliken⁹, Donald Brownlee¹⁰, David Joswiak¹⁰, Miki Takahashi¹, Kazuhiko Ninomiya¹¹, Tadayuki Takahashi³, Takahito Osawa¹², Kentaro Terada¹¹, Frank E. Brenker¹³, Beverley Tkalcec¹³, Yuki Kimura¹⁴, Satoshi Tanaka⁸, Housei Nagano¹⁵, Rosario Brunetto¹⁶, Alice Aléon-Toppani¹⁶, Queenie Chan¹⁷, Mathieu Roskosz¹⁸, Esen Ercan Alp¹⁹, Pierre Beck²⁰, Aiko Nakato⁸, Takaaki Noguchi²¹, Masahiko Tanaka²², Takahiro Hiroi⁹, Eri Tatsumi²³, Faith Vilas²⁴, Amanda R. Hendrix²⁴, Camilo Jaramillo²⁵, Gerardo Dominguez²⁶, Cecile Engrand¹⁶, Jean Duprat¹⁶, Hidenori Genda²⁷, Kousuke Kurosawa²⁸, Sara Russell²⁹, Ashley King²⁹, Enrica Bonato³⁰, Chi Ma³¹, Kentaro Uesugi⁷, Akihisa Takeuchi⁷, Jyunya Matsuno²¹, Akira Miyake²¹, Satomi Enju³², Masahiro Yasutake⁷, Toru Matsumoto³³, Shota Okumura²¹, Aki Takigawa³, Shohei Yamashita³⁴, Takahiro Kawai³, Jean-Christophe Viennet¹⁸, Barbara Lavina¹⁹, Toshiaki Tanigaki³⁵, Kazuo Yamamoto³⁶, Deborah Domingue Lorin²⁴, Ferenc Borondics³⁷, Zélia Dionnet¹⁶, Donia Baklouti¹⁶, Zahia Djouadi¹⁶, Celine Lantz¹⁶, Stefano Rubino¹⁶, Laszlo Vincze³⁸, Bart Vekemans³⁸, Gerald Falkenberg³⁹, Pieter Tack³⁸, Ella De Pauw³⁸, Miles Lindner¹³, Benjamin Bazi³⁸, Shinya Yamada⁴⁰, Kenya Kubo⁴¹, Shunsaku Nagasawa³, Taiga Wada¹, Satoshi Takeshita³⁴, Akihiro Taniguchi²¹, Shin Watanabe^{3, 8}, Izumi Umegaki³⁴, Chiu I-Huan¹¹, Yasuhiro Miyake³⁴, Kosuke Inoue⁴², Seiji Sugita³, Kohei Kitasato⁴³, Hisayoshi Yurimoto¹⁴, Ryuji Okazaki³³, Hikaru Yabuta⁴⁴, Hiroshi Naraoka³³, Kanako Sakamoto⁸, Shogo Tachibana^{3, 8}, Seiichiro Watanabe¹⁵, Yuichi Tsuda⁸ and the Hayabusa2-initial-analysis Stone team.

¹Tohoku University, Japan, ²NASA/JSC, USA, ³The University of Tokyo, Japan, ⁴University of New Mexico, USA, ⁵Arizona State University, USA, ⁶Ritsumeikan University, Japan and CAS, GIG, China, ⁷JASRI/SPring-8, Japan, ⁸ISAS/JAXA, Japan, ⁹Brown University, USA, ¹⁰University of Washington, USA, ¹¹Osaka University, Japan, ¹²Japan Atomic Energy Agency, Japan, ¹³Goethe University Frankfurt, Germany, ¹⁴Hokkaido University, Japan, ¹⁵Nagoya University, Japan, ¹⁶University of Paris-Saclay, France, ¹⁷University of London, UK, ¹⁸Muséum National d'Histoire Naturelle, France, ¹⁹Argonne National Laboratory, USA, ²⁰Université Grenoble Alpes, France, ²¹Kyoto University, Japan, ²²National Institute for Materials Science, Japan, ²³Instituto de Astrofísica de Canarias, Spain, ²⁴Planetary Science Institute, USA, ²⁵Pennsylvania State University, ²⁶California State University, USA, ²⁷Tokyo tech, Japan, ²⁸Chiba tech, Japan, ²⁹Natural History Museum, UK, ³⁰Deutsches Zentrum für Luft- und Raumfahrt, Germany, ³¹Caltech, USA, ³²Ehime University, Japan, ³³Kyusyu University, Japan, ³⁴High Energy Accelerator Research Organization (KEK), Japan, ³⁵Hitachi, Ltd., Japan, ³⁶Japan Fine Ceramics Center, Japan, ³⁷SOLEIL Synchrotron, France, ³⁸Ghent University, Belgium, ³⁹DESY, Germany, ⁴⁰Rikkyo University, Japan, ⁴¹International Christian University, Japan, ⁴²Kanazawa University ⁴³University of Aizu, Japan, ⁴⁴Hiroshima University, Japan.

As a part of the initial analysis of the Ryugu samples, we perform a variety of analyses of millimeter-sized "stones". Our goals are to elucidate the entire formation process of Cb-type asteroid Ryugu from the viewpoint of petrology and mineralogy and obtain necessary information by sample analysis, and then simulate the formation of Ryugu based on the evidence obtained from sample analysis. Eighteen stones (8 from the chamber A and 10 from the chamber C) were received from the ISAS curation facility on June 1, 2021, and placed into a fully nitrogen-displaced glove box at Tohoku University. At the same time, we also received the powder samples from the chamber A and the chamber C. All the allocated samples were put in the sample transport containers prepared by ISAS in the nitrogen atmosphere inside the clean chamber system dedicated to Ryugu samples. The containers were then transferred to the nitrogen glovebox at ISAS, where all the containers were completely sealed in plastic bags with moisture and oxygen absorbers. No moisture or oxygen was detected when the bags were opened in the glove box at Tohoku University, so it was confirmed that there was no exposure to the atmosphere during transport.

To date, a number of analyses have been carried out successfully and within schedule margins. The analysis started with the measurement of reflectance spectra, which are sensitive to atmospheric oxidation, hydroxylation, and adsorbed water. The ultraviolet, visible, near-infrared, and mid-infrared reflectance spectra were measured while the samples were kept airtight. The spectra of powder samples and stone samples (as aggregates and as a single stone) were successfully obtained. Concurrent with the analyses described below were ultra-violet spectral observations on stone samples, also transported and performed in an inert environment, conducted at the University of Illinois Urbana-Champaign (USA).

A major feature of the stone team's analysis is the use of synchrotron radiation facilities around the world. Since this analysis is non-destructive, stone samples whose reflectance spectra were measured were sent to KEK, SPring-8, ESRF (France), SOLEIL (France), DESY (Germany), and APS (USA). Using these synchrotron radiation facilities, high spatial resolution and sensitivity XRD, STXM, XANES, CT [1], IR-CT, FT-IR [2, 3], XRF, and Mössbauer [4] analyses were performed. Most of the analyses were carried out under airtight conditions on the stone samples and the particulates separated from the stone samples. These analyses allowed us to determine the three-dimensional distribution of solid phases and elements, redox state, density, and porosity of the stone samples.

Furthermore, as a characteristic analysis of the stone team, light elemental analysis using negative Muon was performed at the MLF facility of J-PARC with an exceptionally long allocation of machine time. This is the non-destructive method to measure the concentration of light elements in the whole (not the surface) of stone samples. Because the characteristic X-rays produced

by muon irradiation are much higher in energy than the fluorescent X-rays produced by X-ray irradiation, there is little effect of self-absorption by the sample, and therefore, the concentration of light elements such as carbon, oxygen, and sodium in the entire "stone" sample can be determined.

Some stone samples are currently being measured for thermal conductivity and strengths in order to understand the physical properties of asteroid Ryugu. The data obtained from these measurements are useful for interpreting the remote-sensing data taken from the surface layer of the asteroid Ryugu [5-8]. It is also important for understanding the behavior of the Ryugu material during impact events.

The surfaces of many stone samples were observed by electron microscopy and other techniques, especially on natural "flat" surfaces formed on 5 stones. As a result, characteristic mineral aggregates formed by the reactions with water and characteristic impact features were observed on some samples. Based on the observations of surfaces and the synchrotron measurements of the whole stones, important objects such as characteristic structures and specific crystal aggregates for understanding the formation history of the asteroid were identified, and these parts were separated from the stone samples using a Xe beam (pFIB) and analyzed by various methods including transmission electron microscopy and synchrotron radiation analysis. Many stone samples, from which important objects have been separated, are embedded in epoxy resin and cut to produce many polished sections. Electron microscopy and spectroscopic measurements of the polished surfaces are being carried out to reveal the detailed mineralogical properties and elemental distribution inside the stone samples. In this fall, the allocated beam time for synchrotron radiation will begin, and we plan to analyze single crystals and characteristic objects separated from the stone samples. Photometric measurements in the ultra-violet and visible to near-infrared will also be made this fall on the powders produced in the structural experiments to facilitate comparisons with the ONC-T and NIRS3 remote sensing observations.

Acknowledgement

We thank Drs. H. Nakao (KEK), K. Nitta (JASRI/SPring-8), O. Sekizawa (JASRI/SPring-8) for support in synchrotron analysis and Dr. O. Sasaki for support in CT analysis at Tohoku University.

References

[1] Tsuchiyama A. et al. in this volume. [2] Dionnet Z. et al. in this volume. [3] Rubino S. et al. in this volume. [4] Viennet J-C. et al. in this volume [5] Watanabe S. et al. 2019. Science 364:268. [6] Sugita S. et al. 2019. Science 364:252. [7] Kitazato K. et al. 2019. Science 364:272. [8] Okada T. et al. 2020. Nature 579:518.

Mineralogy and surface modification of small grains recovered from the asteroid 162173 Ryugu

T. Noguchi¹, T. Matsumoto¹, A. Miyake¹, Y. Igami¹, M. Haruta¹, H. Saito², S. Hata², Y. Seto³, M. Miyahara⁴, N. Tomioka⁵, H. A. Ishii⁶, J. P. Bradley⁶, K. Ohtaki⁶, E. Dobrică⁶, T. Nakamura⁷, M. Matsumoto⁷, A. Tsuchiyama^{8,9}, M. Yasutake¹⁰, J. Matsuno⁸, S. Okumura¹, K. Uesugi¹⁰, M. Uesugi¹⁰, A. Takeuchi¹⁰, M. Sun⁹, S. Enju¹¹, A. Takigawa¹², H. Leroux¹³, C. Le Guillou¹³, D. Jacob¹³, M. Marinova¹³, F. de la Peña¹³, F. Langenhorst¹⁴, D. Harries¹⁴, P. Beck¹⁵, T. H. V. Phan¹⁵, R. Rebois¹⁵, N. M. Abreu¹⁶, T. Zega¹⁷, P.-M. Zanetta¹⁷, M. Thompson¹⁸, M. Lee¹⁹, L. Daly¹⁹, P. A. Bland²⁰, R. Stroud²¹, K. Burgess²¹, J. C. Bridges²², L. Hicks²², M. E. Zolensky²³, D. R. Frank⁶, J. Martinez²⁴, H. Yurimoto²⁵, K. Nagashima⁶, N. Kawasaki²⁵, R. Okazaki², H. Yabuta⁴, H. Naraoka², K. Sakamoto²⁶, S. Tachibana¹², S. Watanabe²⁷, Y. Tsuda²⁶, and the Hayabusa2 Initial Analysis Team

¹Kyoto Univ., Japan; ²Kyushu Univ., Japan; ³Kobe Univ., Japan; ⁴Hiroshima Univ., Japan; ⁵Kochi Core Center, JAMSTEC, Japan; ⁶Univ. of Hawaii, USA; ⁷Tohoku Univ., Japan; ⁸Ritsumeikan Univ., Japan; ⁹Guangzhou Institute of Geochemistry, China; ¹⁰JASRI, Japan; ¹¹Ehime Univ., Japan; ¹²Univ. of Tokyo, Japan; ¹³Univ. de Lille, France; ¹⁴Univ. of Jena, Germany; ¹⁵Univ. Grenoble Alpes, France; ¹⁶Penn State, USA; ¹⁷Univ. of Arizona, USA; ¹⁸Purdue Univ., USA; ¹⁹Univ. of Glasgow, UK; ²⁰Curtin Univ., Australia; ²¹US Naval Research Laboratory, USA; ²²Univ. of Leicester, UK; ²³JSC/NASA, USA; ²⁴Jacobs Engineering, USA; ²⁵Hokkaido Univ., Japan; ²⁶JAXA/ISAS, Japan; ²⁷Nagoya Univ., Japan

Introduction: Surface material on airless bodies exposed to the interplanetary space experienced the bombardment by low-energy (~1 keV/nucleon) solar wind particles and micrometeoroid impacts. These processes, alongside the resultant surface modifications, and spectral darkening and reddening are called space weathering [1]. Space weathering of the Moon and the asteroid 25143 Itokawa belonging to S-type asteroids have been investigated intensively [e.g. 1-5]. The *Hayabusa 2* spacecraft returned samples from the asteroid 162173 Ryugu C-type asteroid. The Ryugu samples give us the first opportunity to investigate space weathering of C-type asteroids. The Mineralogy-Petrology Fine (M-P F or Sand) sub-team mainly investigates small grains (typically ~100 μm across). The main purposes of the M-P F sub-team are to understand the variation of mineralogy of the allocated grains and the nature of space weathering of the asteroid Ryugu. The M-P F sub-team is comprised of 51 members belonging to 25 universities and laboratories.

Sample and methods: Numerous small Ryugu grains, ~100 μm across on average, were allocated to the M-P F sub-team. Surface morphology of >350 grains from the chamber A of the sample canister have been observed by JEOL JSM-7001F field emission scanning electron microscope (FE-SEM) at Kyoto Univ. and by Thermo Scios focused ion beam (FIB)-SEM at Kyushu Univ. Elemental mapping analysis was also performed using Energy dispersive spectrometer (EDS) equipped on the FE-SEM. Most of the grains were attached to Au plates with small amounts of epoxy glue in N₂ filled glove box for SEM observation. Some grains were just placed on Pt plates without using any glue to make FIB sections in response to requests from some members. One sample was prepared by Reichelt Ultracut ultramicrotome at Kyoto Univ. In addition to the small grains, the Chemistry sub-team loaned a polished sample of a fragment originating from a large grain A0026 (~3 mm wide) because the sample has a bubble-rich material on its surface. Seven samples were able to be prepared for the detailed analysis. Up to now we have prepared ~80 FIB sections from 40 grains and >30 FIB sections have already been distributed to the members. To understand mineralogy and petrology down to the nanometer of these grains and to clarify the detailed mineralogical analyses of space weathering of the C-type asteroid Ryugu, we are now performing (scanning) transmission electron microscopy ((S)TEM), synchrotron radiation X-ray absorption fine structure (XANES and EXAFS) analysis, nanotomography, and atom probe analysis at 15 universities and laboratories.

Results: Major minerals of the small Ryugu grains are phyllosilicates (saponite and serpentine), Fe-bearing sulfides, magnetite, dolomite, and a lesser amount of breunnerite. It is obvious that the asteroid Ryugu experienced severe aqueous alteration and did not experience heating enough to make secondary anhydrous minerals such as olivine, pyroxene and Fe metal, which are common in severely heated carbonaceous chondrites. Serpentine in these Ryugu grains may have better crystallinity than that in Orgueil and Ivuna CI chondrites [e.g., 6]. Typical spacing of (001) of saponite is ~1.0-1.3 nm, which suggests partial dehydration of interlayer H₂O molecules. Minor minerals so far observed are hydroxyapatite, ilmenite, magnesiochromite, manganochromite, Cr oxide, Cu-bearing ZnS, (Fe, Ni)₂P, FeCr₂S₄, cubanite, Na- and Mg-bearing phosphate, forsteritic olivine, and Fe-free low-Ca pigeonite. A moissanite crystal was also identified, which could be a presolar grain.

The surfaces of the most Ryugu grains investigated have highly euhedral pyrrhotite crystals. Their surfaces preserve quite sharp steps, which may reflect growth or dissolution in aqueous solutions. Magnetite crystals that form framboidal aggregates have shapes as rounded as those in Orgueil and Ivuna. In addition, some magnetite crystals have facets as sharp as those in

Tagish Lake C ungrouped meteorite. The presence of these Fe sulfide and oxide suggests that these surfaces did not experience enough exposure to the interplanetary space to degrade the surfaces of these minerals.

After scrutinizing >350 small Ryugu grains by FE-SEM and FIB-SEM, we found 10 small Ryugu grains having obviously different surface morphology. Figure 1 shows an example of such grains with abundant open bubbles. The bubble-rich surfaces form a continuous layer containing abundant bubbles. In Fig. 1(b), the bubble walls are as thick as $\sim 0.5 \mu\text{m}$ at the thickest places. Most bubble-rich layers have $\sim 50 - \sim 500 \text{ nm}$ thick, but the layer of A0026 has up to $\sim 3 \mu\text{m}$ thick. The bubble-rich layer in Fig. 1(b) is amorphous and contains abundant tiny Fe sulfide crystals based on selected area electron diffraction (SAED) patterns and electron diffraction mapping. Preliminary analysis of energy-loss near-edge structures of Fe L_{2,3} edge of the bubble-rich layer and the subsurface phyllosilicate suggests that the former is much more enriched in Fe^{2+} than the latter. More detailed description of the rugged Fe sulfide and the other phases will be presented in another presentation [7].

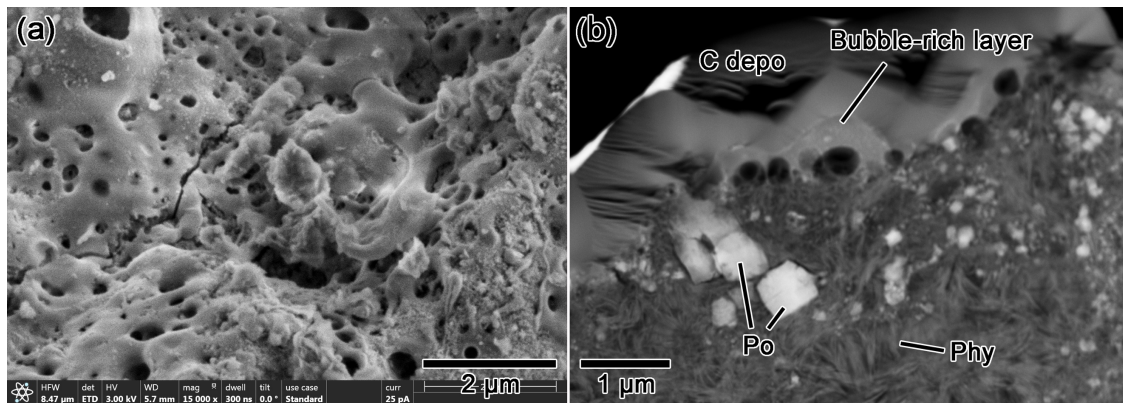


Fig. 1 Secondary electron and annular dark-field images of a small Ryugu grain with a bubble-rich surface. (a) The surface is covered by a gently rolling layer with abundant open bubbles. Abundant bright tiny speckles are on the surface. (b) A cross-section of the bubble-rich layer and the interior. Abbreviations: Po: pyrrhotite; Phy: phyllosilicate; depo: deposition.

Discussion and conclusion: These major minerals and the petrography of the small Ryugu grains indicate that the asteroid Ryugu experienced severe aqueous alteration that can be classified as C1. The mineralogy and petrology of these grains are similar to CI chondrites but these grains lack ferrihydrite and sulfates, both common among CI chondrites [e.g., 6, 8 and references therein]. The formation of ferrihydrite and sulfates may have occurred by terrestrial weathering. The spacing of (001) of saponite increased to $\sim 1.3 \text{ nm}$ on average by using ethylene glycol as the trough liquid during ultramicrotomy, which means that saponite in the Ryugu samples can rehydrate.

Morphology of the bubble-rich layers is apparently similar to melt sheets (Fig. 1a). However, it does not necessarily mean that all the layers were formed through melting by meteoroid impacts. The formation of similar bubble-rich amorphous layers by H^+ or He^+ ion irradiation has already been reported [9-11]. Although the size and number density of bubbles in the amorphous layer are different from the irradiation experiments and the natural samples, the difference can be interpreted by the different fluxes between them. Therefore, we believe that at least thin bubble-rich layers were related to solar wind irradiation. Unlike the irradiation experiments, the bubble-rich layer in Fig. 1(b) is more enriched in Fe, S, and Ca than the subsurface phyllosilicate. Recondensation of elements derived from the surrounding phases may have also played a role in the compositional difference. Because the thickness of the bubble containing layer is quite variable, the relative contribution of irradiation and micrometeoroid impacts that resulted in vaporization and recondensation of elements may be quite different at places. The M-P F sub-team continues to assess the role of recondensation in the space weathering of the Ryugu C-type asteroid. Although small Ryugu grains with the space weathering rims are quite rare among the investigated samples, it does not necessarily mean that such grains are rare on the surface of Ryugu because most of the surfaces are exposed to the interplanetary space may have been destroyed during the sampling sequence using Ta projectiles. If most of the space exposed surface had the bubble-rich amorphous layer on Ryugu, the bubble-rich amorphous surface layers might have affected the reflectance spectra of the asteroid Ryugu.

References [1] Noguchi T. et al. 2011. *Science* 333, 1121-1125. [2] Noguchi T. et al. 2014. *Meteorit. Planet. Sci.* 49, 188-214. [3] Matsumoto T. et al. 2015 *Icarus* 257, 230-238. [4] Thompson, M. et al. 2014. *Earth Planet. Space* 66, 89. [5] Burgess K.D. and Stroud K.D. 2018. *J. Geophys. Res. Planets* 123, 2022-2037. [6] Tomeoka K. and Buseck P. 1985 *Geochim. Cosmochim. Acta* 52, 1627-1640. [7] Matsumoto T. et al. this symposium. [8] Brearley A. and Jones R. 1998. *Planetary Materials*, pp. C1. [9] Thompson M. et al. 2020. *Icarus* 346, 113775. [10] Lacznik D.L. et al. 2020. *Icarus* 364, 114479. [11] Noguchi T. et al. 2017. *Hayabusa 2017 Symp. & 8th Symp. Pol. Sci.* (abstract).

Initial Analysis of Volatile Components in the Hayabusa2 Samples

Ryuji Okazaki¹, Bernard Marty², Henner Busemann³, Yayoi N. Miura⁴, Keita Yamada⁵, Saburo Sakai⁶, Ko Hashizume⁷, Ken-ichi Bajo⁸, Shun Sekimoto⁹, Fumio Kitajima¹, Kevin Righter¹⁰, Alex Meshik¹¹, Jamie Gilmour¹², Naoyoshi Iwata¹³, Evelyn Füre², Sarah Crowther¹², Naoki Shirai¹⁴, Mitsuru Ebihara¹⁵, Yoshinori Takano⁶, Akizumi Ishida¹⁶, Reika Yokochi¹⁷, Olga Pravdivseva¹¹, Jisun Park^{18, 19}, Toru Yada²⁰, Kunihiko Nishiizumi²¹, Keisuke Nagao²², Jong Ik Lee²², Michael Broadley², David Byrne², My Riebe³, Patricia Clay¹², Akihiro Kano⁴, Marc Caffee²³, Shinsuke Kawagucci⁶, Yohei Matsui⁶, Ryu Uemura²⁴, Makoto Inagaki⁹, Daniela Krietsch³, Colin Maden³, Mizuki Yamamoto¹, Hisayoshi Yurimoto⁸, Tomoki Nakamura¹⁶, Takaaki Noguchi⁹, Hiroshi Naraoka¹, Hikaru Yabuta²⁵, Kanako Sakamoto²⁰, Shogo Tachibana^{4, 20}, Sei-ichiro Watanabe²⁴ and Yuichi Tsuda²⁰

¹Kyushu Univ., ²CRPG, ³ETH, ⁴Univ. of Tokyo., ⁵Tokyo Inst. Tech., ⁶JAMSTEC, ⁷Ibaraki Univ., ⁸Hokkaido Univ., ⁹Kyoto U., ¹⁰NASA JSC, ¹¹Washington Univ., ¹²Univ. Manchester, ¹³Yamagata Univ., ¹⁴Tokyo Metro., ¹⁵Waseda Univ., ¹⁶Tohoku Univ., ¹⁷Chicago Univ., ¹⁸Kingsborough Comm. Coll., ¹⁹AMNH, ²⁰JAXA, ²¹UC Berkeley, ²²KOPRI, ²³Purdue Univ., ²⁴Nagoya Univ., ²⁵Hiroshima Univ.

The major objectives of the Hayabusa2-initial-analysis volatile team are (1) to determine the pristine volatile components in the parental materials of the returned Ryugu samples, and (2) to elucidate the origin and chronological history of the asteroid Ryugu, as well as the evolution of the solar system through determination of volatile carrier phases and abundances of volatile components (e.g., presolar grain abundances). Our analytical data will be linked with remote sensing (NIRS3, ONCs, TIR, and LIDAR) data and theoretical modeling [e.g., 1-5]. For example, the erosion rate and the degree of gardening of the surface layer of the asteroid Ryugu can be estimated based on trapped solar wind (SW) and cosmic ray produced (cosmogenic) nuclides, which will be discussed in conjunction with the results based on the remote sensing data [3-5]. Taken together, these will provide characteristics of the surface materials, such as the degree and duration of the alteration by SW/cosmic ray irradiation and micrometeorite bombardments.

Our analytical plan for the Ryugu samples consists of three approaches (Fig. 1): One is analyses of native volatiles in the Ryugu samples which have been treated WITHOUT air-exposure throughout the whole process, since the collection from the asteroid Ryugu to the gas extraction in the laboratories. The goal of this work is to quantify the indigenous compositions with as minimal terrestrial (atmospheric, biological, and unintentional man-made pollution) contamination as possible. We will obtain

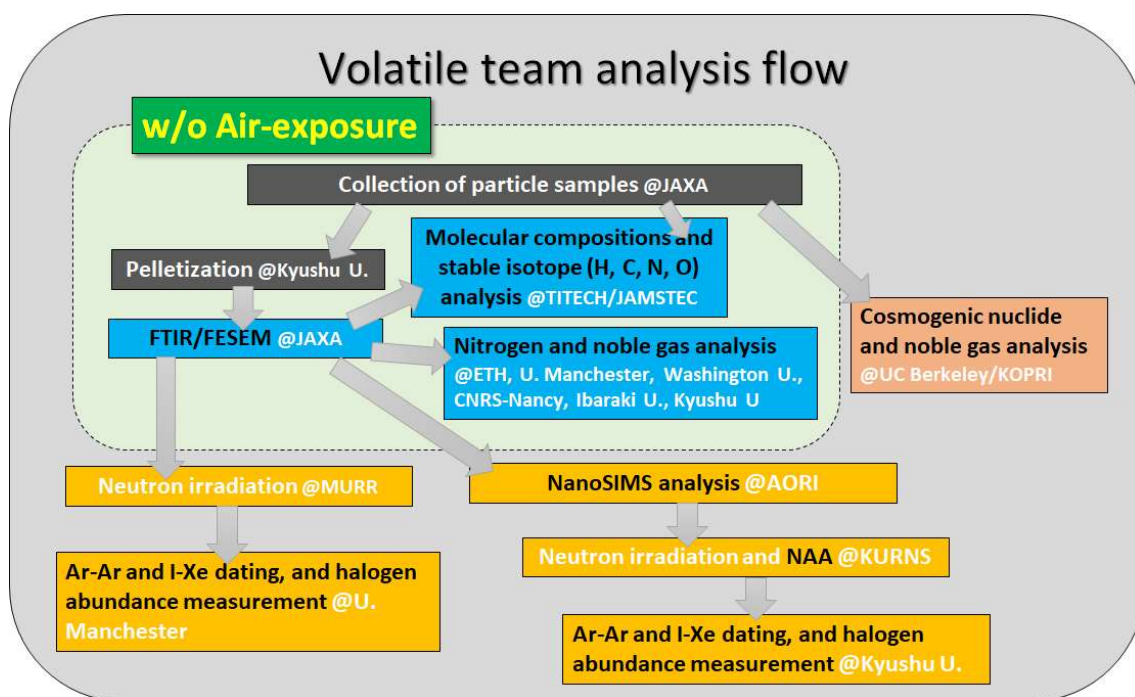


Figure 1. Analytical flow of the volatile team of the Hayabusa2 initial analysis.

the abundances and isotopic compositions of nitrogen, noble gases, and volatile elements (e.g., H and C in H₂, CO, and CO₂, methane, and ethane).

The second approach is analyses of the neutron-irradiated samples to determine the Ar-Ar and I-Xe ages and halogen abundances by noble gas isotope measurements at U. Manchester and Kyushu U., and to obtain abundances of minor/trace elements (e.g., Co, Ni, and Ir) by neutron activation analysis (NAA) at KURNS. Prior to neutron-irradiation, nanoSIMS analysis will be carried out at AORI on the same samples that are used for the Ar-Ar/I-Xe/halogen analysis at Kyushu U. to understand the distribution and isotopic compositions of volatile elements (H, C, N, and O).

The third approach is measurements of cosmogenic long-lived nuclides and noble gas isotopes, which are performed for different samples prepared under an atmospheric environment. The preliminary result of cosmogenic nuclides is reported by [6].

Most of Hayabusa2 samples allocated to the volatile team have been transported to Kyushu Univ. from JAXA, and located in a N₂ glove box installed at Kyushu Univ., and pelletized without air-exposure in June 2021, except for two particles for the volatile element analysis at TITECH/JAMSTEC and five samples for cosmogenic nuclides which were directly allocated to Berkeley U. from JAXA. Twenty four pellets have been prepared (Fig. 2), and sent back to JAXA to perform FTIR and FESEM observations. After these observations, 16 out of 24 samples have been distributed to our team laboratories, ETH, U. Manchester, Washington U., CNRS-Nancy, Ibaraki U., TITECH/JAMSTEC, and Kyushu U. to measure native volatile compositions. Before analysis, we measured the sample weight without air-exposure by using a small weighing container (Fig. 3). These careful operations enable us to obtain the most intact, fresh volatile compositions of the asteroid Ryugu.

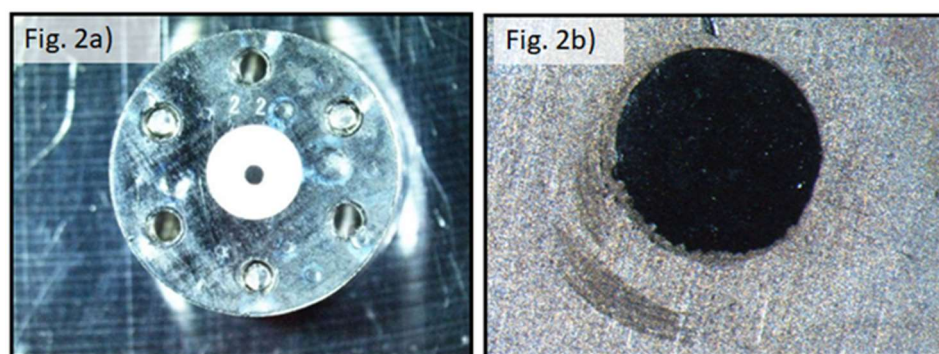


Figure 2. The Hayabusa2 samples pelletized onto a Cu disk without air-exposure (2a). The Cu disk is installed in a metal holder for NanoSIMS analysis and transportation. Enlarged view of the sample is shown in Fig. 2b.



Figure 3. The small weighing container developed for the Hayabusa2 initial analysis.

The remainder of the samples, six pellets have been transported to Tohoku U. and coated with Os and Pt as an antistatic treatment. These samples have now been exposed to the atmosphere. After coating, the 6 samples were shipped to AORI and investigate with NanoSIMS in August 2021. The result of the nanoSIMS analysis will be reported by Drs. Hashizume and Ishida somewhere else.

Following NanoSIMS analysis, the 6 pellet samples were transported to Kyushu U. for installation in diamond container for the NAA. The neutron irradiation and NAA are scheduled to be completed in October. After the NAA, the 6 samples will be analyzed for Ar-Ar age dating. For I-Xe dating and halogen analysis, two other pellet samples, different from the 6 samples that have been analyzed for nanoSIMS and NAA, have been distributed to U. Manchester in July. Now all of these preparatory steps are over and the Ryugu samples are ready for the experiments. We believe that all analyses will proceed successfully.

References

- [1] Sugita S. et al. 2019. Science 364, eaaw0422 1-11.
- [2] Kitazato K. et al. 2019. Science 364, 272-275.
- [3] Tatsumi E. et al. 2021. Nature Astronomy doi.org/10.1038/s41550-020-1179-z.
- [4] Morota T. et al. 2020. Science 368, 654-659.
- [5] Tachibana S. et al. 2021. in review.
- [6] Nishiizumi K. et al. 2021. This issue.

An initial look at the distributions and compositions of organic macromolecules in the asteroid Ryugu samples

Hikaru Yabuta¹, George Cody², Cecile Engrand³, Yoko Kebukawa⁴, Bradley De Gregorio⁵, Lydie Bonal⁶, Laurent Remusat⁷, Rhonda Stroud⁵, Eric Quirico⁶, Larry Nittler², Minako Hashiguchi⁸, Mutsumi Komatsu⁹, Taiga Okumura¹⁰, Yoshio Takahashi¹⁰, Yasuo Takeichi¹¹, Emmanuel Dartois³, Jean Duprat⁷, Jeremie Mathurin³, David Kilcoyne¹², Zita Martins¹³, Scott Sandford¹⁴, Shohei Yamashita¹¹, Ariane Deniset³, Alexandre Dazzi³, Yusuke Tamenori¹⁵, Takuji Ohigashi¹⁶, Hiroki Suga¹⁵, Daisuke Wakabayashi¹¹, Maximilien Verdier-Paoletti⁷, Smail Mostefaoui⁷, Gilles Montagnac¹⁷, Jens Barosch², Kanami Kamide¹, Miho Shigenaka¹, Laure Bejach³, Takaaki Noguchi¹⁸, Hisayoshi Yurimoto¹⁹, Tomoki Nakamura²⁰, Ryuji Okazaki²¹, Hiroshi Naraoka²¹, Kanako Sakamoto²², Shogo Tachibana^{10,22}, Sei-ichiro Watanabe⁸, and Yuichi Tsuda²²

¹Hiroshima Univ., ²Carnegie Institution of Washington, ³Université Paris Sud, ⁴Yokohama National Univ., ⁵Naval Research Laboratory, ⁶Université Grenoble Alpes, ⁷Muséum national d'Histoire naturelle, ⁸Nagoya Univ., ⁹The Graduate Univ. for Advanced Studies (Sokendai), ¹⁰Univ. of Tokyo, ¹¹High Energy Accelerator Research Organization, ¹²Advanced Light Source, ¹³Universidade de Lisboa, ¹⁴NASA Ames Research Center, ¹⁵SPRING8, ¹⁶UVSOR, IMS, ¹⁷ENS de Lyon, ¹⁸Kyoto Univ., ¹⁹Hokkaido Univ., ²⁰Tohoku Univ., ²¹Kyushu Univ., ²²JAXA

Hayabusa2 is JAXA's asteroid sample return mission that targeted the carbonaceous (C-type) asteroid (162173) Ryugu. The mission aims to unveil the origin and evolution of organic compounds and water in the early Solar System as life's building blocks [1]. Following the arrival of the Hayabusa2 spacecraft at Ryugu on June 27, 2018, observations by onboard remote sensing instruments revealed that Ryugu is a top-shaped asteroid with a very low geometric albedo [2-4] and that its surface is probably partially dehydrated [5]. The Mobile Asteroid Surface Scout (MASCOT) lander observed two types of boulders on the surface of Ryugu: one type was dark and cauliflower-like with a similar morphology to primitive carbonaceous chondrites, and another type was bright and smooth [6]. The lander's radiometer revealed that Ryugu has low thermal conductivity and high porosity unlike any chondritic meteorites, while these thermal properties have similar values to comets [7]. Thanks to the formation of the artificial crater on Ryugu's surface by a small carry-on impactor [8], two successful touchdowns on February 22 and July 11, 2019 have enabled collections of samples from two distinct locations on the asteroid, providing an advantage for investigating the origin and evolution of the Solar System as well as the surface processes of the asteroid. After the sample return on December 6, 2020, the curatorial work on the Ryugu sample has been conducted at JAXA for the first 6 months [9]. With the significant guidance from the observations and curation, the initial sample analysis has a one-year mission from June 2021 to June 2022 to address the question of what kind of asteroid Ryugu is.

Organic compounds are a major component of interstellar dust as along with silicates and water ice due to the high abundances of their elements (C, H, O, N, S, P) in the Galaxy. The initial molecular inventory of the Solar System, inherited from the parental molecular cloud, was modified and new complex molecules formed through a variety of processes in the protoplanetary disk and planetesimals, which resulted in the diverse compositions of asteroids and comets. These small bodies are thought to have contributed to the formation of our habitable planet, through exogenous delivery of organics and water as life's building blocks to the early Earth.

Organic macromolecules from chondritic meteorites have been often characterized as a dark, complex, acid-insoluble organic matter (IOM). IOM accounts for a major portion of total organic carbon in primitive carbonaceous chondrites (CCs). The intact chemical structure of IOM in CCs is still unknown, although a number of previous studies have suggested that it is composed of aromatic network crosslinking with short-branched aliphatic chains and various oxygen-bearing functional groups [10, 11]. Whether IOM was formed in interstellar cloud [12], outer solar nebula [13] or planetesimals [14], is still under debate. Nevertheless, elemental, molecular and isotopic variations of IOM from various types of small body materials, such as chondritic meteorites [15-20], interplanetary dust particles (IDPs) [21], cometary dusts [21-23], and Antarctic micrometeorites (AMMs) [24-27], have enabled our comprehensive understanding of chemical history of the early Solar System.

The Hayabusa2-initial-analysis IOM team consists of 36 members from Japan, USA, France, and Portugal. The scientific goals of IOM team include: i) Decoding the chemical relationship(s) between organics and minerals on a C-type asteroid parent body, ii) Elucidating formation pathways of organic macromolecules in a C-type asteroid, iii) Determining the origin(s) of organics in a C-type asteroid, iv) Investigating the asteroid-comet continuum, v) better understanding Solar System formation and volatile delivery, and vi) Understanding the role of organic macromolecules in the origin of life. In order to accomplish the goals, we aim to unveil the elemental, isotopic, and functional group compositions, structures and textures of organic macromolecules from the Ryugu samples. The analytical procedures are configured by combination of micro-Fourier

Transform Infrared Spectroscopy (FTIR), micro-Raman spectroscopy, synchrotron-based scanning transmission x-ray microscope (STXM), Scanning Transmission Electron Microscopy (STEM) coupled with Electron Energy Loss Spectroscopy (EELS) and Energy Dispersive X-ray Spectroscopy (EDS), Atomic Force Microscope based Infrared Spectroscopy (AFM-IR), and nano-secondary ion mass spectrometry (NanoSIMS). The analytical procedures are applied to the intact Ryugu samples and the IOM isolated by HCl/HF treatment of the Ryugu samples, respectively.

For the first measurements, Chamber A aggregates (A0108) collected upon the first touchdown and Chamber C aggregates (C0109) collected upon the second touchdown have been analyzed. The individual particles from A0108 and C0109 range from 200 to 900 μm in size. Some of the particles were crushed on a diamond window for micro-FTIR, micro-Raman, and NanoSIMS. Slices of other particles were prepared with a focused ion beam workstation (FIB) and/or an ultramicrotome to obtain ultra-thin sections for STXM, STEM-EELS, AFM-IR and NanoSIMS. The water/solvent/HCl extraction residues of other aggregates of Chamber A (A0106) and Chamber C (C0107), which were transferred by SOM team, were treated with 6N HCl and 1N HCl/9N HF to yield IOM for future measurements.

Organic macromolecules have been identified from the Ryugu samples by all the analytical techniques. The organic macromolecules were associated with secondary minerals formed through aqueous alteration [28], and they often exhibited D and/or ^{15}N -rich regions [29, 30]. These results show that the observed organics are of extraterrestrial origin. The FTIR [31] and Raman [32] spectroscopic features as well as the isotopic features [29, 30] of organic macromolecules from the Ryugu samples were comparable with those of the primitive carbonaceous CI/CM chondrites, while the other features were not necessarily consistent with the typical CI/CM, demonstrating that Ryugu samples record heterogeneous chemical history in a pristine state [28, 29].

References

- [1] Tachibana et al. 2014. *Geochem. J.* 48:571. [2] Watanabe et al. 2019. *Science* 364:268. [3] Sugita et al. 2019. *Science* 364: eaaw0422. [4] Tatsumi et al. 2020 *A&A*, 639:A83. [5] Kitazato et al. 2019. *Science* 364:272. [6] Jaumann et al. 2019. *Science* 365:817. [7] Grott et al. 2019. *Nature Astronomy* 3:971. [8] Arakawa et al. 2020. *Science* 368:67. [9] Yada et al. et al. 2021. under review. [10] Glavin et al. 2018. In: *Primitive Meteorites and Asteroids: Physical, Chemical and Spectroscopic Observations Paving the Way to Exploration* (Ed. Abreu N.) pp. 205-271. [11] Martins et al. 2020. *Space Sci. Rev.* 216:54. [12] Alexander et al. 2007. *GCA* 71:4380. [13] Remusat et al. 2010. *Astrophys. J.*, 713:1048. [14] Kebukawa et al. 2013. *Astrophys. J.* 771:19. [15] Cody and Alexander, 2005. *GCA* 69:1085. [16] Yabuta et al. 2005. *GCA* 40:779. [17] Bonal et al. 2006. *GCA* 70:1849. [18] Cody et al. 2008. *Earth Planet. Sci. Lett.* 272:446. [19] Kebukawa et al. 2011. *GCA* 75:3530. [20] Quirico et al. 2018. *GCA* 241:17. [18] Messenger, 2000. *Nature* 404:968. [21] Sandford et al. 2006. *Science* 314:1720. [22] Cody et al. 2008. *MAPS* 43:353. [23] De Gregorio et al. 2011. *MAPS* 46:1376. [24] Duprat et al. 2010. *Science* 328:742. [25] Yabuta et al. 2017. *GCA* 214:172. [26] Noguchi et al. 2017. *GCA* 208:119. [27] Mathurin et al. 2019. *A&A* 622:A160. [28] Stroud et al. this conference. [29] Nittler et al. this conference. [30] Remusat et al. this conference. [31] Kebukawa et al. this conference. [32] Bonal et al. this conference.

Soluble Organic Matter (SOM) analysis of the Hayabusa2 samples: The first results

Hiroshi Naraoka¹, Yoshinori Takano², Jason P. Dworkin³, Kenji Hamase¹, Aogu Furusho¹, Minako Hashiguchi⁴, Kazuhiko Fukushima⁴, Dan Aoki⁴, Yasuhiro Oba⁵, Yoshito Chikaraishi⁵, Saburo Sakai², Nanako O. Ogawa², Naohiko Ohkouchi², Toshihiro Yoshimura², Toshiki Koga², Haruna Sugahara⁶, Hajime Mita⁷, Daniel P. Glavin³, Jamie E. Elsila³, Eric T. Parker³, José C. Aponte^{3,8}, Hannah L. McLain^{3,8}, Heather V. Graham³, John M. Eiler⁹, Francois-Regis Orthous-Daunay¹⁰, Cédric Wolters¹⁰, Véronique Vuitton¹⁰, Roland Thissen¹⁰, Junko Isa¹¹, Philippe Schmitt-Kopplin¹², Norbert Hertkorn¹², Alexander Ruf¹³, Hisayoshi Yurimoto⁵, Tomoki Nakamura¹⁴, Takaaki Noguchi¹⁵, Ryuji Okazaki¹, Hikaru Yabuta¹⁶, Kanako Sakamoto⁶, Shogo Tachibana^{6,17}, Seiichiro Watanabe⁴ and Yuichi Tsuda⁶

¹Kyushu Univ., ²JAMSTEC, ³NASA Goddard Space Flight Center, ⁴Nagoya Univ., ⁵Hokkaido Univ., ⁶JAXA, ⁷Fukuoka Inst. Tech., ⁸Catholic Univ/CRESST, ⁹California Inst. Tech., ¹⁰Univ. Grenoble Alpes CNRS IPAG, ¹¹Tokyo Inst. Tech., ¹²Helmholtz-Zentrum Muenchen, ¹³Aix-Marseille Univ., ¹⁴Tohoku Univ., ¹⁵Kyoto Univ., ¹⁶Hiroshima Univ., ¹⁷Univ. Tokyo

The Hayabusa2 spacecraft successfully collected the surface and possible sub-surface materials of the asteroid 162173 Ryugu. Ryugu is a C-type asteroid characterized by a low-albedo surface probably consisting of hydrous minerals and carbonaceous materials. [1] The direct optical and spectral analysis of the returned samples indicates that Ryugu material is dominated by hydrous carbonaceous chondrite-like matter (similar to CI chondrites) [2]. Since carbonaceous chondrites have generally yielded various types of organic matter, the collected Ryugu grains are expected to contain diverse types of organic compounds including bio-related molecules. The occurrence of organic compounds in the Ryugu surface will provide clues to the evolution of prebiotic molecules and their preservations associated with aqueous alteration of the primitive asteroid. The initial analysis of soluble organic matter (SOM) of the Hayabusa2-returned samples has been performed by an international team consisting of 32 members. Because the sample amount available for comprehensive SOM analyses is limited, and because the SOM is expected to be present as a complex mixture of various types of organic compounds with very small concentrations of each compound, high-sensitivity and high-resolution analytical techniques have been developed using carbonaceous meteorites [e.g. 3].

Two aggregate samples of the Ryugu grains (A106 and C107) were allocated for the solvent extractions and total carbon (C), hydrogen (H), nitrogen (N), sulfur (S) and oxygen (O) measurements. The A106 sample was collected during the 1st sampling in February 2019 and the C107 sample was collected during the 2nd sampling in July 2019 after the Small Carry Impactor (SCI) operation. They consist mainly of particles smaller than 1 mm in diameter, and each sample mass was 38-39 mg. They were firstly investigated spectroscopically in the near infrared wavelength range by the Stone Team prior to the solvent extractions. Other small grains (A0080 and C0057) were also allocated for this study to investigate the spatial distribution of organic compounds on the sample surface. The extraction and analytical measurements implemented by the SOM Team are summarized in Figure 1. Each powder sample was extracted sequentially with non-polar to polar solvents, i.e., hexane, dichloromethane (DCM), methanol (MeOH) and H₂O, for non-targeted analysis to reveal the compound composition. Each solvent extract was analyzed by solution state nuclear magnetic resonance (NMR) spectroscopy [4], Fourier transform ion cyclotron resonance/mass spectrometry (FT-ICR/MS) with ESI and APPI ionization [5] and by high-resolution mass spectrometry using Orbitrap MS coupled with nano-liquid chromatography (nanoLC/Orbitrap MS) [6], and using two dimensional gas chromatography/mass spectrometry (GC×GC/MS). The extracted residues were passed to the Chemistry Team for further inorganic element analysis. The other powder sample was subjected to the hot water extraction for amino acid analyses including chiral isomer separation, which was performed by three-dimensional (3D) high-performance liquid chromatography (HPLC) with high-sensitivity fluorescence detection (FD) [7] and by HPLC/FD coupled with quadrupole-time of flight/mass spectrometry (QToF/MS) [8]. After the hot water extraction, the residue was split into two halves. One half was further extracted with hydrochloric acid (HCl) to analyze for amino acids in bound-form. The other half was sequentially extracted with DCM/MeOH (1/1) to analyze semi-polar compounds such as polycyclic aromatic hydrocarbons (PAHs) by GC/MS, followed by further extraction with formic acid to analyze polar heterocyclic compounds, and subsequent extraction with HCl to detect bound-form polar compounds. The extracted residues were passed to the IOM Team for the analysis of insoluble organic matter (IOM). Compound-specific stable isotope analyses will be performed using GC/combustion/isotope ratio mass spectrometry (GC/C/IRMS) if the compound concentration is high enough to enable such an isotopic measurement. All extraction procedures were performed on an ISO 6 (Class 100) clean bench inside an ISO 5 (Class 1000) clean room. Baked serpentine powder was also analyzed as a procedural blank. *In situ* organic compound analysis with the molecular imaging was performed using desorption electrospray ionization (DESI) equipped with Orbitrap MS [9, 10], followed by

A first look at the interior and exterior of Ryugu preserved in samples collected by Hayabusa2

Eizo Nakamura¹, Katsura Kobayashi¹, Ryoji Tanaka¹, Tak Kunihiro¹, Hiroshi Kitagawa¹, Christian Potyszil¹, Tsutomu Ota¹, Chie Sakaguchi¹, Masahiro Yamanaka¹, Yusuke Yati¹, Tomohiro Usui², Yuichi Tsuda², Seichiro Watanabe³, Masanao Abe², Tatsuaki Okada², Toru Yada²

¹*The Pheasant Memorial Laboratory, Inst. for Planetary Materials, Okayama Univ. at Misasa, Tottori 682-0193, Japan.*

²*Inst. Space Astronaut. Sci., Japan Aerosp. Explor. Agency (JAXA), Kanagawa 252-5210, Japan*

³*Dept Earth Planet. Sci., Grad. Sch. Sci., Nagoya Univ., Nagoya 464-8601, Japan.*

Sample return missions represent great opportunities to study materials from known locations. The Hayabusa mission returned material to Earth from the asteroid Itokawa in 2010 and revealed through geochemistry and micro-petrography that it is genetically related to ordinary chondrite meteorites and the surface of the modern-day asteroid is being actively bombarded by hyper-velocity small particles (e.g., Kawaguchi *et al.*, 2003; Nakamura *et al.*, 2012). The Hayabusa2 mission returned material to Earth from Ryugu on 6th of December, 2020 (Tsuda *et al.*, 2020). Based on the very low geometric albedo indicated by remote observations (Sugita *et al.*, 2019; Kitazato *et al.*, 2019), abundant organic matter on Ryugu, compared to those in carbonaceous chondrites, might be expected (Potyszil *et al.*, 2020). The initial uncontaminated and non-destructive observations for the entire set of returned samples in the Phase-1 Curation at JAXA/ISAS (Yada *et al.*, 2021) demonstrated that Hayabusa2 retrieved the representative and unprocessed (albeit slightly fragmented) Ryugu sample. The data further expanded on the indications from the remote sensing observations that Ryugu is dominated by hydrous carbonaceous chondrite-like materials, similar to CI chondrites, but with an optically darker, more porous, and more fragile nature.

In order to analyze both organic and inorganic matter, the pieces of Ryugu were subject to in-depth investigations in the Pheasant Memorial Laboratory (PML), Okayama University at Misasa. The 16 particles of Ryugu sample (A0022, A0033, A0035, A0048, A0073, A0078, and A0085 from the natural surface of the equatorial region of Ryugu, and C0008, C0019, C0027, C0039, C0047, C0053, C0079, C0081, and C0082 from the surrounding site of the artificial impact crater on Ryugu; total ~55 mg) were selected during the Phase-1 Curation. The selected samples were then transferred to the ultimate clean room in the PML for Phase-2 Curation, to catalog the samples via a comprehensive analytical strategy.

The particles were first characterized under digital optical microscope and then their volume and mass were measured to determine their densities. The average density was $1530 \pm 250 \text{ kg m}^{-3}$, which was systematically larger than the value reported in Yada *et al.* (2021). To elucidate the systematic differences among the 16 pieces, both plainer surfaces and powder were created from each piece using an ultra-microtome equipped with a diamond knife. The surface was observed using optical microscope and SEM, the major element distribution and mineral phases were determined by EDS installed in SEM, micro-Raman spectroscopy, micro-XRD and TEM, all without coating. Subsequently, major and trace element compositions were determined from a given powder by ICP-MS. Element and isotope compositions of H, C, N and O were determined by gas-source mass-spectrometry, and those of Ne were determined by laser-heating noble-gas-mass-spectrometry using small broken pieces. Solvent soluble organic matter was extracted from sample powders using various solvents, including water, acetonitrile, ethyl acetate and formic acid. Meanwhile, insoluble organic matter was isolated after solvent extraction and demineralization by HCl, HF and boric acid. After the first-round characterization, the microtomed surfaces were surveyed using micro-Raman spectroscopy, SIMS and desorption electrospray ionization-orbitrap-mass spectrometry (DESI-OT-MS).

The 16 pieces were found to consist of magnetite, carbonate, phosphates, sulfides and minor silicate fragments interfiled by matrix (modal abundance of 86-96%) that was dominated by sub-micron-sized phyllosilicates. Average modal abundances of the aforementioned phases (excluding matrix) were 3.7, 2.4, 0.8, 2.5 and 0.4 %, respectively. The phyllosilicates were mainly composed of the serpentine and smectite groups. As noted by the Phase-1 Curation, the existence of high-temperature nebular products, such as refractory inclusions and chondrules were not found. The magnetite was present as micron-sized euhedral to subhedral grains and sub-micron-sized grains with a framboidal and plaque texture. Non-carbonate carbon-rich phases of several micrometers in size, were discovered embedded in the matrix (modal abundance is ~0.2%). The presence of soluble and insoluble organic matter was confirmed by DESI-OT-MS and FTIR and micro-Raman spectroscopy, respectively. Further characterization of the solvent soluble fraction via HPLC-OT-MS and GC-MS is currently underway. The organic matter is ubiquitous in the matrix according to observations by SIMS and micro-Raman spectroscopy.

The major and trace element compositions and O isotope composition are homogenous, with the major and trace element compositions representing the proto-solar abundance of Lodders (2020). However, a significant variation of H, C, N and Ne isotopic compositions at the sub-mm scale among the particles was found, which suggests that Ryugu has experienced a complex evolutionary history.

In this talk, preliminary results from the Misasa Phase2 Curation team will be presented.

References

- Kawaguchi, J. *et al.*, The MUSES-C mission for the sample and return—its technology development status and readiness, *Acta Astronautica*, 52, 117-123, 2003.
- Kitazato, K., *et al.*, The surface composition of asteroid 162173 Ryugu from Hayabusa2 near-infrared spectroscopy, *Science* 364, 272-275, 2019.
- Lodders, K., Relative Atomic Solar System Abundances, Mass Fractions, and Atomic Masses of the Elements and Their Isotopes, Composition of the Solar Photosphere, and Compositions of the Major Chondritic Meteorite Groups. *Space Science Reviews*, 217, 1-33, 2021.
- Nakamura, E. *et al.*, Space environment of an asteroid preserved on micrograins returned by the Hayabusa spacecraft, *Proceedings of the National Academy of Sciences of the United States of America*, 109, E624-E629, 2012.
- Potyszil, K. *et al.*, The Albedo of Ryugu: Evidence for a High Organic Abundance, as Inferred from the Hayabusa2 Touchdown Maneuver, *Astrobiology*, 20, 916-921, 2020.
- Sugita, S. *et al.*, The geomorphology, color, and thermal properties of Ryugu: implications for parent-body processes, *Science* 364, eaaw0422, 2019.
- Tsuda, Y. *et al.*, Hayabusa2 mission status: landing, roving and cratering on asteroid Ryugu, *Acta Astronautica* 171, 2-54, 2020.
- Yada, T. *et al.*, Ryugu: A brand-new planetary sample returned from a C-type asteroid, *Nature Astronomy*, in press, 2021.

The C-type asteroid Ryugu: A first detailed look by Phase2 Curation Kochi (Ph2K)

M. Ito¹, N. Tomioka¹, M. Uesugi², A. Yamaguchi³, N. Imae³, N. Shirai⁴, T. Ohigashi⁵, M. Kimura³, M-C. Liu⁶, R.C Greenwood⁷, K. Uesugi², A. Nakato⁸, K. Yogata⁸, H. Yuzawa⁵, Y. Kodama^{9*}, M. Yasutake², R. Findlay⁷, I.A Franchi⁷, J.A. Malley⁷, K. Hirahara¹⁰, A. Tsuchiyama¹¹, A. Takeuchi², I. Sakurai¹², I. Okada¹², Y. Karouji¹³, T. Yada⁸, M. Abe⁸, T. Usui⁸, S. Watanabe¹², and Y. Tsuda⁸.

¹JAMSTEC Kochi, ²JASRI/SPring-8, ³NIPR, ⁴Tokyo Met. Univ., ⁵UVSOR/IMS, ⁶UCLA, ⁷Open Univ., ⁸JAXA/ISAS, ⁹MWJ, ¹⁰Osaka Univ., ¹¹Ritsumeikan Univ., ¹²Nagoya Univ., ¹³JAXA/JSEC, *Toyo Corp.

The Hayabusa2 spacecraft successfully returned to Earth surface materials from the C-type asteroid 162173 Ryugu on December 6th 2020. The sample capsule contained a large number of small grains (a few to several mm in size), collected from touchdown sites 1 and 2 on Ryugu, with a total mass of ~5.4 g [1, 2]. After initial characterization of the grains by JAXA curation (e.g., size, weight, FTIR and MicrOMEGA spectroscopic survey), we received eight grains (four from Room A and four from Room C) on June 17, 2021 (Figure 1 and Table 1). Detailed study of the materials returned from Ryugu will provide critical information about the origin and early evolution of the Solar System and in particular, the nature of the asteroid-meteorite connection, water-rock interactions on asteroids, the evolution of organics on small bodies, the diversity and history of asteroid families in the main belt.

On June 19, 2021, we started initial characterization studies of all our samples using synchrotron radiation-based CT and XRD at the SPring-8. An air-tight sealed carbon nano-tube sample holder was used for CT analysis. In order to avoid degradation and contamination due to interaction with the terrestrial atmosphere (water vapor and oxygen gas) [3], all of the sample preparation (chipping by a chisel, cutting by a counter balanced diamond wire saw, and epoxy mount preparation) was conducted in a glove box in an atmosphere of pure, dry N₂ (Dew point: -80 to -60°C, O₂ ~50 to 100 ppm). Once we had acquired high-resolution, detailed three-dimensional structural and crystallographic information (0.85 μm/pixel for CT) for each of our samples, we were able to define a priority list for the next phase of the analytical campaign, which involved coordinated micro and bulk analysis.

The micro-analysis plan proposed by Ph2K involves the use of a wide range of multi-beam instruments to acquire detailed micro-textural and chemical information about the samples at a sub-micrometer scale. Ongoing studies have involved the use of FIB, STXM-NEXAFS, NanoSIMS and TEM [4]. In parallel, we are conducting bulk analysis of the samples using SEM-EDS, EPMA, Raman spectroscopy, XRD, large geometry type SIMS, high precision O isotopic analysis by laser fluorination and INAA. We have used air-tight containers (a facility-to-facility transfer container, FFTC [4]) for sample transportation to nation-wide institutes by hand carry. With the assistance UK embassy in Tokyo, a few representative grains were delivered to the Open University without any potentially invasive inspection (i.e., X-ray).

In this talk, we will present the preliminary results of the Ph2K coordinated micro-analysis and systematic bulk chemical analysis campaign, which is focused on providing a detailed understanding of these precious Ryugu returned samples.

References: [1] Morota T. et al. 2020. *Science* 368, 654–659. [2] Yada et al. 2021. Abstract#2008, 52nd LPSC. [3] Uesugi M. et al. 2020. *Rev. Sci. Instrum.* 91, 035107. [4] Ito M. et al., 2020. *Earth, Planets and Space* 72, 133.

Figure 1. Largest Ryugu sample (A0002) for the Phase 2 curation Kochi. (a) optical and (b) 3D-reconstruct images

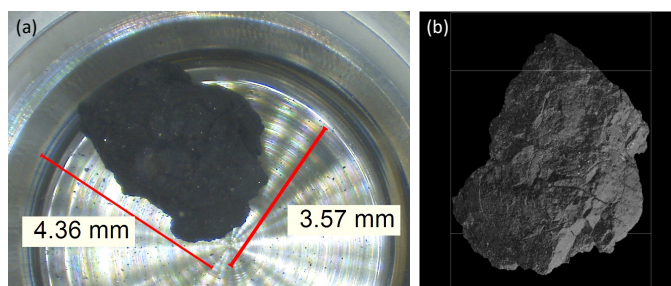


Table 1. The Ryugu samples for the Phase2 curation Kochi

Sample No.	mg	μm	SPring-8	Microanalysis (STXM, NanoSIMS, TEM)	Bulk Analysis (SEM-EDS, EPMA, Raman)	High Precision O isotopes	SIMS	INAA	XRD
A0002	19.3	4,092	HR-CT, XRD, XRD-CT	Y				Y	
A0029	9.1	3,069	HR-CT, XRD, XRD-CT	Y	Y			Y	Y
A0037	7.8	3,129	HR-CT, XRD, Phase-contrast CT	Y	Y		Y	Y	Y
A0098	1.9	1,868	HR-CT			Y		Y	
C0009	11.1	3,520	HR-CT, XRD, XRD-CT	Y	Y		Y		
C0014	6.8	3,527	HR-CT		Y	Y			
C0068	1.68	1,980	HR-CT	Y	Y	Y		Y	
C0087	2	3,242	HR-CT			Y			Y

JAXA Detailed Description -Variation of surface characteristics of Ryugu returned samples-

Aiko Nakato¹, Toru Yada¹, Kasumi Yogata¹, Akiko Miyazaki¹, Kentaro Hatakeda^{1,2}, Kazuya Kumagai^{1,2}, Masahiro Nishimura¹, Yuya Hitomi^{1,2}, Hiromichi Soejima^{1,2}, Kana Nagashima¹, Jean-Pierre Bibring³, Cedric Pilorget³, Vincent Hamm³, Rosario Brunetto³, Lucie Riu³, Lionel Lourit³, Damien Loizeau³, Tania Le Pivert-Jolivet³, Guillaume Lequertier³, Aurelie Moussi-Soffys⁴, Masanao Abe¹, Tatsuaki Okada¹ and Tomohiro Usui¹

¹*Institute of Space and Astronautical Science, Japan Aerospace Exploration Agency*, ²*Marine Works Japan, Ltd.*, ³*Institut d'Astrophysique Spatiale, Université Paris-Saclay, CNRS*, ⁴*Centre National d'Etudes Spatiales*

The Ryugu sample brought back by the Hayabusa2 spacecraft in December 2020 weighed ~5.4 g, which is much larger than we expected [1, 2]. After the samples were delivered to JAXA Extraterrestrial Curation Center, individual grains have been picked up and stored into sapphire dish, and analyzed by optical microscope, weighting, FTIR spectroscopy, and MicrOmega hyperspectral imaging [3] for initial description [2]. The obtained data will open in early 2022 for International Announcement of Opportunity (AO) through curatorial Database System for Ryugu Sample [4]. During the first 6 months, we observed 205 individual grains, 100 from chamber A and 105 from chamber C. There are some unique characteristic features on the surface. Here, we propose a morphological classification of these surface features into 4 groups, based on visible characteristics of Ryugu samples. 1/ Dark and fluffy: these features are dominant in Ryugu samples; 2/ Dark and glossy: they are present either on a part or on the entire of grain; 3/ Bright: also present either on a part or on the entire of grain; 4/ White regions: they are observed over 300 µm in size. Those characteristics may be observed alone or in duplicate on a single grain.

In July 2021, 4 grains showing those different features, were allocated as JAXA detailed description (JAXA-DD) (Fig.1). We conduct petrological and mineralogical observation by SEM and XRD to understand the linkage with surface characteristics obtained by the initial description. The purpose of this study is to contribute to the sample selection by researchers at Int'l AO.

FE-SEM/EDS observation was performed using Hitachi SU6600 equipped with slow purge system in order to non-air-exposure transportation from glove box to SEM, on the front surface where the main initial description was made. For two grains A0017 and C0094, where the entire front surface shows unique characteristics, SEM observation was also performed on the back surface. After these observations, we performed a sample chipping under pure N₂ atmosphere inside Glove Box. A specially developed tantalum chisel is used for the division. Since tantalum is also used as a bullet when collecting samples on the asteroid, it was selected as materials for the purpose of unifying the potential sources of sample contamination. From the divided sample, we separated small portions showing each of the four characteristics and we performed additional SEM observations. We handled the samples under non-air-exposure environment until the sample division. The small portions are attached to carbon fiber with glue for future XRD analysis using RIGAKU RA-Micro7 HFMR.

In this presentation, we will introduce the variations of Ryugu sample surface characteristics, reflecting variations of their mineralogy and petrography, coordinated with JAXA initial description.



Figure 1. Optical microscopic images of 4 grains allocated to JAXA-DD.

- a) A0042 : Dark and fluffy feature is dominant in Ryugu samples. b) C0094: Dark and glossy characteristic is appeared on entire surface. c) A0017: Bright area cover most of the front surface. d) C0041: White region is shown at the right bottom and left top of grain.

References: [1] Tachibana S. et al. (2021) LPS, XXXXXII, Abstract #1289. [2] Yada T. et al. (2021) LPS, XXXXXII, Abstract #2008. [3] Bibring J.-P. et al (2017) Space Sci. Rev. 208, 401-412. [4] Nishimura M. et al. (2021), Astromaterials Data Management in the Era of Sample-Return Missions Community Workshop, Abstract.

Overview of the features of returned samples from the C-type asteroid 162173 Ryugu based on optical microscope observations and their weights

A. Miyazaki¹, T. Yada¹, M. Abe^{1,2}, A. Nakato¹, K. Yogata¹, K. Nagashima¹,
K. Hatakeda^{1,4}, K. Kumagai^{1,4}, M. Nishimura¹, Y. Hitomi^{1,4}, H. Soejima^{1,4}, M. Yoshitake¹, A. Iwamae^{1,4},
S. Furuya^{1,3}, K. Sakamoto¹, T. Okada^{1,3}, S. Tachibana^{1,3}, H. Yurimoto^{1,5}, T. Usui¹

¹*Institute of Space and Astronautical Science, Japan Aerospace Exploration Agency,*

²*The Graduate University for Advanced Studies (SOKENDAI),* ³*University of Tokyo,*

⁴*Marine Works Japan, Ltd.,* ⁵*Hokkaido University.*

Hayabusa2 collected the surface and sub-surface material from the C-type near-Earth asteroid 162173 Ryugu and brought back 5.4 g of samples in total to the Earth [1]. The samples were collected during the two touch-down operations: the samples collected for the first touch-down (TD1) were stored in the Chamber A of the sample catcher, and those collected for the second touch-down (TD2), which was done near the artificial crater made by the SCI [2], were stored in the Chamber C [3]. In the clean chamber dedicated to Hayabusa2 samples [4], the samples in the Chambers A and C were first put in individual sapphire containers for the initial characterization of bulk properties. The samples were first observed with an optical microscope and it was found that the samples from both chambers were aggregation of black-colored mm-sized pebbles and sub-mm sized fine powder, with millimeter-scale particles being the most common [5]. A few centimeter-sized pebbles were also found in the samples recovered from the Chamber C [1]. Then, weight analysis, optical spectroscopy and visual multispectral imaging were performed for the initial characterization. We will present here the features of the individual returned samples based on the microscopic observations and weight analyses.

Pebbles of 1–10 mm in size were removed from the sapphire containers to individual small sapphire dishes. For the first six months after the sample receipt, 100 pebbles from the Chamber A and 105 from the Chamber C were hand-picked one-by-one with vacuum tweezers in the clean chamber under ultra-purified nitrogen atmosphere without exposing to terrestrial atmosphere [6]. The samples in the sapphire dishes are first photographed with an optical stereomicroscope equipped above the clean chamber through a glass window. The size of the individual samples is measured from the microscopic images. Then, the gross weight of the sample and the sapphire dish in the stainless steel capsule was measured with a microbalance equipped in the CC. The weight of an individual sample inside the dish is calculated based on the gross weight of the dish in the stainless steel capsule which was measured in advance.

The preliminary results were reported in [3] and [5]. The observed Ryugu samples have dark spectral features. Many bright and patchy fine inclusions are observed on the surface of some pebbles, but no apparent high temperature components like chondrules nor Calcium-Aluminum-rich-Inclusions (CAI) has been observed with optical microscope analyses [5]. These pebbles show significant morphological variations; grains with rugged surface and with smooth surfaces are observed [3]. These two types of features were also found on the surface textures on Ryugu boulders [7]. Many pebbles are also found to feature curved and straight cracks and some pebbles show elongated block-like morphologies [3]. Densities of individual grains are estimated from the grain weight and the volume of approximated spheroid evaluated from the optical observation, leading to the average density of $1282 \pm 231 \text{ kg m}^{-3}$. This density is much lower than the typical grain density of CI chondrites [5]. We will present more detailed features of the returned individual samples.

References

[1] Yada T et al., 2021. 52nd LPSC, abstract#2008. [2] Arakawa M. et al. 2020, Science 368:67. [3] Tachibana S. et al. Submitted to Science. [4] Abe M. et al., 2021. This meeting. [5] Yada T. et al. Submitted to Nature Astronomy. [6] Yada T. et al., 2014. Meteoritics Planet. Sci. 49:135. [7] Cho Y. et al., Submitted to Planet. Space Sci.

Initial description of Ryugu returned samples: characteristics of individual grains by FT-IR analysis

Kentaro Hatakeda^{1,4}, Toru Yada¹, Masanao Abe^{1,2}, Tatsuaki Okada^{1,3}, Aiko Nakato¹, Kasumi Yogata¹, Akiko Miyazaki¹, Kazuya Kumagai^{1,4}, Masahiro Nishimura¹, Yuya Hitomi^{1,4}, Hiromichi Soejima^{1,4}, Kana Nagashima¹, Miwa Yoshitake¹, Ayako Iwamae^{1,4}, Shizuho Furuya^{1,3}, Tomohiro Usui¹, Shogo Tachibana^{1,3}, Kanako Sakamoto¹, Kohei Kitazato⁵, Hisayoshi Yurimoto⁶

¹*Institute of Space and Astronautical Science, Japan Aerospace Exploration Agency, Sagamihara 252-5210, Japan,*

²*The Graduate University for Advanced Studies (SOKENDAI), Hayama 240-0193, Japan*

³*University of Tokyo, Bunkyo, Tokyo 113-0033, Japan,*

⁴*Marine Works Japan, Ltd., Yokosuka 237-0063, Japan,*

⁵*The University of Aizu, Aizu-Wakamatsu 965-8580, Japan,*

⁶*Hokkaido University, Sapporo 060-0810, Japan.*

A total of ~5.4 g of sample was collected at the surface of the C-type asteroid 162173 Ryugu and successfully returned to Earth [1] [2]. The collected samples were transported to the curation facility in ISAS, Sagamihara, Japan, and stored in purified nitrogen condition, except for a few grains picked up under vacuum condition, to keep the samples as physically and chemically pristine as possible. Approximately 100 grains have been picked up from each of those in Chamber A, uppermost centimeter-scale layer of Ryugu collected during the first touch-down sampling (TD1), and in Chamber C, surface to subsurface layer (~1 m) of Ryugu collected close to the artificial crater during the second touch-down sampling (TD2). Then, initial descriptions, such as weighing, optical imaging, FT-IR spectroscopy in 1-5 μm range, MicrOmega as a hyperspectral NIR microscope, and visual multispectral imaging, have been performed for characterization of these samples. Here we present the preliminary result of FT-IR spectral analysis for individual grains.

The measurement system consists of the spectrometric unit outside the clean chamber and the sample chamber connected to the clean chamber (Figure 1). Although purified nitrogen gas flowed inside the spectrometric unit, absorption bands of O-H (e.g., H_2O) and that of C-O (CO_2) appeared in the reflectance spectra of reference material (Infragold) measured after the sample analysis, indicating the influence of spectral absorption in the atmosphere. In addition, the spot size of the incident beam, approx. 1 mm in diameter at the focal position, was slightly larger than the sizes of individual grains in many cases, and these data were contaminated by the reflectance from the sapphire dish at the bottom of the sample holder. The reflection from the sapphire dish increased the albedo, changed the spectral slope between 1 and 2.5 μm from positive to negative, and decreased the absorption band depth (Figure 2).

Except for the samples with significant effect of sapphire dish, reflectance spectra of individual grains generally show a similar trend to those of bulk samples [3] in the wavelength range between 2.5 and 4 μm . The depth of absorption bands varied between grains, and the band-depth variation is observed not only between the individual grains but also within the single grain. We also found grains with unique spectral profiles, of which abundance is ~1% or less. These grains basically contain relatively large inclusions, which are apparently different from the surrounding matrix.

We are now planning to modify the FT-IR system to extend to the mid to far-infrared wavelength range, and expect to get further information on the collected Ryugu samples.

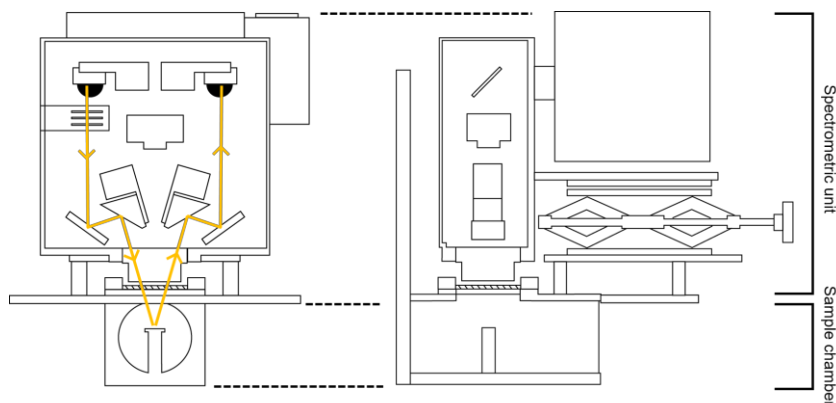


Figure 1. Overview of the FT-IR measurement system

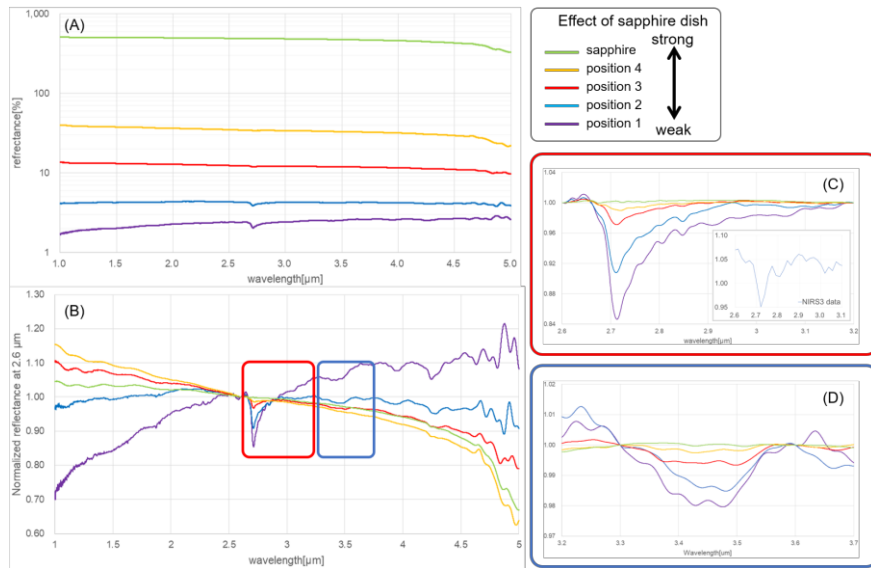


Figure 2. The mixing effect of the sapphire dish reflectance. The larger effect was observed with increasing the area where incident beam illuminated the sapphire dish; A) Reflectance spectra (%), B) Normalized reflectance at 2.6 μm, C) Normalized reflectance with continuum at 2.6-3.2 μm and NIRS3 spectral data [4], D) Normalized reflectance with continuum at 3.3-3.6 μm.

References

- [1] Tachibana S. et al. (2021) LPS, XXXXXII, Abstract #1289. [2] Yada T. et al. (2021) LPS, XXXXXII, Abstract #2008. [3] Yada T. et al. in press. Nature Astronomy. [4] Kitazato et al. (2019) Science **364**: 272.

MicrOmega detections of C-rich phases in Ryugu returned samples within the Hayabusa2 JAXA Extraterrestrial Curation Center

Bibring¹, J.-P.; Brunetto¹, R.; Carter¹, J.; Gondet¹, B.; Pilorget¹, C.; Hamm¹, V.; Hatakeda², K.; Langevin¹, Y.; Lantz¹, C., Le Pivert-Jolivet¹, T.; Loizeau¹, D.; Nakato², A.; Okada², T.; Riu^{1,2}, L.; Usui², T.; Yada², T.; Yogata², K., ¹*Institut d'Astrophysique Spatiale, Université Paris-Saclay, CNRS*, ²*Institute of Space and Astronautical Science, Japan Aerospace Exploration Agency*

The Ryugu samples brought back by the Hayabusa2 spacecraft in December 2020 have been delivered to the JAXA Extraterrestrial Curation Center [1, 2]. Bulk samples and then individual grains have been deposited onto sapphire dishes, weighted, and analyzed with optical microscopy, FTIR spectroscopy, and MicrOmega hyperspectral imaging [3] for initial description [2]. The MicrOmega instrument used in the JAXA Extraterrestrial Curation Center is a NIR hyperspectral microscope. It images samples ~ 5 mm x 5 mm large, with 250x256 pixels of ~22 μm in size. Its spectral capability covers the range from 0.98 μm to ~3.6 μm , which gives access to primary and secondary minerals and organic matter, in particular through their OH, CO₃, and CH features [4, 5].

As presented in the Yada et al. and Pilorget et al. talks (this conference), the averaged spectra of Ryugu returned samples present two major features, centered around 2.7 and 3.4 μm , attributed to OH-rich and CH-rich compounds respectively. Thanks to the MicrOmega capability to characterize the spectral signatures of returned grains down to the few tens of μm scale, a variety of C-rich compositions do show up, through the following features:

- variability in the central position and shape of the 3.4 μm dominant absorption, with a minimum varying from 3.35 μm to 3.45 μm , and the occasional presence of several local minima with varying spectral band areas. These observations suggest organic matter of varying composition and structure is present over the entire samples;
- the presence of coupled spectral features such as at around 2.85 μm , 3.1 μm or 3.55 μm , with their associated band ratios. Additional spectral structures < 2.7 μm are in some cases observed and correlate with them. These bands collectively suggest organic carbon is at times bound to non-C groups or intimately mixed with specific minerals.
- the ratio between the 2.7 μm and 3.4 μm band depths spans a very wide range of values, with some grains highly depleted in either OH-rich or CH-rich phases.

These spectral features are diagnostic of specific C-rich compositions and of their spatial heterogeneity in the collected samples at the scale of few tens to few hundred microns. We shall present a preliminary review of the observed diversity, and discuss it in terms of the composition and origin of the potential carriers.

References

- [1] Tachibana S. et al. (2021) LPS, XXXXXII, Abstract #1289. [2] Yada T. et al. (2021) LPS, XXXXXII, Abstract #2008. [3] Bibring J.-P. et al (2017) Space Sci. Rev. 208, 401-412. [4] Pilorget C. and Bibring J.-P. (2014) PSS 99, 7-18. [5] Pilorget C. et al. (2021) this conference.

MicrOmega detections of carbonates in Ryugu returned samples within the Hayabusa 2 JAXA Extraterrestrial Curation Center

Loizeau, D.¹; Bibring, J.-P.¹; Brunetto, R.¹; Pilorget, C.¹; Okada, T.^{2,3}; Carter, J.¹; Gondet, B.¹; Hamm, V.¹; Hatakeda, K.^{2,4}; Langevin, Y.¹; Lantz, C.¹; Le Pivert-Jolivet, T.¹; Nakato, A.²; Riu, L.²; Usui, T.^{2,3}; Yada, T.²; and Yogata, K.²;

¹*Institut d'Astrophysique Spatiale, Université Paris-Saclay, CNRS, France*

²*Institute of Space and Astronautical Science, Japan Aerospace Exploration Agency, Japan* ³*University of Tokyo, Bunkyo, Japan,* ⁴*Marine Works Japan, Ltd., Japan*

The Ryugu samples brought back by the Hayabusa2 spacecraft in December 2020 have been delivered to the JAXA Extraterrestrial Curation Center [1, 2]. Bulk samples and then individual grains have been picked up and stored into sapphire dishes, weighted, and analyzed with an optical microscope, FTIR spectroscopy, and MicrOmega hyperspectral imaging [3] for initial description [2]. The MicrOmega instrument used in the JAXA Extraterrestrial Curation Center is a NIR hyperspectral microscope. It has a total field of view of 5 mm x 5 mm, with resolution of ~22 $\mu\text{m}/\text{pixel}$ in the focal plane. It covers the spectral domain from 0.99 μm to ~3.6 μm . Its capabilities enable the identification of organic matter and of different minerals in the returned samples [4]. Initial analyses with MicrOmega were first made on the bulk samples from chambers A and C of the Hayabusa 2 returned capsule, and then on individual grains stored in their sapphire dishes. 137 out of the 205 extracted grains have been analyzed with MicrOmega as of September 30, 2021 [5].

In the spectral domain of MicrOmega, carbonates have a strong characteristic double absorption band in the 3.3-3.5 μm area, accompanied by two other weaker bands around 2.5 and 2.3 μm . The exact spectral position of these bands varies with the cation content of the carbonate [6]. Iron-bearing carbonates also show a strong absorption below 1.5 μm .

First detections of carbonates were made in grains included in the bulk samples from both chambers A and C. Some small grains seem to be entirely carbonate-rich and are up to ~450 μm , down to <50 μm in size. Carbonate inclusions were also detected in larger grains, with sizes up to ~380 μm in a >1.5 mm-sized grain, and down to <50 μm (figure 1-A).

From the first 130 analyzed extracted grains, MicrOmega detected carbonate inclusions with high confidence in 19 of those grains. The largest detection was made on grain C0041, covering ~0.25 mm, or ~10% of the visible surface of the grain (figure 1-B). This grain is one of the grains with "White regions" as described in Nakato et al. [7].

In terms of spectral characteristics, they all present a double band at 3.31-3.47 μm and a band centered at 2.71 μm . The largest grains and inclusions also exhibit spectral bands at 2.51 and 2.30 μm , also characteristic of carbonates, and a deep absorption below 1.5 μm . Some detections also have a band at 2.77 μm (present in many carbonate reference spectra), and some between 3.07 and 3.10 μm . The presence of a strong absorption below 1.5 μm indicates the likely presence of Fe^{2+} in the carbonate mineral, although the position of the bands around 2.3, 2.5 and 3.4 μm is shifted to shorter wavelength compared to a purely Fe^{2+} carbonate (siderite), and would better fit Mg-bearing carbonates like dolomite or magnesite. The iron-bearing magnesite breunnerite is a likely candidate for these detections. Smaller grains and inclusions do not show the absorption below 1.5 μm , while the other absorptions are centered around the same positions than for the larger grains (figure 1-C). Likely candidates include dolomite and magnesite.

Such carbonate grains and inclusions within the returned samples from Ryugu are a key to understand the evolution of the asteroid. MicrOmega can help mapping and quantifying the presence of these carbonates throughout the collection.

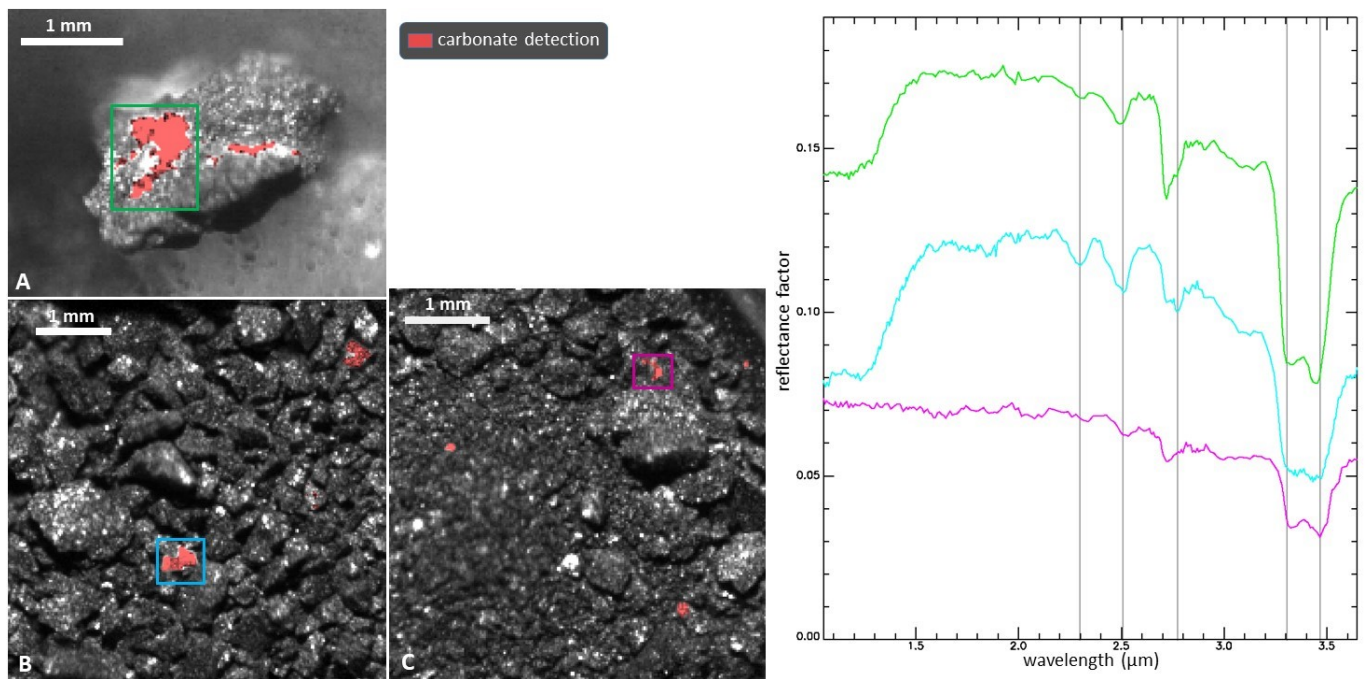


Figure 1. Example of carbonate detections with MicrOmega on bulks from chamber A and C, and on an extracted grain from chamber C. Left: MicrOmega images with red pixels where carbonate is detected. A: extracted grain C0041. B: bulk samples from chamber A. C: bulk samples from chamber C. Right: Average spectra of pixels with carbonate detections within the colored boxes in the left images.

References

- [1] Tachibana S. et al. (2021) LPS, XXXXXII, Abstract #1289. [2] Yada T. et al. (2021) LPS, XXXXXII, Abstract #2008. [3] Bibring J.-P. et al (2017) Space Sci. Rev. 208, 401-412. [4] Pilonget C. and Bibring J.-P. (2014) PSS 99, 7-18. [5] Pilonget C. et al. (2021) this conference. [6] Hunt G.R. and Salisbury J.W. (1971) Visible and near infrared spectra of minerals and rocks. II. Carbonates. Modern Geology 2, 23–30. [7] Nakato A. et al. (2021) this conference.

The 2.7 μ m OH band in different grains of Ryugu from the two collection sites, as seen by MicrOmega in the Hayabusa2 Curation Facility

Tania Le Pivert-Jolivet¹, Jean-Pierre Bibring¹, Rosario Brunetto¹, Cedric Pilorget¹, Tatsuaki Okada², John Carter¹, Brigitte Gondet¹, Vincent Hamm¹, Kentaro Hatakeda^{2,3}, Yves Langevin¹, Cateline Lantz¹, Damien Loizeau¹, Aiko Nakato², Lucie Riu^{1,2}, Tomohiro Usui², Toru Yada² and Kasumi Yogata²

¹IAS, Université Paris-Saclay, CNRS, France, ²Institute of Space and Astronautical Science, Japan Aerospace Exploration Agency, ³Marine Works Japan, Ltd

Hayabusa2 is the first space mission to study and collect samples from a C-type asteroid. In December 2020, the spacecraft brought back to Earth ~5.4g of materials from the surface of asteroid (162173) Ryugu. The samples were collected from two different sites TD1 and TD2 [1] at the surface of the asteroid, possibly sampling surface and subsurface materials. The samples were delivered to JAXA (Japan Aerospace eXploration Agency) Extraterrestrial Curation Center for preliminary analyses. Individual grains were extracted and analyzed in a controlled N₂ environment by an optical microscope, a FTIR microscope and MicrOmega, a near-infrared (0.99-3.65 μ m) hyperspectral microscope. MicrOmega acquires images of 256x250 pixels with a spatial resolution of 22.5 μ m. The total field of view covers ~5x5mm [2].

In addition to the bulk samples, observations of individual grains, extracted from the bulks, were performed with MicrOmega at different azimuth angles to optimize the coverage and avoid potential photometric biases. In order to extract average spectra of the individual grains (typical size 1-4.5 mm), we developed a novel procedure using thermal emission maps measured by MicrOmega: first the grains were isolated from the rest of the field of view (the sample holder) thanks to their difference in terms of thermal emission, then their pixels were averaged at each azimuth orientation. Spectral parameters were finally calculated to characterize the position and the depth of the 2.7 μ m OH feature. This band is believed to be related to the presence of metal-OH stretching modes in phyllosilicates [3], and it is observed at large scale over the surface of Ryugu [4].

We shall present the distribution of the spectral parameters of the 2.7 μ m feature observed by MicrOmega on grains extracted from chamber A and chamber C, corresponding to TD1 and TD2 respectively. We will discuss the potential variations of the spectral parameters, in particular with regards to the observations performed at a much larger scale by NIRS3, and their possible implications regarding the hydrothermal and space weathering history of the asteroid.

References

[1] Tachibana et al. (2020) LPS XXXXXI Abstract #2027. [2] Bibring et al. (2017) Space Sci. Rev. 208, 401-412. [3] Madejová et al. (2017) Developments in Clay Science, 8, 107-149. [4] Kitazato et al. (2019) Science, 364, 272-275

Microscale Diversity of H, C, and N Isotopes in Asteroid Ryugu

Larry R. Nittler¹, Jens Barosch¹, Bradley T. De Gregorio², Rhonda M. Stroud², Hikaru Yabuta³, and The Hayabusa2-initial-analysis IOM team, Hisayoshi Yurimoto⁴, Tomoki Nakamura⁵, Takaaki Noguchi⁶, Ryuji Okazaki⁷, Hiroshi Naraoka⁷, Kanako Sakamoto⁸, Shogo Tachibana^{8,9}, Sei-ichiro Watanabe¹⁰ and Yuichi Tsuda⁸

¹*Carnegie Institution of Washington, Washington DC, USA*, ²*US Naval Research Laboratory, Washington DC, USA*, ³*Hiroshima Univ.*, ⁴*Hokkaido Univ.*, ⁵*Tohoku Univ.*, ⁶*Kyoto Univ.*, ⁷*Kyushu Univ.*, ⁸*JAXA*, ⁹*Univ. of Tokyo*, ¹⁰*Nagoya Univ.*

Understanding the nature and origin of organic matter in asteroid 162173 Ryugu is one of the key science goals of the Hayabusa2 sample-return mission. Macromolecular organic matter (MOM) makes up to a few % of primitive meteorites and displays a wide range of H, C, and N isotopic ratios on whole-rock to sub- μm scales [1]. Both its origin (for example, whether in the protosolar molecular cloud or in the protoplanetary disk) and the degree to which it is modified on asteroidal parent bodies is debated, but it may represent the dominant form of C delivered to early Earth. NanoSIMS-based isotopic imaging surveys of both bulk CI, CR, CM, and CO chondrites and purified MOM residues from them [2-6] have revealed that, while bulk samples are typically modestly enriched in D and ¹⁵N, relative to the Earth, a small fraction of the material shows much more extreme enrichments and/or depletions in these isotopes. Large ¹³C enrichments and depletions are also seen in chondrites, both in presolar circumstellar SiC and graphite grains [7], and in rare cases in MOM particles [8].

We have begun conducting similar NanoSIMS surveys of Ryugu samples. Four grains from Chamber A aggregates (A0108) were embedded in S and sectioned with an ultramicrotome equipped with a diamond knife. Relatively thick (250-nm) slices were deposited onto Si wafers for NanoSIMS analysis while adjacent thin sections were kept for coordinated analysis by transmission electron microscopy (TEM) and synchrotron X-ray microscopy (STXM). After the S was sublimated, we applied a thin Au coat to the Si wafers and analyzed them with a NanoSIMS 50L ion microprobe in multicollection imaging mode. Microtome sections were first analyzed for C and N isotopes (as ¹²C₂, ¹²C¹³C, ¹²C¹⁴N, and ¹²C¹⁵N, plus ¹⁶O, ²⁸Si, MgO and secondary electrons) with a 0.4 pA, <200-nm Cs⁺ beam. The sections were then re-analyzed at the same magnification with a 1-pA beam and collection of ¹H, D, and ¹²C secondary ions and secondary electrons. Five of the sections were subsequently re-measured for C and N to improve the counting statistics. Total counting times varied but were typically of order $\sim 0.1 \text{ s}/0.01 \mu\text{m}^2$ for each run.

The measurements reveal broadly similar results to similar data obtained on primitive carbonaceous chondrites. The four particles show modest bulk enrichments of D and ¹⁵N, with D/H and ¹⁵N/¹⁴N ratios in general agreement with those of CI chondrites. The NanoSIMS images show that much of the C is present as particles typically a few hundred nm in size, but ranging up to 2 μm . As in chondrites, a fraction of these particles show more extreme enrichments or depletions (“hotspots” and “coldspots”) which span ranges similar to those recently seen in the least-altered CM chondrites Asuka 12169, Asuka 12236, and Paris [3]. A much smaller fraction of C-rich grains shows ¹³C anomalies, associated both with presolar grains and organic particles. The bulk and microscale isotopic distributions vary to some extent among the four Ryugu grains, indicating heterogeneity at the 100- μm scale. Planned TEM and STXM measurements of slices from the same grains will help unravel the chemical nature of the organic particles and their relationship to inorganic phases in the asteroid.

References

- [1] Alexander C. M. O'D. et al. 2017. *Chemie der Erde - Geochemistry* 77:227. [2] Busemann H. et al. 2006. *Science* 312:727. [3] Nittler L. R. et al. 2021. Abstract #6063. 84th Meteoritical Society Meeting. [4] Remusat L. et al. 2010. *The Astrophysical Journal* 713:1048. [5] Nittler L. R. et al. 2019. *Nature Astronomy* 3:659. [6] Nittler L. R. et al. 2018. *Geochimica et Cosmochimica Acta* 226:107. [7] Zinner E., 1.4 - Presolar grains, in: A.M. Davis (Ed.), *Meteorites and Cosmochemical Processes* (Vol. 1), *Treatise on Geochemistry* (Second Edition, eds: H. D.

Holland and K. K. Turekian), Elsevier-Pergamon, Oxford, 2014, pp. 181–213. [8] Floss C. et al. 2009. *Astrophysical Journal* 697:1242.

Diversity of Insoluble Organic Matter at the Nanoscale in Asteroid Ryugu

Rhonda M. Stroud¹, Bradley T. De Gregorio¹, Larry R. Nittler², Jens Barosch², Hikaru Yabuta³, and The Hayabusa2-initial-analysis IOM team, Hisayoshi Yurimoto⁴, Tomoki Nakamura⁵, Takaaki Noguchi⁶, Ryuji Okazaki⁷, Hiroshi Naraoka⁷, Kanako Sakamoto⁸, Shogo Tachibana^{8,9}, Sei-ichiro Watanabe¹⁰ and Yuichi Tsuda⁸

¹US Naval Research Laboratory, Washington DC, USA, ²Carnegie Institution of Washington, Washington DC, USA, ³Hiroshima Univ., ⁴Hokkaido Univ., ⁵Tohoku Univ., ⁶Kyoto Univ., ⁷Kyushu Univ., ⁸JAXA, ⁹Univ. of Tokyo, ¹⁰Nagoya Univ.

Acid-insoluble, macromolecular organic matter represents up to 4 wt% of the matrix of carbonaceous chondrites (CC). Many properties of the insoluble organic matter (IOM), including microstructure, functional group chemistry, and mineralogical associations strongly correlate with asteroid parent body grouping and alteration history [1]. However, the IOM of many chondrites shows significant variation in structure, chemistry, and isotopic composition at the nanoscale [2,3]. The microstructure of CC IOM ranges from discrete sub-micron blebs called nanoglobules; to micrometer and larger sized veins; diffuse intergranular material; OM intercalated into phyllosilicates, and poorly-graphitized carbonaceous grain coatings. In addition, the IOM can serve as host to inorganic carbonaceous phases, such as presolar nanodiamond [4] and phase-Q [5]. This variation results from a combination of inherited molecular cloud chemistry, nebular processing, parent body and terrestrial alteration. Studies of the nanoscale variation in the IOM in the returned samples of Ryugu provide the first chance to examine the IOM of a CC parent body largely free of terrestrial alteration signatures, in order to better constrain the alteration history of a specific asteroid, and provide unprecedented constraint on the evolution of carbon in the early solar system.

Our primary method for the Initial Analysis of the nanoscale diversity of Ryugu IOM microstructure and functional chemistry is scanning transmission electron microscopy (STEM), in coordination with scanning transmission x-ray absorption spectroscopy (STXM), and isotopic characterization with NanoSIMS. The STEM measurements are carried out with the Nion UltraSTEM 200-X at the Naval Research Lab, operated at 60 kV to minimize electron beam damage. STEM measurements include annular dark field (ADF) imaging, electron energy loss spectroscopy (EELS), and energy dispersive x-ray spectroscopy (EDS). The EELS and EDS data are collected as simultaneous spectrum images to allow direct correlation of the elemental composition with the C functional chemistry, and microstructure [6]. As of this abstract submission, we have examined slices of three grains from Chamber A (A0108), one prepared as a focused ion beam (FIB) lift-out section, and two prepared as sulfur-embedded ultramicrotome slices. The FIB section was analyzed with STXM at Photon Factory BI-19 prior to the STEM analysis. Adjacent microtome slices of were prepared for coordinated STXM and NanoSIMS measurements at the Advanced Light Source and Carnegie Institution of Washington, respectively. Measurements of additional FIB and microtome slices of Chamber A and Chamber C particles are planned.

Overall, our STEM measurements indicate IOM microstructures and functional chemistry consistent with low temperature aqueous alteration, broadly consistent with CI and CM chondrites. Small nanoglobules (< 400 nm) are abundant, but larger nanoglobules > 1000 nm are less common. Diffuse carbon intercalated into phyllosilicates is also common. Carbonate and nanoscale Fe, Ni sulfides are also found in association with IOM. Coordination of the STEM results with the ongoing STXM and NanoSIMS measurements of slices from the same grains will ultimately help constrain the nature of Ryugu and its relationship to known carbonaceous chondrites, and the history of the organic matter it contains.

References

[1] Alexander C. M. O'D. et al. 2017. *Chemie der Erde - Geochemistry* 77:227. [2] De Gregorio B. T. et al. 2013. *Meteoritics & Planetary Science* 48:904. [3] C. Le Guillou et al. 2014. *Geochemica et Cosmochemica Acta* 131: 368. [4] Garvie, L.A.J. (2010), Lunar and Planetary Science Conference, #1388. [5] Amari, S., et al. 2013. *Astrophysical Journal* 778:37. [6] Stroud R. M. et al. *Microscopy and Microanalysis* 27(S1):2546.

Infrared transmission spectra of Ryugu particles and their unique adsorption behavior

Yoko Kebukawa¹, Lydie Bonal², Eric Quirico², Emmanuel Dartois³, Cécile Engrand⁴, Jean Duprat⁵, Jérémie Mathurin⁶, Alexandre Dazzi⁶, Ariane Deniset-Besseau⁶, Hikaru Yabuta⁷ and The Hayabusa2-initial-analysis IOM team, Hisayoshi Yurimoto⁸, Tomoki Nakamura⁹, Takaaki Noguchi¹⁰, Ryuji Okazaki¹¹, Hiroshi Naraoka¹¹, Kanako Sakamoto¹², Shogo Tachibana^{12,13}, Sei-ichiro Watanabe¹⁴ and Yuichi Tsuda¹²

¹*Yokohama National Univ.*, ²*IPAG, Univ. Grenoble Alpes, CNRS CNES* ³*ISOM*, ⁴*IJCLab*, ⁵*IMPMC/MNHN*, ⁶*ICP*, ⁷*Hiroshima Univ.*, ⁸*Hokkaido Univ.*, ⁹*Tohoku Univ.*, ¹⁰*Kyoto Univ.*, ¹¹*Kyushu Univ.*, ¹²*JAXA*, ¹³*Univ. of Tokyo*, ¹⁴*Nagoya Univ.*

The Hayabusa2 spacecraft successfully obtained samples from two different locations from Ryugu, a C-type asteroid, and returned them to the Earth on December 6, 2020. The first touchdown samples and second touchdown samples were separately stored in sample container chamber A and chamber C, respectively. The initial analyses began in June 2021, after curation at ISAS/JAXA. The insoluble organic matter (IOM) subteam has so far conducted in-situ analyses of the Ryugu particles, in order to decipher the nature of the organic matter and its origin, parent body processing, and interaction with water and minerals. Fourier transform infrared (FTIR) spectroscopy is a nondestructive technique for functional group chemistry and structures which is suitable for both organic and inorganic compounds. To date, IR absorption (transmission) spectra have been obtained from various chondrites and other astromaterials such as interplanetary dust particles (IDPs), micrometeorites and cometary dust particles [e.g., 1-7]. IR spectroscopy is often employed for astronomical observations and remote sensing. The reflectance spectra of solar system bodies provide information of the compositions of their surfaces. To compare the laboratory samples and the surfaces of asteroids, IR reflectance spectra have been commonly used [e.g., 8-10]. Both IR transmission and reflectance spectra give intrinsically similar information as both reflect the absorptions of IR frequencies by the target samples, although some differences do exist. As a part of the initial analysis in the IOM team, IR absorption spectra were obtained using FTIR microspectroscopy, to provide initial characterization of the Ryugu particles and search for organic matter, as well as for comparison with the surface reflectance spectra of Ryugu. Several samples were analyzed in parallel in the team, in Japan (Yokohama National Univ., YNU) and in France (IPAG, Grenoble and Orsay-lab teams) to increase the robustness of the analysis.

Each particle (sub-millimeter in diameter) from the aggregates in chamber A (A0108) or chamber C (C0109), was further decomposed by gently crushing between two glass slides, or by separation of a fragment with a scalpel. The small fragments were then further crushed between two diamond windows (YNU and IPAG) and in a diamond compression cell under an optical microscope to optimize the thickness for further atomic force microscope based infrared spectroscopy (AFM-IR) measurements (Orsay-lab). In YNU, IR absorption spectra were collected from each diamond window with a micro-FTIR (JASCO FT/IR-6100+IRT-5200), equipped with a ceramic IR light source, a germanium-coated KBr beam splitter, a mercury-cadmium-telluride (MCT) detector, and $\times 16$ Cassegrain mirrors, with typically $20 \times 20 \mu\text{m}$ aperture. The microscope and the FTIR were continuously purged with dry N_2 . To remove adsorbed water further from the sample, a heating stage (Linkam 10036L) was employed. The IR absorptions from water were satisfactorily removed typically by 60°C under N_2 flow. Micro-FTIR measurements were also conducted at IPAG with a Hyperion 3000 Bruker FTIR microscope, operating with a $\sim 50 \times 50 \mu\text{m}$ spot and an environmental cell placing the sample under secondary vacuum ($< 10^{-6}$ mbar) and gentle heating ($< 80^\circ\text{C}$) to remove adsorbed water. IR spectra by the Orsay-lab team were taken during a week of beamtime at the SOLEIL synchrotron (SMIS beam line). The synchrotron beam was coupled to a Nicolet Continuum 2 IR microscope equipped with a MCT detector and a $\times 32$ Cassegrain optics, under dry air. For these measurements, the IR spot size was optimized with an aperture of $6 \times 6 \mu\text{m}$, close to the diffraction limit, and hyperspectral maps of Ryugu samples were acquired over several hundreds of μm in size.

The IR absorption spectra of both A0108 and C0109 particles were almost identical, and typically consistent with CI chondrites. However, some local heterogeneity exists, e.g., IR spectra from some areas were dominated by carbonate features, and opaque minerals are seen in high resolution hyperspectral maps. They display Mg-rich phyllosilicate bands at $\sim 1000 \text{ cm}^{-1}$ (Si-O stretching) and $\sim 3700 \text{ cm}^{-1}$ (OH group in phyllosilicates), organic bands (aliphatic C-H) at $3000\text{-}2800 \text{ cm}^{-1}$. The position and narrowness of the OH band fit those observed in spectra collected in-situ by the spacecraft [11]. Compared to the reflectance spectra obtained by JAXA curation [12], the OH band and aliphatic C-H bands features in the absorption spectra were roughly consistent, but the abundance of aliphatic C-H peaks were lower than the reflectance spectra. Such differences could be due to the difference between reflectance spectra and transmission spectra of sample particles. Also, interesting behavior was observed during FTIR analysis, in that the aliphatic C-H peak increased during analysis for a few hours, likely due to adsorption of environmental volatile organic compounds (VOCs). It is known that porous OH bearing silicates adsorb

VOCs [e.g., 13-15], particularly when fresh surfaces are exposed by sample crushing [16], however the Ryugu samples appear unusually reactive and absorb VOC very rapidly, considering that the Ryugu sample analysis was conducted in a clean environment without abundant contamination sources. This behavior indicates that Ryugu samples are fresh and highly porous. Measurements conducted under vacuum and gentle heating reveal a rapid and dramatic disappearance of adsorbed water, along with an increase of the aliphatic band intensity. This has been previously observed for CI chondrites [6,17,18], and confirms the high adsorption properties of Ryugu samples. Tight interactions between organics and -OH in phyllosilicates may account for this spectral evolution.

Overall, the FTIR organic signatures of the Ryugu samples do not point to a significant post-accretional heating as observed in heated CM/CI chondrites [19]. Acid extraction of Ryugu samples very soon will provide a fresh IOM isolate, and thereby enable quantitative characterization of chemical group abundances.

References

- [1] Keller L. P. et al. 2004. *Geochimica et Cosmochimica Acta* 68: 2577. [2] Osawa T. et al. 2005. *Meteoritics & Planetary Science* 40: 71-86. [3] Sandford S. A. et al. 2006. *Science* 314: 1720. [4] Beck P. et al. 2014. *Icarus* 229: 263. [5] Dartois E. et al. 2018. *Astronomy & Astrophysics* 609: A65. [6] Battandier M. et al. 2018. *Icarus* 306: 74. [7] Kebukawa Y. et al. 2019. *Meteoritics & Planetary Science* 54: 1632. [8] Cloutis E. A. et al. 2011. *Icarus* 212: 180. [9] Cloutis E. A. et al. 2011. *Icarus* 216: 309. [10] Cloutis E. A. et al. 2012. *Icarus* 217: 389. [11] Kitazato K. et al. 2019. *Science* 364: 272. [12] Yada T. et al. 2021. *Nature Portfolio*, under review. [13] Pires J. et al. 2001. *Microporous and Mesoporous Materials* 43: 277. [14] Li X. et al. 2020. *Separation and Purification Technology* 235: 116213. [15] Zhu L. et al. 2020. *Journal of Hazardous materials* 389: 122102. [16] Kebukawa Y. et al. 2009. *Meteoritics & Planetary Science* 44: 545. [17] Beck P. et al. 2010. *Geochimica et Cosmochimica Acta* 74: 4881. [18] Takir D. et al. 2013. *Meteoritics & Planetary Science* 48: 1618. [19] Nakamura T. et al. 2005. *Journal of Mineralogical and Petrological Sciences* 100: 260.

Thermal history of Ryugu based on Raman characterization of Hayabusa2 samples

Lydie Bonal¹, Eric Quirico¹, Mutsumi Komatsu², Gilles Montagnac³, Hikaru Yabuta⁴ and The Hayabusa2-initial-analysis IOM team, Hisayoshi Yurimoto⁵, Tomoki Nakamura⁶, Takaaki Noguchi⁷, Ryuji Okazaki⁸, Hiroshi Naraoka⁸, Kanako Sakamoto⁹, Shogo Tachibana^{9, 10}, Sei-ichiro Watanabe¹¹ and Yuichi Tsuda⁹

¹*Institut de Planétologie et d'Astrophysique de Grenoble, Université Grenoble Alpes, CNRS CNES, Grenoble, France*

²*SOKENDAI, The Graduate Univ. for Advanced Studies*

³*Laboratoire de géologie de Lyon, CNRS/INSU - ENS de Lyon, Lyon, France*

⁴*Hiroshima Univ.*, ⁵*Hokkaido Univ.*, ⁶*Tohoku Univ.*, ⁷*Kyoto Univ.*, ⁸*Kyushu Univ.*, ⁹*JAXA*, ¹⁰*Univ. of Tokyo*, ¹¹*Nagoya Univ.*

Introduction: The degree of structural order of the polyaromatic carbonaceous matter present in extraterrestrial samples is a tracer of the thermal history they experienced (e.g., primitive chondrites: [1-4]; micrometeorites: [5-6]). To characterize Ryugu's thermal history (long vs. short thermal heating and extent of thermal heating), we thus perform Raman characterization of several Ryugu particles returned by the Hayabusa2 mission. In order to be fully confident in the obtained data and interpretation, Raman characterization was led independently by two groups of persons in Japan and in France on distinct Ryugu particles. The results were subsequently compared.

Samples and methods: Raman point analyses were performed on several fragments of six particles from Chamber A aggregates (A0108) and six particles from Chamber C aggregates (C0109). To be able to combine in situ IR and NanoSIMS measurements on the same samples, fragments of particles were manually selected under a binocular and pressed onto diamond windows. The Raman spectra were acquired with a 532 nm laser in both Japan and France. Because some Raman bands related to carbonaceous matter are dispersive, data for Ryugu particles and comparison samples have been acquired and analyzed consistently in both Japan and in France. In particular, a Renishaw InVia Reflex equipped with a 1800 l/mm grating at Materials Characterization Central Laboratory was used in Waseda University (Japan). The laser was focused at the sample surface through a 50× objective (spot size around 3-4 μm) and its power was set at 0.24 mW and 1 mW. Each acquisition comprised five integrations of 10 s that were averaged to make the final spectrum. In France, Raman measurements were performed at the Ecole Normale Supérieure de Lyon (Laboratoire de Géologie de Lyon—Terre, Planètes, Environnement) using a LabRam Raman spectrometer (Horiba Jobin-Yvon) equipped with a 600 g/mm grating. The laser was focused through a 100× objective to obtain a <2 μm spot size. The power on the sample was 0.3 mW. Each acquisition comprised six integrations of 15 s that were averaged to make the final spectrum.

Results and discussion: More than 200 spectra were acquired on 12 different particles. The Raman data acquired in Japan and in France are fully consistent. Each acquired spectrum is characterized by a high fluorescence background and by the presence of the Raman D- (~ 1350 cm⁻¹) and G-bands (~ 1580 cm⁻¹), related to the presence of polyaromatic carbonaceous matter. The spectral parameters derived from the mathematical fitting of the individual spectra, that is, the band widths (FWHM-D, FWHM-G), the band positions (ω_D , ω_G), and the band intensity ratio (I_D/I_G) are comparable between particles. No systematic differences have been observed to date between the spectral parameters of Chamber A and Chamber C particles. This point will be further investigated on insoluble organic matter isolated by acid treatment of Ryugu samples.

The Ryugu particles contain polyaromatic carbonaceous matter that is poorly structured, as reflected by the high fluorescence background superimposed to wide D- and G-Raman bands, present at relatively low Raman shifts. The comparison of these spectral parameters with similarly characterized chondrites shows that the structural order of the polyaromatic carbonaceous matter present in Ryugu particles is comparable to that in primitive (type 1, type 2) carbonaceous chondrites. Ryugu thus escaped significant degree of long duration radiogenic thermal metamorphism (as typically experienced by type 3 chondrites), as well as short-duration heating as experienced by some type 2 chondrites (e.g., [4]).

References

[1] Bonal et al. 2006. *Geochimica Cosmochimica Acta* 70 :1849. [2] Bonal et al. 2016. *Geochimica Cosmochimica Acta* 189: 312. [3] Busemann et al. 2007. *Meteoritics & Planetary Science* 42: 1387. [4] Quirico et al. 2018. *Geochimica Cosmochimica Acta* 241 : 17 [5] Dobrica et al. 2011. *Meteoritics & Planetary Science* 46 : 1363. [6] Battandier et al. 2018. *Icarus* 306 : 74.

Elemental and isotopic compositions of organic grains from asteroid Ryugu

Laurent Remusat¹, Maximilien Verdier-Paoletti¹, Smail Mostefaoui¹, Lydie Bonal², Hikaru Yabuta³ and The Hayabusa2-initial-analysis IOM team, Hisayoshi Yurimoto⁴, Tomoki Nakamura⁵, Takaaki Noguchi⁶, Ryuji Okazaki⁷, Hiroshi Naraoka⁷, Kanako Sakamoto⁸, Shogo Tachibana^{8,9}, Sei-ichiro Watanabe¹⁰ and Yuichi Tsuda⁸

¹Museum National d'Histoire Naturelle, CNRS, Sorbonne Université, Paris, France. ²Institut de Planétologie et d'Astrophysique de Grenoble, Université Grenoble Alpes, CNRS CNES, Grenoble, France ³Hiroshima Univ., ⁴Hokkaido Univ., ⁵Tohoku Univ., ⁶Kyoto Univ., ⁷Kyushu Univ., ⁸JAXA, ⁹Univ. of Tokyo, ¹⁰Nagoya Univ.

Introduction: Isotope composition of organic material found in extraterrestrial samples is a powerful proxy for tracking its origin and evolution during the solar system events [1,2]. *In situ* investigation of isotope and elemental compositions unravel the heterogeneity and diversity of organic particles embedded within the fine-grained minerals of chondrites and IDPs [3,4]. Understanding the origin of organic matter on carbonaceous asteroids and its subsequent evolution due to secondary processes as well as space weathering is one of the prime goals of the Hayabusa2 sample-return mission [5]. To document Ryugu's inventory of organic material, we have employed NanoSIMS imaging of intact grains, without any chemical treatments, from both Chamber A and Chamber C. We present here the first set of data acquired on the NanoSIMS installed at the National Muséum of Natural History in Paris, and compare the composition of organic particles from the two sampling sites to evaluate the influence of space weathering and aqueous alteration.

Samples and methods: Several fragments of 3 particles from Chamber A aggregates (A0108) and 3 particles from Chamber C aggregates (C0109) were manually selected under a binocular and pressed on diamond windows. After their analysis by Raman and transmission FTIR, samples were gold coated (about 25 nm thick) before NanoSIMS imaging. In the first step, secondary ions of ¹⁶O, ¹²C₂, ¹²C¹⁴N, ¹²C¹⁵N and ³²S were imaged in multicollection mode, to investigate N-isotope distributions as well as N/C, O/C and S/C elemental ratios. A 2-3 pA primary Cs⁺ beam with a spatial resolution around 200 nm was rastered over 20 by 20 μm², divided into 256 by 256 pixels, in association with an electron flooding gun for charge compensation. Dwell time was set at 2 ms/pixel and about 60 frames were stacked.

Results and discussion: About 11,600 and 9,600 μm² surface area were imaged, of Chamber A and Chamber C samples, respectively. Individual organic particles were identified using the L'image software developed by Larry Nittler (Carnegie Institution of Washington). The ¹⁵N/¹⁴N ratios of individual particles are comparable to the values for isotope anomalies in CI and CM insoluble organic matter [3,6,7] whilst samples from Chamber C tend to exhibit a slightly larger ¹⁵N enrichment. In addition, bulk organic δ¹⁵N is in the range of IOM in CI chondrites. These values are consistent with independent NanoSIMS measurements of other Ryugu aggregates [8]. The corresponding elemental ratios point to a larger content in N in the organic particles from Chamber A, while the particles from Chamber C are more O-rich. Overall, S content is similar in organic particles from both chambers. It must be noted that O/C and S/C may be biased by the occurrence of fine scale association of oxides/silicates and sulfides with the organic particles, as observed by TEM [9]. The elemental composition of particulate organic matter will be further investigated on insoluble organic matter isolated by acid treatment of Ryugu samples. Our data suggest differences between aggregates from the two sampling sites in terms of elemental and isotope compositions of individual organic particles.

References

[1] Remusat et al. 2010. ApJ 713:1048. [2] Alexander C. M. O'D. et al. 2017. Chemie der Erde - Geochemistry 77:227. [3] Busemann et al. 2006. Science 312 :727. [4] Remusat et al. 2009 ApJ 698 :2087. [5] Tachibana et al. 2014. Geochem. J. 48:571. [6] Alexander et al. 2010. GCA 74:4417. [7] Remusat et al. 2019. GCA 263:235. [8] Nittler et al. 2021. This conference. [9] Stroud et al. 2021. This conference.

Exposure Conditions of Samples Collected on Ryugu's Two Touchdown Sites Determined by Cosmogenic Nuclides

Kunihiko Nishiizumi¹, Marc W. Caffee², Keisuke Nagao³, Ryuji Okazaki⁴, Hisayoshi Yurimoto⁵, Tomoki Nakamura⁶, Takaaki Noguchi⁷, Hiroshi Naraoka⁴, Hikaru Yabuta⁸, Kanako Sakamoto⁹, Shogo Tachibana^{9,10}, Sei-ichiro Watanabe^{9,11}, Yuichi Tsuda⁹, and Hayabusa2 Initial Analysis Volatile Team

¹Space Sci. Lab., Univ. of California, Berkeley, CA 94720-7450, USA., ²Dept. of Phys. & Astro., Purdue Univ., West Lafayette, IN 47907-2036, USA., ³KOPRI, Incheon 21990, Korea, ⁴Kyushu Univ., Fukuoka 819-0395, Japan, ⁵Hokkaido Univ., ⁶Tohoku Univ., ⁷Kyoto Univ., ⁸Hiroshima Univ., ⁹ISAS/JAXA, ¹⁰Univ. of Tokyo, ¹¹Nagoya Univ.

Hayabusa2 arrived at the C-type asteroid 162173 Ryugu in Jun. 2018, and successfully collected surface samples from two sampling sites, returning ~5.4 g of samples to Earth on Dec. 6, 2020. Surface samples stored in Chamber A were collected by the 1st touchdown (TD) on Ryugu's surface on Feb. 21, 2019. A crater (diameter of ~14 m) on Ryugu's surface was made using a collision device - denoted "Small Carry-on Impactor (SCI)" - on Apr. 5, 2019 [1]. Samples in Chamber C were collected proximal to this artificial crater and are possibly ejecta from the north side of the crater by the 2nd TD on Jul. 11, 2019 [2].

Our studies are based on the measurement of those nuclides produced in asteroidal surface materials by cosmic rays - both solar and galactic cosmic rays. Cosmic-ray-produced (cosmogenic) nuclides are used to determine the duration and nature of the exposure of materials to energetic particles. Our goals are to understand both the fundamental processes on the asteroidal surface and the evolutionary history of its surface materials. They are also key to understanding the history of Ryugu's surface and asteroid-meteoroid evolutionary dynamics. For Hayabusa2 samples, there are several specific questions we aim to address: (1) are the Chamber C samples, collected during the 2nd touchdown ejecta deposits from the artificial crater, (2) if so, what is the original depth of each recovered sample in the Ryugu regolith, and (3) what is the surface exposure time, mixing rate, and erosion/escape rate of Ryugu's surface? To answer these questions, we were allocated and received 2 particles from Chamber A (A0105-19 and -20) and 3 particles from Chamber C (C0106-09, -10, and -11) for measurements of cosmogenic radionuclides and noble gases. Each sample is several hundred μm in size.

We transferred the individual grains to acid cleaned sapphire containers, with ~2 mm diameter hole, using a vacuum tweezer at the JAXA curation facility. The five samples were hand carried to the Space Sciences Laboratory (SSL), University of California, Berkeley. Each sample was gently crushed by a mortar and pestle made from sapphire and then divided into two fractions, one fraction for cosmogenic radionuclides and one for noble gases. The samples were individually transferred to a small Al weighing boat and the masses were determined using an ultra-micro balance. For cosmogenic radionuclide analysis, the sample was transferred to a Teflon bomb from the Al boat and dissolved with a few drops of HF-HNO₃ mixture in the presence of clean Be, Al, Cl, and Mn carriers. After Cl was separated as AgCl, a small analysis aliquot was taken for chemical analysis by ICP-OES (Table 1). Beryllium and Al were separated by ion chromatography, using 1 mL anion and cation ion exchange columns, and purified for accelerator mass spectrometry (AMS) measurements. To serve as a baseline comparison, three grains of the Nogoya CM2 chondrite were analyzed using the same protocols.

Beryllium-10 ($t_{1/2} = 1.36 \times 10^6$ yr) AMS analysis was performed at PRIME lab, Purdue University [3] and result was shown in Table 1. Analyses of ²⁶Al (7.05×10^5 yr) and ³⁶Cl (3.01×10^5 yr) as well as noble gases will be done in the near future.

Table 1. Chemical compositions and cosmogenic nuclide ¹⁰Be concentration in Hayabusa2 samples and Nogoya CM2 chondrite.

Sample	Mass (mg)	Mg (%)	Ti (ppm)	Mn (ppm)	Fe (%)	Co (ppm)	Ni (%)	¹⁰ Be (dpm/kg)
Hayabusa2 A0105-19	0.2429	8.18	470	-	17.6	590	1.00	12.76 ± 0.37
Hayabusa2 A0105-20	0.2061	8.41	720	(2010)	18.0	460	1.03	12.75 ± 0.29
Hayabusa2 C0106-09	0.1228	6.05	690	(2090)	19.5	580	1.36	7.10 ± 0.30
Hayabusa2 C0106-10	0.1543	7.97	490	-	21.0	440	1.43	7.48 ± 0.26
Hayabusa2 C0106-11	0.1898	8.45	450	-	21.5	430	1.29	7.21 ± 0.43
Nogoya CM2	0.4594	9.96	480	1800	20.0	580	1.18	2.09 ± 0.13
Nogoya CM2	0.3437	9.61	480	1680	19.9	540	1.17	2.12 ± 0.09
Nogoya CM2	0.2049	11.27	410	1710	19.8	380	1.20	2.00 ± 0.13

Mn concentrations in parentheses are large uncertainty.

Although the chemical compositions of all 5 Hayabusa2 particles are very similar, the concentrations of Fe and Ni of the 3 Chamber C samples are ~10 % higher than that of Chamber A samples. Our measurements of the 5 Hayabusa2 samples indicate that the chemical composition of Ryugu is closer to those of CI or CM carbonaceous chondrites, rather than CV or CO.

To validate our procedures we measured the ^{10}Be concentrations in 3 individual grains from Nogoya. The concentrations from the Nogoya grains are nearly identical and in good agreement with our previous measurement of 2.22 ± 0.10 dpm/kg. The measurements reported here used ~ 3 orders of magnitude less sample mass than the measurements made years ago, have essentially the same uncertainties. For Ryugu, we were able to obtain high quality ^{10}Be measurements using ~ 100 μg sample.

The surface of Ryugu is bombarded by cosmic ray in a 2π exposure geometry, similar to surface of the Moon. On the Moon, the production profile of cosmogenic ^{10}Be from the surface to a depth of over 400 g/cm^2 is well established by measurements of ^{10}Be concentrations in the Apollo 15 drill core and 15008/7 core, shown in Fig. 1 [4, 5]. The ^{10}Be concentrations in A0105-19 and -20 are equivalent to the saturation value measured at the surface of the Moon. The simplest scenario is that both A0105-19 and -20 were collected from a depth of $0\text{-}30$ g/cm^2 on Ryugu. Both samples have been continuously exposed to cosmic ray at a similar depth for more than several Myr. A more precise depth can be obtained by measurement of ^{26}Al , which has a different production profile than ^{10}Be , and is also produced by solar cosmic ray at shallow depth (\leq several g/cm^2). Since the ^{10}Be activity is saturated, the total exposure age must be obtained by measurements of longer half-life (3.7×10^6 yr) ^{53}Mn and cosmogenic noble gases. Beryllium-10 concentrations in three Chamber C samples are lower than that of the Chamber A samples but nearly the same as each other. The sampling location of the 2nd TD is close to the "ejecta ray 3" described by [1]. Assuming that the Chamber C samples were shielded during their exposure to cosmic rays and then were incorporated into the ejecta deposits from the artificial crater by SCI impact, we can calculate the depth at which they were exposed. All three Chamber C samples were ejected from a depth of $150 - 180$ g/cm^2 from Ryugu (see Fig. 1). This depth corresponds to $1.3 - 1.5$ m, assuming the regolith density is the same as Ryugu's bulk density of 1.2 g/cm^3 [6]. Since the depth of the crater floor from the initial surfaces was determined 1.7 m by a digital elevation map (DEM) [1], three Chamber C samples were ejected from near bottom of the crater. Alternatively, if we assume these were not ejecta, but were resident on the surface, the lower ^{10}Be activities would indicate that these grains have shorter exposure ages, ~ 1 Myr. Based on their location near the artificial crater ejecta ray, we consider this scenario unlikely. Aluminum-26 and ^{36}Cl measurements of these samples will further constrain ejection depth and condition.

For our work, we obtained 5 similar sized, $\sim 0.5 - 1$ mm, grains. We don't know whether the sizes we observe now are representative of the grain's original sizes on Ryugu's surface; it is possible that they were broken during the collection process or during sample handling. We are certain though that independent of their original size on Ryugu, the three Chamber C grains were exposed to cosmic rays at the same depth. These grains had ample ^{10}Be for measurement, ^{10}Be measurements are possible in smaller grain sizes. A logical next step would be the measurement of ^{10}Be in grains of different sizes to investigate whether any possible association of grain size and ejection depth.

Based on saturated ^{10}Be in surface samples and from ejecta samples we conclude that the surface of Ryugu has been exposed to cosmic rays for more than several Myr and that the upper $1 - 2$ m of regolith have been relatively undisturbed for more than several Myr. Our observation shows that the surface of Ryugu is more stable than the surface of Itokawa and the estimation by geomorphological indicators [7]. Additional cosmogenic nuclide measurements, especially stable noble gases, will allow a detailed understanding of the surface evolution of Ryugu.

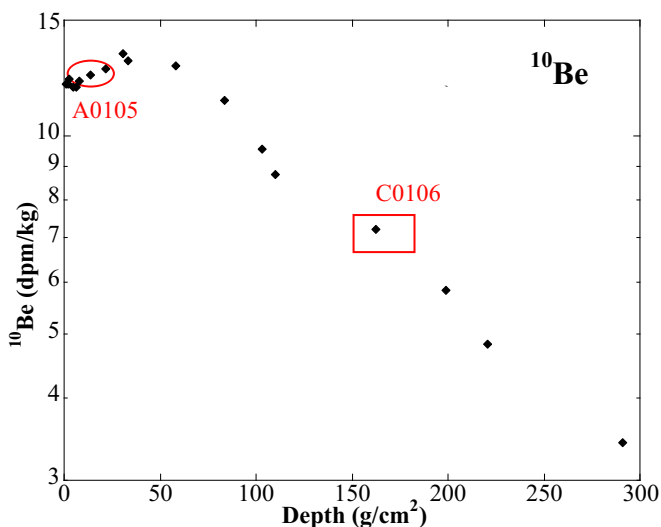


Figure 1. The depth profile of ^{10}Be production on the Moon. Black diamonds indicate ^{10}Be concentration vs. depth on the Moon measured in undisturbed Apollo 15 drill core and 15008/7 core [4, 5]. Observed ^{10}Be concentrations in Hayabusa2 samples are plot at estimate depths on Ryugu and marked red circle (A0105) and square (C0106).

References: [1] Arakawa M. et al. 2020. Science 368, 67-71. [2] Tsuda Y. et al. 2020. Acta Astronautica 171, 42-54. [3] Sharma P. et al. 2000. NIM B172, 112-123. [4] Nishiizumi K. et al. 1984. EPSL 70, 157-163. [5] Nishiizumi K. and Caffee M. W. 2019. MAPS 54, 6087pdf. [6] Watanabe S. et al. 2019. Science 364, 268-272. [7] Sugita S. et al. 2019. Science 364, eaaw0422.

Acknowledgments: We thank Hayabusa2 project and initial analysis team, especially Hayabusa2 curation members. Z. Nett and K. C. Welten helped a part of laboratory works. Nogoya was obtained from Field Muse. of Nat. His. This work was supported by NASA's LARS program.

Small grains from Ryugu: handling and analysis pipeline for Infrared Synchrotron Microspectroscopy

Stefano Rubino¹, Zélia Dionnet¹, Alice Aléon-Toppani¹, Rosario Brunetto¹, Tomoki Nakamura², Donia Baklouti¹, Zahia Djouadi¹, Celine Lantz¹, Obadias Mivumbi¹, Ferenc Borondics³, Stephane Lefrançois³, Christophe Sandt³, Francesco Capitani³, Eva Hériprié⁴, David Troadec⁵, Megumi Matsumoto², Kana Amano², Tomoyo Morita², Hisayoshi Yurimoto⁶, Takaaki Noguchi⁷, Ryuji Okazaki⁷, Hikaru Yabuta⁸, Hiroshi Naraoka⁷, Kanako Sakamoto⁹, Shogo Tachibana⁹⁻¹⁰, Sei-ichiro Watanabe¹¹, Yuichi Tsuda⁹, and the Hayabusa2-initial-analysis Stone team

¹IAS, Université Paris-Saclay, CNRS, France, ²Tohoku University, Japan, ³SMIS-SOLEIL, France

⁴CentraleSupélec, Université Paris-Saclay, CNRS, France, ⁵IEMN, Université de Lille, France, ⁶Hokkaido University, Japan,

⁷Kyushu University, Japan, ⁸Hiroshima University, Japan, ⁹ISAS/JAXA, Japan, ¹⁰The University of Tokyo, Japan, ¹¹Nagoya University, Japan

Introduction: In December 2020, the sample return mission Hayabusa2 (JAXA) brought 5.4g of matter from the surface of C-type primitive asteroid (162173) Ryugu [1]. This extremely precious material is now the object of multiple studies with state-of-the-art techniques in laboratories all around the world (Initial Analysis phase). These studies will grant new insight on the origin and evolution of primitive hydrated planetesimals, and ultimately on the early stages of our solar system. Within the Hayabusa2-initial-analysis “Stone” team [1] led by T. Nakamura, we received several microscopic particles in July 2021, with the goal of performing IR hyper-spectral imaging and IR micro-tomography studies.

Samples transfer and handling: Ryugu samples are kept in a controlled N₂ environment at Sagami-hara (JAXA) in order to avoid exposure to the terrestrial atmosphere. We took several steps in order to minimize the samples' exposure to air, before, during and after measurements. Prior to receiving the samples, we designed a custom sample-holder (Figure 1) for transferring particles from Japan to France and for their preliminary analysis. Particles from Ryugu were deposited on a gold mirror inside the sample-holder at Tohoku University (Japan). A KBr window installed in the cover of the sample-holder allowed us to acquire measurements of the particles while the sample-holder was still sealed. This custom-made sample-holder was kept as clean and sterile as possible (to avoid terrestrial contamination) and it had to fulfill two major requirements: fit on the microscope stages for our IR imaging and microspectroscopy studies and keep the samples in a dry N₂ environment (to avoid alteration from the atmosphere). The sample-holder was assembled inside a glovebox under N₂ atmosphere ($\Delta P \sim 6$ mBar, H₂O = 1.0 ppm, O₂ = 1.2 ppm). Multiple interfaces were used in order to prevent the mixing of the clean N₂ atmosphere and the ambient air (gold gasket, cleanroom static shielding bags), but also to avoid issues from shocks and vibrations (membrane boxes, foam-padded case). Once in Sendai, the empty sample holders were opened in a glovebox, and were loaded with 32 microscopic particles from Ryugu (distributed among four sample-holders: 14 particles from the first touchdown site in SH2 and SH3, and 18 particles from the second touchdown site in SH1 and SH4).

To monitor the atmosphere's changes in our sample-holders, these were accompanied by a “control”-holder, with grains of olivine and Fe dust (to monitor hydration and oxidation). A second “control”-holder, loaded with drierite (calcium sulfate) and some Fe dust, was kept in France, to monitor hydration and oxidation when not under dry N₂ conditions.

Samples reception and characterization: Upon arrival at synchrotron SOLEIL (France) in early July, the sample holders were inspected with a binocular through the KBr windows. We were able to identify at least 24 out of 32 of the original Ryugu particles, either based on their morphological correspondence with the grains prepared at Tohoku, and/or thanks to their clear IR “Ryugu-like” spectral signatures (mainly the 2.7 μm feature [2]). The particle size range was from 20 to 80 μm , with a particularly large particle in SH4 larger than 100 μm .

The analytical pipeline started with a full spectral characterization using the IR synchrotron beam while keeping the sample-holder closed, in order to minimize exposure to air. During the first three weeks of July, we analyzed all the identified Ryugu grains in their sample holders using three different FTIR microscopes: (1) a mid-IR large wavelength range MCT/B-equipped and synchrotron-radiation-fed microscope, (2) a far-IR bolometer-equipped microscope, (3) an FPA-equipped imaging microscope. Multiple detectors were used to access different wavelength ranges, covering from near-IR to far-IR (1 μm to 35 μm). This large spectral coverage allowed us to detect carbonates, organics, and phyllosilicates with different band positions [3]. Most of the IR spectra showed interesting features. Hyperspectral maps in the mid-IR of the individual particles were also acquired, in order to assess the compositional heterogeneity at the 5-10 μm scale. A few Raman spectra and maps were also acquired on isolated fragments, to assess the presence and structure of endemic organics in Ryugu's particles and to get complementary information on the mineralogy.

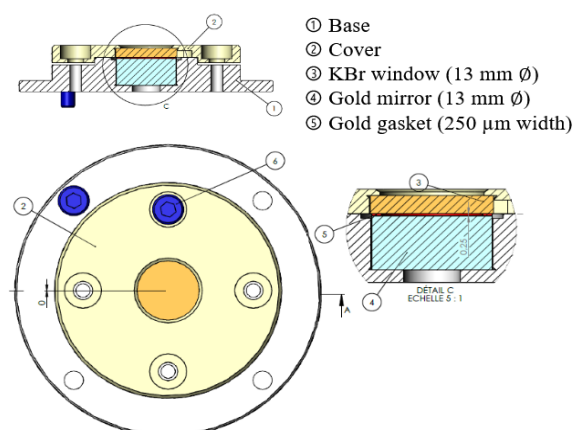


Figure 1. Sample-holder description

Thanks to a Raman measurement on a μm -spot on the gold substrate, we managed to detect remotely molecular oxygen inside SH2, which indicates the holders at some point lost their air-shut condition, probably in flight from Japan to France. We estimate that the grains were exposed to air for about 72-96 hours, before we received them and we put them again into a dry N_2 environment. However, we did not observe any modification of the KBr (a control KBr window we exposed to air for 24h showed clear modifications), and the anhydrous control samples we sent along the Ryugu sample holders showed no evidence of water adsorption nor hydration. So we inferred that Ryugu grains remained in a relatively dry environment, although in presence of O_2 , probably thanks to the presence of desiccants that prevented an increase in humidity.

In mid- and late-July, we opened sample holders SH2 and SH3, and we mounted 6 Ryugu grains on W or Al needles using two different FIB-SEM microscopes in Saclay and in Lille [4]. These grains were then measured in both transmission and reflectance mode, by Infrared Computed Tomography [5] (IR-CT) and Infrared Surface Imaging [6] (IR-SI) respectively. IR-CT allows us to assess the compositional heterogeneity of small particles in a 3D space, while IR-SI allows us to assess the surface composition for larger particles, treating the grain as a planetary surface by projecting the 2D IR hyper-spectral maps on a 3D shape model. Data processing and analysis of this large set of data is still ongoing. Our primary method of analysis, IR spectroscopy, is totally non-destructive, which implies that after our measurements a few particles can be sent to other analytical teams in the scope of combining different studies on the same sample. Some of these particles are now being analyzed by X-ray computed tomography at SPring-8 (Japan) [7].

Overall, the outcome of the last months has shown that the agreed handling, transfer and analysis pipelines are valid and may be applied for future sample-return missions.

Acknowledgements: We thank Moe Matsuoka for her precious help in preparing and sending Ryugu's particles from Sendai-Japan all the way to Orsay-France. This work is part of the multi-analytical sequence of the Hayabusa2 "Stone" MIN-PET group, led by Tomoki Nakamura. Zélia Dionnet was supported by a CNES postdoctoral allocation and this work was supported by the Centre National d'Etudes Spatiales (CNES-France, Hayabusa2 mission). The micro-spectroscopy measurements were supported by grants from Region Ile-de-France (DIM-ACAV) and SOLEIL.

References

[1] T. Nakamura et al., *abstract in this volume* ; [2] K. Kitazato et al., *Science*, 2019, 364, 272–275. ; [3] Z. Dionnet et al, *abstract in this volume* ; [4] A. Aléon-Toppani et al., *Meteorit. Planet. Sci.*, 2021, 56, 1151–1172. ; [5] Z. Dionnet et al. 2020. *Meteoritics & Planetary Science* 55 ; [6] Z. Dionnet et al., *in preparation*, 2021. ; [7] A. Tsuchiyama et al., *abstract in this volume*.

Preliminary results from FTIR hyper-spectral imaging campaign on Ryugu small grains and fragments.

Zélia Dionnet¹, Stefano Rubino¹, Alice Aléon-Toppiani¹, Rosario Brunetto¹, Tomoki Nakamura², Donia Baklouti¹, Zahia Djouadi¹, Celine Lantz¹, Ferenc Borondics³, Christophe Sandt³, Eva Hérigné⁴, David Troadec⁵, Megumi Matsumoto², Kana Amano², Tomoyo Morita², Hisayoshi Yurimoto⁶, Takaaki Noguchi⁷, Ryuji Okazaki⁷, Hikaru Yabuta⁸, Hiroshi Naraoka⁷, Kanako Sakamoto⁹, Shogo Tachibana⁹⁻¹⁰, Seiichiro Watanabe¹¹, Yuichi Tsuda⁹ and the Hayabusa2-initial-analysis Stone team.

¹IAS, Université Paris-Saclay, CNRS, France, ²Tohoku University, Japan, ³SMIS-SOLEIL, France

⁴CentraleSupélec, Université Paris-Saclay, CNRS, France, ⁵IEMN, Université de Lille, France, ⁶Hokkaido University, Japan,

⁷Kyushu University, Japan, ⁸Hiroshima University, Japan, ⁹ISAS/JAXA, Japan, ¹⁰The University of Tokyo, Japan, ¹¹Nagoya University, Japan

Introduction: Hayabusa2 is the first sample return mission to study and return samples from a primitive carbonaceous asteroid. It thus allows the study of the same small body at very different scales, from the km down to the atomic scale. Infrared (IR) spectroscopy plays a crucial role in this respect, helping to build a bridge between the remote sensing observations of the asteroid's surface, performed by NIRS3 [1,2] and the chemical and physical processes operating at a smaller scale and characterized in the laboratory on the returned samples. In December 2020, the Hayabusa2 reentry capsule delivered 5.4 g of material coming from asteroid Ryugu. This extremely precious material was then recovered by JAXA and pre-characterized inside the ISAS curation facility [3,4]. A fraction of this material was then given to six Initial Analysis sub teams, including the "Stone" team led by T. Nakamura which studies mineralogy and petrology at a large scale [5].

Material and Methods: We will present the result of FTIR hyperspectral imaging on six micrometric Ryugu fragments (ranging from 30 to 80 μm in size). These fragments originate from 2 bigger millimetric grains (A0064 and C0046). We analyzed these small grains in multiple configurations (see detailed analytical plan and transportation issues in [6]). After the first characterization in reflectance mode on their gold substrate, we mounted these small grains at the top of metallic needles to analyze them at different rotating angles both in transmission and reflection modes. The obtained data in transmission mode, IR-CT [7] (Infrared Computed Tomography), were then analyzed to reconstruct 3D distributions of the molecular components inside the grains, while reflectance data were projected on a 3D shape model of the grains. In this case, the fragments were treated as a planetary surface, which will also help to reinforce the link between remote sensing and laboratories measurements. Taking advantage of each configuration, the preliminary results of the combination of the different measurements will be shown and discussed.

Results and Discussion: We will present the average spectra in the 2.5 – 30 μm range. Several grains have IR signatures at 2.7 μm , 3.0-3.1 μm , 3.4 μm , and 3.9 μm , in a good agreement with the bands identified by NIRS3 or by MicOmega and FTIR in the JAXA curation facility [3, 4], plus several mid-IR signatures of great interest, such as bands attributed to Si-O stretching in phyllosilicates, and C=O stretching in organics and carbonates. A comparison of the IR spectra of the different grains with those of a large variety of carbonaceous chondrites acquired with the same set-up will be presented. Finally, we will discuss the heterogeneity within individual grains, with particular emphasis on the following issues: (i) detection and heterogeneity of the 2.7 μm band (ii) spatial correlation between phases (phyllosilicates, carbonates, opaque phases, organics) and (iii) identification and quantification of the carbonates. These spectral observations and parameters will help to better constrain the 3D μm -scale assembly of minerals and organics in Ryugu, and will provide information on the origin and evolution of Ryugu.

Perspectives: Our multi-analytical sequence started with non-destructive IR hyperspectral imaging and continues now with more destructive techniques. One grain has been sliced into 3- μm thin sections and will be analyzed in 2D with higher resolution IR hyperspectral imaging and complementary analyses [8]. The rest of the samples have been sent back to Japan, to be analyzed at the BL47XU of SPring-8 synchrotron by XCT [9] in order to obtain complementary information concerning the 3D physical, chemical and morphological properties.

Acknowledgments: We thank Moe Matsuoka for her precious help in preparing and sending Ryugu's particles from Sendai-Japan all the way to Orsay-France. This work is part of the multi-analytical sequence of the Hayabusa2 "Stone" MIN-PET group, led by Tomoki Nakamura. Zélia Dionnet was supported by a CNES postdoctoral allocation and this work was supported by the Centre National d'Etudes Spatiales (CNES-France, Hayabusa2 mission). The micro-spectroscopy measurements were supported by grants from Region Ile-de-France (DIM-ACAV) and SOLEIL.

References: [1] Kitazato et al. 2019 Science 364-6437: 272. [2] Watanabe, S.-I., Tsuda, Y., Yoshikawa, M., et al. 2017, Space Science Review, 208: 3. [3] Bibring et al. 2021. Metsoc Abstract #6276. [4] Yada et al. 2021. Metsoc Abstract #6186. [5] Nakamura et al. in this volume. [6] Rubino et al. in this volume. [7] Dionnet et al. 2020. Meteoritics & Planetary Science 55: 1645-1664. [8] Aléon-Toppiani et al. 2021. Meteoritics & Planetary Science. [9] Tsuchiyama A. et al. 2011. Science 333-6046: 1125.

Iron valence state and mineralogy in particles from asteroid Ryugu

Jean-Christophe Viennet¹, Mathieu Roskosz¹, Pierre Beck², Esen Ercan Alp³, Barbara Lavina^{3,4}, Michael Hu³, Jiyong Zhao³, Tomoki Nakamura⁵, Kana Amano⁵, Mizuha Kikui⁵, Tomoyo Morita⁵, Hisayoshi Yurimoto⁶, Takaaki Noguchi⁷, Ryuji Okazaki⁸, Hikaru Yabuta⁹, Hiroshi Naraoka⁸, Kanako Sakamoto¹⁰, Shogo Tachibana^{10,11}, Seiichiro Watanabe¹², Yuichi Tsuda¹⁰, and the Hayabusa2-initial-analysis Stone team.

¹*Institut de Minéralogie, de Physique des Matériaux et de Cosmochimie, Museum National d'Histoire Naturelle, CNRS, Sorbonne Université, Paris, France.* ²*Institut de Planétologie et d'Astrophysique de Grenoble, Université Grenoble Alpes, CNRS CNES, Grenoble, France.* ³*Center for Advanced Radiation Sources, The University of Chicago, Chicago, IL 60637, USA.* ⁴*Advanced Photon Source, Argonne National Laboratory, Argonne, IL 60439, USA.* ⁵*Tohoku Univ.* ⁶*Hokkaido Univ.* ⁷*Kyoto Univ.* ⁸*Kyushu Univ.* ⁹*Hiroshima Univ.* ¹⁰*JAXA.* ¹¹*Univ. of Tokyo,* ¹²*Nagoya Univ.*

Introduction: Iron is a major element in rocky material from the solar system that can occur under multiple valence state. As such it can be used to trace geological processes that occurred on asteroid Ryugu, including thermal metamorphism and aqueous alteration. Observations of the mineralogy of carbonaceous chondrites have revealed the presence of minerals assemblages that are barely in thermodynamic equilibrium. Even at the micron-scale, iron is often present under multiple valence state (most frequently 0, +2, or +3) in a wide range of minerals (primary or secondary in nature), including silicates, oxy-hydroxide, sulfides, sulfates, clay minerals and carbonates. Such heterogeneous assemblages are the results of post-accretion processes that often triggered a partial textural and chemical equilibration, associated to a modification of primary Fe-bearing minerals and their valence state. It is therefore tricky to disentangle the different processes recorded by the iron mineralogy of chondritic materials. Furthermore, since most Fe-bearing phases are redox-sensitive, exposure to terrestrial atmosphere may also induce iron oxidation and additional, late modifications of the iron mineralogy. In this context, Hayabusa2 sampled Ryugu, an asteroid that did not suffer extensive thermal metamorphism, and returned rocks to Earth with minimal air exposure. It offers a unique opportunity to study the redox state of carbonaceous asteroids and evaluate the overall redox state of the most oxidized primitive rocks of the solar system.

Samples and methods: Here, we determine the mineralogy and the redox state of Fe-bearing minerals from ten Ryugu samples (five from the chamber A used for the first sampling and five from the chamber C for the second sampling) prior to and after exposure to air. We use Synchrotron Mössbauer Spectroscopy (SMS) technique that enables to probe the bonding environment of iron at the microscopic scale. These measurements are combined with co-aligned X-ray diffraction, permitting to assess locally the mineralogy and valence state of iron in Ryugu particles. We also apply conventional Mössbauer spectroscopy on a couple of large (mm-size) Hayabusa returned samples from the chambers A and C.

Results and discussion: We will present the bulk proportions of iron-bearing minerals and the Fe redox state ($\text{Fe}^{3+}/\text{Fe}_{\text{tot}}$) at the 'Stone' scale. We will then provide the first estimate of the redox state of Ryugu as compared to the large array of bulk redox data collected over several decades on meteorites. We will also describe the redox states of iron-bearing clay minerals before any air contamination. The first clues on the ageing of these minerals after exposure to air will be discussed based on data collected on the same sample before and after exposure to air. We will compare in greater details Ryugu samples to a series of well-known chondritic meteorites including Orgueil and Murchison. We will show, more specifically, that most of the iron is accommodated in magnetite and sulfides (pyrrhotite and pentlandite). Clay minerals also contain a fraction of the total iron. Overall, the investigated Ryugu samples appears to be (or are) more reduced than the Orgueil, both considering the bulk composition and the clay minerals fraction. The redox state recorded in a pristine sample and in the same sample exposed to air for more than two months do not show clear evidence of oxidation suggesting that, as far as iron is concerned, samples can be prepared and analyzed at ambient conditions at least for several weeks if stored in vacuum or in inert gas after preparation.

Three-dimensional analysis of Ryugu sample particles using X-ray nanotomography.

Akira Tsuchiyama^{1,2}, Megumi Matsumoto³, Junya Matsuno¹, Tomoki Nakamura³, Takaaki Noguchi^{4,5}, Kentaro Uesugi⁶, Akihisa Takeuchi⁶, Masanori Yasutake⁶, Miyake Akira⁴, Shota Okumura⁴, Yuri Fujioka³, Mingqi Sun², Aki Takigawa⁷, Toru Matsumoto⁴, Satomi Enju⁸, Itaru Mitsukawa⁴, Yuma Enokido³, Tomoyo Morita³, Naoto Nakano⁴ and Stefano Rubino⁹, Tsukasa Nakano¹⁰ Hisayoshi Yurimoto¹¹, Ryuji Okazaki¹², Hikaru Yabuta¹³, Hiroshi Naraoka¹², Kanako Sakamoto¹⁴, Shogo Tachibana^{7,14}, Seiichiro Watanabe¹⁵ and Yuichi Tsuda¹⁴, and the Hayabusa2-initial-analysis Stone and Sand teams
¹Research Organization of Science and Technology, Ritsumeikan University, ²CAS, Guangzhou Institute of Geochemistry, ³Graduate School of Science, Tohoku University, ⁴Graduate School of Science, Kyoto University, ⁵Faculty of Arts and Science, Kyushu University, ⁶SPRING8/JASRI, ⁷Graduate School of Science, University of Tokyo, ⁸Graduate School of Science and Engineering, Ehime University, ⁹Université Paris-Saclay, CNRS, Institut d'Astrophysique Spatiale, ¹⁰GSA/AIST, ¹¹Graduate School of Science, Hokkaido University, ¹²Graduate School of Science, Kyushu University, ¹³Graduate School of Advanced Science and Engineering, Hiroshima University, ¹⁴ISAS/JAXA

We have performed initial analysis of samples returned from asteroid 162173 Ryugu by the Hayabusa2 spacecraft using synchrotron radiation-based X-ray nanotomography to elucidate the 3D structures and features of the samples with sub-micron spatial resolution as parts of the Hayabusa2 initial analysis Stone and Sand sub-teams.

We analyzed 29 and 20 particles from the first and second touchdown sites (chambers A and C), respectively. Particles of 10 ~ 150 μm in apparent size were picked up and attached to the tips of Ti needles with Pt deposition using FIB or amorphous carbon fibers with glycol phthalate. They were imaged by two different methods (dual-energy tomography (DET) [1] and scanning-imaging X-ray microscopy (SIXM) [2]) at BL47XU of SPring-8 [3]. In DET, X-ray absorption contrast images were obtained as the spatial distribution of linear attenuation coefficient (LAC) at two different X-ray energies of 7 and 7.35 keV, which are below and above the K-absorption energy of Fe (7.11 keV), respectively. The LAC images at 7 keV correspond closely to compositional (Z) contrasts, except for Fe, and those at 7.35 keV strongly depended on Fe content. In SIXM, we obtained X-ray differential phase contrast images as the spatial distribution of refractive index decrement (RID), which is the difference between the X-ray refractive index (RI) and unity ($\text{RI} = 1 - \text{RID}$), at X-ray energy of 8 keV. The RID image is closely proportional to the density of the object. The voxel sizes of LAC 7 keV, LAC 7.35 keV and RID images are $47.4 \times 47.4 \times 47.4 \text{ nm}^3$, $51.1 \times 51.1 \times 51.1 \text{ nm}^3$ and $111.1 \times 111.1 \times 109.2 \text{ nm}^3$, respectively.

The image analysis was made by combining ImageJ and codes made with C and Python. The registration among the three types of images was made with the reference of LAC 7 keV images. Then, RGB-CT images were made by assigning blue, red, and green to LAC 7 keV, LAC 7.35 keV, and RID images, respectively. Different phases including organic materials show different colors in the RGB-CT images. Minerals are quantitatively discriminated by comparing the LAC and RID values of the objects in CT images and those of minerals with known chemical compositions and densities. The solid portions of the sample particles images were extracted in LAC 7.35 keV using Chan-Base segmentation. The volume, V , surface area, S , 3-axial lengths, $A \geq B \geq C$, fractal dimension, FD , and closed porosity, p_0 , were then obtained. Porosity by considering pores and cracks that are open to the outside, named as open porosity, p_∞ , were also estimated by a wrapping method [4]. The density, ρ , was estimated from the averaged RID value of the particle as the lower limit. Density considering open pores, ρ_∞ , was calculated as $\rho \times (1 - p_\infty)$. Sphere-equivalent diameter, D , was calculated from V and sphericity, Ψ , from V and A .

No distinct difference between the samples from chambers A and C was recognized. The sample particles are mainly composed of Mg-rich phyllosilicates (serpentine and/or saponite; $\text{Mg}\# \sim 0.8\text{-}0.9$) in the matrix (Fig. 1A). The phyllosilicates are not homogeneous in some particles (Fig. 1B) probably due to the difference of $\text{Mg}\#$ and/or nanoporosity below the spatial resolution. FeS (mostly pyrrhotite and minor pentlandite) grains are commonly present as hexagonal plates shown as a rectangle shape in a slice image (Fig. 1A). We found whiskers of probably FeS (Fig. 1C) in some matrices as well. Magnetite grains with different morphologies (framboidal, spherulitic, plaquette and equant) are also commonly present (Fig. 1A). Sub-micron grains of FeS and magnetite are usually present in the matrix. Dolomite is usually present mostly as aggregates of euhedral or subhedral grains (Fig. 1A) and contains minor amounts of Fe and some heavy element (possibly Mn). Aggregates of micron-sized dolomite grains are also present (Fig. 1B). Breunerite is present as a rhombohedron in shape and have the composition roughly estimated as $(\text{Mg}_{0.6}\text{Fe}_{0.4})\text{CO}_3$ (Fig. 1D). CaCO_3 (aragonite or calcite) is rarely present. Apatite is usually present mostly as aggregates of subhedral or anhedral grains (Fig. 1E). Small grains of forsterite or enstatite ($\text{Mg}\# \sim 1$) are rarely observed. Small objects (mostly $< 1 \mu\text{m}$) of probably organic materials are commonly present in the matrix (Fig. 1B) but their abundance is small (probably a few % or less). Inclusions, which are empty or filled with low-Z materials, were observed in FeS, dolomite, breunerite and apatite grains (Fig. 1D). Spherical objects of phyllosilicate surrounded by fine grains of FeS

or dolomite (Fig. 1E) and object composed of Fe-rich and mostly anhydrous silicates (Fig. 1E) and fine grains of FeS and/or magnetite named “dark inclusion” (Fig. 1A) were sometimes observed. In addition to the above phases, several unidentified phases are observed as well. Some sample particles are unique; a low-density material ($\sim 1 \text{ g/cm}^3$) with a lot of fine cracks and organic-like material with embedded mineral grains. Porous objects like the ultra-porous lithology in Acfer 094 [3] were not observed.

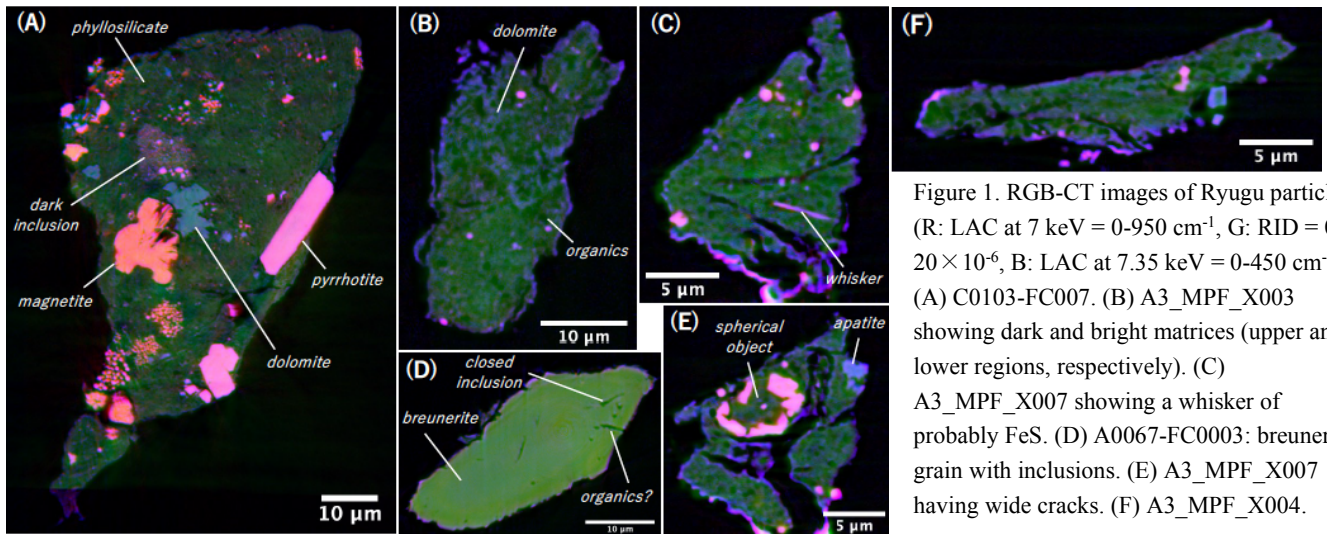


Figure 1. RGB-CT images of Ryugu particles (R: LAC at 7 keV = 0-950 cm^{-1} , G: RID = 0-20 $\times 10^{-6}$, B: LAC at 7.35 keV = 0-450 cm^{-1}). (A) C0103-FC007. (B) A3_MPF_X003 showing dark and bright matrices (upper and lower regions, respectively). (C) A3_MPF_X007 showing a whisker of probably FeS. (D) A0067-FC0003: breunerite grain with inclusions. (E) A3_MPF_X007 having wide cracks. (F) A3_MPF_X004.

D ranges from 9 to 60 μm . The 3D shape distribution indicates that the Ryugu particles ($B/A=0.66$ and $C/B=0.65$ in average) are less spherical in shape than the Itokawa particles and fragments of impact experiments (*c.f.*, silver ratio: $B/A=C/B=0.71$) [1]. Some particles examined here may not be the original impact fragments on the Ryugu surface but artificial fragments during the sampling by the space craft and/or in the laboratory. Ψ is small (<0.4) and FD of some particles are <3 together with a weak correlation between them, indicating that the particle shapes are irregular and complicated. Some surfaces of the particles are convexo-concave indicating fragmentation, while some are more or less smooth and may be formed by mechanical abrasion on the asteroid as proposed for Itokawa particles [4]. Cracks less than a few μm in width are commonly present in all particles except for those composed of single crystals. Some cracks develop along the boundaries of some objects and mineral grains (Fig. 1E), implying that they are cracks formed due to shrinkage by dehydration. Some cracks are subparallel to flattened particle surfaces probably due to impact (Fig. 1F). p_0 is usually less than a few%. p_∞ mostly ranges from 5 to 20% (Fig. 2), which is less than the porosity of the CI chondrite Orgueil (34.9% [5]). This can be explained by the different size of pores; the p_∞ counts relatively large pores ($>\sim$ a few hundred nm) while that of CI counts nanopores. ρ mostly ranges from 1.3 to 1.8 g/cm^3 and ρ_∞ from 1.1 to 1.6 g/cm^3 (Fig. 2). They are not inconsistent with the bulk density of Orgueil (1.57 g/cm^3 [5]) if we consider ρ and ρ_∞ as the lower limits.

The examined samples closely resemble CI in mineralogy and textures although we did not surely find any sulfates, such as gypsum, epsomite and blödite. The porosity and density are also consistent with those of CI. Any signature of dehydration as suggested from the IR spectrum [6] was not recognized. Highly porous materials as expected from the low thermal inertia [7] were not observed. FIB sections were prepared based on the 3D information and examined by TEM [8, 9]. The present examination is ongoing and we note that some of the ranges of physical properties, such as D , B/A , C/B , Ψ , FD , p_0 , p_∞ , ρ and ρ_∞ , are still preliminary.

References

- [1] Tsuchiyama A. et al. 2013. *Geochim. Cosmochim. Acta* 116;5. [2] Takeuchi A. et al. 2014. *J. Synchrotron Radiat.* 20:793.
- [3] Matsumoto M. et al. 2019. *Science Advances* 5;eaax5078. [4] Tsuchiyama A. et al. 2011. *Science* 333;1125. [5] Flynn G. J. et al. 2018. *Chemie der Erde* 78: 269. [6] Kitazato K. et al. 2019. *Science* 268:272. [7] Okada T. et al. 2020. *Nature* 579:518.
- [8] Nakamura T. et al. 2021. Abstract in this volume. [9] Noguchi T. et al. 2021. Abstract in this volume.

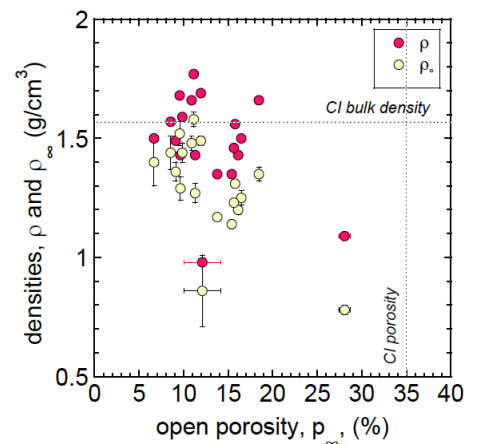


Figure 2. Density, ρ , estimated from the averaged RID value (lower limit) and density considering open pores, ρ_∞ , plotted against open porosity, p_∞ .

Surface morphologies and space weathering features of Ryugu samples

T. Matsumoto¹, T. Noguchi¹, A. Miyake¹, Y. Igami¹, M. Haruta¹, H. Saito², S. Hata², Y. Seto³, M. Miyahara⁴, N. Tomioka⁵, H. A. Ishii⁶, J. P. Bradley⁶, K. Ohtaki⁶, E. Dobrică⁶, T. Nakamura⁷, M. Matsumoto⁷, A. Tsuchiyama^{8,9}, M. Yasutake¹⁰, J. Matsuno⁸, S. Okumura¹, K. Uesugi¹⁰, M. Uesugi¹⁰, A. Takeuchi¹⁰, M. Sun⁹, S. Enju¹¹, A. Takigawa¹², H. Leroux¹³, C. Le Guillou¹³, D. Jacob¹³, M. Marinova¹³, F. de la Peña¹³, F. Langenhorst¹⁴, D. Harries¹⁴, P. Beck¹⁵, T. H. Van Phan¹⁵, R. Rebois¹⁵, N. M. Abreu¹⁶, T. Zega¹⁷, P.-M. Zanetta¹⁷, M. Thompson¹⁸, M. Lee¹⁹, L. Daly¹⁹, P. Bland²⁰, R. Stroud²¹, K. Burgess²¹, J. C. Bridges²², L. Hicks²², M. E. Zolensky²³, D. R. Frank⁶, J. Martinez²⁴, H. Yurimoto²⁵, K. Nagashima⁶, N. Kawasaki²⁵, R. Okazaki², H. Yabuta⁴, H. Naraoka², K. Sakamoto²⁶, S. Tachibana¹², S. Watanabe²⁷, Y. Tsuda²⁶, and the Hayabusa2 Initial Analysis Team

¹Kyoto Univ., Japan; ²Kyushu Univ., Japan; ³Kobe Univ., Japan; ⁴Hiroshima Univ., Japan; ⁵Kochi Core Center, JAMSTEC, Japan; ⁶Univ. of Hawaii, USA; ⁷Tohoku Univ., Japan; ⁸Ritsumeikan Univ., Japan; ⁹Guangzhou Institute of Geochemistry, China; ¹⁰JASRI, Japan; ¹¹Ehime Univ., Japan; ¹²Univ. of Tokyo, Japan; ¹³Univ. de Lille, France; ¹⁴Univ. of Jena, Germany; ¹⁵Univ. Grenoble Alpes, France; ¹⁶Penn State, USA; ¹⁷Univ. of Arizona, USA; ¹⁸Purdue Univ., USA; ¹⁹Univ. of Glasgow, UK; ²⁰Curtin Univ., Australia; ²¹US Naval Research Laboratory, USA; ²²Univ. of Leicester, UK; ²³JSC/NASA, USA; ²⁴Jacobs Engineering, ²⁵USA, Hokkaido Univ., Japan; ²⁶JAXA/ISAS, Japan; ²⁷Nagoya Univ., Japan

Introduction: Asteroids are leftover remnants of planet formation and provide clues as to the origin and evolution of the early solar system. C-type asteroids have been expected to be parent bodies of carbonaceous chondrites, containing hydrated silicates and volatile compounds that could be the origin of water and life on the Earth. JAXA's *Hayabusa 2* spacecraft explored C-type asteroid Ryugu and collected surface materials at two landing sites on Ryugu [1]. The spacecraft delivered its re-entry capsule to the Earth, and subsequent initial investigation of the *Hayabusa 2* sample container found that millimeter pebbles and fine grains were successfully recovered from the surface of Ryugu [2]. Geologic maps and variations in the reflectance spectra of Ryugu's surface suggest that geologic activities and alteration of regolith occur over time [3]. Ryugu samples will provide an opportunity to understand the dynamic evolution of surface materials on C-type asteroids. Materials exposed to the space environment are expected to have altered optical, physical, or chemical properties. This process is defined as space weathering, which includes alteration by micrometeoroid bombardments, solar wind implantation, and solar radiation heating [4]. Analyses of lunar soils and regolith particles from S-type asteroid Itokawa have revealed that the uppermost surfaces of regolith grains record the space weathering features, such as amorphization, melting, and vapor-deposition [5,6]. Thus far, the space weathering of carbonaceous asteroids is not well understood. The surface microstructures of Ryugu samples will offer insight into the ongoing alteration of the regolith on Ryugu. In this study, we report the surface morphologies and mineral structures of Ryugu samples investigated in the initial analysis by the Mineralogy-Petrology Fine (Sand) sub-team.

Samples and methods: Ryugu samples from the two sampling sites were preserved in chambers A and C of the sample catcher inside the sample container [2]. We have mainly investigated the fine grains (< 300 μm) picked up from both chambers at the Extraterrestrial Sample Curation Center of JAXA. After the samples were allocated from JAXA, we handled them in a dry glove box filled with nitrogen at Kyoto University. For surface observation, the fine grains were fixed on gold plates using an Araldite adhesive. We examined the surface features of the Ryugu samples using a field emission scanning electron microscope (FE-SEM: JSM-7001F). We then extracted electron-transparent sections of regions of interest on the Ryugu grains for transmission/scanning transmission electron microscopy (TEM/STEM) studies, using a focused ion beam (FIB) system (Helios NanoLab G3 CX at Kyoto University, Thermo Scios at Kyushu University). We are now performing TEM/STEM analysis, synchrotron radiation X-ray absorption fine structure analysis, nano-tomography, and atom probe analysis.

Results: *Surface features of Ryugu grains:* Fine Ryugu grains have massive, platy, and granular shapes. The majority of the grain surfaces consist of phyllosilicates with rough surfaces. Coarse and fine surface textures are identified on the phyllosilicates. Cracks/gaps exist between phyllosilicates and other mineral phases. TEM analysis shows that the phyllosilicates are composed mainly of serpentine and saponite (detailed TEM observations are described in [7]). The second major mineral phases on the grain surfaces are sulfides, magnetite, and carbonates. These minerals are ubiquitous, although their abundance varies from grain to grain. Most of the sulfides are pyrrhotite crystals. They appear as hexagonal plates, cuboids, and irregular shapes with sizes up to a few tens of micrometers. The pyrrhotite plates exhibit sharp growth steps on their surfaces. Some pyrrhotite crystals with irregular surfaces have numerous voids. Pentlandite often coexists with pyrrhotite. Tiny sulfides (< 1 μm), including zinc, chromium, and/or copper, occur as minor phases. Magnetite appears as framboidal aggregates, plaquettes, spherulites, and irregular shapes. The framboidal magnetite on Ryugu grains have distinct sharp edges, when compared to framboidal magnetites

with rounded morphologies in thermally metamorphosed CI chondrites (e.g., Y980115) in which thermal sintering has likely occurred. The carbonate phases found on the Ryugu grains are mainly dolomite and minor magnesite-breunnerite. They have euhedral, fractured, and irregular surfaces. Calcium phosphate, oxides (chromite, ilmenite), and iron phosphides are found as minor phases. Na-Mg bearing phosphate with an irregular shape is present as a rare phase and is commonly attached loosely to the grain surfaces. Anhydrous minerals found on Ryugu grains are forsteritic olivine, low-calcium pyroxene and pure spinel with sizes up to a few micrometers. These phases are rare. Most of them have fractured surfaces.

Space weathering features: We found impact craters, melted drops, splashes, melt sheets, glassy spherules on Ryugu grains by SEM observation (Fig. 1). Studies of lunar soils and Itokawa particles have shown that these objects are likely products of micro-impacts on airless bodies [8, 9]; hence, the grain surfaces with the impact products may have been exposed to the space environment. The abundance of the impact products varies from grain to grain. Phyllosilicates on the grain surfaces are altered to have smooth surface textures with tiny voids (Fig. 1 in [7]). TEM analysis shows that the uppermost surface is surrounded by an amorphous rim with a thickness from 50 nm to 2-3 μm . Tiny vesicles and iron compounds appear in the rim. EDX analysis shows a change in chemical composition near the surface. The altered surfaces of pyrrhotite and pentlandite have shallow depressions (200 nm – 300 nm in depth) with rugged textures (Fig. 1). Iron metals protrude from the iron sulfide surfaces, and some are in the form of curved whiskers (Fig. 1). Dark-field TEM imaging suggests disordering of the lattice near the sulfide surface. Carbonates and magnetite have altered surfaces with rough textures. The breunnerite grain we examined by TEM has a distinct rim with disordered lattice and a thickness of approximately 90 nm. Selected area diffraction patterns obtained from the rim imply the appearance of periclase ((Mg,Fe)O) particles in the rim.

Discussion: The dominance of phyllosilicates and the scarcity of anhydrous minerals indicate that Ryugu samples have experienced a high degree of aqueous alteration. The morphologies of the major mineral phases, such as the unique shapes of magnetite, suggest a close similarity between Ryugu samples and CI chondrite [10].

Previous ion irradiation experiments simulating space weathering suggest that the uppermost surface of phyllosilicates can be modified by space weathering [11]. The altered phyllosilicate rim found in our analysis may have been formed by solar wind implantation and impact events [7]. Iron metallic whiskers on iron sulfides have recently been identified as space weathering products in lunar soils and Itokawa particles [12,13]. The iron metals are likely to have formed via selective sulfur loss, accumulation of excess iron atoms, and subsequent growth of iron metals. These alteration processes may be caused by various phenomena including solar wind implantation, thermal effects produced by micrometeoroid bombardments and solar heating [12]. The appearance of iron whiskers on Ryugu samples implies that the space weathering of iron sulfides on Ryugu is similar to that on the Moon and Itokawa. The thickness of the altered rim on breunnerite is roughly consistent with the maximum depth at which extensive atomic displacement is produced by implanted solar wind ions (~ 1 keV/nucleon) [6]. Hence, solar wind implantation may have contributed to the rim formation of the carbonate. Based on our initial analysis, we tentatively conclude that the Ryugu samples record the combined processes of space weathering on the aqueously altered asteroid, implying that remote sensing data should be reassessed considering the space weathering effect.

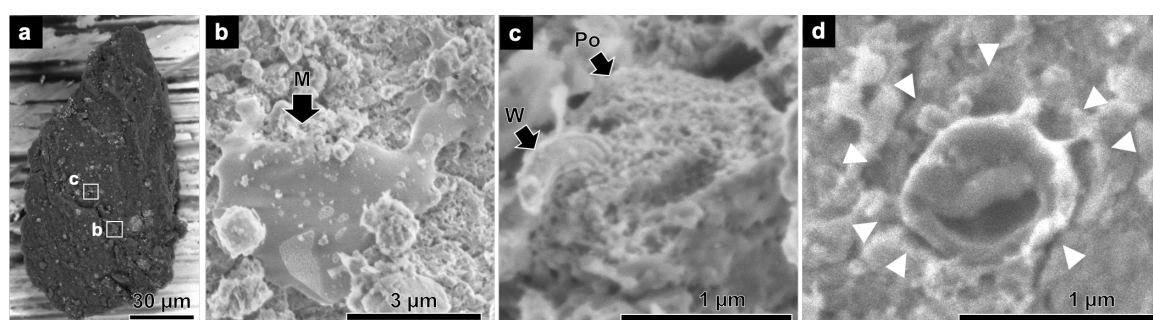


Fig. 1 Space weathered Ryugu grain. (a) Backscattered electron image of a fine Ryugu grain. (b-d) Secondary electron images of a melted drop (b), pyrrhotite with an iron whisker (c), and an impact crater with a residue on phyllosilicates (d). The image (d) was obtained from another fine Ryugu grain. M: melted drop, Po: pyrrhotite, W: iron whisker. Triangles in (d) indicate the crater rim.

References: [1] Watanabe S. et al. 2019. Science 364, 268-272. [2] Yada T. et al. 2021. Abstract# 2548 in 52nd LPSC. [3] Sugita S. et al. 2019 Science 364, 252. [4] Pieters C. and Noble S. K. 2016. J. Geophys. Res. Planet 121, 1865-1884. [5] Keller L. P. and McKay D. S. 1993 Science 261, 1305-1307. [6] Noguchi T. et al. Science 333, 1121-1125. [7] Noguchi T. et al. this symposium. [8] McKay D. S. et al. 1991. Lunar Sourcebook. [9] Matsumoto T. et al. 2018. Icarus 303, 22-33. [10] Brearley A. 2006, Meteorites and the early solar system II, 587-624. [11] Thompson M. et al. 2020. Icarus 346, 113775. [12] Matsumoto T. et al. 2020. Nat. Commun. 11, 1-8. [13] Matsumoto T. et al. 2021. Geochim. Cosmochim. Acta 299, 69-84.

CNHOS contents with their isotopic compositions and preliminary organic profiles from the Hayabusa2 samples

Yoshinori Takano¹, Hiroshi Naraoka², Nanako O. Ogawa¹, Yasuhiro Oba³, Toshiki Koga¹, Toshihiro Yoshimura¹, Saburo Sakai¹, Naohiko Ohkouchi¹, Hisayoshi Yurimoto³, Tomoki Nakamura⁴, Takaaki Noguchi⁵, Ryuji Okazaki², Hikaru Yabuta⁶, Kanako Sakamoto⁷, Shogo Tachibana^{7,8}, Sei-ichiro Watanabe⁹, Yuichi Tsuda⁷ and the Hayabusa2-initial-analysis SOM team

¹ JAMSTEC, ² Kyushu Univ., ³ Hokkaido Univ., ⁴ Tohoku Univ., ⁵ Kyoto Univ.,
⁶ Hiroshima Univ., ⁷ JAXA, ⁸ Univ. Tokyo, ⁹ Nagoya Univ.

The successful collection and recovery of the Ryugu sample [1,2] are leading us to a valuable opportunity for revealing the properties of the carbonaceous asteroid in the Solar System history; -What is Ryugu? -What are the origins and characteristics of light elements (C, N, H, O, and S)? -What do their isotopic compositions tell us? -How do they record the primordial chemical evolution on the asteroid? -How did the interaction of water, organic matter, and minerals affect the evolution and diversity of indigenous molecules? To answer those important issues by using state-of-the-art small-scale analysis, the SOM (Soluble Organic Matter) team have been firstly focusing on (i) the initial bulk profiles, especially for the elemental abundance of carbon (C), nitrogen (N), hydrogen (H), oxygen (O), sulfur (S) with the isotopic compositions of $\delta^{13}\text{C}$, $\delta^{15}\text{N}$, δD , $\delta^{18}\text{O}$ and $\delta^{34}\text{S}$, respectively, and (ii) the molecular profiles to understand more deeply for nature of indigenous SOM [3-5]. For instance, if endogenous water-mineral interactions occurred in the asteroid, some aqueous alteration signatures (e.g., process relevant products including carbonates and other precipitates) should have been recorded to the pristine sample in the bulk and molecular levels. Assuming the interactions above mentioned, we can trace the potential *in-situ* temperature of the alteration process by using clumped isotope surveys of minerals [6]. To assess the objectives, we have been conducting rehearsal analyses for analytical optimizations and sequential sample processes [3-5, e.g., Figure 1], with a scope of solid and soluble organic aspects [6-9]. In order to deal with samples of unknown identity, especially for bulk nitrogen scale, we validated the dynamic range of $\delta^{15}\text{N}$ profiles covered on the basis of pioneering works and compilations for the Inner and Outer Solar System [e.g., 10].

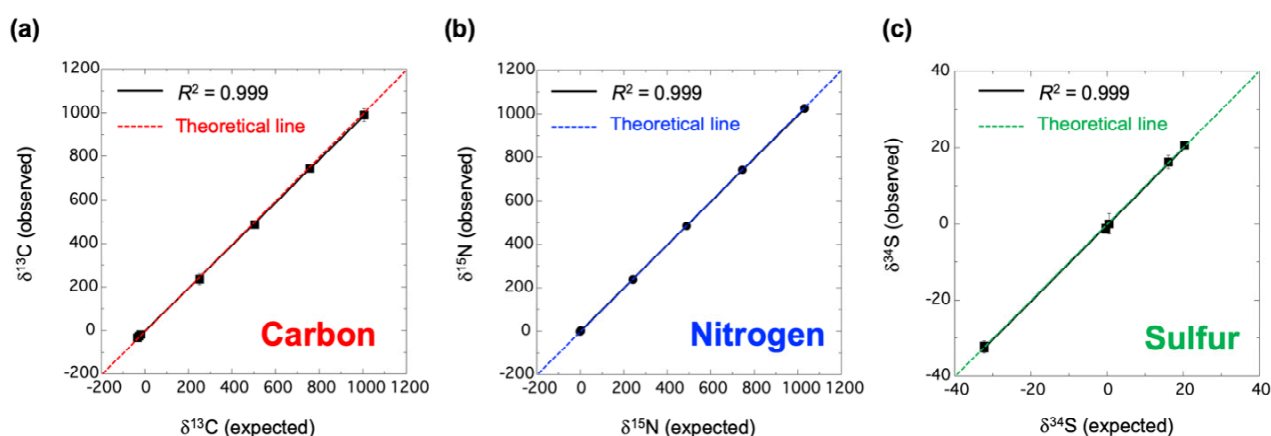


Figure 1 The high precision and high accuracy analytical optimization using reference standards of carbon (C), nitrogen (N), and sulfur (S) for covering wide range isotopic compositions: **(a)** $\delta^{13}\text{C}$, ‰ vs. VPDB; within ^{13}C -enriched and ^{13}C -depleted profiles, **(b)** $\delta^{15}\text{N}$, ‰ vs. Air; within ^{15}N -enriched and ^{15}N -depleted profiles, **(c)** $\delta^{34}\text{S}$, ‰ vs. VCDT; within ^{34}S -enriched and ^{34}S -depleted profiles. The x-axis and y-axis stand for the nominal value (= expected) and the measured value (= observed), respectively. Prior to the Hayabusa2 samples, those analytical validations using the nano-EA/IRMS system [3,4,7] were performed during the rehearsal analyses (e.g., several carbonaceous chondrite of CM2 and C2-ungrouped: unpublished data) at JAMSTEC. We have confirmed that there was no memory effect in the analytical lines due to sequential process. For further of optimization ultra-small-scale sulfur (S) quantification with $\delta^{34}\text{S}$ validation, please see the latest update [11].

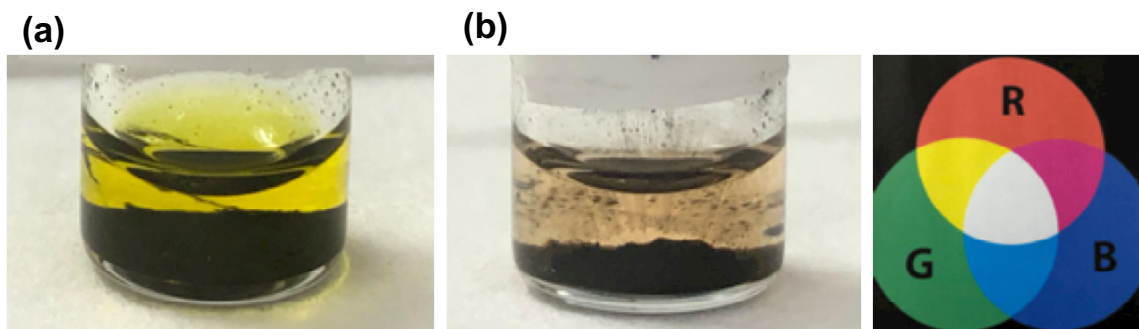


Figure 2 (a, b) Capturing the representative colors during the sequential solvent extraction and the wet chemical treatment for the Hayabusa2 samples (Ryugu, sample ID: A106 & C107). After solid-liquid separation, the colored supernatant with yellowish and pinkish colors were observed in both A106 and C107, the photo taken in the cleanroom at Dept. Earth Planet Sci., Kyushu Univ. Since dissolved inorganic elements and organic-inorganic complex molecules also have some kind of chromaticity depending on the affinity of the solvent, we are in the process of conducting detailed verification. Please see also the residue of insoluble organic matter (IOM, black color) on the bottom of the vial. The onsite RGB color scale is shown.

We observed some of the colored supernatant during the sequential solvent extraction processes of Ryugu sample (Figure 2). These extraction samples have been safely distributed to the SOM team members and are being analyzed in detail at their laboratories [12]. The residue of IOM fraction has been also seamlessly transported to the other initial analysis team for further description [13]. Here, we note that the colors of the extract show the chemical responses of the extractable indigenous organic molecules to the inherent affinity of the solvent from low to high polarity (i.e., dependent on hydrophilicity, hydrophobicity, and amphiphilicity with both properties). Also, the colored supernatant may indicate that there is a certain amount of components with a significant absorption spectrum (e.g., chemically various carbon skeleton with N-, S-, O-hetero structures). Regarding the molecular-level analysis, we are currently in the process of combining the pieces of the raw data profiles [12], and we expect synergistic discussions at this symposium in terms of native organic properties within the history of the Ryugu.

References

- [1] Tachibana S. et al., #1289, 52nd LPSC (2021); Tachibana S. et al., *Geochem. J.* 48, 571-587 (2014).
- [2] Yada T. et al., #2008, 52nd LPSC (2021).
- [3] Naraoka H., Takano Y., Dworkin, J. P. et al., #6314, 82nd Met Soc (2019); Naraoka H. et al., #1362, 51st LPSC (2020).
- [4] Ogawa N. O. et al., 51st LPSC (2020); Ogawa N. O. et al. *Earth, Life, Isotopes*, Kyoto Univ. Press. (2010).
- [5] Yoshimura T. et al., #1971, 51st LPSC (2020); Yoshimura, T. et al. *J. Chromatogr. A* 1531, 157-162 (2018).
- [6] Wang Z. et al., *Anal. Chem.* 92, 2034-2042 (2019); Bonifacie M. et al., *Geochim. Cosmochim. Acta* 200, 255-279 (2017).
- [7] Kebukawa Y. et al., *Meteorit Planet Sci.* 56, 1311-1327 (2021); Kebukawa Y. et al., *Geochim. Cosmochim. Acta* 271, 61-77 (2020); Chan H. S., et al., *Earth, Planets Space*, 68, 7 (2016).
- [8] Oba Y. et al., *Nature Commun.* 10, 4413 (2019); Oba Y. et al., *Nature Commun.* 11, 6243 (2020).
- [9] Takano Y. et al., *Inter. J. Mass Spectrom.* 462, 116529 (2021).
- [10] Kerridge J.F. *Geochim. Cosmochim. Acta* 49, 1707-1714 (1985); Füri, E. and Marty B., *Nature Geosci.* 8, 515-522 (2015).
- [11] Ogawa N. O. et al., #PR0203, *Geochem. Soc. Jpn.* (2021).
- [12] Naraoka H., Takano Y., Dworkin, J. P., this symposium. & the other reports from the Hayabusa2-initial-analysis SOM team.
- [13] Initial reports from the Hayabusa2-chemistry, -stone, -sand, -volatile, -IOM team at this symposium.

Compound distribution determined by nanoLC-Orbitrap MS

Francois-Regis Orthous-Daunay¹, Cédric Wolters¹, Véronique Vuitton¹, Roland Thissen¹, Junko Isa², Hiroshi Naraoka³, Hisayoshi Yurimoto⁴, Tomoki Nakamura⁵, Takaaki Noguchi⁶, Ryuji Okazaki⁷, Hikaru Yabuta⁸, Kanako Sakamoto⁹, Shogo Tachibana^{9,10}, Seiichiro Watanabe¹¹ and Yuichi Tsuda⁹, and the Hayabusa2-initial-analysis SOM team

¹Univ. Grenoble Alpes CNRS IPAG, ²Tokyo Inst. Tech., ³Kyushu Univ., ⁴Hokkaido Univ., ⁵Tohoku Univ., ⁶Kyoto Univ., ⁷NASA Goddard Space Flight Center, ⁸Hiroshima Univ., ⁹JAXA, ¹⁰Univ. Tokyo, ¹¹Nagoya Univ

The Hayabusa2 mission is no less than the first opportunity to infirm or confirm theories about the formation of C-type asteroids [1], [2]. The origin and nature of the organic molecules Ryugu bears will tell which part of this chemistry takes place on this type of airless bodies and which part is inherited by accretion. The comparison with carbonaceous chondrite will be the method to evaluate if what has been interpreted from well-studied meteoritical samples is still valid for actual asteroid regolith. This study focuses on the molecular mixture complexity observed thanks to the combination of two analytical methods: liquid phase chromatography and high-resolution mass spectrometry [3]. Samples from the first (named A106) and second (C107) encounter with Ryugu were washed with different solvents in order to extract the soluble organic compounds in a sequence of increasing polarity in Kyushu University. Each extract was separated on an amide column with limited volume and flow in a so-called nano-liquid-chromatography (nano-LC) protocol. The chemical separation is monitored through time by Orbitrap-mass-spectrometry (Orbitrap-MS).

This provides three observables for each compound present in the Ryugu soil extract: an intensity evaluating its relative abundance, a retention time depending on its structure and a molecular weight equivalent to its atomic composition. With thousands of different compounds, mixtures usually exhibit peculiar patterns in this three-dimensional framework. For instance, the relative abundance of phospholipids in terrestrial living cells varies by orders of magnitude if the carbon atoms number is odd or even, making contamination by fingerprints easy to detect. We used the ATTRIBUTOR routines developed at University of Grenoble Alpes to extract relevant patterns in the Ryugu extracts chromatograms [4].

The most remarkable feature found in both meteorites and Ryugu samples is a ubiquitous polymerization pattern [5]. Almost each measured mass is part of a network linking it to other molecules with one more carbon atom, two more hydrogen atoms or any combination of these. A typical bell-shaped intensity distribution indicates that the whole mixtures are likely to be of one single synthesis origin [6]. Variability of the distribution characteristics goes with a complex origin of subsequent processes. This type of mass and intensity patterns is difficult to find in other terrestrial natural samples.

The less polar molecules found in Murchison have extremely broad distributions, only matched by some of the Ryugu's compounds and other chondrites. For these molecules, the best analogues are solid residues generated out of gas mixtures in plasma chambers [7]. Experimental polymers synthesized in liquid phase or by irradiation of ices have significantly different polymerization patterns [8].

The chemical structure of compounds found in Ryugu slightly differs from the one in the CM2 Murchison chondrite. As of preliminary identification, the less polar compounds are similar between Ryugu and Murchison while the most polar molecules have significantly different retention times. Assuming polar compounds are more likely to be part of a reaction in liquid water, the discrepancy between Murchison and Hayabusa2 samples could be due to different degree of aqueous alteration on their parent bodies.

References

- [1] Tachibana, S. *et al.* 2021.*Lunar Planet. Sci. Conf.*p. 1289 [2] Yada, T. *et al.* 2021.*Lunar Planet. Sci. Conf.*p. 2008 [3] Naraoka, H.Takano, Y.Dworkin, J. P.and SOM Analysis Team. 2020.*Lunar Planet. Sci. Conf.*p. 1362 [4] Orthous-Daunay, F.-R.Thissen, R.and Vuitton, V. Apr. 2019.*Proc. Int. Astron. Union.*vol. 15, no. S350.pp. 193–199 [5] Naraoka, H.Yamashita, Y.Yamaguchi, M.and Orthous-Daunay, F. R. 2017.*ACS Earth Sp. Chem.*vol. 1, no. 9.pp. 540–550 [6] Orthous-Daunay, F.-R. *et al.* 2019.*Geochem. J.*vol. 53, no. 1 [7] Bekaert, D. V. *et al.* 2018.*Astrophys. J.*vol. 859, no. 2.p. 142 [8] Vinogradoff, V.Bernard, S. Le Guillou, C.and Remusat, L. 2017.*Icarus.*vol. 305.pp. 358–370

Highest molecular diversity and structural complexity revealed with ultrahigh resolution mass spectrometry and nuclear magnetic resonance spectroscopy of Ryugu's samples

Philippe Schmitt-Kopplin^{1,2}, Norbert Hertkorn², Marianna Lucio², Marco Matzka², Mourad Harir², Philippe Diederich², Hiroshi Naraoka³, Hisayoshi Yurimoto⁴, Tomoki Nakamura⁵, Takaaki Noguchi⁶, Ryuji Okazaki³, Hikaru Yabuta⁷, Kanako Sakamoto⁸, Shogo Tachibana^{8,9}, Seiichiro Watanabe¹⁰ and Yuichi Tsuda⁸
and the Hayabusa2-initial-analysis SOM team

¹ *Technische Universität Muenchen, Germany*, ² *Helmholtz Zentrum Muenchen, Germany*,
³ *Kyushu Univ., Japan*, ⁴ *Hokkaido Univ., Japan*, ⁵ *Tohoku Univ., Japan*, ⁶ *Kyoto Univ., Japan*,
⁷ *Hiroshima Univ., Japan*, ⁸ *JAXA, Japan*, ⁹ *Univ. Tokyo, Japan*, ¹⁰ *Nagoya Univ., Japan*.

The surface and possible sub-surface materials of the asteroid Ryugu were recovered during the two touch-down sampling by the Hayabusa2 spacecraft. Here we present the first results on the solvent soluble organic matter (SOM) using ultrahigh-resolution Fourier transform ion cyclotron resonance mass spectrometry (FTICR/MS) complemented with high field nuclear magnetic resonance spectroscopy (NMR) [1-3]. The two samples A106 (first touchdown) and C107 (second touchdown) were sequentially extracted in the Hayabusa2-initial-analysis SOM team with various polar and apolar solvent extracts and demonstrate a never seen molecular complexity and diversity.

We confirm herewith the close similarity and the possible comparison of the solvent extracts with meteoritic material to the Hayabusa2 return samples. We analyzed the sequential hexane, dichloromethane (DCM), methanol and water extracts with NMR and with electrospray ionization (ESI) and atmospheric pressure photoionization (APPI) [4] FTICR/MS systematically for both negative and positive ions. The hundred thousands of signals were filtered, converted and assigned into more than 24,000 elementary compositions consisting of carbon (C), hydrogen (H), nitrogen (N), oxygen (O) and/or sulfur (S). Organomagnesium compounds (CHOMg, CHOSMg) were not found and this reflects the low temperature processes on the parent body [5, 6]. As shown for carbonaceous chondrites previously, our results confirm that the extraterrestrial chemical diversity is much higher compared to terrestrial biological and biogeochemical spaces and consists in a regular continuum (i) of small to macromolecules (ii) of carbon oxidation states from apolar (CH, polycyclic aromatic hydrocarbons and branched aliphatics) to polar small molecules (CHO) with increasing functionalized oxygen and heteroatom contents (CHN, CHS, CHNO, CHOS) leading to the observed differential solvent type solubility. We revealed specific known molecular targets (CHN⁺, CHNO⁺) [4] and show evidences of multiple chemosynthesis pathways in describing the carbon oxidation state distribution and heteroatom contributions to the assembly of multiple complex endogen molecules; these also reflect cold hydrothermalism involved on the parent body [5,6]. We also confirm the high importance of chemical processes involving specific nitrogen and sulfur chemistry [7, 8]. The two fractions analyzed show an extreme coverage in structural features in APPI and only slight differences in the apolar solvents in ESI. The A106 sample showed slight differences only with higher mass range and more oxygenated compounds. The C107 sample had increased abundance and uniqueness of more unsaturated carbon and low oxygenated compounds that may have disappeared due to surface processing (some hypothesis could be cosmic irradiation at the surface). These samples presents a unique opportunity of having a direct and low invasive insight into the complex organic diversity present on 162173 Ryugu.

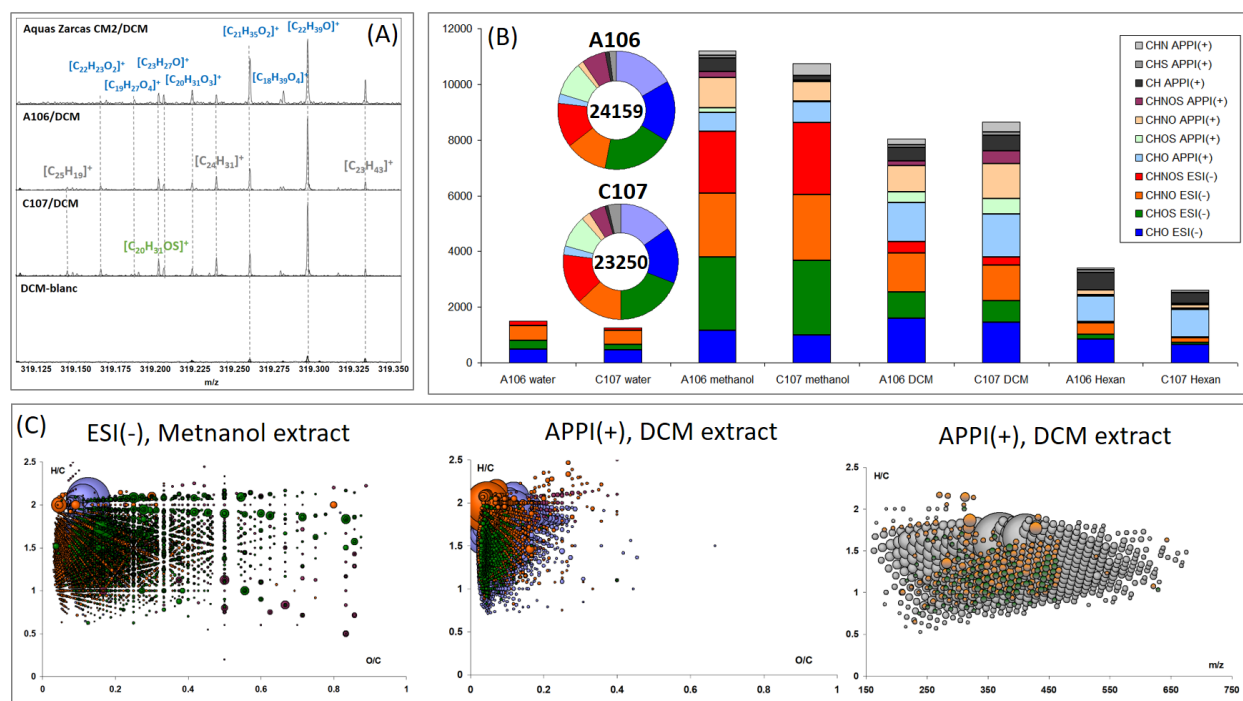


Figure 1. Selected results from the analysis of the solvent extracts of A106 (24159 formula) and C107 (23250 formula) analyzed with Fourier transform ion cyclotron resonance mass spectrometry (FTICR-MS) in electrospray ionization negative mode (ESI(-)) and atmospheric pressure photoionization (APPI(+)). **(A)** nominal mass 319 details of dichloromethane (DCM) extracts of the CM2 Aguas Zarcas, A106, C107 and the DCM-blanc with the annotated elementary compositions as CH, CHO and CHNO from ultrahigh resolution. **(B)** counting of the thousands of elementary compositions in the C, H, O, N, S space as obtained from ESI(-) and APPI(+), and their abundance variations within the different extraction solvents for the A106 and C107 samples. **(C)** visualization of the structural information retrieved from the elementary compositions as van Krevelen diagram plots describing the differences in oxygenations between the two ionization modes ESI(-) and APPI(+), and the profiles of the non-oxygenated CH, CHS and CHN compounds.

References

- [1] Schmitt-Kopplin, P. et al. 2010. *Proc. Natl. Acad. Sci. U.S.A.*, 107:2763.
- [2] Ruf, A. et al. 2018. *Life* 8:18.
- [3] Hertkorn, N. et al. 2015 *Magn. Reson. Chem.*, 53:754.
- [4] Herzog J. et al. 2019. *Life*, 9:48.
- [5] Ruf, A. et al. 2017 *Proc. Natl. Acad. Sci. U.S.A.*, 2017, 114:2819.
- [6] Matzka, M. et al. 2021. *Astrophys. J. Lett.*, 915:L7.
- [7] Danger, G. et al. 2021. *Nat. Commun.*, 12:1.
- [8] Danger, G. et al. 2020. *Planet. Space Sci.*, 1:55.

The Winchcombe Meteorite: A Pristine Sample of the Outer Asteroid Belt

Ashley J. King¹, Luke Daly², Katie H. Joy³, Helena C. Bates¹, James F. J. Bryson⁴, Queenie H. S. Chan⁵, Patricia L. Clay³, Hadrien A. R. Devillepoix⁶, Richard C. Greenwood⁷, Sara S. Russell¹, Martin D. Suttle⁷ & the Winchcombe Consortium
¹Natural History Museum, London, ²University of Glasgow, ³University of Manchester, ⁴University of Oxford, ⁵Royal Holloway, University of London, ⁶Curtin University, ⁷The Open University (a.king@nhm.ac.uk)

At 21:54 (UT) on the 28th February 2021 a bright fireball was observed travelling approximately W to E over the United Kingdom. The fireball lasted ~7 seconds and was recorded by 16 stations operated by the six meteor camera networks of the UK Fireball Alliance (UKFALL); it was also caught on numerous dashboard and doorbell cameras and there were >1000 eyewitness accounts, including reports of a sonic boom. Following an appeal in the national media, the main mass (~320 g) of the meteorite was discovered by a family in Winchcombe, Gloucestershire. The stone landed on the family's driveway, shattering into a pile of dark mm- to cm-sized fragments and powder, most of which they collected wearing gloves and sealed within plastic bags ~12 hours after the fall. Further meteorites were recovered in the local area over the following week by members of the public and during an organised search by the UK planetary science community, with the largest piece being a 152 g fusion-crust stone found on the 6th March 2021 on farmland. In total, >500 g of the Winchcombe meteorite was recovered less than seven days after the fall, with no significant rainfall having occurred during that time.

The entry velocity of the Winchcombe meteoroid was ~14 kms⁻¹ and the videos clearly show several fragmentation events in the atmosphere. Preliminary analysis of the video footage combined with the measurement of short-lived cosmogenic radionuclides suggest that the original body was small (<100 kg). The calculated pre-atmospheric orbit of the Winchcombe meteoroid suggests an origin in the outer asteroid belt; the orbit is similar to those previously reported for the Sutter's Mill (C) and Maribo (CM2) meteorites, but distinct from Tagish Lake (C2_{ung}) and Flensburg (C1_{ung}) [1–4].

Inspection of stones and fragments “by-eye” and petrographic observations of 18 polished samples by optical and electron microscopy indicate that Winchcombe is a CM (“Mighei-like”) carbonaceous chondrite. It consists of chondrules and calcium-aluminium-rich inclusions (CAIs) set within a matrix (SiO₂ ~28 wt%, FeO ~24 wt%, MgO ~18 wt%, total ~80 wt%) of phyllosilicates, carbonates, magnetite and sulphides. X-ray diffraction (XRD) analysis of several fragments show that the phyllosilicates are a mixture of Fe- and Mg-bearing serpentines present at >80 vol%. Many of the polished samples, plus mm-sized chips characterised using computed tomography (CT), show evidence for brecciation and contain multiple distinct lithologies with sharp boundaries. Most lithologies record a high degree of aqueous alteration (CM2.0 – 2.2 on the Rubin et al. [5] scale); chondrules and CAIs retain well preserved fine-grained rims (FGRs) but have been extensively replaced by secondary minerals including abundant tochilinite-cronstedtite intergrowths (TCIs) and carbonates. A rare lithology containing unaltered chondrules and metal has also been identified. The sulphides are mainly pyrrhotite and pentlandite, and magnetite typically has a framboidal structure. Several large (~50–100 μm) sulphate grains have been found embedded within the matrix, with their textural setting suggesting that they formed from a fluid on the parent body.

The classification of Winchcombe as a CM chondrite is further supported by bulk major and minor element abundances and oxygen ($\delta^{17}\text{O} = 2.75 \text{ \& } 0.94$; $\delta^{18}\text{O} = 9.48 \text{ \& } 7.29$; $\Delta^{17}\text{O} = -2.18 \text{ \& } -2.85$) and titanium isotopic compositions. The bulk water content of Winchcombe is ~12 wt% and analysis of two chips by stepped combustion yielded carbon (~2.0 wt%) and nitrogen abundances and isotopic compositions consistent with other highly altered CM chondrites [e.g. 6]. The release profiles indicated the presence of multiple carbon- and nitrogen-bearing organic components and low voltage SEM characterisation of unprepared chips less than a week after the fall identified several carbon-rich regions with “globule-like” morphologies. However, initial analysis by gas chromatography-mass spectrometry (GC-MS) suggests that the total amino acid abundance in Winchcombe is significantly lower than in most CM chondrites [e.g. 7].

The Winchcombe meteorite is only the fifth carbonaceous chondrite fall with a known pre-atmospheric orbit, and due to its rapid recovery is likely the most pristine member of the CM group. The mineralogical, elemental, and organic properties of Winchcombe provide a snapshot of conditions in the protoplanetary disk and new insights into the chemical and dynamic evolution of volatiles in the early solar system. The nature of the Winchcombe meteorite and timing of the fall makes it complementary to samples of asteroids Ryugu and Bennu collected by the Hayabusa2 and OSIRIS-REx missions, offering an opportunity to develop and rehearse analytical protocols on fresh, carbonaceous materials.

References: [1] Jenniskens et al. (2012) *Science* 338:1583. [2] Borovička et al. (2019) *M&PS* 54:1024. [3] Brown et al. (2000) *Science* 290:320. [4] Borovička et al. (2021) *M&PS* 56:425. [5] Rubin et al. (2007) *GCA* 71:2361. [6] Alexander et al. (2013) *GCA* 123:244. [7] Glavin et al. (2006) *M&PS* 41:889.

Thermal History of Dehydrated CY Chondrites Reconstructed from their Fe-sulfide Grains

Catherine S. Harrison^{1,2}, Ashley J. King¹, Rhian H. Jones² and Tobias Salge¹

¹*Department of Earth Sciences, Natural History Museum, London, SW7 5BD, UK*

²*Department of Earth and Environmental Sciences, University of Manchester, Manchester, M13 9PL, UK*

Introduction: Following low temperature (<200 °C) aqueous alteration, the CY carbonaceous chondrites experienced significant post-hydration heating (>500 °C) on their parent body, evidenced by dehydrated phyllosilicates, secondary recrystallized olivine, the destruction and modification of organics, low water contents, and melting of Fe-sulfides [e.g., 1-4]. However, the timing, duration and mechanism of this heating is currently poorly defined. Constraining the thermal history of the CY chondrites is an important step to understanding the evolution of the water-rich C-complex asteroids, and the distribution and transport of volatiles in the early solar system. Our studies also provide a framework for interpreting the samples returned from Ryugu, as the initial results of JAXA's Hayabusa2 mission suggest that materials on Ryugu record periods of both aqueous and thermal alteration [5].

Sulfides are widespread in the carbonaceous chondrites and are sensitive to both aqueous alteration and thermal metamorphism. The unheated CM and CR chondrites contain primary and secondary Fe-sulfides that can provide a detailed record of the conditions within the nebula prior to accretion, as well as aqueous alteration on the parent bodies [6-9]. The CY chondrites contain a third generation of sulfides, specifically pyrrhotite ([Fe,Ni]_{1-x}S) containing inclusions of pentlandite ([Fe,Ni]₉S₈), that formed from the cooling of a monosulfide solid solution (MSS, [Fe,Ni]_{1-x}S) during the metamorphic event [e.g., 6, 7]. Experimental work on synthesized MSS compositions has shown that the textural features and compositions of these sulfides are diagnostic of their cooling histories [10-12].

Here, we have systematically characterized the pyrrhotite-pentlandite grains within the matrices of CY chondrites of heating stages III (peak temperature 500-700 °C) and IV (peak temperature >750 °C) [13], to infer their thermal history.

Samples and Methods: We have characterized up to 20 coarse (>40 µm) sulfide grains within each of five CY chondrites: Yamato (Y-) 82162 and Y-86029 (both Stage III [2]), Y-86789 and Y-86720 (likely paired, Stage IV [2, 14]), and Belgica (B-) 7904 (Stage IV [2]). Scanning electron microscopy (SEM) and energy dispersive spectrometry (EDS) has been carried out at 20 kV and 1.5 nA for one polished section of each sample using a ZEISS Evo 15LS SEM equipped with an Oxford Instruments Aztec EDS system at the Natural History Museum (NHM). To improve the spatial EDS resolution to the sub-micrometre scale, one grain in B-7904 was analysed at 6 kV using an FEI Quanta field emission SEM and Bruker annular EDS detector at the NHM.

Results: The sulfide grains can be separated into two assemblage types - pyrrhotite containing inclusions of pentlandite (PoPn), and pyrrhotite containing inclusions of both pentlandite and metal (PoPnM). Table 1 summarizes the number of grains belonging to each assemblage type, the average nickel content of the pyrrhotite and pentlandite, and the typical size of the pentlandite and metal inclusions. Within each sample, the pentlandite inclusions are commonly associated with cracks in the pyrrhotite, and occasionally occur as isolated blebs within the pyrrhotite grains. In Y-82162, the pentlandite inclusions are oriented laths, whereas in Y-86029, Y-86720, Y-86789 and B-7904 they are irregular in shape and randomly oriented. The PoPnM grains are only present in the Stage IV meteorites Y-86720, Y-86789 and B-7904, and can contain both Ni-rich (up to 56 wt% Ni) and Ni-poor (<6 wt% Ni) metal inclusions (Figure 1). In B-7904 the metal inclusions are anhedral and typically <5 µm in size, although the largest inclusion is ~20 µm in size. In Y-86720 and Y-86789 the metal inclusions are irregular in shape and tend to form along the outer edge of the sulfide grains. Large area elemental EDS mapping of complete sections show that the paired meteorites Y-86789 and Y-86720 both contain a sulfide-rich and a sulfide-poor lithology. All analysed grains within the sulfide-rich lithology are PoPnM type, while in the sulfide-poor lithology they are PoPn type.

Table 1. Properties of the Fe-sulfide grains in Stage III and IV CY chondrites.

Sample (section number)	Heating Stage	No. of PoPn grains	No. of PoPnM grains	Avg. Po Ni content (wt%)	Avg. Pn Ni content (wt%)	Typical Pn inclusion size	Typical M inclusion size
Y-82162 (45-1)	III	11		0.15 ± 0.10 [106]	14.9 ± 1.9 [74]	<5 µm	
Y-86029 (51-A)	III	10		0.15 ± 0.04 [57]	12.1 ± 2.3 [58]	<5 µm	
B-7904 (64-A)	IV		7	0.18 ± 0.08 [38]	14.7 ± 1.4 [17]	<15 µm	<5 µm
Y-86720 (59-A)	IV	9	11	0.13 ± 0.04 [52]	14.4 ± 2.4 [15]	<12 µm	<10 µm
Y-86789 (81-A)	IV	8	8	0.11 ± 0.07 [61]	15.0 ± 1.8 [46]	<10 µm	<10 µm

Po = pyrrhotite, Pn = pentlandite, M = metal, No. = number. Avg. = average. The number of data points for the average Ni contents are in parentheses.

Discussion: Annealing experiments on synthesized MSS compositions show a sequence of pentlandite exsolution textures that evolve with time, where the final morphology of the pentlandite is largely dependent on the cooling rate [10-12]. The quickest cooling rates (<10 K/hr) produce irregular and randomly oriented pentlandite inclusions, while slower cooling rates (>100 K/hr) result in oriented blades/lamellae of pentlandite [11]. The oriented laths of pentlandite within Y-82162 suggest that the sulfides within this sample experienced a slower cooling rate in comparison to those observed in Y-86029, B-7904, Y-86720 and Y-86789. If impacts were the source of heat, this possibly suggests that Y-82162 samples a deeper layer of insulating regolith than the other CY chondrites. Alternatively, Y-82162 might originate from the surface of a parent body that orbited sufficiently close to the sun for solar radiation to keep temperatures elevated for a longer period of time [15]. However, other factors such as the peak metamorphic temperature and the initial MSS composition (metal:S ratio and Fe:Ni ratio) also affect the final pentlandite abundance and morphology. While the experimental work of [10-12] is useful for estimating relative cooling rates between meteorite samples, the ranges of sulfide compositions and environmental conditions considered in these studies are not directly comparable to those on the parent body(ies) of the CY chondrites. For example, the experimental work did not produce any metal-bearing sulfide grains like those observed in Y-86720, Y-86789 and B-7904. It has been suggested that the Fe,Ni-metal inclusions formed through the thermal decomposition of pentlandite and pyrrhotite at temperatures >610 °C under reducing conditions at an fS_2 near the iron-troilite buffer [7, 16], but the influence of the metal inclusions on the texture and morphology of pentlandite requires further experimental work.

Kimura et al. [6] and Harries and Langenhorst [7] also studied the sulfides within Y-86720 (section 71-3 and fragment 86, respectively) and B-7904 (section 94-1 and fragment 114, respectively). In both samples, they only identified metal-bearing sulfide grains that lacked pentlandite (i.e. PoM grains). In contrast, we observed only PoPnM grains within B-7904, and identified two different lithologies within Y-86720 and Y-86789 that contain either PoPnM or PoPn grains. This is consistent with these meteorites being breccias and suggests that the different lithologies each experienced different thermal histories. Based on the thermal decomposition of pentlandite into Fe,Ni-metal with higher temperatures [7, 16], we suggest a decreasing order of peak metamorphic temperature between the lithologies to be PoM > PoPnM > PoPn. Evidence for heterogeneous heating among the different lithologies could explain variable estimates for peak metamorphic temperatures within the literature. For example, estimates for Y-86720 range from 500 °C [17] up to 850 °C [18], while for B-7904 they vary between 400 °C [19] and 900 °C [18].

Heterogeneous heating within the CY chondrites could result from highly localized variations in the metamorphic conditions.

Alternatively, the PoM lithology might have been heated to a greater extent than the PoPn lithology during the metamorphic event, before impacts mixed different lithologies to form a heterogeneous breccia. It is also possible that the primary and/or secondary sulfides within each lithology were compositionally very different prior to heating.

Summary: There are differences in the textural features of the sulfide grains and their associations with Fe,Ni-metal among each of the CY samples, and also among different lithologies within the samples. This suggests the CY chondrites experienced varied thermal histories. Deciphering the cause of these differences will allow us to further develop thermal models for hydrous asteroids.

References: [1] Ikeda (1992) *Proc. NIPR Symp. Antarct. Meteorites* **5**:49. [2] King et al. (2019) *Geochem* **79**:125531. [3] Tonui et al. (2014) *GCA* **126**:284. [4] Quirico et al. (2018) *GCA* **241**:17. [5] Kitazato et al. (2019) *Science* **364**:272. [6] Kimura et al. (2011) *M&PS* **46**:431. [7] Harries and Langenhorst (2013) *M&PS* **48**:879. [8] Schrader et al. (2015) *M&PS* **50**:15. [9] Singerling and Brearley (2020) *M&PS* **55**:496. [10] Durazzo and Taylor (1982) *Miner Deposita* **17**:313. [11] Kelly and Vaughan (1983) *Mineral. Mag.* **47**:453. [12] Etschmann et al. (2004) *Am. Mineral.* **89**:39. [13] Nakamura et al. (2005) *J. Min. Petrol. Sci.* **100**:260. [14] Matsuoka et al. (1996) *Proc. NIPR Symp. Antarct. Meteorites* **9**:20. [15] Chaumard et al. (2012) *Icarus* **220**:65. [16] Harries (2018) *Hayabusa Symposium* (abstract). [17] Zolensky et al. (1993) *GCA*. **57**:3123 [18] Akai (1992) *Proc. NIPR Symp. Antarct. Meteorites* **5**:120. [19] Zolensky et al. (1991) *Proc. NIPR Symp. Antarct. Meteorites* **16**:195.

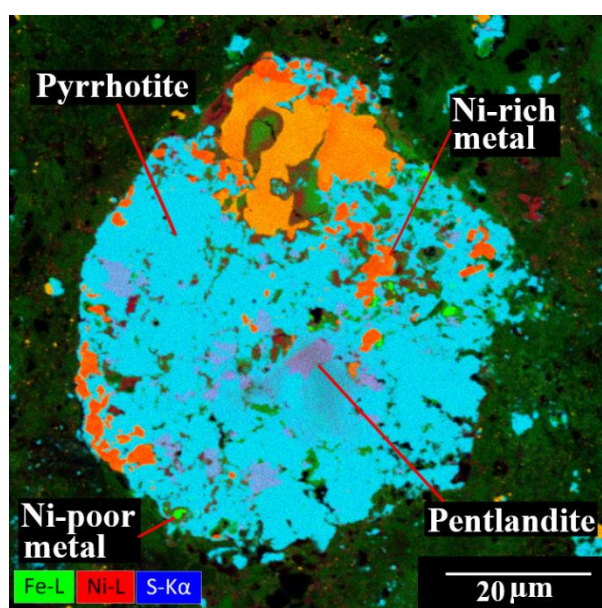


Figure 1. EDS net intensity map of a PoPnM sulfide grain in B-7904. (6V, 890 pA, 319 kcps, 1680x1680 pixels, 50 nm pixel size, 129 min). Fe – green, Ni – red, S – blue.

Hydrothermal history of (162173) Ryugu's parent body inferred from remote-sensing data

Eri Tatsumi^{1,2,3}, Naoya Sakatani⁴, Lucie Riu⁵, Moe Matsuoka⁵, Rie Honda⁶, Tomokatsu Morota³, Shingo Kameda⁴, Tomoki Nakamura⁷, Michael Zolensky⁸, Rosario Brunetto⁹, Takahiro Hiroi¹⁰, Sho Sasaki¹¹, Sei'ichiro Watanabe¹², Satoshi Tanaka^{5,13}, Jun Takita¹⁴, Cédric Pilorget⁹, Julia de León^{1,2}, Marcel Popescu¹⁵, Juan Luis Rizo^{1,2}, Javier Licandro^{1,2}, Ernesto Palomba¹⁶, Deborah Domingue¹⁷, Faith Vilas¹⁷, Humberto Campins¹⁸, Yuichiro Cho³, Kazuo Yoshioka³, Hiroataka Sawada⁵, Yasuhiro Yokota⁵, Masahiko Hayakawa⁵, Manabu Yamada¹⁹, Toru Kouyama²⁰, Hidehiko Suzuki²¹, Chikatoshi Honda²², Kazunori Ogawa⁵, Kohei Kitazato²², Naru Hirata²², Naoyuki Hirata²³, Yuichi Tsuda^{5,13}, Makoto Yoshikawa^{5,13}, Takanao Saiki⁵, Fuyuto Terui⁵, Satoru Nakazawa⁵, Yuto Takei⁵, Hiroshi Takeuchi^{5,13}, Yukio Yamamoto^{5,13}, Tatsuaki Okada^{5,3}, Yuri Shimaki⁵, Kei Shirai²³, Fernando Tinaut^{1,2}, Sunao Hasegawa⁵, Seiji Sugita^{3,19}

¹*Instituto de Astrofísica de Canarias (etatsumi-ext@iac.es)*, ²*Dept. Astrophysics, Univ. La Laguna*, ³*The University of Tokyo*, ⁴*Rikkyo University*, ⁵*Institute of Space and Astronautical Science (ISAS)*, ⁶*Kochi University*, ⁷*Tohoku University*, ⁸*NASA Johnson Space Center*, ⁹*Université Paris-Saclay, CNRS, Institut d'Astrophysique Spatiale*, ¹⁰*Brown University*, ¹¹*Osaka University*, ¹²*Nagoya University*, ¹³*SOKENDAI*, ¹⁴*Hokkaido Kitami Hokuto High School*, ¹⁵*Astronomical Institute of the Romanian Academy*, ¹⁶*INAF, Instituto di Astrofisica e Planetologia Spaziali*, ¹⁷*Planetary Science Institute*, ¹⁸*University of Central Florida*, ¹⁹*Planetary Exploration Research Center, Chiba Institute of Technology*, ²⁰*National Institute of Advanced Industrial Science and Technology*, ²¹*Meiji University*, ²²*The University of Aizu*, ²³*Kobe University*.

1. Summary

Small rubble pile asteroids record the thermal evolution of their much larger parent bodies. However, recent space weathering and/or solar heating create ambiguities between the uppermost layer observable by remote-sensing and the pristine material from the parent body. Hayabusa2 remote-sensing observations find that on the asteroid (162173) Ryugu both north and south pole regions preserve the least space-weathered material, which is spectrally blue carbonaceous chondritic material with a 0 – 3% deep 0.7- μm band absorption, indicative of Fe-bearing phyllosilicates [1]. We report that spectrally blue Ryugu's parent body experienced intensive aqueous alteration and subsequent thermal metamorphism at 570 – 670 K (300 – 400 °C), suggesting that Ryugu's parent body was heated by radioactive decay of short-lived radionuclides possibly because of its early formation 2-2.5 Ma. The samples being brought to Earth by Hayabusa2 will give us our first insights into this epoch in solar system history. Moreover, we found the NUV-VIS spectral similarity between Ryugu and Polana–Eulalia family members, suggesting plausible origin from inner main belt predicted by the dynamical simulation [2].

2. Observation on polar regions

Ryugu could be an ideal body to study the thermal history and water/rock ratio of pre-disruption parent bodies, much larger (~100 km) than Ryugu. Our objective is to find the most pristine material on Ryugu and to study evidence for proposed thermal metamorphism of its original parent body and consequent processes after its catastrophic disruption and re-accumulation. Stratigraphic analyses have suggested that the possible surviving, unprocessed materials are bluer than the average Ryugu reflectance spectrum [3,4]. Slightly bluer materials than the average were found on the equatorial ridge, which might be uncovered by regolith migration from the ridge to the middle latitudinal regions. Furthermore, the global observations obtained by the Hayabusa2 spacecraft discovered that the bluest materials are distributed at the polar regions of Ryugu [3]. This motivated us to conduct detailed surveys of the polar regions to investigate the unprocessed materials. Effects after the formation of Ryugu, such as solar wind irradiation, micrometeoroid bombardment, and radiative heating caused by close encounter to the Sun, need to be deconstructed.

Spectrally blue (negative visible spectral slope) material is concentrated on both poles, as clearly shown. Furthermore, blue material is associated with a relatively deeper 0.7- μm band absorption. Phyllosilicates in CM/CI chondrites become progressively enriched in Mg (and depleted in Fe) as aqueous alteration proceeds [5]. Thus, Fe-bearing phyllosilicates showing 0.7- μm band absorption are a strong indication of the specific water/rock ratio condition during the parent body formation. To examine the cause of the distribution of blue materials with 0.7- μm band absorption, the maximum temperature in an asteroidal year and the normalized solar photon dose were calculated based on the TIR measurements [6], the shape model and current orbital elements. The comparison indicates that areas and facets with low solar wind irradiation fluxes exhibit blue spectra and relatively deeper 0.7- μm absorption, while the influence of solar heating does not clearly correlate with the spectral characteristics. On the north pole, the concentration of the material with blue spectral slope, and deeper 0.7- μm band absorption were well correlated with the regions experiencing the lowest temperatures and least solar wind irradiation due to the large incidence angle during the whole asteroidal year. The correspondence between the color variation and those

processes shows that solar wind irradiation is a more likely cause for the color changing from blue to red and the decrease in the 0.7- μm band absorption depth

3. Possible connection with (3200) Phaethon

(3200) Phaethon, the target of the DESTINY+ Mission, exhibits blue spectra in the visible wavelength range and turn-up in the UV. Recently, many ground-based observations were made over a wide wavelength range, which reported that the variation in visible spectral slope depends on rotational phase. The range of spectral slope variation in one rotation is -0.5 to $0.05 \mu\text{m}^{-1}$ and that of the relative R-band magnitude is ± 0.15 [7,8]. Moreover, a correlation between brighter and bluer spectra was also observed [7]. The similarity for both Ryugu and Phaethon, that neither exhibits a strong UV nor 2.7- μm OH-band absorption for the entire rotational phases [9], might result in similar spectral changes due to space weathering on both asteroids. Thus, the majority of Phaethon's surface could be explained by freshness due to rejuvenation caused by the recent encounter with the Sun, i.e. fresh cometary activity.

4. Search for F types in the main belt

Ryugu is an F-type asteroid with a flat spectral shape in near-ultraviolet ($0.4 - 0.55 \mu\text{m}$) [10]. In order to put in context the results from the Hayabusa2 spacecraft and of its returned sample analyses, it is critical to know the abundance of F-types across the Solar System. However, after Eight Color Asteroid Survey (ECAS) [11], there is no major spectroscopic survey that covers the near-ultraviolet wavelength range. We started ground-based near-ultraviolet observations using telescopes at Roque de Los Muchacho Observatory, La Palma, Spain. Also we revisited our previous observations and reanalyzed the data in this wavelength range. We collected the spectral data of Themis, Polana, and Eulalia family members from our observations and ECAS. The largest members of these families are known to have negative visible spectral slope. Polana and Eulalia families are the plausible origin of Ryugu based on the dynamical calculation [2]. When we compared only the visible slope, those family members cannot be distinguished. However, if we use near-ultraviolet spectral slope, Themis family members are quite different from Polana and Eulalia family members. While Themis members show deep absorption in near-ultraviolet, Polana and Eulalia members exhibit flatter in this region. Ryugu is consistent with variation of the Polana and Eulalia members. Moreover, Bennu, the target asteroid of NASA's OSIRIS-REx [12], is also consistent with the Polana and Eulalia group. We found the connection between Ryugu and Polana and Eulalia members spectroscopically. Thus, now the idea that Ryugu is originated from the inner main belt is supported also from spectroscopy.

References

- [1] Tatsumi, E. et al. 2021. Nature Commun.
- [2] Campins, H. et al. 2013. ApJ **146**:26.
- [3] Sugita, S. et al. 2019. Science **364**. eaaw0422.
- [4] Morota, T. et al. 2020. Science **368**. 654.
- [5] McAdam, M. M. et al. 2015. Icarus **245**. 320.
- [6] Shimaki et al. 2020. Icarus **348**. 113835.
- [7] Ohtsuka, K. et al. 2020. PSS **191**. 104940.
- [8] Kareta, T. et al. 2018. ApJ **156**. 6.
- [9] Takir, D. et al. 2020. Nature Commun. **11**. 2050.
- [10] Tatsumi, E. et al. 2020. A&A **639**. A83.
- [11] Zellner, B. et al. 1985. Icarus **61**. 355.
- [12] Lauretta, D. S. et al. 2019. Nature **568**. 55.

Multiband thermal radiometry and related laboratory studies, indicating possible origin and evolution of Ryugu

M. Hamm^{1,2}, M. Grott², H. Senshu³, J. Knollenberg², J. de Wiljes¹, V. E. Hamilton⁴, F. Scholten², K. D. Matz², H. Bates^{5,6}, A. Maturilli², Y. Shimaki⁷, N. Sakatani⁸, W. Neumann^{2,9}, T. Okada⁷, F. Preusker², S. Elgner², J. Helbert², E. Kührt^{10,11}, T.-M. Ho¹², S. Tanaka⁷, R. Jaumann^{13,2}, S. Sugita¹⁴

¹*Institute of Mathematics, University of Potsdam, Potsdam, Germany*, ²*Institute of Planetary Research, German Aerospace Center (DLR), Berlin, Germany*, ³*Planetary Research and Exploration Center, Chiba Institute of Technology, Narashino, Japan*, ⁴*Southwest Research Institute, Boulder, CO USA*, ⁵*Department of Earth Sciences, Natural History Museum, Cromwell Road, London, SW7 5BD UK*, ⁶*Atmospheric, Oceanic and Planetary Physics, Oxford University, Parks Road, Oxford, OX1 3PU, UK*, ⁷*Institute of Space and Astronautical Science, Japan Aerospace Exploration Agency, Sagami-hara, Japan*, ⁸*Department of Physics, Rikkyo University, Toshima, Japan*, ⁹*Universität Heidelberg, Heidelberg, Germany*, ¹⁰*Institute of Optical Sensor Systems, German Aerospace Center, Berlin, Germany*, ¹¹*Qian Xuesen Laboratory of Space Technology, China Academy of Space Technology, Beijing, China*, ¹²*German Aerospace Center (DLR), Institute of Space Systems, Bremen, Germany*, ¹³*Freie Universität Berlin, Berlin, Germany*, ¹⁴*University of Tokyo, Bunkyo, Japan*

The MASCOT lander's radiometer [1] observed the diurnal variation of the surface temperature of single boulder on the surface of (162173) revealing a low thermal inertia and high porosity [2]. While the instrument observes the surface through six filters, two broad band filter and four bands pass transmitting the region between 6 and 16 μm , only the data of the 8 – 12 μm broadband filter was used in the previous studies [2, 3]. Coupling a thermophysical model to a combined DEM of boulder and landing site [4], and applying a data assimilation scheme for efficient parameter estimation [2], the analysis of the full radiometer data becomes feasible. The thermal inertia and emissivity of the surface within the filter's spectral ranges could be retrieved. The thermal inertia is estimated to be $255 - 265 \text{ J m}^{-2} \text{ K}^{-1} \text{ s}^{-1/2}$, corresponding to a high porosity of $46 \pm 1 \%$. The emissivity in the broad filters is estimated to be 0.98 ± 0.1 .

The emissivity estimates in the narrowband filters shows significant differences from band to band. In the 5.5 – 7 μm band the emissivity drops to band to 0.85 (-0.02, +0.01), reaches its maximum in the 8 – 9.5 μm band with 0.98 ± 0.01 , drops in the adjacent 9.5 – 11.5 μm band to 0.94 (-0.02, +0.01), and rises again to 0.97 ± 0.01 in the 13.5 – 15.5 μm region. We form the ratios of the emissivity within the 9.5-11.5 μm band and the 13.5 – 15.5 μm band with respect to the emissivity within the 8 - 9.5 μm band and compare them to equivalent emissivity ratios of mid-infrared spectra of powdered and thin section samples of various carbonaceous chondrites. We find that respective ratios of aqueously altered CM and CI chondrites form a common trend and our results for Ryugu lies within this cluster of CM and CI chondrites. The CI chondrites appear to be the best spectral match in the mid-infrared. Our study indicates that despite the partially dehydrated appearance of the surface in the visible to near-infrared wavelength range [5,6,7], the mid-infrared shows strong signs of aqueous alteration, and the Ryugu materials might be less dehydrated than previously thought.

References

- [1] Grott, M., et al., 2017, Space Science Reviews, 208, 413–431. [2] Grott, M., et al., 2019, Nature Astronomy, 3, 971 – 976. [3] Hamm, M., et al., 2020, Monthly Notices of the Royal Astronomical Society, 496, 3, 2776-2785. [4] Scholten, F., et al., 2019, Astronomy & Astrophysics, 632, L5. [5] Sugita, S., et al., 2019, Science, 364. [6] Kitazato, et al., 2019, Science eaav7432. [7] Kitazato, et al., 2021, Nature Astronomy, 5, 246–250.

Color Mapping of Asteroid Bennu

D.N. DellaGiustina¹ and the OSIRIS-REx Science Team
¹Lunar and Planetary Laboratory, University of Arizona

To evaluate relationships between color and morphology on Bennu, we radiometrically and photometrically corrected multispectral images acquired by the MapCam instrument of the OSIRIS-REx Camera Suite (OCAMS) [1-4]. Calibrated images were subsequently mosaicked to develop band-ratio and principal component analysis (PCA) maps. We mapped ~1600 boulders and ~700 craters, extracted their average MapCam spectra, and examined statistically meaningful trends between color, reflectance, and these morphological features. We also compared the global color distribution of Bennu to that of Ryugu.

The color of the largest craters (>100 m) on Bennu is indistinguishable from that of the average terrain. However, many small (≤ 25 m) craters are redder than average in the visible to near-infrared wavelengths (VIS to NIR; MapCam b' to x bands; neutral to red spectral slopes). The size distribution of these small reddish craters implies that they are the youngest component of the global crater population, in turn implying that redder colors are related to younger exposure ages [4]. We interpret this finding to indicate that space weathering leads to spectral bluing on Bennu [4].

On the basis of reflectance and color, we have categorized Bennu's boulders into four types [4]: 1) Dark boulders are equivalent to or darker than Bennu's average surface, are subangular, and commonly have rough, undulating surface textures. They encompass a wide range of sizes including the largest boulders on the asteroid (25 to 100 m in diameter) and are the dominant boulder type. 2) Bright boulders are brighter than the average surface of Bennu, have blue spectral slopes in the mid-VIS to NIR (MapCam v to x bands), and exhibit smooth, typically angular textures. They occur only at diameters less than ~10 m. 3) Rare, very bright boulders (reflectance up to 0.26; ~1% in number) show evidence of an absorption at 1 μm (downturn in the x band), which was confirmed to be indicative of exogenic pyroxene using data acquired by the OSIRIS-REx Visible and InfraRed Spectrometer (OVIRS) [5]. 4) Rare boulders (~2% in number) that have an absorption feature detectable above the OCAMS radiometric uncertainty at 0.7 μm (absorption depth of 2 to 10%) are inferred to contain Fe-bearing phyllosilicates. The 0.7- μm absorption has been observed in spectra of primitive asteroids and carbonaceous meteorites and has been attributed to the Fe²⁺-Fe³⁺ intervalence charge transfer associated with hydrated clay-bearing phyllosilicates [5].

This variety of boulders indicates that Bennu's surface is highly diverse, encompassing primitive material potentially from different depths in its parent body [4], as well as exogenic material delivered to the parent body from another asteroid family [5].

The multi-band cameras onboard the Hayabusa2 and OSIRIS-REx spacecraft use similar photometric filters in the visible wavelengths, allowing for direct comparison of the spectra from each [1, 6]. The variation in reflectance on Bennu is 1.7 times that on Ryugu, and Bennu exhibits a bluer overall color [4]. Ryugu shows large-scale latitudinal color differences, which have been attributed to regolith migration from the equator to mid-latitudes during a period of rotational deceleration [6]. A latitudinal color trend is also observed on Bennu, but the difference is small compared with its overall color variation [4]. Bennu's slightly bluer equatorial region may indicate the presence of more mature material, which is consistent with its increasing rotation rate and the associated global patterns of mass movement across the asteroid [7]. Unlike Ryugu, color variation on Bennu appears to be dominated by heterogeneity at the meter scale, likely driven by individual boulders [4]. This suggests that the extent of recent large-scale mass wasting on Bennu may not have been as widespread as the effect of regolith mixing [4].

References

- [1] Rizk, B., et al. "OCAMS: the OSIRIS-REx camera suite." *Space Science Reviews* 214.1 (2018): 26.
- [2] Golish, D. R., et al. "Ground and in-flight calibration of the OSIRIS-REx camera suite." *Space Science Reviews* 216.1 (2020): 12.
- [3] Golish, D. R., et al. "Disk-resolved photometric modeling and properties of asteroid (101955) Bennu." *Icarus* (2020): 113724.
- [4] DellaGiustina, D. N., et al. "Variations in color and reflectance on the surface of asteroid (101955) Bennu." *Science* 370.6517 (2020).
- [5] DellaGiustina, D. N., & Kaplan, H. H., et al. "Exogenic basalt on asteroid (101955) Bennu". *Nature Astronomy*, (2021): 5.1.
- [6] Sugita, S., et al., "The geomorphology, color, and thermal properties of Ryugu: Implications for parent-body processes". *Science* (2019): 364.
- [7] Jawin, E. R., et al., "Global patterns of mass movement on asteroid (101955) Bennu". *JGR Planets*, (2020):125.

The Mineralogy and Organic Composition of Bennu as Observed by VNIR and TIR Spectroscopy

V. E. Hamilton¹, A. A. Simon², H. H. Kaplan², P. R. Christensen³, D. C. Reuter², D. N. DellaGiustina⁴, C. W. Haberle⁵, L. B. Breitenfeld⁶, B. E. Clark⁷, and D. S. Lauretta⁴

¹*Southwest Research Institute, Boulder, CO, USA (hamilton@boulder.swri.edu)*

²*NASA Goddard Space Flight Center, Greenbelt, MD, USA*

³*Arizona State University, Tempe, AZ, USA*

⁴*University of Arizona, Tucson, AZ, USA*

⁵*Northern Arizona University, Flagstaff, AZ, USA*

⁶*Stony Brook University, Stony Brook, NY, USA*

⁷*Ithaca College, Ithaca, NY, USA*

NASA's Origins, Spectral Interpretation, Resource Identification, and Security — Regolith Explorer (OSIRIS-REx) mission characterized the surface composition of the carbonaceous asteroid Bennu at visible to infrared wavelengths (~0.4 - 100 μm). Spectral features of hydrated minerals (phyllosilicates) are dominant at both visible to near infrared (VNIR) [1, 2] and thermal infrared (TIR) wavelengths [1], with ~90 vol.% of the silicates being comprised of phyllosilicates (\leq 10 vol.% olivine plus pyroxene) [3]. Features of iron oxides are observed in both the VNIR (magnetite, goethite) [4] and the TIR (magnetite) [1]. In the 3.2-3.6 μm region, we observe spatially variable evidence for carbonate minerals (some associated with meter-long, cm-wide veins) and organic compounds comparable to insoluble organic material (IOM), with classification results showing little or no evidence of any correlation between these features and surface morphology or spectral slope/band depth [5-9]. A half-dozen isolated, meter-sized boulders exhibit pyroxene signatures consistent with those in the howardite-eucrite-diogenite (HED) meteorites from (4) Vesta [10]. There is evidence for non-uniform deposits of dust (~5-10 μm thick) superposed on a largely boulder-dominated surface [3]. The majority of VNIR features show only small band depth variations across the surface [4] and the TIR features appear to vary dominantly with particle size [3]. Nanophase magnetite produced by space weathering may account for Bennu's visible blue slope [12]. Two populations of rocks are observed in visible imaging, distinguished by albedo and surface texture [11], but spectral data analyzed to date have not shown any evidence of these two populations having different compositions.

The observed mineralogy of Bennu has been identified as being most consistent with a highly aqueously altered, CI- or CM-like, carbonaceous chondrite (CC) composition. In addition, we have recently recognized that GRO 95577 (CR1) also exhibits NIR and TIR spectra that are compatible with the observed spectroscopy and inferred mineralogy of Bennu (Figures 1 and 2). (We note that none of the NIR analogues shown here are good matches to Bennu at visible wavelengths, where the best fit is to a sample of Ivuna (CI) heated to 700°C [14]; however, the effects of space weathering on Bennu are not represented by the analogue spectra.) Isolated boulders containing pyroxene are interpreted as exogenic, basaltic material from Vesta, the preserved evidence of inter-asteroid mixing that occurred after the conclusion of planetesimal formation [10]. The manifestation of carbonate veins at scales much larger than has been observed in CC meteorites suggests that Bennu's parent body experienced fluid flow and hydrothermal deposition on kilometer scales for thousands to millions of years [6]. In October 2020, OSIRIS-REx collected a sample of the surface of Bennu for return to Earth in September 2023. We predict that the returned sample will contain the minerals and compounds described here (phyllosilicates, iron oxides, carbonates, and organics), representing a significant degree of alteration. In addition, minerals that are difficult to detect with remote sensing data, such as sulfides, also may be present, as well as exogenous materials.

References

[1] Hamilton, V. E. et al. 2019. *Nature Astronomy* 4:332. [2] Praet, A. et al. 2021. *Icarus* 363:114427. [3] Hamilton, V. E. et al. 2021. *Astronomy & Astrophysics* 650:A120. [4] Simon, A. A. et al. 2020. *Astronomy & Astrophysics* 644:A148. [5] Simon, A. A. et al. 2020. *Science* 370:eabc3522. [6] Kaplan, H. H. et al. 2020. *Science* 370:eabc3557. [7] Kaplan, H. H. et al. 2021. *Astronomy & Astrophysics* 653:L1. [8] Barucci, A. et al. 2020. *Astronomy & Astrophysics* 637, L4. [9] Ferrone, S. et al. 2021. *Icarus* 368:114579. [10] DellaGiustina, D. N. et al. 2020. *Nature Astronomy* 5:31. [11] DellaGiustina, D. N. et al. 2020. *Science* 370:eabc3660. [12] Trang, D. et al. 2021. *Planetary Science Journal* 2:68. [13] Takir, D. et al. 2013. *Meteoritics & Planetary Science* 48:1618. [14] Clark, B. E. et al. 2011. *Icarus* 216:462.

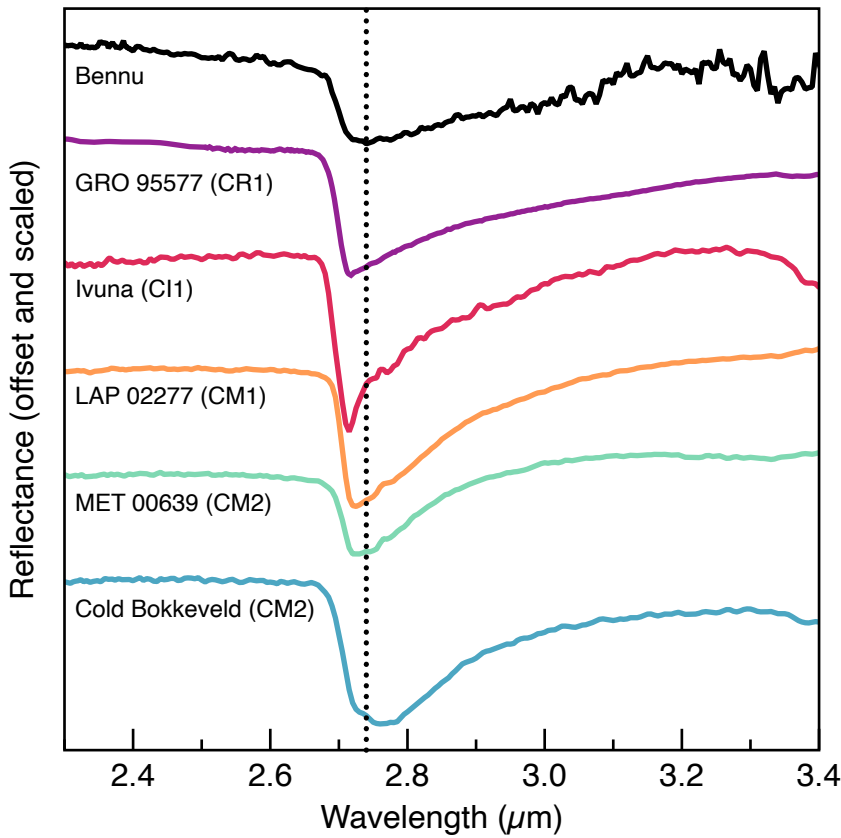


Figure 1. OVIRS spectrum of Benu [1] in the “3- μ m region” as compared to spectra of CC meteorites from [13] and a RELAB spectrum of GRO 95577.

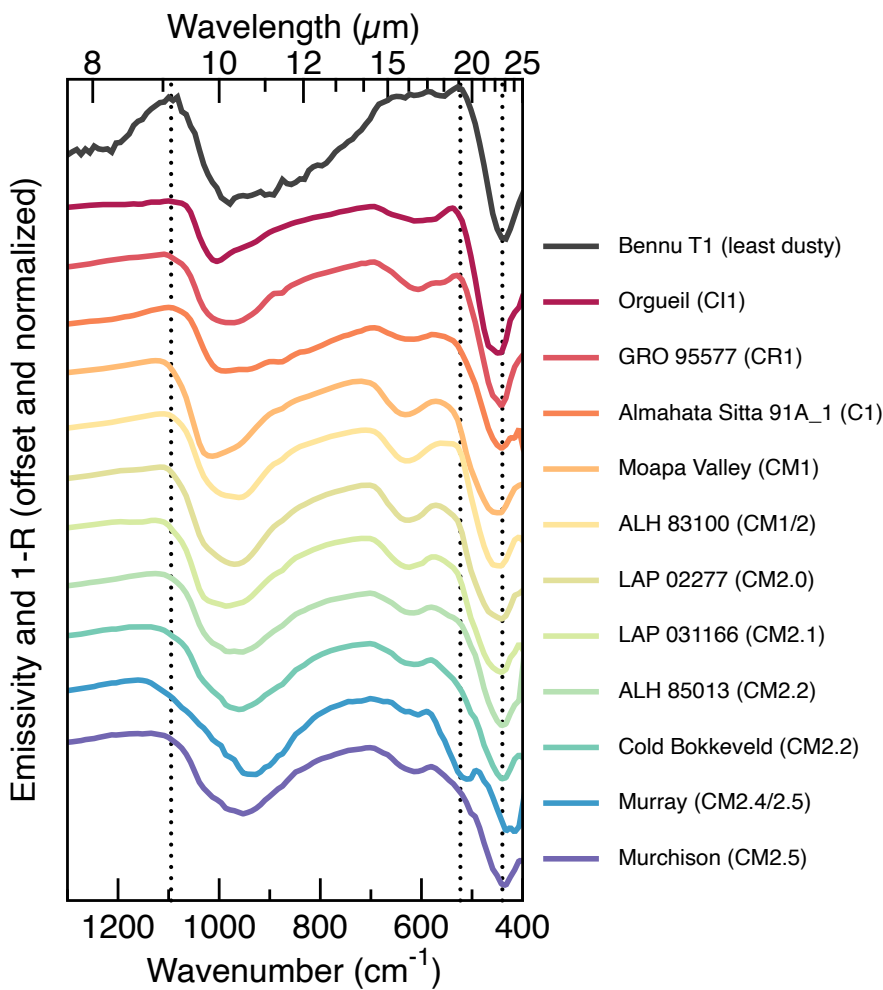


Figure 2. OTEs spectrum of Benu [3] as compared to CC analogues. The Christiansen feature (~ 1090 cm^{-1} , ~ 9.2 μm) is not particularly diagnostic. However, the peak at 528 cm^{-1} (18.9 μm) is a diagnostic feature in the Benu spectrum, and it weakens and shifts with increasing abundances of anhydrous silicates (e.g., pyroxene and olivine). As the abundance of anhydrous silicates increases, the Si-O bending mode (the minimum at ~ 440 cm^{-1} or 22.7 μm) broadens and features of pyroxene and olivine become apparent (e.g., Cold Bokkeveld, Murray, Murchison).

The Nature of Extraterrestrial Amino Acids in Carbonaceous Chondrites and Links to Their Parent Bodies

Daniel P. Glavin¹, José C. Aponte^{1,2}, Jason P. Dworkin¹, Jamie E. Elsila¹, Hannah L. McLain^{1,2}, and Eric T. Parker¹

¹*NASA Goddard Space Flight Center, Greenbelt, Maryland 20771, USA*

²*Catholic University of America, Washington, District of Columbia 20064, USA*

Meteorites and samples returned from asteroids and comets provide an important record of the physical and chemical processes that occurred in the early solar system and represent some of the oldest solid materials currently available for laboratory analyses. The delivery of organic matter by extraterrestrial material to the early Earth could have been an important source of complex prebiotic organic molecules available for the emergence of life. Analyses of primitive carbonaceous chondrites over the last five decades have revealed a major insoluble organic component [1,2], as well as a complex and highly diverse suite of soluble organic molecules of prebiotic importance [3,4] that includes carboxylic acids, N-heterocycles, sugars, amino acids, amines, and many other organic molecules that have not yet been identified [5]. Amino acids continue to be a primary focus of many soluble organic analyses in carbonaceous chondrites because (1) these molecules are essential components of life (as the monomers of proteins), (2) they have structural diversity (multiple possible isomers) that can be used to help constrain formation mechanisms and parent body conditions, and (3) most amino acids identified in carbonaceous chondrites are chiral, a property that can be used to distinguish between amino acids of extraterrestrial and terrestrial origins. The degree of parent body hydrothermal alteration has been shown to have a major influence on the formation and destruction of amino acids in carbonaceous meteorites as observed in the measured abundances and molecular distributions [6]. Aqueous alteration in primitive asteroids could have also led to the preferential enrichment of some left-handed amino acids over their right-handed forms, an astounding discovery that suggests that the origin of life on Earth or elsewhere was biased toward left-handed amino acid homochirality [7,8]. This talk will give an overview of what is known about the amino acid composition of carbonaceous chondrites, present some key unanswered questions, and discuss how the analysis of samples returned from asteroids Ryugu and Bennu will further advance our understanding of parent body chemistry and potential contributions from carbonaceous asteroids to the origin of life on Earth or elsewhere.

References

- [1] Alexander, C.M.O'D. et al. 2007. *Geochimica et Cosmochimica Acta* 71: 4380. [2] Yabuta, H. et al. 2007. *Meteoritics and Planetary Science* 42: 37. [3] Glavin D.P., Alexander, C.M.O'D., Aponte, J.C., Dworkin, J.P., Elsila, J.E., and Yabuta, H. 2018. The origin and evolution of organic matter in carbonaceous chondrites and links to their parent bodies, in *Primitive Meteorites and Asteroids*, ed. N. Abreu, Elsevier, pp. 205-271. [4] Furukawa, Y. et al. 2019. *Proceedings of the National Academy of Sciences USA* 116: 24440. [5] Schmitt-Kopplin, P. et al. 2010. *Proceedings of the National Academy of Sciences USA* 107: 2763. [6] Elsila, J.E. et al. 2016. *ACS Central Science* 2: 370. [7] Cronin, J. R. and Pizzarello, S. 1997. *Science* 275: 951. [8] Glavin, D.P. et al. 2020. *Chemical Reviews* 120: 4616.

Oxygen isotopes and water in bulk matrix of CM2 Murchison as an analog for Ryugu matrix

Aditya Patkar¹, Trevor Ireland², Janaina Avila³, and Michael Zolensky⁴

¹RSES, Australian National University, Australia 0200 (aditya.patkar@anu.edu.au); ²SEES, University of Queensland, Australia 4067; ³GCSCR, Griffith University, Australia 4111; ⁴ARES, NASA JSC, Houston (TX), USA

Introduction: Fine-grained phyllosilicates like serpentine and saponite form a dominant component in CM and CI chondrites. The triple oxygen isotope composition of the matrix phases in carbonaceous chondrites (CC) is poorly characterised due to their small grain size and the unavailability of suitable standards for SIMS analysis. CM chondrites may be considered as a good analog for the materials from the C-type asteroid Ryugu [1]. Since Ryugu samples are observed to be almost entirely made of matrix material like CI chondrites, it is essential to characterise in situ bulk matrix isotope composition using SIMS in Ryugu and the matrix-rich CCs.

Samples and methodology: We measured triple oxygen isotopes and water in the ‘bulk’ matrix of CM2 Murchison using the Sensitive High Resolution Ion Microprobe Stable Isotope (SHRIMP SI) at RSES, Australian National University. A chip of the rock was mounted in Bi-Sn alloy, a new mounting technique developed to measure trace amounts of water in nominally anhydrous minerals (NAMs). In this case it is also useful in the measurement of oxygen isotopes to avoid contamination from epoxy in the porous CC matrix in high-precision analyses. ¹⁶O⁻, ¹⁷O⁻ and ¹⁸O⁻ ions were measured in multi-collection mode using Faraday cups followed by ¹⁶O¹H peak characterisation from automated mass scans on the same spots. A spot size of 30 μm was used. The measurements were referenced to San Carlos Olivine (SCO). An antigorite serpentine reference material was also analysed to establish any issues with the OH⁻ peak tailing under ¹⁷O⁻.

Results: Triple oxygen isotope analysis in 27 spots from Murchison matrix were acquired. The observed range in the isotope ratios are $\Delta^{17}\text{O} \approx +1$ to $+7\%$ (mean 2SE at 95% confidence $\approx 0.21\%$), $\delta^{17}\text{O} \approx +2$ to $+7\%$ (mean 2SE $\approx 0.5\%$), $\delta^{18}\text{O} \approx -3$ to $+5\%$ (mean 2SE $\approx 0.25\%$). External reproducibility of $\Delta^{17}\text{O}_{\text{SCO}}$ was $\approx 1\%$. Any instrumental mass fractionation effects are expected to affect $\delta^{17}\text{O}$ and $\delta^{18}\text{O}$ but not $\Delta^{17}\text{O}$. The water abundance (¹⁶O¹H/¹⁶O ratios) ranges from 0.025 to 0.06, and so is significantly larger than ¹⁷O. Figure 1a shows the plot of ¹⁶O¹H/¹⁶O vs $\Delta^{17}\text{O}$.

We also measured water in olivine grains scattered in the Murchison matrix. The apparent ¹⁶O¹H/¹⁶O ratios in the Murchison olivines vary from 6×10^{-6} to 9×10^{-6} . Additionally, the ¹⁶O¹H/¹⁶O ratios in SCO span the same range of $\sim 6 \times 10^{-6}$ to 9×10^{-6} . Calibration using multiple reference materials shows a water concentration of ~ 10 -15 ppm in Murchison olivines as well as SCO [2].

Discussion: There is a distinct lack of studies characterising in situ CC matrix oxygen isotope compositions. One analysis of isolated Murchison matrix fraction using BrF₅-catalysed extraction of oxygen from silicates has yielded $\delta^{18}\text{O} = 12.70\%$, $\delta^{17}\text{O} = 4.72\%$, $\Delta^{17}\text{O} = -1.88\%$ [3]. This analysis is isotopically ‘heavier’ than the whole-rock values for Murchison but lies on the same 2-component mixing line as the host rock. The $\Delta^{17}\text{O}$ range observed in this work is ≈ 2 to 8% higher than the analysis reported in [3]. This disparity may be potentially related to the tailing of the OH⁻ peak under ¹⁷O⁻ peak due to their similar mass [4]. A 100 μm collector slit on SHRIMP SI and optimum peak tuning ensures good separation of the two ion species seen in figure 1b. However, in case of an interference, OH counts/sec should be proportional to the tailing effects, i.e., a rise in $\delta^{17}\text{O}$. Compared to the $R^2 = 0.82$ value for ¹⁶O¹H/¹⁶O vs $\Delta^{17}\text{O}$ in figure 1a, correlation with $\delta^{17}\text{O}$ shows $R^2 \approx 0.3$. Can the positive $\Delta^{17}\text{O}$ values be trusted? The covariation seen in water vs $\Delta^{17}\text{O}$ agrees with the two-

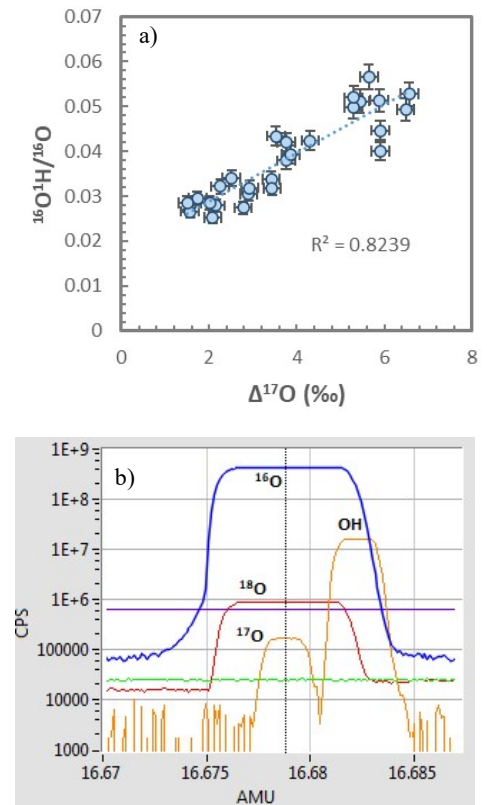


Figure 1: a) Plot of ¹⁶O¹H/¹⁶O vs $\Delta^{17}\text{O}$ in Murchison matrix. 10% uncertainty is assumed for the water ratios; b) Mass scan in Murchison matrix showing well-resolved ¹⁷O⁻ and ¹⁶OH⁻ peaks. Vertical line through the peaks is the position of the magnet during data acquisition.

component mixing model between a solar reservoir and heavy water reservoir for variable water : rock ratios [3]. More work is underway to constrain the nature of these in situ measurements and ascertain any instrumental artefacts.

The water observed in the Murchison olivines stands in contrast to the elevated water concentrations from chondrule olivines in CM chondrites reported in recent studies, and the difference is likely due to different sample preparation methods [5,6]. Water in olivines from different meteorites and Ryugu would be crucial to constrain the formation conditions of the olivines that make up a majority of the chondrules and are scattered throughout the CC matrix.

Conclusions: CM Murchison matrix should be a good analog for the matrix from Ryugu samples. In situ bulk matrix analysis of CM Murchison using SHRIMP SI yield a $\Delta^{17}\text{O}$ range of +1 to +7‰, which is at least 2‰ higher than the whole-rock isotope composition range for CM chondrites. There is good covariation between the water content measured in the 27 spots and the $\Delta^{17}\text{O}$ values. If there is any interference of the OH^- ion species into ^{17}O , the covariation should be strong for $\delta^{17}\text{O}$ values too. However, that is not the case. A more robust dataset measuring matrix from other hydrous CCs like CI and CR chondrites is needed to constrain the nature of these in situ bulk matrix measurements. Moreover, water in the NAM olivine from Murchison chondrules and matrix show ~10-15 ppm water which is in contrast to recent studies and has implications on the formation and evolution of their host components.

Acknowledgements: This work is supported by an Australian Research Council Discovery Project (DP210101798) grant to Trevor Ireland and Michael Zolensky.

References: [1] King, A. et al. (2019) *M&PS*, 54(3), 521-543; [2] Turner, M. et al. (2015) *JAAS*, 30, 1706-1722; [3] Clayton, R. and Mayeda, T. (1999) *GCA*, 63(13-14), 2089-2104; [4] Ireland, T. (2013) *Treatise on Geochemistry*, 15, 385-409; [5] Stephant et al. (2017) *GCA*, 199, 75-90; [6] Azevedo-Vannson et al. (2021) *52nd LPSC*, abstract #2548.

Anomalous and ungrouped carbonaceous chondrites in the US Antarctic meteorite collection and their potential relevance to Ryugu and Bennu

Kevin Righter¹, Nicole G. Lunning¹, Catherine M. Corrigan², and Timothy J. McCoy²

¹*Mailcode XI2, NASA Johnson Space Center, Houston, TX 77058*

²*Smithsonian Institution, Department of Mineral Sciences, Washington, DC 20560*

With two different carbonaceous asteroid sample return missions in full swing, attention has focused on what connections can be made between the asteroid samples and the wide range of carbonaceous chondrite meteorites in worldwide collections. The US Antarctic meteorite collection contains nearly 1000 carbonaceous chondrites of various types including many in well-established groups as well as ungrouped, unusual or anomalous groups [1]. Some of the latter have been included in, or are possibly related to, recently proposed new carbonaceous chondrite classifications – CA and CY chondrites [2,3]. In addition to these, there are numerous ungrouped samples that have properties intermediate between established groups (like CM and CO; [4]), distinct from any other groups [5], or have anomalous properties that might be attributable to parent body processes such as heating, fluid interaction, or impacts [6].

Some CM anomalous or ungrouped chondrites share spectral features with Ryugu, which has a small hydration peak arguably due to hydrated minerals left after either impact heating or shock in carbonaceous chondrites [7]. PCA 91008, PCA 02012, GRO 95566, and LEW 85311 are all CMs that have experienced heating or metamorphism that may be due to impacts, solar radiation, or radiogenic decay [6]. These samples all have low H contents, C/H (bulk), and low $\Delta^{17}\text{O}$ [6,8] and may hold clues to understanding the mineralogy of Ryugu, or interpretations of its spectral properties.

WIS 91600, on the other hand, appears to be related to several other highly altered CM [6], and shares properties with the newly proposed CY chondrites [6]. An understanding of this grouplet will also aid in the interpretation of Bennu samples which have strong hydration features. In addition, ungrouped carbonaceous chondrites may provide valuable insights into the aqueous alteration potentially recorded in Bennu and Ryugu samples; such as the relatively moderate aqueous alteration recognized and dated at 4-5 myr after CAIs in MAC 88107 (C2-ungrouped) by [9] to the extensive aqueous alteration apparent in MIL 090292 (C1-ungrouped) [10].

Finally, LON 94101/94102 is a brecciated CM chondrite with numerous lithologies. Its appearance is similar to some of the brecciated lithologies visible at the surface of Bennu and Ryugu [11]. Although CM chondrites with multiple lithologies are common (e.g., [12]), the lithologies are often difficult to resolve at the hand specimen scale and only after some detailed e-beam characterization are the subtle lithologic differences evident (e.g., [13]). LON 94102 contains visibly distinct clasts at the hand specimen scale, relatively rare for CM breccias.

The largest CM chondrites by mass from the U.S. Antarctic meteorite collection may provide insights into the extent of brecciation and heterogeneity within more typical CM chondrite-like source asteroids. For example, recent curation CT scans [14] show possible clasts within in a subsplit of ALH 83100 (CM1/2) which is the largest CM chondrite or CM chondrite pairing group in the U.S. Antarctic collection with an original mass of 3.019 kg. Similar work on additional subsplits or meteorites may aid our understanding of heterogeneity within CM chondrites from Antarctica.

Initial classification of CM chondrites in the U.S. Antarctic meteorite collection includes preliminary pairing when petrographically similar CM chondrites that have been previously found in the same field area. The two largest CM chondrite preliminary pairing groups by mass are the ALH 83102 (CM2) pairing group with an original mass of 2.554 kg and the EET 96005 (CM2) pairing group with an original mass of 1.125 kg. However, preliminary pairing groups assigned at classification—intrinsically—do not include stones that are petrographically distinct. Rigorous pairing group studies of CM chondrites from specific field sites are needed to investigate if there is unrecognized heterogeneity in CM chondrites from Antarctica that may represent common asteroid impactors (pre-atmospheric entry asteroids/meteoroids). Detailed pairing studies have the potential to recognize initial stones with multiple lithologies and investigate if there are stones that only sample one of those respective lithologies in the collection.

These groups of heated CMs, extensively hydrated CMs, intermediate between CM and CO chondrites, and brecciated samples are all potentially relevant to Bennu and Ryugu samples, where heating, hydration, and brecciation have all come into play. These bodies might also be comprised of material intermediate to CM and CO chondrites, or at least distinct from the well-established CC groups. These small and unusual groups of carbonaceous chondrites may help to unlock new information about early solar system processes and aid in the understanding of the evolution of these carbonaceous asteroids.

References

- [1] <https://curator.jsc.nasa.gov/antmet/index.cfm>. [2] King AJ et al. (2019) *Geochemistry* 79: 125531. [3] Kimura M et al. (2021) *Meteoritics & Planetary Science*, in press. [4] Prestgard T et al. (2021) *Meteoritics & Planetary Science* 56, 1758–1783. [5] Davidson J et al. (2020) LPSC 51st, #1623. [6] Choe WH et al. (2010) *Meteoritics & Planetary Science* 45: 531-554. [7] Kitazato K (2019) *Science* 364: 272-275. [8] Alexander CMD et al. (2018) *Space Science Reviews* 214: 1-47. [9] Doyle PM et al. (2015) *Nature Communications* 6, 1-10. [10] Jilly-Rehak C et al. (2018) *Geochimica et Cosmochimica Acta* 222, 230-252. [11] Walsh K et al. (2019) *Nature Geoscience* 12: 242-246. [12] Zolensky et al. (2020) *Meteoritics & Planetary Science* 56: 49-55. [13] Telus M et al. (2019) *Geochimica et Cosmochimica Acta* 260, 275-291. [14] <https://curator.jsc.nasa.gov/antmet/samples/petdes.cfm?sample=ALH83100>

VOLATILES IN CHONDRITES AND ACHONDRITES

M. Bose¹, T. M. Hahn², Ziliang Jin³

¹School of Earth and Space Exploration, Arizona State University, Tempe, AZ 85287

²Jacobs, Johnson Space Center, Houston, TX 77058

³Macau University of Science and Technology, Macau.

(*Correspondence: Maitrayee.Bose@asu.edu)

The abundance and distribution of volatiles in Solar System objects are vital for understanding planet formation and evolution. The presence of water and organic molecules is critical for the emergence of life and the habitability of planetary environments. Although some information on volatiles can be obtained from analysis of meteorites, they are prone to alteration and exchange in Earth's environment. Additionally, lack of context, i.e., which specific asteroid body, sampling location within the asteroid etc. results in an incomplete understanding. Returning samples allows for the use of state-of-the-art laboratory analyses, providing extremely high-precision, high-sensitivity, and high-resolution. More importantly, returned samples can be placed into geologic context and provide complementary information with other studies of the parent object.

A successful sample return mission from asteroid Itokawa by JAXA's Hayabusa spacecraft led to our excellent understanding about the parent bodies of ordinary chondrite meteorites. Minute details of the asteroid's history was gleaned through thorough and detailed laboratory investigations including compositions, mineralogy, and chronology. One such investigation led to the measurement of hydrogen isotopes and water in tiny Itokawa particles, which show that the silicate minerals can contain between 400-800 ppm of water and translated to up to 0.5 Earth's oceans to be delivered to proto-Earth by S-type asteroids¹. On the other hand, the proportions of various chondritic materials accreted to form Mars are distinct from those for Earth. Recent accretion models for terrestrial planets using chondritic components suggests that S-type asteroids (specifically, H chondrites) would have contributed up to 50% the mass of proto-Mars². Based on analysis of recent confirmed falls, Chelyabinsk and Benenitra, we ascertained that only about ½ of water contained within the martian mantle can be explained by accretion of S-type asteroids; We speculate that pebble accretion may have played a significant role in forming Mars³.

Asteroids Bennu and Ryugu are the targets of ongoing sample return missions from C-type asteroids. The spectral features are similar to those of aqueously altered CM-type carbonaceous chondrites (CCs). Murchison and Aguas Zarcas are CM2 chondrite falls and potential meteorite analogs for Bennu and Ryugu. We studied these two CCs and their components to constrain the evolution of hydrogen in C-type asteroids⁴. In addition, we studied stones from Ureilites and Brachinites⁵, primitive achondrites that are likely better planet forming starting materials because of their early accretion ages. I will discuss the data, and discuss how both chondrites and achondrites that formed in the inner solar system could be the source of volatiles during the early accretion stages of terrestrial planets.

References.

- (1) Jin Z. and Bose M. (2019) *Science Advances* 5:eaav8106.
- (2) Mah J. and Brasser R. (2021) *Icarus* 354: 114052
- (3) Jin Z. and Bose M. (2020) *LPS XXXXI*, Abstract #1470.
- (4) Bose M., Hahn Jr. T. M., and Jin Z. (2021) 84th Annual Meeting of the Meteoritical Society, Abstract #6078.
- (5) Bose M., Hahn Jr. T. M. (2021) 84th Annual Meeting of the Meteoritical Society, Abstract #6227.

Space weathering of sulfides and silicate minerals from asteroid Itokawa

Laura Chaves¹, Michelle Thompson¹

¹ *Purdue University*

Space weathering refers to the progressive spectral, microstructural, and chemical alterations of mineral grains on the surfaces of airless planetary bodies [1]. These changes are produced by high-velocity micrometeoroid impacts and solar wind irradiation, causing vesiculation, melt and vapor deposits, sputtering, ion implantation, and amorphization on regolith grains. Spectrally, space weathering produces multiples alterations in the visible near-infrared (VNIR) wavelengths, including reddening, darkening, and attenuated absorption bands [1]. The spectral anomalies have been attributed to the presence of Fe nanoparticles (npFe) that are mainly composed of metallic iron (npFe⁰). Analyses on individual lunar grains show that the spectral alterations in the VNIR depend on the particle size, where npFe with diameters < 5 nm produce reddening, whereas particles >10nm produce darkening [2]. In 2010, the Japan Aerospace Exploration Agency (JAXA) Hayabusa mission successfully collected 1534 regolith particles from the surface of S-type asteroid Itokawa [3]. Prior to sample return, S-type asteroids were hypothesized to be the parent bodies of ordinary chondrites; however, the spectral characteristics of the meteorites in our collections differed from these asteroids. Geochemical analyses in Itokawa particles indicated a composition similar to LL4-LL6 chondrites [3], corroborating the link between ordinary chondrites and S-type asteroids and demonstrating the importance of space weathering studies for accurate characterization of asteroidal surfaces.

Previous studies have identified space weathering features in Itokawa regolith particles, including disordered rims, chemically distinct layers, whisker-like structures, sulfur depleted rims, and Fe⁰ and FeS nanoparticles [4,5,6,7,8]. Most space weathering studies have concentrated on understanding the response of silicate minerals to interplanetary space [4,9,10] as these phases are the most common in lunar samples and Itokawa particles. However, our understanding of the behavior of other minerals under space weathering conditions is still in a very early stage. Among these understudied minerals are sulfides which are present in the sample collection of asteroid Itokawa [11] and are relevant minerals in carbonaceous chondrites [12], thought to be meteoritic counterparts of asteroids Bennu, Ryugu, and Psyche [13,14,15].

To compare the responses of silicates and sulfides under space weathering conditions, we performed coordinated analyses of the RC-MD01-0025 Itokawa grain previously identified to contain olivine, low-Ca pyroxene, and Fe-Ni- sulfides. We embedded the particle in low-viscosity epoxy and prepared electron transparent thin sections with an approximate thickness of 50 nm using a Leica EM UC7 ultramicrotome. To identify microstructural and chemical properties associated to space weathering in silicate and Fe-Ni- sulfide grains in the Itokawa particle, we used a FEI Talos 200 KeV transmission electron microscope (TEM) coupled with a Super-X silicon drift detector (SDD) energy-dispersive X-ray spectrometer (EDS). The sample preparation of the Itokawa particle and the electron microscopy analyses of the ultramicrotomed samples were performed at Purdue University.

Bright-field (BF) TEM imaging shows the presence of a ~50 nm mottled rim in an olivine grain (Fig. 1a). Chemically, EDS maps show the rim presents three layers (Fig. 1b,c). Layer 1 (L1) thickness is ~30 nm and shows similar O, Mg, Fe, and Si concentrations as the bulk grain. Layer 2 (L2) has a thickness of 5-10 nm and presents depletion of Mg, Fe, and enrichment of Si compared to L1. Layer 3 (L3) has a thickness of 5-10 nm and is Si depleted compared to L1 and L2; it is enriched in Fe and Mg compared to L2 but depleted in these elements compared to L1. High resolution (HR) TEM images show an amorphous region in the rim's outer 5-10 nm with some nanocrystalline regions. The nanocrystalline domains present d-spacing values of 0.20 nm that correspond to npFe⁰. Metallic iron nanoparticles were previously identified in silicates and Fe-sulfides in Itokawa regolith particles [4,5]. The identification of chemically distinct layers in returned samples [4,6,7] and in H⁺ irradiation experiments on olivine [16] suggests this multilayer rim might correspond to a combination of sputtering, redeposition, and ion irradiation damage processes.

High resolution (HR) TEM imaging of the Fe-Ni- sulfide grain shows d-spacing values of 0.28 nm similar to (222) pentlandite and the presence of a ~5-10 nm rim that presents nanocrystallinity (Fig. 2a). EDS mapping shows that the rim is depleted in Ni and S but enriched in Fe compared to the bulk mineral (Fig. 2b,c). Previous studies in Itokawa samples have identified sulfur-depleted rims Fe-sulfides [5,17], and the origin of these rims is attributed to solar wind damage. The depletion in S and Ni and the enrichment of Fe of the rim suggest it might have formed in a complex process of sputtering and redeposition. The microstructural and chemical characteristics in the olivine and pentlandite grains further indicate that solar wind irradiation is

the main contributor to the space weathering of both mineral phases. Future work will include the TEM and EDS analyses of the low-Ca pyroxene grains present in the RC-MD01-0025 regolith particle. In addition to TEM and EDS, we will perform electron energy-loss spectroscopy (EELS) to compare the oxidation state of Fe between the mineral grains and the space weathered rims. Understanding how different mineral phases respond to space weathering conditions using returned samples is crucial to accurately interpret remote sensing observations of the surfaces of airless bodies and adequately characterize the regolith samples collected from asteroids Ryugu and Benu.



Figure 1. Space weathered rim on olivine grain. a) Bright field (BF) TEM image shown the ~50 nm mottled rim on olivine. b) High-angle annular dark field image overlain with EDS maps (O, Mg, Si, Fe). c) EDS line scan showing the chemical layering of the rim.



Figure 2. Space weathered rim on Fe-Ni sulfide grain. a) High-resolution (HR) TEM showing the presence of a 5-10 nanocrystalline rim. b) High-angle annular dark field (HAADF) image overlain with EDS maps of S, Fe, and Ni. c) EDS line scan showing the Ni and S depletion on rim compared to the bulk mineral.

References

- [1] Hapke B. 2001. *Journal of Geophysical Research* 106, 10039-10073. [2] Keller L. P. 1998. 29th Lunar and Planetary Science Conference. Abstract #1762. [3] Nakamura T. et al. 2011. *Science* 333, 1113-1116. [4] Noguchi T. 2011. *Science* 333, 1121-1125. [5] Keller. L. P. et al. 2014. *Earth, Planets and Space* 66:71. [6] Thompson. M. S. et al. 2014. *Earth, Planets, and Space* 66:89. [7] Noguchi. T. et al. 2014. *Meteoritics & Planetary Science* 49, 188-214. [8] Matsumoto T. et al. 2020. *Nature Communications* 11, 1-8. [9] Keller L. P. and McKay D. S. 1997. *Geochimica et Cosmochimica Acta*, 61, 11, 2331-2341. [10] Loeffler M. J. et al. 2016. *Meteoritics and Planetary Science* 51, 2, 261-267. [11] Nakamura T. et al. 2011. *Science* 333, 1113-1116. [12] Bland A. et al. 2004. *Meteoritics & Planetary Science* 39, 3-16. [13] Clark B. E et al., 2011. *Icarus* 216, 462-475. [14] Kitazato K. et al. 2019. *Science* 364, 272-275. [15] Elkins-Tanton L. T. *Journal of Geophysical Research* 125, 1-23. [16] Laczniak D. L. et al. 2021. *Icarus* 364, 1-23. [17] Burgess K. D. and Stroud R. M. *Meteoritics and Planetary Science* 56, 1109-1124.

Space weathering of iron sulfides on airless bodies

Toru Matsumoto¹

¹*The Hakubi Center for Advanced Research, Kyoto University*

Introduction: Solar wind implantation, micrometeorite impacts, and solar radiation cause the alteration of the optical, physical, and chemical properties of surface materials on airless bodies. Space weathering refers to these alteration processes, which affect rocks and soils on airless surfaces over time [1]. Microstructures indicative of space weathering are important in understanding geological processes occurring in the dynamically evolving regolith, such as regolith motion, volatile distribution, and replenishment of soils [2]. Space weathering features also shed light on the evolution of solids in interstellar environments and at the surface of the proto planetary disk, where free-floating particles could be bombarded by energetic ions. Extensive studies of lunar soils and particles from S-type asteroid Itokawa have revealed microproducts caused by space weathering, such as vapor depositions, partly/completely amorphized rims, and nanophase iron/iron compounds [e.g., 3, 4]. Our knowledge of space weathering has progressed based on analyses of the major constituents of rock forming minerals such as silicates and oxides, whereas the behavior of other minerals in space-exposed environments remains poorly investigated. Iron sulfides represent solid reservoirs of sulfur, which is a major, moderately volatile element in early solar system materials. The space weathering features of iron sulfides will provide clues to understanding the evolution of sulfur compounds and the distribution of sulfur on airless bodies. Here, the author reports recent studies on space weathering of iron sulfides in lunar soils and Itokawa particles using electron microscopy techniques [5, 6].

Methods: Itokawa particles and lunar mare soils from Apollo 11 and 17 landing sites were used in the studies. The sizes of the samples are smaller than 200 μm . Itokawa particles have mineral components corresponding to those of LL chondrites, and contain 2 vol% of iron sulfides [7]. Lunar mare basalts include < 1 wt% of iron sulfides, with the sulfur content being higher in mare basalts than in highland rocks [8]. Surface structures of iron sulfides were observed using scanning electron microscopy (SEM). Then, electron-transparent sections were prepared using focused ion beam (FIB) systems from regions of interest on the samples. The sections were analyzed using transmission electron microscopy (TEM).

Results: SEM observations revealed that altered surfaces of iron sulfides have vesicular textures and elongated iron metals (whiskers) on their surfaces (Fig. 1). These microstructures were identified in Itokawa particles and lunar soils and are similar to each other. TEM analysis showed that the upper zone of iron sulfides from the surface to a depth of up to 80–100 nm is distinct from the non-altered area; this zone is defined as the space-weathered rim. The space-weathered rim is characterized by crystallographic misorientations and the disappearance of superstructure reflections of troilite in electron diffraction patterns. The rim contains opened vesicles that are aligned along the c-plane of the sulfides, as well as numerous tiny vesicles. The Fe/S ratio on the surface of the rim is higher than in non-altered regions, indicating selective sulfur loss from the surface. Iron whiskers protrude from the space-weathered rim and consist of polycrystalline metallic iron. The sulfide rims and the iron whiskers are both coated with vapor-deposited materials.

Discussions: The crystallographic modifications of the sulfides are probably produced by solar wind irradiation. The loss of sulfur atoms may be caused by combined processes including selective sputtering of sulfur atoms during solar wind implantation, chemical reaction with solar wind hydrogen, and thermal effects produced by micrometeorite bombardments. The whiskers may have been formed by continued sulfur loss and accumulation of excess iron atoms that lead to the growth of metallic nuclei on the sulfide surfaces. Thermal stress induced by thermal cycling could also have contributed to the whisker growth.

The sulfur loss by the space weathering of iron sulfides may contribute to sulfur depletion detected on the surface of S-type asteroid Eros [9]. Furthermore, the sulfur loss from iron sulfides likely causes mass-dependent fractionation of sulfur in regolith grains and supports the notion that the enrichment of heavy sulfur isotopes in mature lunar soils is due to sulfur loss by space weathering [e.g., 10]. Thus, iron sulfides are highly susceptible to decomposition by space weathering, which may change the chemical properties of regolith. The general similarities of space weathering of iron sulfides between the Moon and Itokawa indicate that the alteration of iron sulfides is common among airless bodies in the solar system.

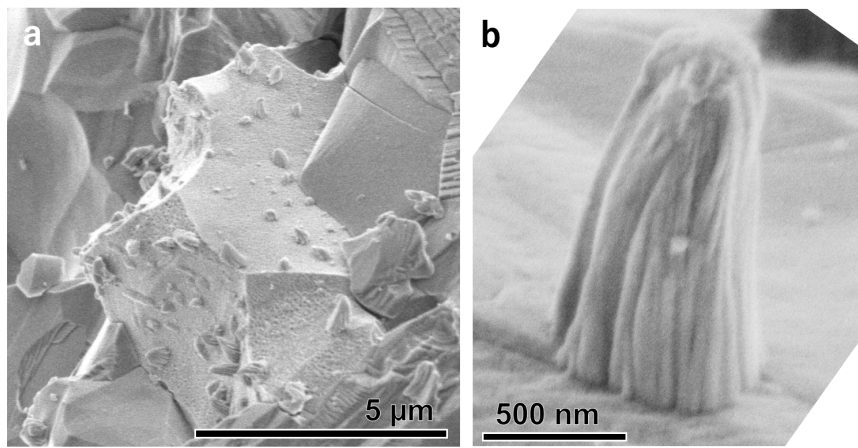


Fig.1 . Secondary electron images of whiskers on iron sulfide surfaces. (a) Iron sulfide grain on an Itokawa particle. Numerous whiskers appear on the sulfide. (b) Enlarged image of an iron whisker on a sulfide surface of an Itokawa particle.

References:

- [1] Pieters C. and Noble S. K. 2016. *J. Geophys. Res. Planet* 121, 1865-1884. [2] Matsumoto T. et al. 2016. *Geochim. Cosmochim. Acta* 187, 195-217. [3] Keller L. P. and McKay D. S. 1993 *Science* 261, 1305-1307. [4] Noguchi T. et al. *Science* 333, 1121-1125. [5] Matsumoto T. et al. 2020. *Nat. Commun.* 11, 1-8. [6] Matsumoto T. et al. 2021. *Geochim. Cosmochim. Acta* 299, 69-84. [7] Tsuchiyama A. et al. 2011 *Science* 333, 1125-1128. [8] Papike J. et al. 1991. *Lunar Source book*, p121-181. [9] Trombka J. I. et al. 2000, *Science* 289, 2101-2105. [10] Clayton R. N. 1974. *Proc. Lunar Sci. Conf. 5th vol.2*, pp. 1801-1809.

Extraterrestrial Non-Protein Amino Acids Identified in Carbon-Rich Particles Returned from Asteroid Itokawa

Eric T. Parker¹, Queenie H.S. Chan^{2,3}, Daniel P. Glavin¹ and Jason P. Dworkin¹

¹NASA Goddard Space Flight Center, Greenbelt, MD 20771, U. S. A.

²Royal Holloway University of London, Egham, Surrey TW20 0EX, U.K.

³The Open University, Walton Hall, Milton Keynes MK7 6AA, U.K.

In this work, amino acid analyses of the acid hydrolyzed hot water extracts of gold foils containing five Category 3 (*i.e.*, carbon-rich) [1-4] particles returned by the JAXA Hayabusa mission were performed by liquid chromatography with fluorescence detection and time-of-flight mass spectrometry (LC-FD/ToF-MS). In advance of LC-FD/ToF-MS analysis, and after hot water extraction and acid hydrolysis, samples underwent pre-column derivatization using *o*-phthaldialdehyde/*N*-acetyl-L-cysteine (OPA/NAC), which is a fluorescent tagging agent that facilitates chromatographic separation of chiral primary amines. Initial analyses of these particles by JAXA using field emission scanning electron microscopy with energy dispersion X-ray spectrometry suggested the particles possessed significant amounts of carbon. Prior to amino acid analysis, infrared and Raman microspectroscopy analyses revealed highly primitive organic carbon was present in some grains [5]. Some terrestrial contamination, primarily as L-protein amino acids, was observed in all sample extracts. However, several terrestrially uncommon non-protein amino acids were also identified. Some particle extracts were characterized by racemic (D ≈ L) mixtures of the non-protein amino acids β-amino-*n*-butyric acid (β-ABA) and β-aminoisobutyric acid (β-AIB) at low abundances ranging from 0.09 to 0.31 nmol g⁻¹. A larger abundance of β-alanine (9.2 nmol g⁻¹, ≈4.5 times greater than background levels), also a non-protein amino acid, were measured in a combined extraction of three particles. This β-alanine abundance in these Hayabusa particles was ≈6 times higher than that (1.49 nmol g⁻¹) measured in an extract of a grain of the CM2 Murchison meteorite, which was processed in parallel. The comparatively high abundance of β-alanine in these three Hayabusa grains is surprising because Itokawa possesses similar features to that of amino acid poor LL ordinary chondrites, suggesting that perhaps the amino acid content observed in this study may be a result of exogenous delivery, as has been reported in the analyses of other Hayabusa particles [1,6]. Elevated abundances of β-alanine and racemic β-AIB and β-ABA in Hayabusa particles suggest these non-protein amino acids are not of terrestrial origin. These Itokawa results represent the first presentation of amino acids not of terrestrial origin in the extracts of material collected by an asteroid sample-return mission. Furthermore, these results demonstrate the analytical capabilities of the protocols used in this work as viable options with which to explore the soluble organic chemistry of asteroids Ryugu and Bennu returned by the Hayabusa2 and OSIRIS-REx missions, respectively.

References

- [1] Chan Q. H. S. et al. 2021. Scientific Reports 11. [2] Ito M. et al. 2014. Earth, Planets and Space 66. [3] Yabuta H. et al. 2014. Earth, Planets and Space 66. [4] Kitajima F. et al. 2015. Earth, Planets and Space 67. [5] Chan Q. H. S. et al. 2019. Abstract #6223. 82nd MetSoc. [6] Burgess, K.D. and Stroud, R.M. 2021. Communications Earth & Environment 2.

NaCl in an Itokawa Particle: Terrestrial or Asteroidal?

Shaofan Che¹ and Thomas J. Zega^{1,2}

¹*Lunar and Planetary Laboratory, University of Arizona, Tucson AZ*

²*Department of Materials Science and Engineering, University of Arizona, Tucson AZ*

Introduction. The detailed mineralogies and compositions of the particles returned from asteroid Itokawa collected by the Hayabusa mission were extensively studied over the past decade [e.g., 1-3]. However, the full range of nanoscale features of these returned samples are still not well understood. We previously reported NaCl grains in a focused-ion-beam (FIB) section extracted from particle RA-QD-02-0248 [4]. In this study, these NaCl grains are re-examined to better understand their origins and potential implications for the alteration processes on Itokawa.

Methods. The characterization work was conducted on the 200 keV Hitachi HF5000 scanning transmission electron microscope (S/TEM) located at the Kuiper Materials Imaging and Characterization Facility, Lunar and Planetary Laboratory, University of Arizona (Tucson, AZ, U.S.A.). The HF5000 is equipped a cold-field emission gun, third-order spherical aberration corrector for STEM mode, and an Oxford Instruments X-Max N 100 TLE energy-dispersive X-ray spectroscopy (EDS) system with dual 100 mm² windowless silicon-drift detectors providing a solid angle (Ω) of 2.0 sr.

Results. A total of five FIB sections were lifted out from RA-QD-02-0248 during the initial examination in August and September 2016. [4] reported that Section #3 is composed of plagioclase and olivine with abundant NaCl grains, most of which were randomly distributed on the plagioclase surfaces while some appeared be within the thickness of the section. The NaCl grains were reported to vary in size from <20 nm to 200 nm and some of the large grains appeared euhedral, with cubic or elongate shapes. No NaCl grains were found on the adjacent olivine. The plagioclase was also reported to contain thin (<15 nm) K-feldspar lamella along its interface with olivine. We recently re-visited this FIB section to evaluate if the NaCl grains were modified. Our STEM results show that the overall distribution of the grains did not change (Fig. 1). To better compare the NaCl grains analyzed in 2016 and now, we overlaid the secondary electron (SE) images with each other (Fig. 2). The data suggest that some grains grew larger and more euhedral and some adjacent grains merged into larger ones. We also re-examined the Section #4 containing plagioclase and olivine. STEM analysis shows abundant high-Z grains (~30 nm in size) and many of them are on the surface of the FIB section. The EDS elemental mapping of these grains shows a clearly resolved Cl K peak in a summed spectrum. Similar to Section #3, NaCl grains do not occur within the olivine in this Section #4.

Discussion. Halite crystals were previously reported in two ordinary chondrites, Monahans (H5) and Zag (H3-6) [5-6]. Several lines of evidence, such as the widespread distribution of halite in the matrices and the ancient ages derived from the radiogenic isotope dating methods, suggest a pre-terrestrial origin of halite in these meteorites. Micrometer-sized halite is also a ubiquitous phase on the external surfaces of many Itokawa particles [7], and a recent TEM study of two Itokawa particles [8] showed that submicrometer-sized NaCl grains were present on the top surface of plagioclase below the capping layer. These authors also described an outer NaCl rim surrounding plagioclase. Contrary to the halite grains in Monahans and Zag, those in Itokawa particles do not show strong textural or compositional evidence for a pre-terrestrial origin, partly due to their small sizes and extremely reactive nature [7]. Textural modifications of halite in the N₂-filled storage box were previously observed [7].

The NaCl grains in the Itokawa sample RA-QD-02-0248 that we report on here could be contaminants introduced during the ultramicrotomy or FIB sectioning. However, this scenario has difficulty in explaining why NaCl grains only occur on the plagioclase, instead of randomly dispersed in both plagioclase and olivine. Alternatively, NaCl grains might have formed during the TEM analysis. Na in plagioclase could be mobilized by the high-voltage electron beam providing a potential Na source for NaCl grains. However, this scenario has trouble explaining the source of Cl. The coarsening and change of shapes of NaCl grains could be driven by Ostwald ripening due to the relative low humidity in the N₂-filled desiccator. Nonetheless, the lack of changes in the distribution and amount of NaCl grains after 5-year storage in the desiccator proves that significant alteration did not occur during sample preservation.

If the NaCl grains in our FIB sections are native to the asteroid, which the TEM data supports, then such grains could have formed through in situ alteration of plagioclase on Itokawa. Previous studies of phosphates and plagioclase in ordinary chondrites suggest that the initial fluid altering primary merrillite and anorthite was a hydrous brine containing Na, K, Cl and F, and at the waning stage of alteration, the fluid could have become very dry and halogen-rich [9-11]. The saturation of NaCl in the dry fluid could have subsequently resulted in the precipitation of halite [11,12].

Conclusion and further work. Our TEM investigation of Itokawa particle RA-QD-02-0248 suggests that the NaCl grains might be native to Itokawa. We plan to conduct atomic-scale imaging with EDS to further investigate the structure and

chemical composition of the NaCl grains in Section #3. We will also search for NaCl in another FIB section #5 that contains twinned plagioclase.

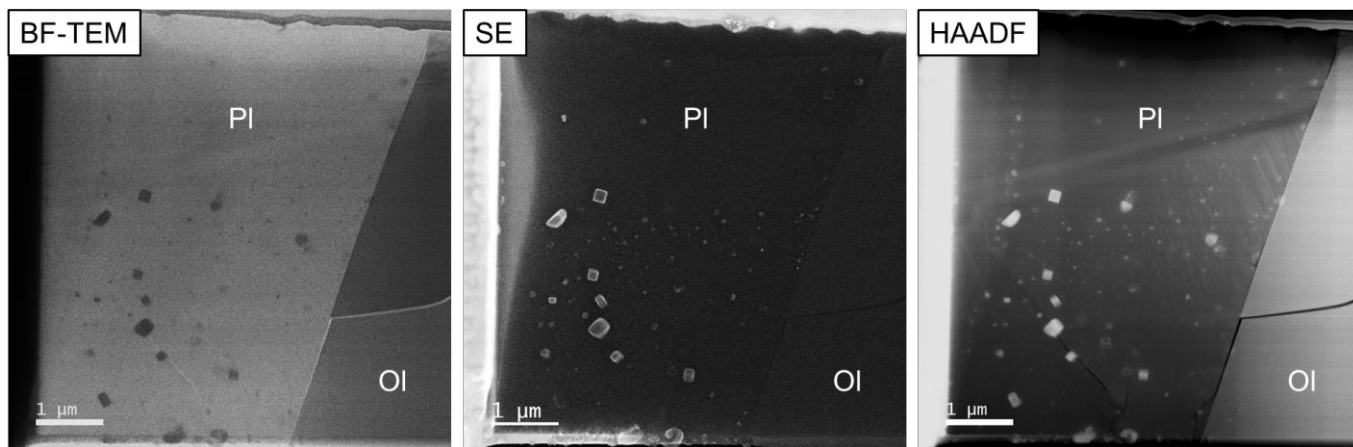


Figure 1. TEM images showing the distribution of NaCl grains on the side surface of plagioclase. The images were obtained on September 10th, 2021.

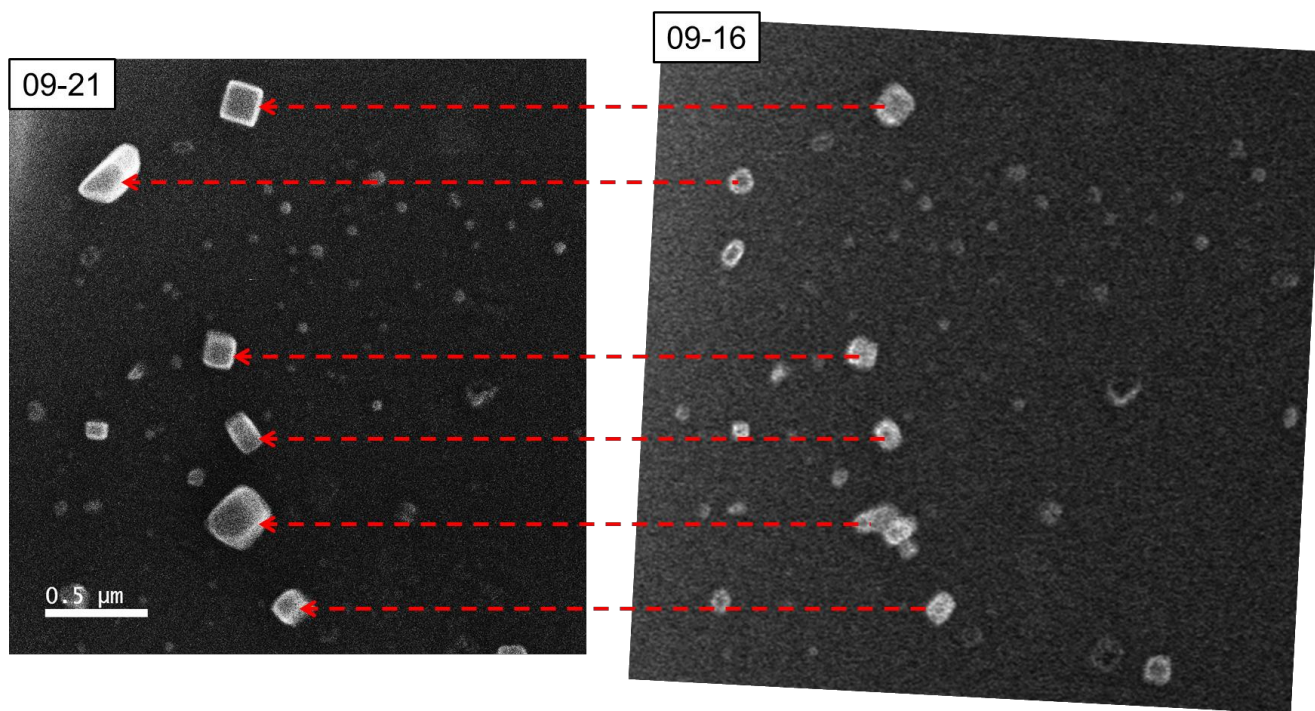


Figure 2. The SE image taken in September 2021 (left) is compared with that taken in September 2015 (right). The NaCl grains have been well preserved, except some of them show changes in size and shape.

References

- [1] Nakamura T. et al. 2011. *Science* 333:6046. [2] Thompson M. S. et al. 2014. *Earth, Planets and Space* 66:1. [3] Matsumoto T. 2020. *Nature communications* 11:1. [4] Zega T. J. et al. 2017. Abstract #3037. 48th LPSC. [5] Zolensky M. E. et al. 1999. *Science* 285:5432. [6] Rubin A. E. et al. 2002. *Meteoritics & Planetary Science* 37:1. [7] Noguchi T. et al. 2014. *Meteoritics & Planetary Science* 49:7. [8] Keller L. P. and Berger E. L. 2017. *The Eighth Symposium on Polar Science/Ordinary sessions*. [9] Jones R. H. et al. 2014. *Geochimica et Cosmochimica Acta* 132. [10] Lewis J. A. and Jones R. H. 2016. *Meteoritics & Planetary Science* 51:10. [11] Jones R. H. et al. 2016. *American Mineralogist* 101:11. [12] Zolotov M. Y. et al. 2005. Abstract #2271. 36th LPSC.

Northwest Africa 5401 CV chondrite: Not oxidized, not reduced, maybe in between?

T.J. Fagan¹, M. Komatsu², Y. Imai¹ and N. Sumiwaka¹

¹*Dept. Earth Sciences, Waseda University, Tokyo, Japan*

²*SOKENDAI, Kanagawa, Japan*

Introduction: Variations in oxidizing vs. reducing conditions in the early solar system are recorded by the CV chondrites. Nickel-poor compositions of troilite and relatively abundant Fe,Ni-rich metal are indicators of reducing conditions in a reduced subgroup (CV3red), whereas Ni-rich sulfide and a paucity of Fe,Ni-rich metal grains are indicators of oxidizing conditions in two oxidized subgroups (CV3oxA similar to Allende and CV3oxB similar to Bali) [1-3]. Raman analyses of temperature-sensitive carbon-rich matter have helped to show that the CV3red subgroup was metamorphosed at lower temperatures than the oxidized subgroups [2,4,5]. However, most CV chondrites appear to fall within one of the three subgroups—samples representing intermediate metamorphic temperatures and red-ox conditions are rare.

In this project, we present petrologic data and Raman spectroscopy analyses to argue that the meteorite Northwest Africa 5401 (NWA 5401) represents an intermediate stage in metamorphic temperature and oxidation, between the CV3red and CV3oxA subgroups. The presence of an intermediate suggests that the CV3red and CV3oxA subgroups represent stages along a continuum of temperature-oxidation conditions, and favors the interpretation that CV chondrites come from a single parent body that experienced a range of metamorphic conditions (cf. [3]).

Samples and Methods: Two polished thin sections and several chips were prepared from a slab of NWA 5401. One of the thin sections contains a texturally distinct clast (similar to dark inclusions reported from other CV chondrites, e.g. [6]) within the main host lithology of NWA 5401. The other thin section includes a coarse-grained Ca-Al-rich inclusion (CAI). The thin sections were imaged using petrographic microscopes, a Hitachi S-3400N scanning electron microscope (SEM) and JEOL JXA 8900 electron probe microanalyzer (EPMA) at Waseda University. Quantitative elemental analyses of minerals were collected by EPMA using a 15 kV, 20 nA, ~1- μ m spot electron beam and well-characterized standards. Modes of chondrite components (chondrules, matrix, amoeboid olivine aggregates (AOAs), CAIs) were collected by manually counting on a grid overlying elemental maps of the two thin sections.

Raman spectra were collected at the Waseda Physical Properties Measurement Center using a laser excitation wavelength of 532 nm and a spot size of ~3-4 μ m focused by a 50x objective lens. The power at the sample surface was ~2.4 mW, the acquisition time was 10 seconds, and spectra were acquired in the range of 500-2200 cm^{-1} . Spectral fitting was conducted using a Lorentzian profile for the D-band, BWF profile for the G-band in the region of 900-1900 cm^{-1} . Model spectra with poor fits to data ($R^2 < 0.97$) were excluded. The D- and G-bands (abbreviated for defect and graphite, respectively) are attributed to molecular vibrations in carbon-rich matter; the full width at half maximum of the D-band (FWHM-D) decreases and peak intensity ratio of I_D/I_G increases with thermal maturity [4].

Results and Discussion: Large chondrules typical of CV chondrites are evident in the host lithology of NWA 5401 (Fig. 1). The clast lithology has much smaller chondrules and a higher matrix/inclusions* ratio (*inclusions used here to represent high-T components of chondrites including chondrules, CAIs and AOAs; see [7]). The NWA 5401 host has matrix/inclusions ~ 0.7-0.8, whereas the clast has matrix/inclusions ~ 3.8. Corresponding values determined by [7] are as follows: ~1.3 for Allende and Tibooburra (CV3oxA); 0.8 and 1.2 for Bali and Mokoia, respectively (CV3oxB); 0.6 and 0.4 for Vigarano and Leoville, respectively (CV3red, though Vigarano is a breccia with some CV3ox affinities). Bonal et al. (2020, ref. [2]) do not use the same matrix/inclusions parameter, but do report matrix mode percentages, with averages ($\pm 1\sigma$) of 48.9 (± 5.6) for CVoxA, 52.3 (± 8.5) for CVoxB and 35.1 (± 7.2) for CVred. The matrix abundance of ~45 mode% of the NWA 5401 host lithology appears typical for the oxidized CV subgroups, but somewhat high for CVred.

The extent of alteration in the coarse-grained CAI (labelled SC-9) in one thin section of NWA 5401 also appears intermediate between observations reported from reduced and oxidized CV chondrites. Coarse-grained CAIs in Allende typically have alkali-FeO-rich minerals near CAI rims and grossular-rich veins extending into CAI interiors [8], whereas coarse-grained CAIs from CVred lack the grossular-rich veins and have only minor abundances of alkali-rich secondary minerals near CAI rims. In contrast, NWA 5401 CAI SC-9 has a widespread domain of alkali-rich minerals near its rim, but lacks the grossular-rich veins typical of Allende CAIs.

Nickel concentrations in sulfides were among the first observations that led [9] to distinguish oxidized CVs (with high-Ni sulfides) from reduced CVs (with low Ni-sulfides); the variations in Ni abundances in sulfides are verified by [3] (Fig. 2). Sulfides in NWA 5401 host lithology are near-endmember troilite with minimal Ni (Fig. 2).

Raman analyses show that the FWHM-D and I_D/I_G parameters of NWA 5401 fit most closely with previously compiled analyses from the CVoxB subgroup, though there is some overlap with CVred (Fig. 3).

In summary, the NWA 5401 host lithology appears similar to the CVoxB and CVred groups in Raman parameters, to the CVred group in sulfide composition, but exhibits greater alteration in a coarse-grained CAI than is typical of CVred CAIs. The matrix/inclusions ratio of NWA 5401 host is above that of most CVred chondrites and comparable to matrix/inclusions of some oxidized CVs. NWA 5401 may represent an intermediate metamorphic history between low-T metamorphism of CVred and higher-T metamorphism typical of oxidized CVs.

References: [1] Weisberg et al. (2006) in Lauretta D.S. & McSween H.Y. (editors) MESS II, p. 19-52. [2] Bonal L. et al. (2020) GCA 276: 363-383. [3] Gattacceca J. et al. (2020) EPSL 547: 116467 (9 pages). [4] Bonal L. et al. (2006) GCA 71: 1849-1863. [5] Bonal L. et al. (2016) GCA 189: 312-337. [6] Buchanan P.C. (1997) GCA 61: 1733-1743. [7] Ebel D.S. et al. (2016) GCA 172: 322-356. [8] Fagan T.J. et al. (2007) MAPS 42: 1221-1240. [9] McSween H.Y. (1977) GCA 41: 1777-1790.

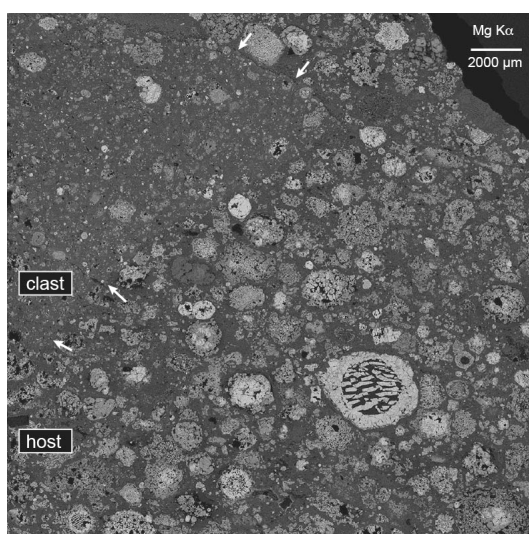


Fig. 1. Mg Ka map of NWA 5401 host and clast lithologies. Arrows highlight boundary.

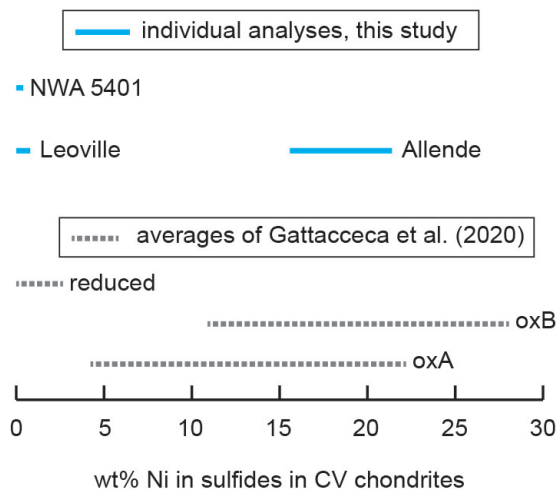


Fig. 2. Nickel concentrations in sulfides in CV chondrites. Ranges of values in the CV subgroups show averages from individual meteorites reported by Gattacceca et al. (2020) and ranges of individual analyses collected for this study.

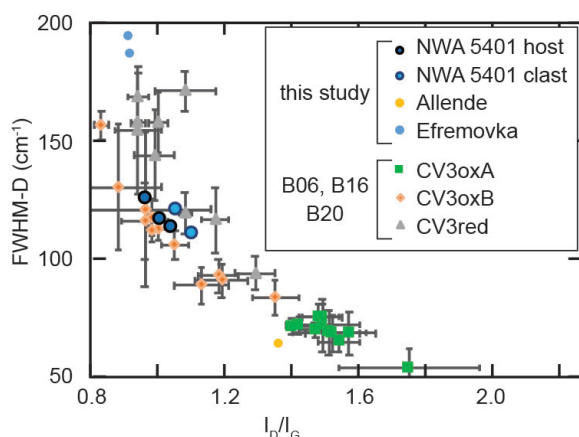


Fig. 3. Raman parameters collected in this study and reported by Bonal et al. (2006; 2016; 2020).

Organics and iron speciation in CI chondrites : a combined STXM and TEM study

Le Guillou C.¹, Leroux H.¹, Bernard S.², Viennet J-C.², Marinova M.¹, Jacob D.¹, De La Pena F.¹, Brearley A.³, El Kemi H.³

¹Unité Matériaux et transformation, Université de Lille, France

²IMPMC-MNHN, Sorbonne Université, Paris, France

³University of New Mexico, Albuquerque, USA

In order to precisely comparing the mineralogy and the nature organic matter of known chondrites with Ryugu samples, we investigated 6 FIB sections of Orgueil and 2 sections of Ivuna CI chondrites. Orgueil insoluble organic matter (IOM) was also measured. We first performed Scanning Transmission X-ray Microscopy (STXM) at the Carbon and Iron edge, to determine the speciation of these elements. We are performing Transmission Electron Microscopy (TEM), with a special focus on the elemental composition of phyllosilicates and organic matter.

STXM delivers hyperspectral dataset that can be processed pixel by pixel using the python hyperspy library [www.hyperspy.org/]. For the Iron L-edge, we fit the background and an arctangente and quantify the $Fe^{3+}/\Sigma Fe$ using previously established calibration (Bourdelle et al., 2013, Le Guillou et al., 2015). For the Carbon K-edge, we fit the background, normalize to the carbon amount and then fit gaussians at given positions to quantify some of the functional groups using previously established calibration (Le Guillou et al., 2018). Thanks to these procedures, we obtain quantitative maps and are able to describe the variability and distribution at the scale of 10s of nanometer.

In Orgueil, Iron in phyllosilicates is oxidized, the $Fe^{3+}/\Sigma Fe$ varies between 65 and 80 %, with a dichotomy likely related to the fine grained/coarse-grained mixture of smectite and serpentine. Sulfides and oxides are also present.

Organics display three families of spectra (in addition to carbonates) :

- Organic particles, which are aromatic-rich and show important variability from one particle to the next. They contain some ketone and/or phenol groups. They are more aromatic than the IOM.
- diffuse organic, with is present all over the section, mixed at a fine scale with phyllosilicates. It is aliphatic and carboxylic rich. The carbon amount is lower than in particles. They are less aromatic than the IOM.
- Carboxylic-rich particles, present locally in some section, they show a carboxylic peak higher than the diffuse OM, and is often accompanied by a hydroxyl and/or a carbonate peak.

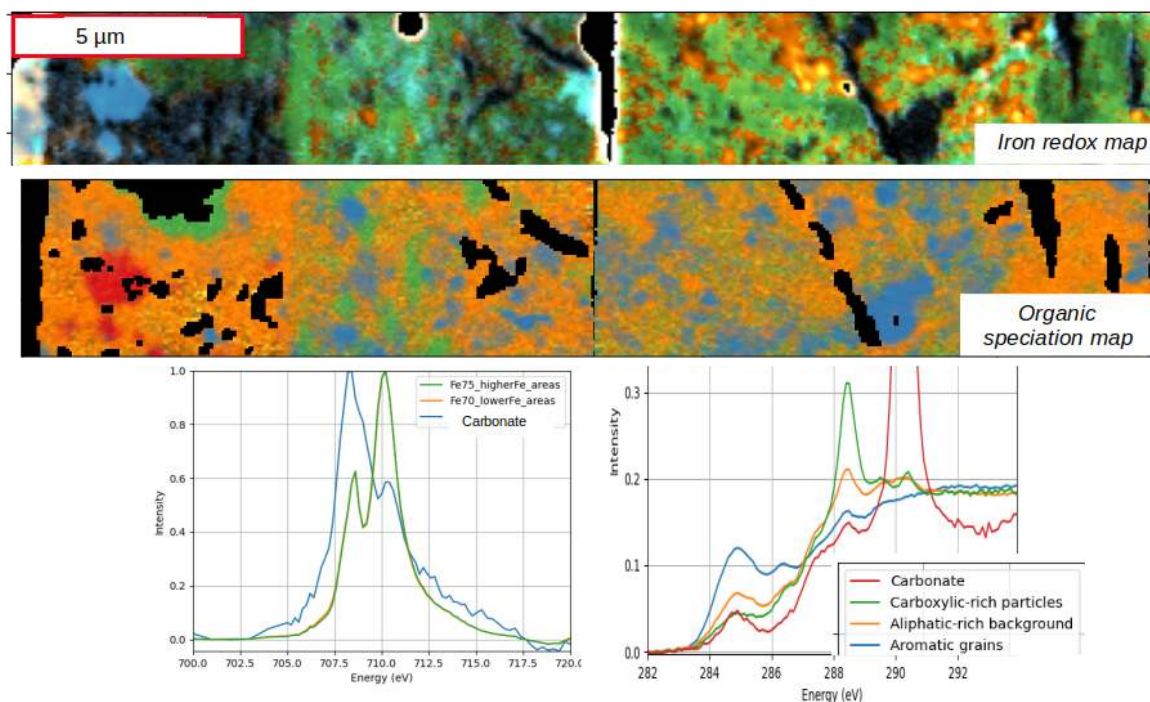


Figure 1. Maps based on linear combination fitting of individual components. On top, map based on the iron L-edge, showing different regions with both slight redox variation but also iron content variation. Below, map based on the carbon speciation showing individual organic particles (blue) embedded in diffuse OM (orange) covering the entire section.

In order to describe the variability, we plotted histograms (Fig. 2).

The iron valency is heterogeneous from section to section, possibly depending on the ratio of coarse/fine grained phyllosilicates that are sampled each time. However, it could also be due to a more global variability of the sample at the micrometer scale. Several areas need therefore to be investigated to fully describe them.

Diffuse OM is very heterogeneous at the FIB section scale, with a tail extending toward aromatic particles. The latter are not really visible on the histograms because they are less abundant. There is also a little variability of the peak distribution, especially in one of the section (G2-2).

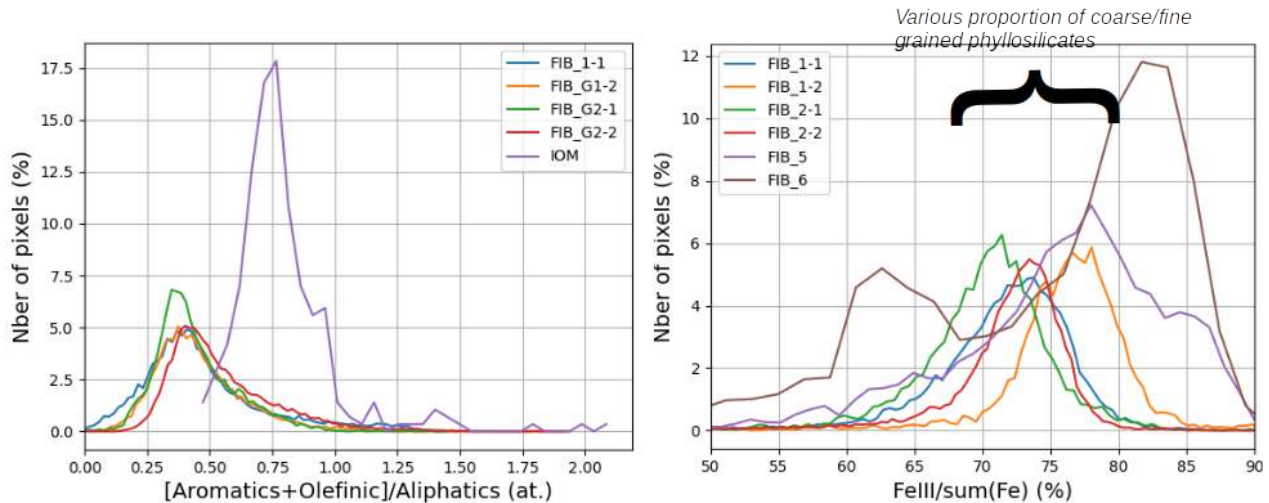


Figure 2. Histograms of quantified proxies at the carbon K-edge (left) and Iron L_edge (right). They allow to visualize the distribution of the composition within each FIB section, as well as the heterogeneity among different FIB sections.

Altogether, these data will help us understand the history of the CI parent body. Similar data obtained on Ryugu samples have been obtained and are presently being processed.

Shocked regolith in asteroid 25143 Itokawa surface

Josep M. Trigo-Rodríguez¹, S. Tanbakouei¹ and Mark Burchell²

¹*Institute of Space Sciences (CSIC-.IEEC), Campus UAB, C/ Can Magrans s/n, 08193 Cerdanyola del Vallés (Barcelona), Catalonia, Spain,*

² *Centre for Astrophysics and Planetary Science, University of Kent, Canterbury Kent CT2 7NR, Kent, United Kingdom,*

A major milestone in space exploration was to achieve the first sample return from an asteroid by the Japanese Space Agency (JAXA) [1]. The detailed images of asteroid 25143 Itokawa transformed a faint point of light seen by telescope into an intricated rubble-pile asteroid, with a complexity that exemplifies the type of challenging bodies we need to confront as source of hazard to humans. These bodies surrounding our planet exhibit challenging properties because they have been exposed over the eons to space weathering processes and numerous impacts. As a consequence, their crumbly surfaces are covered by small particles, pebbles, and boulders [1]. The Japanese JAXA/ISAS Hayabusa mission collected micron-sized particles from the regolith of asteroid 25143 Itokawa [2]. We have studied some regolith grains using different analytical techniques in our Meteorite and Sample Return Clean Lab at the CSIC Institute of Space Sciences in Barcelona in order to unveil some of the processes in which they were formed [3].

There is an important debate about the dominant physical processes at work in the surface of these bodies. Certainly Near Earth Asteroids (NEAs) are exposed to short-perihelion approaches that produce significant thermal stress changes in the rock-forming minerals present in their surfaces. Nowadays, it is usually considered that most small regolith particles are produced by thermal fatigue [4], but obviously impacts should play an important role over longer time scales. Fine-grained regolith could be useful to apply future In Situ Resource Utilization (ISRU) tests in NEAs, so there is specific interest in deciphering the most dominant mechanisms. Then, which of these two mechanisms dominates the production of regolith over a body like Itokawa?. This can be tested in a non-destructive way, just by studying the silicate phases using Raman spectroscopy. Itokawa asteroid is a nice example of a rubble pile and its surface consists of heterogeneously distributed boulders, large rocks and pebbles: In addition, some regions contain fine-grained regolith made of pounded stones and small grits (Saito et al, 2006). A particularly useful mineral to infer the existence of shock is olivine, as pointed out by Harriss and Burchell [5].

We have studied 3 Itokawa particles provided by JAXA with numbers S14, S23 and S47 were investigated (Table 1). The polished upper sides of the three particles are shown in Figure 1. To study their specific mineralogy the samples were analyzed by SEM/EDX (Quanta 650 FEG equipped with EDX Inca 250 SSD XMax20 detector). To identify possible shocked minerals several regions of interest (ROIs) were defined. Then we have performed Micro-Raman spectra using a spot size of about 1 μm and a laser power of 0.6 mW cm^{-2} . We studied carefully the chemical and mineralogical structure to get some clues on their shock history. Raman spectra were taken at room temperature using the 5145 \AA line of an Argon-ion laser with a Jobin-Yvon T-64000 Raman spectrometer attached to an Olympus microscope, and using a CCD detector cooled by liquid nitrogen. We concentrated in the silicate phases, so we decided to acquire the spectra in a working window between 100 and 1400 cm^{-1} . From the EDX images and the peaks found in the Raman spectra we are able to distinguish the major rock-forming minerals (Fig. 1).

Table 1. Catalog numbers, maximum size and composition of the studied regolith samples.

Sample#	Size (μm)	Main mineral phases
RA-QD02-0014	131.2 \pm 0.1	Olivine, low-Ca pyroxene, plagioclase
RA-QD02-0023	149.4 \pm 0.1	Olivine, troilite
RA-QD02-0047	108.0 \pm 0.1	Olivine, low-Ca and high-Ca pyroxene

As the main results of the study of the selected ROIs, our Raman spectra of olivine, found for two out of three grains, show two drifted peaks $P1=820\text{ cm}^{-1}$ and $P2=850\text{ cm}^{-1}$ which are considered characteristics of a shocked phase [6]. A Raman spectrum for S14 particle is shown in Fig. 1. The precise peak location depends on the forsterite (Fo) and fayalite (Fa) content of the olivine [7,8]. A Raman spectrum for S14 particle is shown in Fig. 1. The precise peak location depends on the forsterite (Fo) and fayalite (Fa) content of the olivine [8-9]. In any case, Harriss and Burchell suggested that shocked olivines above 65 GPa exhibit permanent shifts in the 820 and 850 cm^{-1} peaks in their Raman spectra [5].

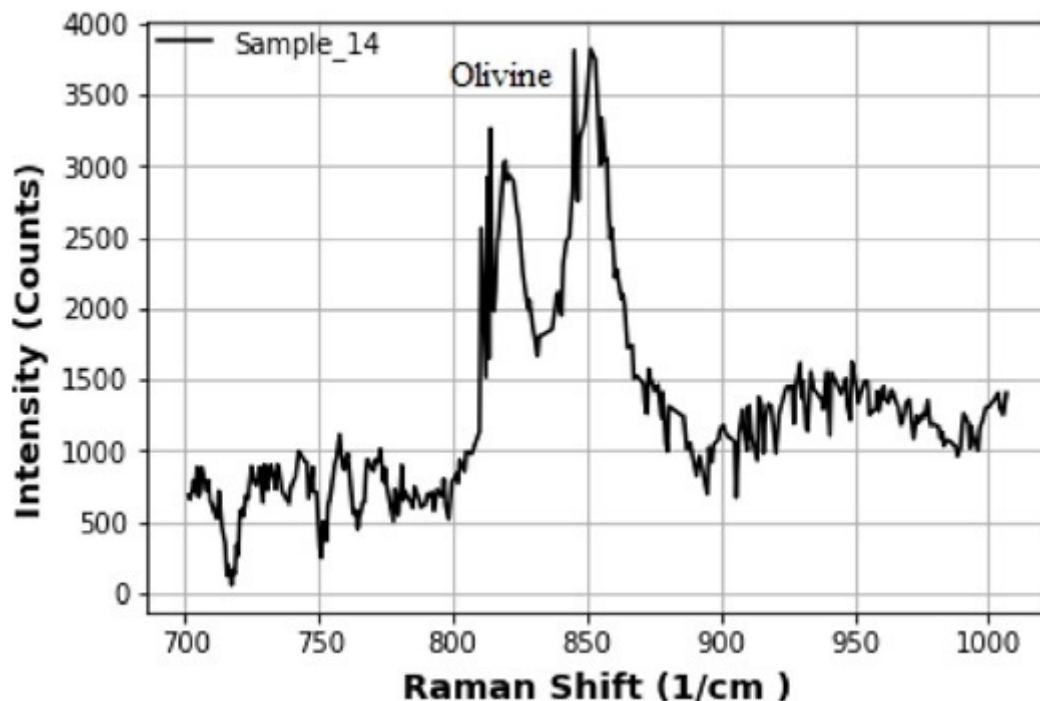


Figure 1. Raman spectrum obtained for olivine in sample RA-QD02-0014

In conclusion, the shock experienced by Itokawa's regolith grains can be inferred from the deformation found in the lattice of the olivine grains. Our Raman study of three particles seems to indicate that a significant fraction of these grains could have experienced collisional processing. Obviously the number of studied grains so far is not statistically significant, but this finding could encourage other groups to complete a more comprehensive study. If these preliminary results are correct, a significant fraction of the regolith particles collected in the Muses Sea were shocked, and fragmented by impact excavation more than by thermal fatigue. In fact, such scenario is likely because nano-indentation studies we performed on these grains [1] seem to point that the minerals exhibit similar mechanical properties than ordinary chondrites of similar composition [3].

Acknowledgements

JMTR and ST acknowledge financial support from research project PGC2018-097374-B-I00, funded by FEDER/Ministerio de Ciencia e Innovación – Agencia Estatal de Investigación (PI: JMTR).

References

- [1] Nakamura T., et al., 2012. *Science* 333, 1113. [2] Saito, J., et al. 2006. *Science*, 312, 1341. [3] Tanbakouei, S., et al., 2019. *Astronomy & Astrophysics*, 629, p.A119. [4] Delbo M. et al. 2014. *Nature*, Volume 508, 233. [5] Harriss, K.H., and Burchell, M.J., 2016. *Meteoritics & Planetary Science* 51, 1289. [6] Mohanan, K., et al. 1993. *American Mineralogist*, 78, 42. [7] Chopelas, A., 1991. *American Mineralogist*, 76, 1101. [8] Kuebler K. E., et al. 2006, *Geochim. Cosmochim. Acta*, 70, 6201. [9] Foster N.F., et al. 2013. *Cosmochimica et Geochimica Acta* 121, 1.

Organic matter in Itokawa particles

Q. H. S. Chan^{1,2}, A. Stephant², I. A. Franchi², X. Zhao², R. Brunetto³, Y. Kebukawa⁴, T. Noguchi⁵, D. Johnson^{2,6}, M. C. Price⁷, K. H. Harriss⁷, M. E. Zolensky⁸, M. M. Grady^{2,9}, E. T. Parker¹⁰, D. P. Glavin¹⁰, and J. P. Dworkin¹⁰

¹Royal Holloway University of London, Egham TW20 0EX, Surrey, UK. ²The Open University, Walton Hall, Milton Keynes MK7 6AA, UK. ³IAS-Université Paris-Saclay, 91405 Orsay, France. ⁴Yokohama National University, Yokohama 240-8501, Japan. ⁵Kyushu University 744, Motoooka, Nishi-ku, Fukuoka 819-0395, Japan. ⁶University of Exeter, Penryn, Cornwall TR10 9FE, UK. ⁷University of Kent, Canterbury CT2 7NH, Kent, UK. ⁸NASA Johnson Space Center, Houston, TX 77058, USA. ⁹The Natural History Museum, London SW7 5BD, UK. ¹⁰NASA Goddard Space Flight Center, Greenbelt, MD 20771, USA.

The first Hayabusa mission returned samples from the near-Earth S-type asteroid 25143 Itokawa to Earth in 2010 [1]. Although Itokawa has a lithology related to ordinary chondrites (OCs) that typically have low organic contents, several Itokawa particles were found to contain organic matter (OM) [2-5]. However, there was not an explicit conclusion to the origin of the observed OM in these early studies. We have extended our search for OM into other Itokawa grains. Here, we report extraterrestrial OM (macromolecular carbon and amino acids) observed in six Itokawa particles (including a category 1 particle: RA-QD02-0162 [#62; also nicknamed “Amazon”), and five category 3 carbon-rich particles: RA-QD02-0012 [#12], RA-QD02-0078 [#78], RB-CV-0029 [#29], RB-CV-0080 [#80] and RB-QD04-0052 [#52]).

All allocated Itokawa samples were initially analysed by spot and point-by-point mapping Raman spectroscopic analysis at the Open University, UK. Amazon was then transferred and mounted into indium on an aluminium stub, which was studied with a NanoSIMS 50L ion microprobe for its H,C,N isotopic compositions. The rest of the samples were mounted in sterile gold foils, and the amino acid contents of their acid hydrolysed hot water extracts were obtained with a liquid chromatography with tandem fluorescence and accurate mass detection at NASA Goddard Space Flight Center, USA.

Based on the observation of the Raman parameters (e.g. the peak locations and widths of the defect (D) and graphite (G) bands) [6], a significant variety of carbonaceous materials has been observed in Amazon. The carbonaceous materials include primitive and unaltered OM that shares similarity with the IOM in primitive (CI,CM,CR) carbonaceous chondrites, as well as OM that has been heavily graphitised. The organic structure of the heated material is best represented by nanocrystalline graphite, comparable to that observed for metamorphosed meteorites (e.g., L3–6 Inman, Tieschitz and New Concord, CV3 Allende, and EH4 Indarch), suggesting peak metamorphic temperatures (PMT) of $>\sim 600^{\circ}\text{C}$. The thermal history recorded in the graphitic OM agrees with PMT estimates for returned Itokawa regolith grains ($600\text{--}800^{\circ}\text{C}$) [7].

We have obtained the H,C,N isotopic compositions for the primitive OM in Amazon, which exhibits unambiguously extraterrestrial isotopic signatures ($\delta\text{D} = +4868 \pm 2288\text{‰}$; $\delta^{13}\text{C} = -24 \pm 5\text{‰}$; $\delta^{15}\text{N} = +344 \pm 20\text{‰}$), contrasting to the typically negative isotopic values obtained for terrestrial organic matter [8]. The δD and $\delta^{13}\text{C}$ values of the organic material in Amazon are comparable to OCs, however, the $\delta^{15}\text{N}$ value is higher than that typically observed for OCs ($\delta^{15}\text{N} = -47$ to $+36\text{‰}$), and is similar to that of CRs ($\delta^{15}\text{N} = +153$ to $+309\text{‰}$) [9]. Our data suggest a genetic link between the primitive organic material observed in Itokawa to CRs and IDPs for they share similar D, ^{13}C and ^{15}N enrichments [10].

The high carbon contents of the five category 3 Itokawa particles suggest potentially higher OM abundances, hence we extracted and analysed amino acids in these samples. Although terrestrial contamination was observed primarily as L-protein amino acids, several terrestrially uncommon non-protein amino acids were also observed at low abundances, such as β -aminoisobutyric acid (β -AIB), β -amino-*n*-butyric acid (β -ABA), and β -alanine. Itokawa amino acid content observed here was dissimilar to thermally altered OCs, but preliminarily analogous to more aqueously altered CR2s.

Continued evolution of Itokawa is evident by the infall of primitive organic material derived from CRs/IDPs, accounting for a complex interplay between the remnant Itokawa silicates with exogenous organics. The results reported here are the first evidence of extraterrestrial OM in asteroid material from a sample-return mission, showcasing a working protocol for analysing samples returned by the Hayabusa2 and OSIRIS-REx missions.

References

- [1] Yada, T., et al. *Meteoritics & Planetary Science*, 2014. **49**(2): p. 135-153. [2] Ito, M., et al. *Earth, Planets and Space*, 2014. **66**(1): p. 91. [3] Yabuta, H., et al. *Earth, Planets and Space*, 2014. **66**(1): p. 1-8. [4] Uesugi, M., et al. *Earth, Planets and Space*, 2014. **66**(1): p. 1-11. [5] Kitajima, F., et al. *Earth, Planets and Space*, 2015. **67**(1): p. 1-12. [6] Tuinstra, F. and J.L. Koenig. *Journal of Chemical Physics*, 1970. **53**(3): p. 1126-1130. [7] Nakamura, T., et al. *Science*, 2011. **333**(6046): p. 1113-1116. [8] Pizzarello, S. *Accounts of Chemical Research*, 2006. **39**: p. 231-237. [9] Alexander, C.M.O.D., et al. *Geochimica et Cosmochimica Acta*, 2007. **71**: p. 4380-4403. [10] Busemann, H., et al. *Science*, 2006. **312**: p. 727-730.

Hayabusa2 curation: from concept, design, development, to operations

Masanao Abe^{1,2}, Tomohiro Usui¹, Shogo Tachibana^{1,3}, Tatsuaki Okada^{1,3}, Shino Suzuki¹, Haruna Sugahara¹, Toru Yada¹, Masahiro Nishimura¹, Kanako Sakamoto¹, Kasumi Yogata¹, Akiko Miyazaki¹, Aiko Nakato¹, Kana Nagashima¹, Rei Kanemaru¹, Kentaro Hatakeda^{1,4}, Kazuya Kumagai^{1,4}, Yuya Hitomi^{1,4}, Hiromichi Soejima^{1,4}, Miwa Yoshitake^{1,X}, Ayako Iwamae^{1,4,Y}, Shizuho Furuya^{1,3}, Tasuku Hayashi¹, Daiki Yamamoto¹, Ryota Fukai¹, Takuya Ishizaki¹, Hisayoshi Yurimoto⁵

¹ *Institute of Space and Astronautical Science, Japan Aerospace Exploration Agency, Sagamihara 252-5210, Japan,*

²*The Graduate University for Advanced Studies (SOKENDAI), Hayama 240-0193, Japan,* ³*University of Tokyo, Bunkyo, Tokyo 113-0033, Japan,* ⁴*Marine Works Japan, Ltd., Yokosuka 237-0063, Japan,* ⁵*Hokkaido University, Sapporo 060-0810, Japan*

Introduction: JAXA conducted and is conducting sample return missions, such as Hayabusa and Hayabusa2, to bring back samples of extraterrestrial materials from asteroids (S-type asteroid Itokawa and C-type asteroid Ryugu, respectively). The returned materials are scientific valuable samples that can provide scientific knowledge about the origin and evolution of the Solar System [1]. Prior to sample return, meteorites were the only accessible extraterrestrial samples to unravel the history of the Solar System. However, meteorites have to be strong enough to fly through the Earth's atmosphere to fall, and, after dropped on the ground, they are contaminated by terrestrial atmosphere, water and materials, changing their properties. On the other hand, sample return missions allow to store the sample in a sealed container and protect them from terrestrial contamination and from heat and shock during re-entry to the Earth. Returned samples are very valuable scientifically, and it is extremely important to handle them without compromising their scientific characteristics.

Scientific requirement: The curation center that handles returned samples has the following scientific requirements to maintain the high scientific value of the returned samples: 1) Do not expose the sample to the Earth's atmosphere; 2) Do not lose the sample; 3) Do not destroy the sample except for when needed. The first requirement is to prevent the samples from being reacted with terrestrial materials to be altered. If the terrestrial compounds are mixed into the sample, the reliability of the analytical results is not ensured. The second requirement should of course be met considering the cost, time, and human resources to get samples back from space. The third requirement is not strict, but refers only to preliminary examination of the samples. The preliminary examination team at the curation center performs first description of the returned samples before detailed initial analysis by the project-lead analysis team. The destructive analysis of the sample should not be performed in the preliminary examination at the curation center in order to enable the initial analysis team to perform a comprehensive analysis that combines the morphological observation of the sample and the destructive chemical analysis.

Role: The curation center is responsible for the receipt and preliminary analysis (we call it “initial description”) of returned samples while satisfying the above requirements as well as the long-term storage and scientific investigation of the samples after the initial description. Examples of the initial description include size and shape description by optical observation, sample mass measurements, non-destructive spectroscopic observations for chemical and mineralogical analysis. In the case of Hayabusa, the total amount of sample brought back from Itokawa was small (i.e., about 1 mg) and spectroscopic observation was difficult. To compare with the data of the X-ray fluorescence spectrometer on-board the Hayabusa spacecraft, elemental analysis was also carried out by SEM/EDS during the initial description stage [2]. All these preliminary analyses have the important role to provide a scientific link between the sample brought back and the target body. Normally, the returned samples are stored in a special storage container, and it is necessary to take out the sample from the container by a special procedure. After the initial description, except for a part of the sample stored separately for future use, around half of samples is distributed for detailed analysis, for example the initial analysis and the AO (Announcement of Opportunity) research, which is open to the science community. The sample distribution also requires curatorial work, such as taking out and storing the samples in a distribution/transport container and tracking the analysis records.

Design: In consideration of the above roles, JAXA has designed clean rooms and clean chamber dedicated to each sample return mission (Hayabusa and Hayabusa2). The primary reason for this is to avoid mixing of samples from different targets but it is also because the method of taking out the samples from the container and the planned analyses for the initial description were different for the two missions. The facility design for the curation center initiated about 5 years before the sample returned to Earth. This is because it was expected to need one year for designing, two years for manufacturing, one year for confirming functions after manufacturing, and one year for rehearsal of the operation for receiving the returned sample. At the design stage, the specification study team from the JAXA curation members, the design team of the spacecraft sampler, and sample scientists from the research community played a central role in establishing the required specifications. After that, the

manufacturer was selected by bidding after receiving the specification approval from the curation steering committee and the Hayabusa/Hayabusa2 project team.

Specifications for Clean room: The specifications of the clean room at the JAXA Curation Center are basically the same for Hayabusa and Hayabusa2. The cleanliness of the clean room where the clean chamber is installed is Class 1000 (US federal standard), equivalent to Class 6 in ISO 14644-1 standard. The floor has a grating structure, and the return airflow travels from the bottom of the grating through the back of the wall to the ceiling and circulates from the ceiling using a ULPA filter to remove dust in the air. The clean room is maintained at a pressure higher than the outside to prevent outside contamination. The positive pressure control is performed with the adjacent downstream room, and the shortage is taken in from the outside air through a filter by approximately 10% of the circulating air volume. Temperature and humidity are controlled and maintained at 24 ± 2 °C and at $50\pm 10\%$ RH, respectively. The humidity is maintained at a high value to suppress the generation of static electricity. The supply pipes for exhaust gas, purified gas, cooling water, compressed air, etc. are connected to the clean chamber through a grating floor. Equipment that degrades the environments (for example, rough grinding pumps) are installed in isolated areas outside the clean room.

Specifications for Clean chamber: The clean chamber of the JAXA curation center is designed to perform all the operations on samples in a vacuum or pure nitrogen gas environment, i.e., sample extraction from the sample storage container, initial description of the samples, and distribution and storage of the samples. In particular, because the structure of the sample storage container of Hayabusa and Hayabusa2 is complex to store and deliver the samples safely, the clean chambers for both missions are required to have the interface to the sample container opening mechanism. Electrolytic polishing was applied to the inner surface of the chambers for quick cleaning recovery and to avoid contamination to the samples as much as possible. Several types of clean chambers are prepared for the purpose of work after opening the sample storage container, and they are connected to each other through gate valves. In principle, the sample container opening work is performed in a vacuum environment, but the sample removal, initial description, and distribution work have been performed through gloves in a high-purity nitrogen environment. Viton gloves were initially used to minimize organic contamination, but due to the difficulty in obtaining them because of the discontinuation of production, mainly Viton coated butyl gloves have recently been used. Materials used for the jigs used in the clean chamber and materials of the chamber itself were chosen to avoid materials other than those used in the sampling device of the spacecraft as much as possible in order to control the contamination. In particular, the containers to store the samples are basically made of synthetic quartz glass or sapphire, and in some cases stainless steel, aluminum, or Teflon are permitted to use. The use of copper- or gold- plated sample holders for certain analyses such as SEM/EDS is also allowed.

Operations and development: The curation center has been operated by the Astromaterials Science Research Group (ASRG) of ISAS, which is responsible for curatorial work (receipt, description, utilization, and storage) on extraterrestrial returned samples and for facility maintenance [3]. Hayabusa 2 samples were returned in December 2020. After opening the sample storage container in a vacuum environment, most of the curation work has been performed by using gloves in a nitrogen environment. The Hayabusa2 science team required the ASRG to pick up a small fraction of samples to store in a vacuum environment for future analytical studies without ever being exposed to nitrogen gas. Therefore, at the JAXA Curation Center, the clean chamber of Hayabusa2 has the new function of observing the inside of the sample storage container and taking out a part of the sample in a vacuum environment. Two millimeter-sized particles were successfully picked up and are now stored in the vacuum environment.

A total of 5.4 g of Ryugu samples were collected from the chambers A and C of the sample container, which were used for the sample collection at the first and second touchdown sites. The maximum particle size of the sample is about 1 cm, and hundreds of samples with a particle size of 1 mm or more have been confirmed. In the curation center, we plan to store each particle in an individual container as much as possible, acquire initial description data for individual particles to list in the sample catalog. The ASRG has independently-developed handling tools and sample containers to improve work efficiency while minimizing contamination. We believe that these developments will also help us receive and curate future returned samples. The ASRG also study Ryugu samples along with the project-lead initial analysis, which will also provide new insights into the origin and evolution of the Solar System.

References

[1] Tachibana S. et al. 2014. *Geochem J* 48:571. [2] Yada T. et al. 2014. *Meteoritics & Planetary Science* 49:135. [3] Abe M. 2021. *Sample Return Missions. The Last Frontier of Solar System Exploration* (book), Chapter 12.

Sample Analysis Plan for NASA's OSIRIS-REx Mission

H.C. Connolly Jr^{1,2}, T.J. Zega², V.E. Hamilton³, J.P. Dworkin⁴, K. Nakamura-Messenger⁵, C.W.V. Wolner², C.A. Bennett², P. Haenecour², and D.S. Lauretta²

¹*Rowan University, Glassboro, NJ, USA (connollyh@rowan.edu)*

²*Lunar and Planetary Laboratory, University of Arizona, Tucson, AZ, USA*

³*Southwest Research Institute, Boulder, CO, USA*

⁴*NASA Goddard Space Flight Center, Greenbelt, MD, USA*

⁵*NASA Johnson Space Center, Houston, TX, USA*

OSIRIS-REx [1,2] is the third mission in NASA's New Frontiers program and its first asteroid sample return mission. In October 2020, the OSIRIS-REx spacecraft successfully performed its Touch-and-Go (TAG) maneuver to collect a sample of regolith [3] from the surface of its target, asteroid (101955) Bennu, and is now on its return cruise to Earth. On 24 September 2023, the Sample Return Capsule (SRC) is scheduled to be released from the spacecraft and gently land in the desert of the western U.S. state of Utah. After it is recovered, the SRC will be placed into an inert environment, safely packed, and flown to Houston, Texas, where it will go directly to the new OSIRIS-REx curation facility located within NASA's Johnson Space Center. Once within the facility, the SRC will be opened, and the sample will be quickly (within hours to days) processed for distribution to the OSIRIS-REx Sample Analysis Team (SAT) for immediate investigation. In addition, the Japan Aerospace Exploration Agency will receive 0.5% of the unprocessed bulk material and the Canadian Space Administration will receive 4%. A catalog of the entire sample will be produced within six months and will enable requests of the remaining material by the scientific community.

The OSIRIS-REx Sample Analysis Plan (SAP) establishes a hypothesis-driven framework for integrated, coordinated analyses of the returned sample with the goal of satisfying the mission requirement to "return and analyze a sample of pristine carbonaceous asteroid regolith in an amount sufficient to study the nature, history, and distribution of its constituent minerals and organic material." Through analysis of the returned sample, the SAT will test a total of 12 primary hypotheses, each encompassing several secondary hypotheses. The primary hypotheses are:

1. Remote sensing of Bennu's surface has accurately characterized its mineral, chemical, and physical properties.
2. Bennu contains prebiotic organic compounds.
3. Bennu contains presolar material derived from diverse sources.
4. Bennu's parent asteroid formed beyond the snow line by accretion of material in the protoplanetary disk.
5. Geological activity occurred in the interior of Bennu's parent asteroid early in solar system history.
6. Bennu's parent body experienced > 3 billion years of solar system history before being destroyed in a catastrophic disruption.
7. Bennu is a rubble pile that formed by re-accumulation of material from the catastrophic disruption of a precursor asteroid.
8. The Yarkovsky effect pushed Bennu far enough inward to reach a dynamical resonance, which flung it out of the main belt and onto a terrestrial planet-crossing orbit.
9. Bennu has experienced surface processing throughout its history.
10. The physical, chemical, and spectral properties of Bennu's surface materials have been modified by exposure to the space environment.
11. The Hokioi Crater in which the Nightingale sample site is located was recently formed and contains relatively unweathered material [4].
12. OSIRIS-REx asteroid proximity operations, the TAG event, and Earth return modified the collected samples, Touch-and-Go Sample Acquisition Mechanism (TAGSAM), and the SRC.

Each hypothesis is mapped to one or more SAT working groups and analytical technique(s) needed to produce the data to test it.

The SAP applies a three-tiered approach to allocating sample mass for analyses. (i) The "baseline" analysis plan assumes that 15 g of sample will be available to the SAT. This mass is based on the assumption of returning 60 g, the mission-required minimum, and the fact that 75% of the sample (in this scenario, 45 g) will be archived for future community analysis. (ii) The "overguide" analysis plan assumes that 62.5 g of sample will be available to the SAT. This mass is based on the best-available spacecraft-based estimate of the total mass of sample stowed, about 250 g [5]. (iii) The "threshold" analysis plan assumes that

3.75 g of sample will be available to the SAT. This mass addresses a contingency scenario in which an anomaly during Earth return results in a significant mass loss, such that only 15 g is recovered. The threshold plan's other purpose is to guide analysis of any rare lithologies that might be returned as part of the bulk sample.

To test the effectiveness of our SAP and ensure that the SAT is prepared for the analysis of the returned sample, the mission will conduct a Sample Analysis Readiness Test (SART) from June 2022 to June 2023. The SART will focus on aspect of the SAP for which verification or demonstration of proficiency is needed such as follow-on analyses, testing of new or updated equipment, and implementation of new software discussed below. During the SART, the mission will implement a new data storage, processing, sharing, and visualization system designed to enable coordinated analysis, called the Sample Analysis Micro-Information System (SAMIS). SAT members will test their proficiency with the two user-facing modules of SAMIS: the Sample Analysis Tracking Application (SATA), which provides real-time tracking of the location and condition of sub-samples as they are shipped between laboratories and the curation facility, and the Sample Analysis Desktop Application (SADA), which provides a central point of upload, download, spatial co-registration, and visualization of analytical data. Finally, because all data from the mission's sample analysis phase will be archived, the SAT will use the SART to practice data archiving. Periodic reviews of the SART will occur during its implementation, and lessons learned will be applied to the SAP, applications, and archiving approach. A final report on the outcomes of the SART will be produced in the summer of 2023 (before the sample is returned to Earth).

References

[1] Lauretta, D.S. et al. 2017. *Space Science Reviews* 212:925. [2] Lauretta, D.S. et al. 2021. In *Sample Return Missions*, Longobardo, A., ed. (Elsevier), ch. 8. [3] Lauretta, D.S., & OSIRIS-REx TAG Team 2021. 52nd LPSC LII, Abstract# 2097. [4] Enos et al. 2020 Abstract #1463. 51st LPSC. [5] Ma, H. et al. (2021) arXiv:2109.05561 [astro-ph.EP].

Scientific importance of the sample analyses of Phobos regolith and the analytical protocols of returned samples by the MMX mission

Wataru Fujiya¹, Yoshihiro Furukawa², Haruna Sugahara³, Mizuho Koike⁴, Ken-ichi Bajo⁵, Nancy L. Chabot⁶, Yayoi N. Miura⁷, Frederic Moynier⁸, Sara S. Russell⁹, Shogo Tachibana¹⁰, Yoshinori Takano¹¹, Tomohiro Usui³, and Michael E. Zolensky¹²

¹Ibaraki University, ²Tohoku University, ³Institute of Space and Astronautical Science, JAXA, ⁴Hiroshima University, ⁵Hokkaido University, ⁶Johns Hopkins University Applied Physics Laboratory, ⁷Earthquake Research Institute, University of Tokyo, ⁸Institut de Physique du Globe de Paris, CNRS, ⁹Natural History Museum, ¹⁰UTOPS, University of Tokyo, ¹¹Japan Agency for Marine-Earth Science and Technology, ¹²NASA Johnson Space Center

The Martian Moons eXploration (MMX) mission by JAXA is a sample return mission from a Martian moon, Phobos, aiming at collecting >10 g of the regolith materials on Phobos. The touchdown operations are planned to be performed twice at different landing sites. The regolith materials will be collected using coring (C-) and pneumatic (P-) sampling systems [1]. We, Sample Analysis Working Team (SAWT) members, are now designing the analytical protocols of returned Phobos samples [2].

The origin of the Martian moons is unclear, but there are currently two favored formation scenarios: (i) the in-situ formation (giant impact) scenario [e.g., 3], and (ii) the captured asteroid scenario [e.g., 4]. If Phobos formed by giant impact, then the Phobos building blocks were likely heated to high temperatures (ca., ~2000 K), and the returned samples will consist of igneous and/or glassy materials produced by the solidification of melt or the condensation of gas [5]. On the other hand, if Phobos is a captured asteroid, then the returned samples would be primitive materials like carbonaceous chondrites as inferred from Phobos' surface spectra resembling D-type asteroids [e.g., 6]. Observations of the returned samples under an optical microscope, quantitative analysis of their chemical compositions, and isotope measurements of, e.g., O, Ti, and Cr, can distinguish between the above formation scenarios, and characterize the Phobos endogenous materials [e.g., 7].

In the case of the giant impact scenario, the volatile loss accompanied by the giant impact can be evaluated using the isotopic compositions of moderately volatile elements like Zn [8]. Radiometric dating by, e.g., Pb-Pb and Rb-Sr systematics, will provide chronological information about the giant impact event [9]. In the case of the captured asteroid scenario, analyses of organic matter, bulk H and N isotopic compositions, and presolar grain abundance will provide insights into the primitiveness of the Phobos endogenous materials. The timing when the Martian gravity captured Phobos can be constrained by the combination of Ar-Ar dating of the returned samples and the crater counting of the Phobos' surface [10]. In either formation scenario, the sample analyses mentioned above can shed light on the material transport in the solar system and the delivery of volatiles to the terrestrial planets.

It should be noted that the Phobos' regolith may contain materials ejected from Mars by impact throughout the Martian history [11]. The Martian materials on Phobos may include fragile ones like sedimentary rock, which cannot be found in Martian meteorites commonly shocked by >5 GPa [12]. These Martian materials will provide crucial information about the surface evolution of Mars. Furthermore, biomarkers or even potential microorganisms could be detected in the Martian materials on Phobos, although MMX has no concern about viable Phobos organisms to be returned [13]. We plan to design the analytical protocols of the returned samples to detect such Martian materials in curation procedures before they are processed for further analyses.

References

- [1] Usui T. et al. 2020. *Space Sci. Rev.* 216:49. [2] Fujiya W. et al. 2021. *Earth Planets Space* 73:120. [3] Hartmann W. K. 1990. *Icarus* 87:236–240. [4] Citron R. I. et al. 2015. *Icarus* 252:334–338. [5] Pignatale F. C. et al. 2018. *Astrophys. J.* 853:118 (12pp). [6] Murchie S. & Erard S. 1996. *Icarus* 123:63–86. [7] Trinquier A. et al. 2007. *Astrophys. J.* 655:1179–1185. [8] Paniello R. C. et al. 2012. *Nature* 490:376–379. [9] Amsellem E. et al. 2020. *Icarus* 339:113593. [10] Schmedemann N. et al. 2014. *Planet. Space Sci.* 102:152–163. [11] Hyodo R. et al. (2019) *Sci. Rep.* 9:19833. [12] Fritz J. et al. 2005. *Meteorit. Planet. Sci.* 40:1393–1411. [13] Hyodo R. & Usui T. 2020. *Science* 373:742.

What should we do with these Martian rocks? A tale of MSR Sample Science and Curation

Aurore Hutzler¹, Gerhard Kminek¹, Michael Meyer², Lindsay E. Hays² and Sanjay Vijendran¹

¹*European Space Agency, The Netherlands*

²*NASA Headquarters, Washington, DC, USA*

The Mars Sample Return (MSR) campaign is the most complex and ambitious sample return mission to date. The first leg of the campaign, Mars 2020, has successfully landed in the Jezero crater, and the rover Perseverance is already sampling Mars. ESA and NASA have allocated substantial budgets to support the development of a partnership formalised through the signature in October 2020 of a NASA-ESA Memorandum of Understanding (MOU) concerning the flight elements of the MSR Campaign. A fundamental aspect of the partnership as stated in the Joint Statement of Intent between NASA and ESA on MSR campaign science benefits signed on 2 July 2019, is that samples would be treated as one collection and jointly managed. This has been a leading principle for all subsequent actions.

To clarify the activities to be done on the collection, the MSR Science Planning Group (MSPG) in 2018, followed by a second MSPG2 in 2020 were jointly chartered by NASA and ESA to develop key technical inputs for the curation and science activities to be done in the first years after sample return. These inputs have been translated into proposed design requirements for the short- to medium-term needed infrastructure [1]. One of the MSPG2 working groups has delivered a framework for the science management of the collection [2]. Final reports and requirements from MSPG2 were delivered in July 2021. In parallel, a Sample Safety Assessment Protocol working group under the umbrella of COSPAR is currently finishing their deliberations and report [3]. This sample safety assessment overlaps with the time critical and sterilisation sensitive science identified by MSPG2 for execution in the above referenced infrastructure. All these community-defined requirements, recommendations and findings are going to feed into the next steps to prepare the ground-segment activities and infrastructure. As a minimum, there is a need for a Sample Receiving Facility (SRF) for the first years after landing. This primary SRF should be jointly-managed between ESA and NASA, and allow for all needed curation, sample handling and sample analysis (pre-Basic Characterization, Basic-Characterization and Preliminary Examination as well as sterilization-sensitive, time-sensitive science and sample safety assessment) to be done in containment. NASA and ESA are planning independent but coordinated studies to clarify the design trade space and cost associated with handling Mars samples. A formalisation of the NASA/ESA partnership for MSR ground-segment is also underway, with an upcoming Science MOU (2021) and a potential agreement on ground infrastructure (planned 2022).

The upcoming decade will be busy with preparing the infrastructure, the science, and the overall management of the samples. There will be ample opportunities for the worldwide community to participate in the preparation activities, with a joint ESA/NASA Announcement of Opportunity expected soon, followed by more AOs later in the 2020's.

References

[1] Carrier B.L. et al. 2021, *Astrobiology* [2] Haltigin T. et al. 2021, *Astrobiology* [3] Kminek G et al. 2021, SSAP

A New Laboratory Facility in the Era of Sample Return: the Sample Analysis Laboratory (SAL) at DLR Berlin

E. Bonato¹, S. Schwinger², A. Maturilli¹, J. Helbert¹

¹Dept. of Planetary Laboratories, Institute of Planetary Research, DLR, Rutherfordstraße 2, 12489, Berlin, Germany

²Dept. of Planetary Physics, Institute of Planetary Research, DLR, Rutherfordstraße 2, 12489, Berlin, Germany

DLR is currently in the process of setting up a new Sample Analysis Laboratory (SAL) – a facility dedicated to the work on rock and dust samples returned from planetary bodies such as asteroids and the Moon. The key question driving the development of SAL is a more in depth understanding of the formation and evolution of planetary bodies.

SAL extends the currently available laboratory facilities at the Institute of Planetary Research at DLR in Berlin, including the Planetary Spectroscopy Laboratory (PSL), the Raman Mineralogy and Biodetection Laboratory (RMBL). SAL is focused primarily on *in situ* mineralogical and geochemical analysis mainly of extra-terrestrial material returned from sample return missions, as well as of meteorites and sample analogue materials.

Housed within ISO5 clean rooms, SAL will be equipped with glove boxes for handling and preparation of the samples. All samples will be stored under dry nitrogen and can be transported between the instruments in dry nitrogen filled containers.

The instrumentation in the first step of the SAL set up consists of:

- Field Emission Gun Electron Microprobe Analyser (FEG-EMPA)
- Field Emission Gun Scanning Electron Microscope (FEG-SEM)
- X-ray Diffraction (XRD):
 - high resolution qualitative and quantitative analyses of powders
 - μ -XRD for *in situ* analysis and mapping
 - Non-ambient stage for dynamic experiments
- Vis-IR-microscope
- Polarized light microscope with automated stage
- supporting equipment for sample preparation and handling within a controlled atmospheric environment.

SAL is currently being set up. Construction work for the laboratories has started and the first instruments will be arriving by summer 2022. SAL will be operational by the end of 2022, on time to welcome samples collected by the Hayabusa2 mission. In collaboration with the Natural History Museum in Berlin will also have the expertise and facilities for carrying out curation of sample return material which will be made available for the whole European scientific community. DLR is already curating a 0.45 mg of Lunar regolith (Figure 1) collected from the Luna 24 Soviet mission and the first analyses of the material are being planned.

SAL follows the approach of a distributed European sample analysis and curation facility as discussed in the preliminary recommendation of EuroCares. Together with other laboratory facilities at the DLR Institute of Planetary Research (such PSL and RMBL) which are part of the Europlanet RI, the new SAL will be from the start open to the scientific community.

Our goal is to establish an excellence center for sample analysis in Berlin within the next 5-10 years building on our collaborations with the Natural History Museum and the Helmholtz Center Berlin in Berlin as well as the universities in Berlin.

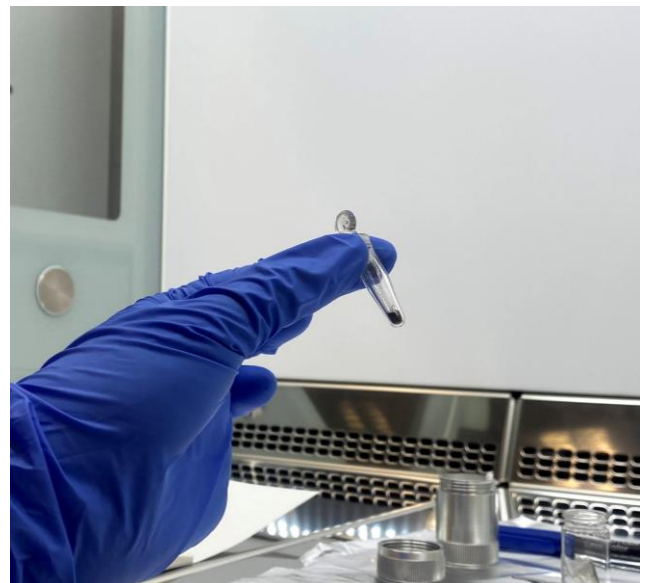


Figure 1. Glass vial containing Lunar regolith collected during the Luna 24 mission.

Milani CubeSat for ESA Hera mission

Tomáš Kohout^{1,2}, Margherita Cardi³, Antti Näsilä⁴, Ernesto Palomba⁵, Francesco Topputo⁶, and the Milani team*

¹University of Helsinki, Faculty of Science, Helsinki University, Finland (tomas.kohout@helsinki.fi)

²Institute of Geology of the Czech Academy of Sciences, Prague, Czech Republic

³Tyvak International, Torino, Italy

⁴VTT Technical Research Centre of Finland, Espoo, Finland

⁵INAF-IAPS, Rome, Italy

⁶Politecnico di Milano, Milano, Italy

*A full list of authors appears at the end of the abstract

Hera is the European part of the Asteroid Impact & Deflection Assessment (AIDA) International collaboration with NASA who is responsible for the DART (Double Asteroid Redirection Test) kinetic impactor spacecraft. Hera will be launched in October 2024 and will arrive at Didymos binary asteroid in January 2027. Milani CubeSat (fig. 1) is developed by Tyvak International with a consortium of European universities, research centers and firms from Italy, Czech Republic and Finland. At arrival it will be deployed and will do independent detailed characterization of Didymos asteroids at distances 5 to 10 km supporting Hera observations. Milani mission objectives are:

1. Map the global composition of the Didymos asteroids.
2. Characterize the surface of the Didymos asteroids.
3. Evaluate DART impacts effects on Didymos asteroids and support gravity field determination.
4. Characterize dust clouds around the Didymos asteroids.

The scientific payloads supporting the achievement of these objectives are “ASPECT”, a visible - near-infrared imaging spectrometer (table 1), and “VISTA”, a thermogravimeter (table 2) aiming at collecting and characterizing volatiles and dust particles below 10 μ m.

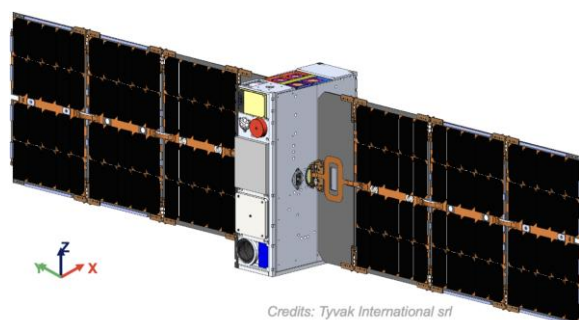


Figure 1. Milani CubeSat

Table 1. ASPECT specifications

Channel	VIS	NIR1	NIR2	SWIR
Field of View [deg]	10° x 10°	6.7° x 5.4°	6.7° x 5.4°	5° circular
Spectral range [nm]	500 – 900	850 – 1275	1225 - 1650	1600 - 2500
Image size [pixels]	1024 x 1024	640 x 512	640 x 512	1 pixel
Pixel size [μ m]	5.5 μ m x 5.5 μ m	15 μ m x 15 μ m	15 μ m x 15 μ m	1 mm
No. spectral bands	Ca. 14	Ca. 14	Ca. 14	Ca. 30
Spectral resolution [nm]	< 20 nm	< 40 nm	< 40 nm	< 40 nm

Table 2. VISTA specifications

Sensor Type	Quartz Crystal Microbalance (QCM)
Resonance frequency	10 MHz
Volume	50mm x 50mm x 38mm
Sensitive area	1.5cm ²
Particles size detection range	5-10 μ m to sub- μ m particles
Methods/Technique used	1. Dust and contaminants accumulation (passive mode) 2. TGA cycles (active mode)
Mass	90g

The young basalts on the Moon: Pb–Pb isochron dating in Chang’e-5 Basalt CE5C0000YJYX03501GP

Dunyi Liu^{1,3}, Alexander Nemchin^{2,1}, Xiaochao Che¹, Tao Long¹, Chen Wang¹, Marc D. Norman⁴, Katherine H. Joy⁵, Romain Tartese⁵, James Head⁶, Bradley Jolliff⁷, Joshua F. Snape⁵, Clive R. Neal⁸, Martin J. Whitehouse⁹, Carolyn Crow¹⁰, Gretchen Benedix², Fred Jourdan², Zhiqing Yang¹, Chun Yang¹, Jianhui Liu¹, Shiwen Xie¹, Zemin Bao¹, Runlong Fan¹, Dapeng Li³, Zengsheng Li³, Stuart G. Webb⁸

¹Beijing SHRIMP Center, Institute of Geology, Chinese Academy of Geological Sciences. ²School of Earth and Planetary Sciences, Curtin University. ³Shandong Institute of Geological Sciences, Jinan, Shandong. ⁴Research School of Earth Sciences, The Australian National University. ⁵Department of Earth and Environmental Sciences, The University of Manchester. ⁶Department of Earth, Environmental, and Planetary Sciences, Brown University. ⁷Department of Earth and Planetary Sciences and The McDonnell Center for the Space Sciences, Washington University in St. Louis, St. Louis. ⁸Department of Civil and Environmental Engineering and Earth Sciences, University of Notre Dame, Notre Dame. ⁹Department of Geosciences, Swedish Museum of Natural History. ¹⁰Department of Geological Sciences, University of Colorado Boulder.

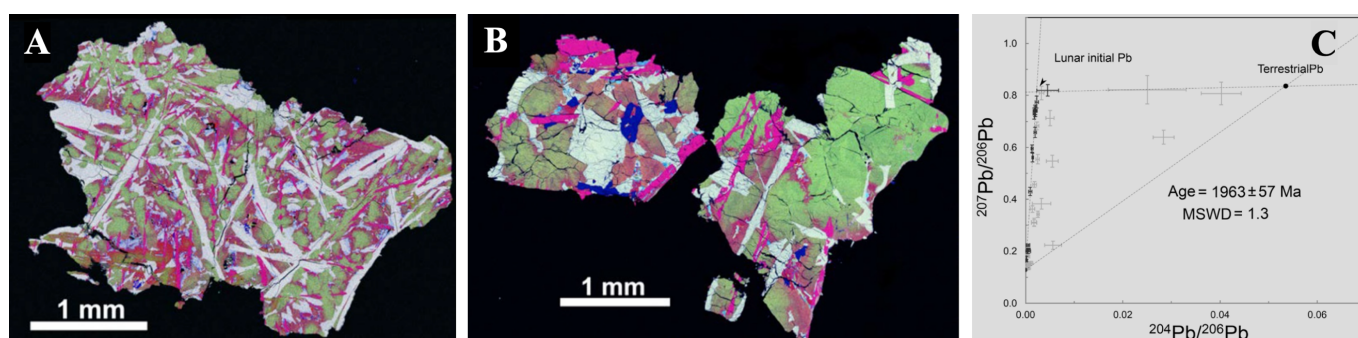


Figure 1. A & B false color energy EDS element maps of the two fragments from CE5C0000YJYX03501GP blue=silica, green=Mg, red=Fe, white=Al, yellow=Ca, pink=Ti, cyan=K. C Pb-Pb isochrons for CE5C0000YJYX03501GP.

China's Chang'e-5 mission collected 1731g lunar samples at 43.1°N, 51.8°W in the northeastern Oceanus Procellarum of the Moon. Basalt fragments is the main lithic type in the lunar soil returned by Chang'e-5 that showed five distinct textural types[1], The two scooped basalt fragments from CE5C0000YJYX03501GP both are equidimensional, approximately 3-4 mm in size and consist of clinopyroxene, plagioclase, olivine, ilmenite, quartz, cristobalite, K-rich glass, barian K-feldspar, troilite and Ca-phosphates, with small amounts of the Zr-rich minerals baddeleyite and zirconolite[Figure 1. A, B]. The pyroxenes and olivines in the two fragments include highly Fe-rich compositions for lunar basalts. and the bulk compositions of both fragments indicate elevated FeO (~22-25 wt.%) and low MgO (~5 wt.%). The mineralogy and bulk compositions of two basalt fragments are consistent with remote sensing data of this region [2]. These 677 ± 3 of $^{238}\text{U}/^{204}\text{Pb}$ ratio (μ -value) for the two fragments imply only a modest (<2%) KREEP component either in their mantle sources or introduced by assimilation during magma ascent [2].

The Pb isotope data were collected using a SHRIMP Ile-MC at Beijing SHRIMP Center, Institute of Geology, Chinese Academy of Geological Sciences, Beijing. $^{204}\text{Pb}^+$, $^{206}\text{Pb}^+$, $^{207}\text{Pb}^+$ and $^{208}\text{Pb}^+$ isotopes were measured simultaneously with multi collectors and the $^{204}\text{Pb}/^{206}\text{Pb}$, $^{207}\text{Pb}/^{206}\text{Pb}$ and $^{208}\text{Pb}/^{206}\text{Pb}$ ratios were calibrated using BCR-2, BHVO-2. Combining all Pb isotope data from Zr-rich minerals, Ca-phosphates, K-rich glass and barian K-feldspar for the two basalt fragments, gives an isochron age of 1963 ± 57 Ma [Figure 1. C]. This age constrains the lunar impact chronology of the inner Solar System and the thermal evolution of the Moon. Studies of other basalt fragments from Chang'e-5 have yielded similar results [3, 4], and showed a relatively low water content [5].

Reference

[1] Li C. et al. 2021. National Science Review. [2] Che X. et al. 2021. Science. [3] Li Q. et al. 2021. Nature. [4] Tian H. et al. 2021. Nature. [5] Hu S. et al. 2021. Nature.

The fundamental deformation of cosmic bodies not depending of their sizes and compositions (from asteroids to Universe)

Kochemasov G. G. IGEM RAS, Moscow, kochem.36@mail.ru

Abstract: Orbits make structures. Not depending sizes and compositions of celestial bodies they acquire tectonic dichotomy (two hemispheres) connected with warping action of fundamental wave.

Keywords; cosmic bodies. orbits, galaxies, planets, satellites, asteroids, fundamental wave

The main point of the wave planetology is: "Orbits make structures". It means that movement in non-round orbits makes waves creating structures (Fig. 1-10) However, any cosmic body moves in several orbits. They all participate in structuring [1]. Their frequencies are divided and multiplied creating new frequencies and corresponding them structures. They are (frequencies) very small and very big. Very slow but very energetic rotation of large cosmic formations (galaxies and the larger assemblies) make very fine oscillations up to microwaves, roentgen and gamma radiations infilling cosmos. From the other end, oscillations passed through fundamental wave and corresponding it tectonic dichotomy of any body. In figures are examples of bodies of various sizes from the Galaxy to small asteroids (Fig.1-8)

The row is finished with small asteroids Itokawa and Ryugu. Both reveal tectonic dichotomy; especially sharp in Itokawa with its convexo-concave shape. Ryugu has unique longitudinal variation in geomorphology: the western side of it has a smooth surface and a sharp equatorial ridge (bulge) [3]. On the opposite side Fossae Tokoyo and Horai occur. Some peculiarities show crater distribution (more than 20 meters in diameter). There are fewer craters in the western bulge and more around the meridian. This cannot be explained by the randomness of cratering [2].

The other end of this row include giant cosmic formations like galaxies and larger ones finishing at Universe. The Universe also is dichotomist divided at uplifted and subsided halves. The humankind occupies the uplifted halve-in the religious sense "paradise", the subsided halve thus is "hell".

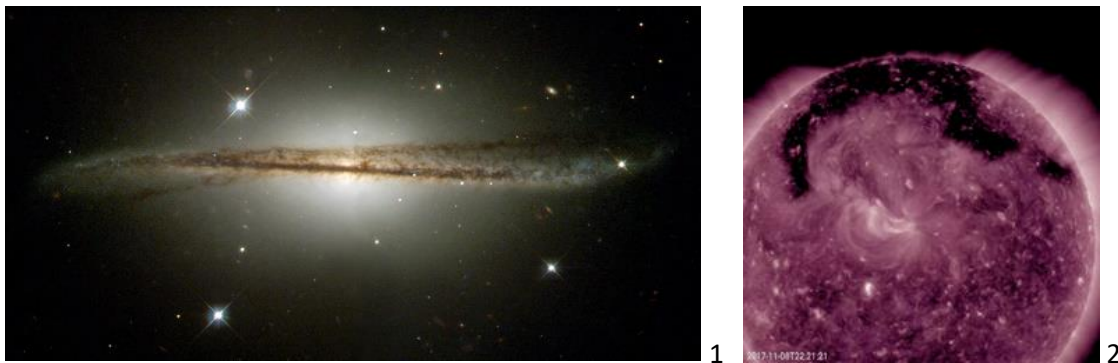


Fig. 1. A spiral Galaxy. ESO 510-613. PIA04213.

Fig.2. PIA22113. Coronal hole all spread out.

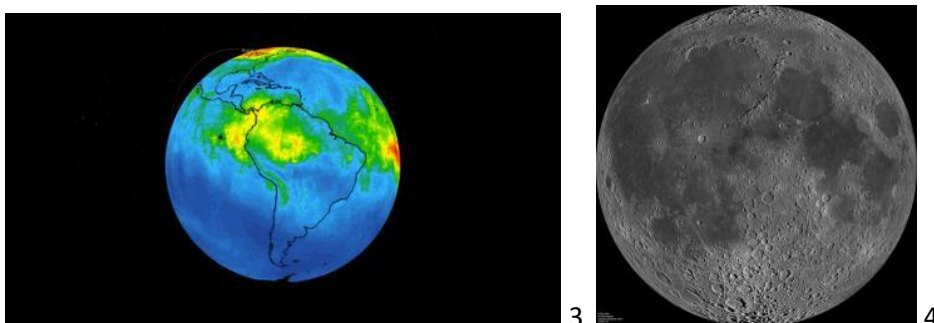


Fig. 3. PIA23356. NASA's AIRS maps carbon monoxide from Brazil fires.

Fig. 4. PIA14011. Moon's nearside

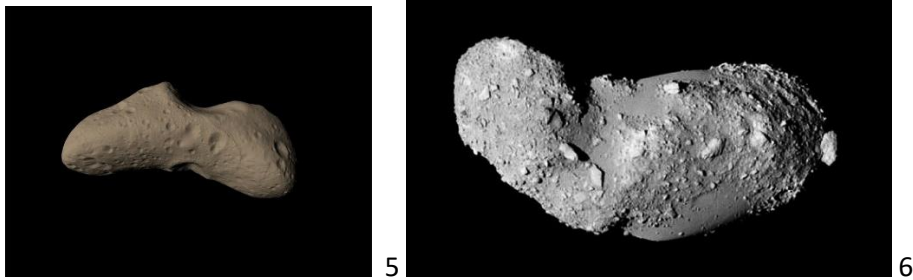


Fig. 5. Asteroid Eros. Convexo-concave shape.

Fig. 6. Asteroid Itokawa. Convexo-concave shape.

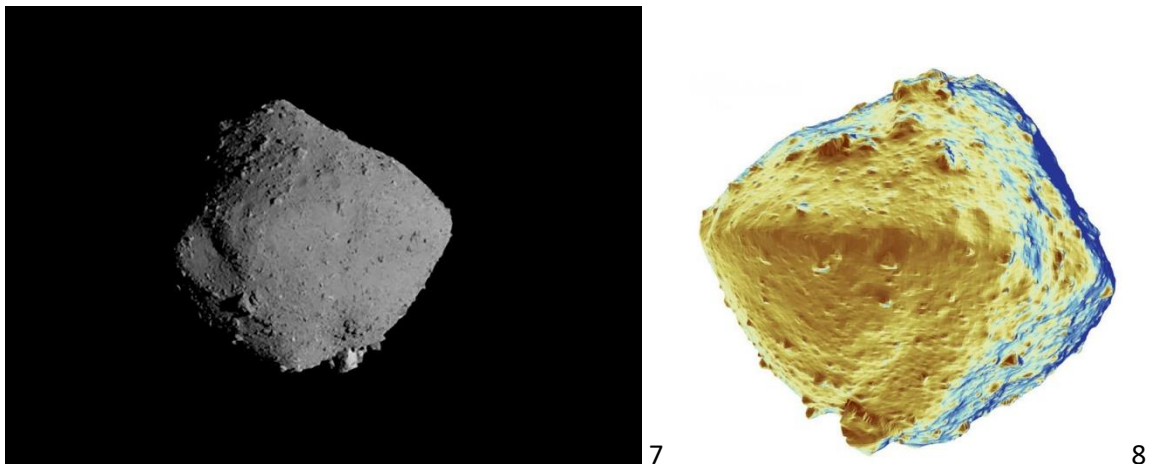


Fig. 7. Asteroid Ryugu. Ab278776d6ce43e581d669ef938497fa.jpg

Fig. 8. Asteroid Ryugu. Dichotomy shows.image_5c91c15458e6c0.69646182.jpg

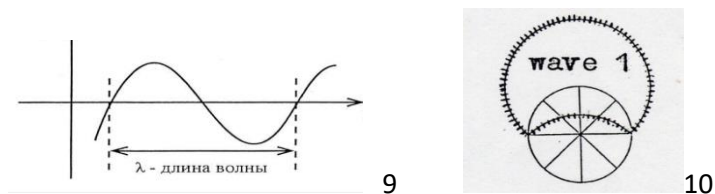


Fig.9, 10. Fundamental wave in line and circle.

Referencs:

- [1] Kochemasov G.G. Modulated wave frequencies in the Solar system and Universe // Journal of Physics and Application 12(4): 68-75, 2018. Doi:10.13189/ujpa.2018.120402.
- [2] N.Hirata, T. Morota, Y.Cho et al. The spatial distribution of impact craters on Ryugu// Icarus , v.338, 1, March 2020, 113527, [https:// doi.org/10.1016/j.icarus.2019.113527](https://doi.org/10.1016/j.icarus.2019.113527)
- [3] H. Masatoshi, T. Eri, M. Hideaki et al. The western Bulge of 162173Ryugu formed as a result of a rotationally driven deformation process // The Astronomical Journal: journal-IOP Publishing, 2019-March (vol.874, #1-P. L10.-ISSN 0004-637X-doi:10.3847/2041-8213/ab0e8b-Bibcode: 2019ApJ...874L.10N-arXiv:1904.03480.

Exogenous copper sulfide in a returned grain from asteroid Itokawa

K. D. Burgess and R. M. Stroud

U.S. Naval Research Laboratory, Washington, DC 20375

Asteroid 25143 Itokawa is an S-type asteroid, and the returned samples are dominated by equilibrated, weakly shocked LL5 and LL6 ordinary chondrite material with some weakly equilibrated LL4 material [1,2]. We present evidence of the presence of a cubanite-chalcopyrite-pyrrhotite-troilite assemblage consistent with low-temperature aqueous alteration in a particle from Itokawa [3]. Most of the materials from Itokawa equilibrated at temperatures near 800°C, with slow cooling to ~600°C [2,4], which indicates this sulfide assemblage must have become part of Itokawa after thermal alteration. Cu-bearing sulfides have been reported in only a few meteorite types [5,6], which suggests the conditions necessary to form such phases occur on only a limited number of planetary bodies. Specifically, cubanite has only been reported in CI chondrites and Wild2 material [7]. Thus, we conclude that this grain, and the other Cu-sulfides noted on Itokawa samples [8] likely originated on a primitive, hydrated asteroid source such as CI chondrite-like parent body or D- or P-type asteroids previously linked to unique, aqueously altered meteorites [9,10].

Particle RB-CV-0038 (C0038) was mounted in epoxy such that most of the grain was available for imaging, then coated by 80 nm of evaporated carbon. SEM images and FIB samples were obtained with an FEI Helios G3 equipped with an Oxford 150 mm² SDD energy dispersive X-ray spectrometer (EDS). After imaging, protective straps of C were deposited on regions of interest, and multiple sections suitable for STEM analysis were extracted using standard techniques. One section, known from SEM-EDS to contain Cu, was attached to a Mo grid. STEM analysis was performed with the Nion UltraSTEM200-X at NRL. The microscope is equipped with a Gatan Enfium ER spectrometer for electron energy loss spectroscopy (EELS) and a windowless, 0.7 sr Bruker SDD-EDS detector. Selected area diffraction patterns were collected using a JEOL 2200FS. Data were collected at 200 kV.

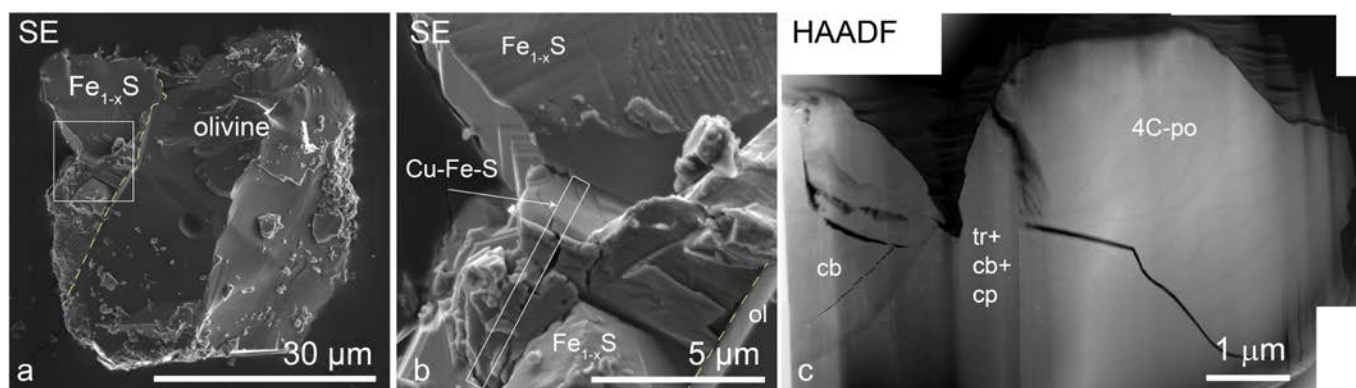


Figure 1. (a,b) Secondary electron (SE) images of particle RB-CV-0038 showing location of cubanite with Fe-sulfide and approximate location of FIB section. (c) HAADF montage of FIB section with cubanite (cb), troilite-cubanite-chalcopyrite (tr+cb+cp) mottled region, and pyrrhotite (4C-po) with “flame” texture.

C0038 is a multiphase grain, ~40 μm across. The particle is predominantly composed of olivine and iron sulfide with minor (adhered?) plagioclase or glass (Fig. 1a). A ~2×5 μm cubanite grain was present in contact with the Fe-sulfide (Fig. 1b). STEM data show several different grains are present within the Fe-sulfide in the FIB section (Fig. 1c). The Cu-Fe-sulfide contains several cracks are, one of which is perpendicular to the FIB section (Fig. 2a). The crack has oxidized Fe-rich edges and is decorated by Cu metal nanoparticles. The cubanite itself shows a tripling of the *c* axis, apparent in SAED patterns (Fig. 2b). Adjacent to the cubanite, the sulfide has a mottled texture (Fig. 2a), and a small amount of Cu is present (~2 at%), concentrated in the bright spots. SAED patterns from the region index to troilite with faint chalcopyrite spots (Fig. 2d). Further from the chalcopyrite, there is no Cu, and the Fe-sulfide has a “flame” exsolution texture of two types of pyrrhotite (Fig. 2c). The pyrrhotite can be indexed to 4C-pyrrhotite. The average measured Fe/S composition for the grain ($x = \sim 0.09$ in $Fe_{1-x}S$) is consistent with a 4C-pyrrhotite or a mixture of 4C and NC-pyrrhotites. In NC-pyrrhotites, NC indicates a variable, non-integral superstructure based on the NiAs-type unit cell where troilite is 2C.

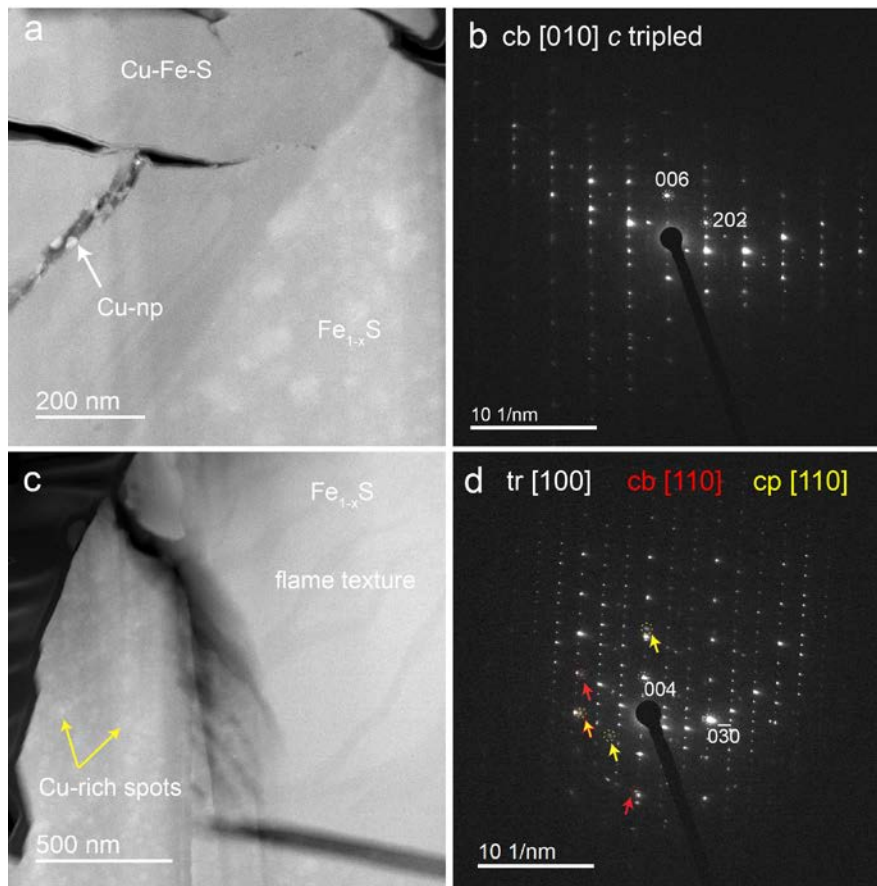


Figure 2. (a,c) HAADF images of cubanite, mottled Fe-sulfide, and pyrrhotite with flame texture. (b) SAED pattern for the cubanite, which shows a tripling of the c axis. (d) SAED pattern for the mottled Fe-sulfide, which has ~2 at% Cu and shows reflections for cubanite and chalcopyrite in addition to troilite.

The presence of cubanite, which forms and is stable only at temperatures below ~250°C [11], together in this grain with 4C-pyrrhotite [7], indicates that this grain must have been brought to Itokawa after thermal alteration and equilibration of the LL-type material. This combination of sulfide phases has previously been identified only in CI chondrite material [7]. However, unlike CI chondrites, no Ni was detected in these sulfides. This could indicate variation in the CI parent body, or that the impactor seen here was from a different parent body, such as the aqueously altered D- or P-type asteroids.

Acknowledgements

The authors thank JAXA and the Hayabusa curation team for access to the samples. Funding was provided by NASA LARS award 80HQTR20T0050 and NNH17AE44I to RMS.

References

- [1] Mikouchi, T., et al. (2014) *Earth, Planets and Space*, 66, 82. [2] Noguchi, T., et al. (2011) *Science*, 333, 1121. [3] Burgess, K.D., and Stroud, R.M. (2021) *Communications Earth & Environment*, 2, 115. [4] Harries, D., and Langenhorst, F. (2018) *Geochimica et Cosmochimica Acta*, 222, 53. [5] Rubin, A.E. (1997) *Meteoritics & Planetary Science*, 32, 231. [6] Rubin, A.E., and Ma, C. (2017) *Geochemistry*, 77, 325. [7] Berger, E.L., et al. (2011) *Geochimica et Cosmochimica Acta*, 75, 3501. [8] Nakamura, E., et al. (2012) *Proceedings of the National Academy of Sciences of the United States of America*, 109, E624. [9] Brown, P.G., et al. (2000) *Science*, 290, 320. [10] Kebukawa, Y., et al. (2019) *Scientific Reports*, 9, 3169. [11] Dutrizac, J. (1976) *The Canadian Mineralogist*, 14, 172.

A Series of Recent Falls of Carbonaceous Chondrites - Perfect Analogues for Returned Hayabusa 2 and Osiris Rex Asteroidal Materials

V.H. Hoffmann¹, K. Wimmer², M. Kaliwoda^{1,3}, W. Schmahl^{1,3}, P. Schmitt-Kopplin⁴. ¹Faculty of Geosciences, Dep. Earth and Environmental Sciences, Univ. Munich; ²Nördlingen; ³Mineralogical State Collection Munich, SNSB; ⁴Helmholtz-Center, Munich; Germany.

Introduction

In recent years, a series of meteorite falls have been reported which produced various types of primitive chondrites. In our contribution we will focus on samples of the following witnessed falls: Flensburg (2019), Kolang and Tarda (both 2020), while Mukundpura (fall 2017) was topic of our earlier studies [1-3]. These meteorites belong to the class of carbonaceous chondrites and play a prominent role in terms of the Hayabusa 2 (successful sample return from asteroid Ryugu in December 2020) and Osiris Rex (sample return from asteroid Bennu planned in 2023) missions [4,5] Both probed asteroids belong to the C type asteroids and are believed to mainly consist of carbon rich materials with a similar composition as primitive chondrites.

The Flensburg meteorite fell in September 2019 in Northern Germany and was classified as a C1 ungrouped carbonaceous chondrite, the first reported fall of this type. Only one small stone was found so far (24.5 gr). For all further details we refer to [2]. The Tarda meteorite fall was reported from Southern Morocco in August 2020, the meteorite (about 4 kg total mass) was classified as a C2 ungrouped carbonaceous chondrite [1,2,6,7]. Only four witnessed falls of this type are known, whereby Tagish Lake is probably the most famous one (fall 2000, [1]). The Kolang meteorite fireball and fall was reportedly observed in Indonesia in August 2020 (four stones with a total mass of 2550 gr). Kolang was classified as a CM 1/2 chondrite and is the first and only witnessed fall known from this meteorite group [8,9].

In our contribution (poster) we will compile our earlier and provide new results of detailed and systematic investigations on the mineral phase composition and distribution of three new meteorite falls [10,11]. Our focus was mainly on the rare/accessory mineralogical components of these meteorites. Specifically we are interested on the carbon-bearing and the magnetic phases. Several unprepared fragments and one individual of Tarda were used for our studies, and additionally one small unprepared fragment of Kolang. Concerning Flensburg, we had a small fragment and a PTS (provided by A. Bischoff, Univ. Münster). We used optical microscopy, LASER Micro Raman Spectroscopy (Horiba XploRa Raman System, MSM/ SNSB) for our study which is perfectly suited for identifying and mapping minor/accessory phases. Being fully non-destructive, allowing high-resolution mapping on natural, broken surfaces without any preparation in 2D or 3D are some of the major advantages of this technique. The surface morphology and mineralogy of the uncoated samples was investigated using a Phenom ProX scanning electron microscope (SEM) in backscattered electron mode equipped with an energy dispersive X-ray spectrometer (EDS) for analyzing the element composition. Magnetic susceptibility was investigated systematically by an SM30 (Hulka Comp., CR).

The results of our Raman spectroscopy experiments on Kolang have to be seen as preliminary as we had only one small fragment for our project. Generally, performing successful LASER Raman experiments on carbonaceous chondrites, here specifically on Flensburg, Tarda and Kolang, required the design of a highly sophisticated experimental setup to avoid or at least minimize alteration effects already during the measurements on the one hand and to guarantee a reasonable signal/noise relationship on the other. Due to the significant brecciation and very fine grained matrix / phases, experiments on Kolang are quite complex. Generally, several phases which have been detected in these primitive carbonaceous chondrites are extremely sensitive against (even minor) heating effects, and therefore any kind of preparation (cutting/grinding etc.), specifically in terrestrial atmospheric conditions has to be minimized. In order to avoid any such effects we decided to investigate only naturally broken unprepared sample materials (PTS of Flensburg is a necessary exception because of representativity but we also had a fragment). The representativity of the data obtained on the available sample material was also topic of our studies: large sets of high resolution mappings in 2D/3D can help to overcome the problem of tiny samples / fragments. Our experiences from the earlier investigations on Hayabusa 1 materials (asteroid Itokawa) were highly profitable in this context [12-14].

Consequently, our main interests were on optimizing and fine tuning our experimental setup. So the series of recent meteorite falls which produced a new set of primitive carbonaceous chondrites provided us directly with unique fresh analogue materials for Hayabusa 2 and Bennu asteroidal samples in our laboratories. We plan to extend our investigations in near future to additional recent falls such as Aquas Zarcas (2019, Costa Rica, CM2) or most recently Winchcombe (2021, England/UK, CM2) [1,3].

References

- [1] Meteor. Bull. Database 10/2021: Flensburg , Tarda, Kolang, Aquas Zarcas, Winchcombe, Mukundpura, Tagish Lake.
- [2] Bischoff A. et al., 2021. The old, unique C1 chondrite Flensburg – Insight into the first processes of aqueous alteration, brecciation, and the diversity of water-bearing parent bodies and lithologies. *Geochem. Cosmochem. Acta*, 293, 142-186.
- [3] <https://www.karmaka.de> (10/2021)
- [4] Hayabusa 2 mission to asteroid Ryugu (finished 12/2020), JAXA: <https://www.hayabusa2.jaxa.jp/en/>
- [5] Osiris Rex mission to asteroid Bennu, NASA: <https://www.nasa.gov/osiris-rex>
- [6] Chennaoui H.A., et al., 2021. Tarda (C2-ung): a new and unusual carbonaceous chondrite meteorite fall from Morocco. 52nd LPSC 2021, #1928.
- [7] Dey S., et al., 2021. Exploring the planetary genealogy of Tarda – a unique new carbonaceous chondrite. 52nd LPSC 2021, # 2517.
- [8] King A.J., et al., 2021. The bulk mineralogy and water contents of the carbonaceous chondrite falls Kolang and Tarda. 52nd LPSC 2021, #1909.
- [9] Jenkins L.E., et al., 2021. Identification of clasts in CM chondrite fall Kolang with S and Ca. 84th Meteor. Soc. Conf., #6161.
- [10] Hoffmann V., et al., 2021. The Kolang (CM1/2) and Tarda (C2 ungrouped) meteorite falls from 2020: first systematic mineralogical investigations by LASER Raman spectroscopy and SEM/EDX. 52nd LPSC 2021, # 2458.
- [11] Hoffmann V., et al., 2021. The Flensburg (C1 ungrouped) 2019 meteorite fall: Raman spectroscopy and compilation of magnetic susceptibility data on C-ungrouped falls/finds. 52nd LPSC 2021, # 2443.
- [12] Mikouchi T., Hoffmann V.H. et. al., 2014. Mineralogy and crystallography of some Itokawa particles returned by the Hayabusa mission. LPSC 2021, #2239.
- [13] Mikouchi T., Hoffmann V.H., et al., 2013. Mineralogy and crystallography of Itokawa particles by electron beam and synchrotron radiation X-ray analyses. Hayabusa Conf. 2013.
- [14] Mikouchi T. and Hayabusa Consortium, 2014. Mineralogy and crystallography of some Itokawa particles returned by the Hayabusa asteroidal sample return mission. *Earth, Planets and Space*, 66/82, 9pp.

Heated Synthetic Murchison Reflectance Spectra

S. Sidhu¹, P. Mann² and E. Cloutis¹

¹Centre for Terrestrial and Planetary Exploration (C-TAPE), The University of Winnipeg

²Department of Geography, The University of Winnipeg

Introduction: Several carbonaceous chondrites (CCs) display evidence of thermal alteration [1]. Remote sensing data from the JAXA Hayabusa2 asteroid sample return mission suggests that asteroid (162173) Ryugu's parent body may have undergone internal or impact-generated heating prior to breakup [2]. Furthermore, models of orbital and thermal evolution of Ryugu suggest that the asteroid was likely exposed to surficial heating during close passes to the Sun. [3]. Recently, geomorphological features observed on Bennu's surface indicate alteration of rocks due to thermal fatigue [4]. Constraining the spectral characteristics of heating will aid in identifying the timing and intensity of heating experienced by Ryugu and its parent body, as well as other extraterrestrial bodies which may have also undergone a period of thermal alteration.

Methods: The Centre for Terrestrial and Planetary Exploration (C-TAPE) at the University of Winnipeg conducted a heating experiment on a synthetic Murchison simulant. The synthetic mixture, named WMM, consisted of various major representative phases in CM carbonaceous chondrites as following: 85 wt. % ASB267, a dark serpentinite representative of CM phyllosilicates. 5 wt. % SHU102, shungite, terrestrial organic representative of organic phases. 5 wt. % TRO203, synthetic troilite representative of sulfides, and 5 wt. % MAG200, magnetite. The simulant consisted of <63 μm powders of serpentinite, shungite, and troilite, and ~20 nm sized magnetite that appeared to be maghemite from X-ray diffractometry (likely due to surface oxidation of the nanoparticles). The samples were heated up to 1200°C at 100°C increments. XRD and reflectance spectra were collected prior to heating, and after each temperature increment. A new sample powder was used for each increment, and samples were heated under continuous nitrogen flow. Samples were heated for one week at intervals of 100°C to 1000°C. However, due to the oven's constraints, samples were only heated for 2 hours at 1100°C and half an hour at 1200°C. The reflectance spectrum for 300°C is unavailable due to an accidental sample spill while removing the powder from the oven. The spectra were collected with an Analytical Spectral Devices (Boulder, CO) LabSpec 4 Hi-Res® spectrophotometer between 350 and 2500 nm. Spectra were measured at a viewing geometry of $i = 30^\circ$ and $e = 0^\circ$ with incident light being provided by an in-house 150 W quartz-tungsten-halogen collimated light source. Sample spectra were measured relative to a Labsphere Spectralon® 100% diffuse reflectance standard and corrected for minor (less than ~2%) irregularities in its absolute reflectance.

Results: Heating the Murchison simulant samples resulted in spectral variation across the temperature increments. The spectra show little change up to ~500°C (Figure 1). Beyond 500°C, the spectra display features associated with Fe³⁺ oxyhydroxides, such as low reflectance below ~500nm, a steep red slope in the visible region, and absorption features near 870 nm. Absorption bands associated with serpentine, at 1400 and 2320 nm, are evident up to ~600-700°C. The spectra generally become brighter up to ~800°C, and then darken substantially beyond this temperature. At and above 1100°C, the spectra are generally dark and featureless, with a broad absorption region centered near 1600 nm.

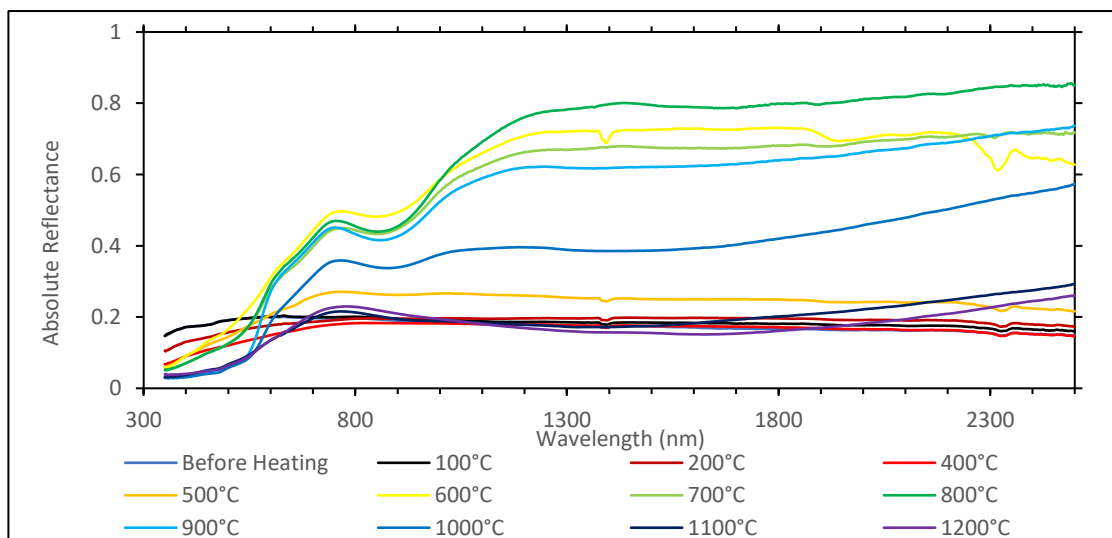


Figure 1. Reflectance Spectra of Simulated Murchison Mixture WMM.

Additionally, we heated end members used to produce the Murchison simulant to better understand the causes of the spectral changes observed. These samples (serpentine, shungite, troilite, and magnetite) were heated under the same conditions as the simulant. Serpentine spectra remained unchanged up to $\sim 200^{\circ}\text{C}$, after which the spectra display an increasing red slope below $\sim 700\text{ nm}$ and an absorption feature near 860 nm , both of which are ascribed to Fe^{3+} oxyhydroxides. Furthermore, the OH absorption bands near 1400 and 2320 nm associated with serpentine were evident up to $\sim 700^{\circ}\text{C}$. Reflectance generally increased up to $\sim 600^{\circ}\text{C}$, and decreased at higher temperatures. Shungite was stable up to $\sim 500^{\circ}\text{C}$. However, at 600°C , the organic component of the sample was volatilized. Troilite remained stable up to $\sim 300^{\circ}\text{C}$, after which Fe^{3+} oxyhydroxides were evident in its spectra. Fine-grained magnetite remained stable up to $\sim 100^{\circ}\text{C}$, after which it also transformed to Fe^{3+} oxyhydroxides.

Discussion: Temperature-induced spectral changes are evident in the Murchison simulant used in this study. XRD measurements confirm that the changes seen in the spectra can be related to the changes in the mineralogy of the samples. The spectral changes occur in multiple wavelength regions, suggesting that various spectral metrics could be robust indicators of temperatures experienced by a serpentine-rich carbonaceous chondrite.

Spectral changes observed in this study are associated with short heating periods (hours to days), and are thus, applicable to short-term heating events such as impact heating. The applicability of these results to long-term heating events, such as internal heating within larger asteroids, is unknown. Furthermore, the dry nitrogen environment under which this heating experiment was conducted only represents one scenario of the conditions which may have prevailed on carbonaceous chondrite parent bodies during any heating events. Nevertheless, the results of our experiments suggest that spectroscopic data in the $350\text{-}2500\text{ nm}$ can provide insights into the intensity and duration of heating events affecting carbonaceous chondrite asteroids. It is also worth noting that naturally-heated carbonaceous chondrites show spectral differences associated with changes in mineralogy [1]. We are in the process of relating the results of these experiments to other carbonaceous chondrite heating experiments [5, 6, 7, 8] and naturally-heated carbonaceous chondrites [9] to better understand the full applicability of our results to observational data.

References

- [1] Cloutis E. et al. 2012. *Icarus* 220:586-617. [2] Sugita S. et al. 2019. *Science* 6437:252. [3] Michel P. & Delbo M. 2010. *Icarus* 209:520-534. [4] Molaro J.L. et al. 2020. *Nature Communications* 11:2913. [5] Hiroi T. et al. 1993. *Science* 261:1016-1018. [6] Hiroi T. et al. 1993. *Symposium on Antarctic Meteorites* 18:93-96. [7] Hiroi T. et al. 1994. *Proceedings of the NIPR Symposium on Antarctic Meteorites* 7:230-243. [8] Hiroi T. et al. 1996. *Meteoritics and Planetary Science* 31:321-327. [9] Hiroi T. et al. 1997. *Lunar and Planetary Science Conference* 28:577-578.

Status of the Curatorial Database System for the Ryugu Samples

M. Nishimura¹, T. Yada¹, M. Abe¹, A. Nakato¹, K. Yogata¹, A. Miyazaki¹, K. Kumagai², K. Hatakeda²,
T. Okada¹, Y. Hitomi², H. Soejima², K. Nagashima¹, T. Usui^{1,3}, and S. Tachibana^{1,3}

¹Inst. Space Astronaut. Sci. (ISAS), Japan Aerosp. Explor. Agency (JAXA), Kanagawa 252-5210, Japan
(nishimura.masahiro2@jaxa.jp), Japan, ²Marine Works Japan Ltd., Yokosuka 237-0063, Japan, ³UTOPS, Grad. Sch. Sci.,
Univ. Tokyo, Tokyo 113-0033

The JAXA's Hayabusa2 spacecraft explored C-type near-Earth asteroid (162173) Ryugu and successfully returned its reentry capsule on December 6, 2020. Particles exceeding ~5 grams in total were safely extracted from two sample chambers in the clean chamber system dedicated to Ryugu samples [1, 2]. After a six-month preliminary examination without exposure to the air by the JAXA Astromaterials Research Group (ASRG), a part of Ryugu samples have been studied by the initial analysis team led by the Hayabusa2 project [3]. Some samples have also been characterized by Phase-2 curation teams outside ASRG [4]. The rest of the samples are continued to be investigated in the clean chamber to be catalogued in a curatorial database system for Ryugu samples (Ryugu DBS), which will be archived to the community in early 2022 for the announcement of opportunity (AO). In this presentation, we report the aim and features of the Ryugu DBS.

The Ryugu DBS has been designed and built to provide the Ryugu sample catalog with the research community and to help the researchers make the sample request through the announcement of opportunity.

The concept design of the Ryugu DBS was made in mid 2019 based on lessons-learned from the operation of DBS for Itokawa samples (Itokawa DBS) [5]. A mockup was first made to check the web interface and the user-friendliness of the system in early 2020. The database system was then developed based on the feedback from the mockup review in Oct. 2020. The system has been used by limited members for further feedback, major updates were made, and a supplemental system such as a data input system was also developed. The Ryugu DBS is run using opensource technologies, such as PHP, PostgreSQL, and Apache, and data servers on Data ARchives and Transmission System (DARTS) at ISAS/JAXA.

The Ryugu DBS provides the information on each individual grain (typically larger than 1 mm along the longest dimension) and on aggregate samples. Because of the presence of large amount of fine particles (relative to Itokawa particles), fine grains are planned to be examined as an aggregate sample put in a single dish. The basic information listed in the DBS includes photomicrographs, weight, size, and spectroscopic data, all of which are obtained in the clean chamber system without exposure to the air. The spectroscopic data can be downloaded with the CSV format. Along with such basic information, the analysis history and data obtained in previous analysis can also be found for each sample. The data obtained by the project-led initial analysis and that from curation work outside JAXA will also be archived in the future.

The release of the Ryugu DBS to the community will be in early 2022.

References

- [1] Tachibana S. et al. (2021) *LPS, XXXXXII*, Abstract #1289. [2] Yada T. et al. (2021) *LPS, XXXXXII*, Abstract #2008. [3] Tachibana S. et al. (2021) submitting for Hayabusa 2021 symposium. [4] Ito M. et al. (2021) submitting for Hayabusa 2021 symposium. [5] Uesugi M et al. (2016) *Journal of Space Science Informatics Japan: Vol 5*, 59-70.

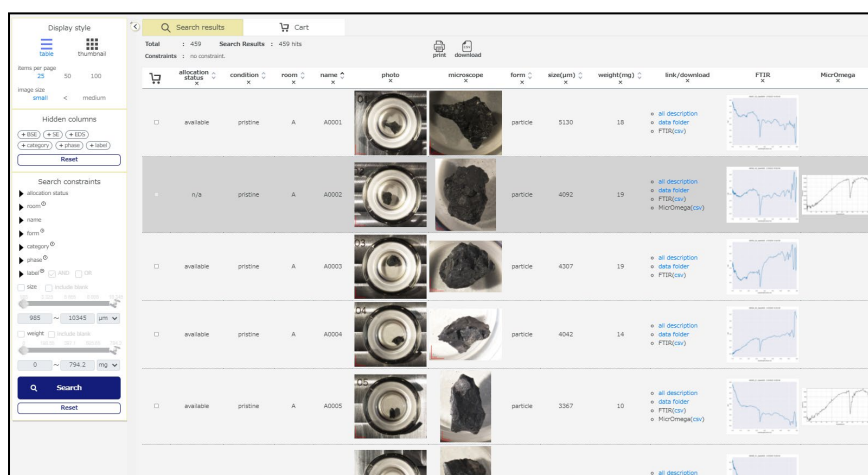


Fig. 1. The interface of the Ryugu DBS.

Methodology of MicrOmega data acquisition/processing in initial description of Ryugu returned samples

Kasumi Yogata¹, Tatsuaki Okada^{1,2}, Kentaro Hatakeda^{1,3}, Toru Yada¹, Masahiro Nishimura¹, Aiko Nakato¹, Akiko Miyazaki¹, Kazuya Kumagai^{1,3}, Yuya Hitomi^{1,3}, Hiromichi Soejima^{1,3}, Kana Nagashima¹, Ritsuko Sawada^{1,3}, Shogo Tachibana^{1,2}, Masanao Abe^{1,4}, Tomohiro Usui¹, Jean-Pierre Bibring⁵, Cedric Pilorget⁵, Vincent Hamm⁵, Rosario Brunetto⁵, Damien Loizeau⁵, Lucie Riu^{1,5}, Lionel Lourit⁵, Guillaume Lequertier⁵, and Hayabusa2 MicrOmega-Curation team^{1,5}

¹Institute of Space and Astronautical Science, Japan Aerospace Exploration Agency, ²University of Tokyo, ³Marine Works Japan, Ltd., ⁴The Graduate University for Advanced Studies (SOKENDAI), ⁵Institut d'Astrophysique Spatiale, Université Paris-Saclay

The Hayabusa2 spacecraft successfully brought samples back to Earth in December 2020, collected at two different locations on the surface of the C-type asteroid Ryugu. The samples, weighing about 5.4 g, have been transported to the Extraterrestrial Samples Curation Center of JAXA and have been installed in vacuum chambers or pure nitrogen-purged chambers. JAXA curation is currently in the progress of producing catalog data to be included in the database, which is planned to be open in early 2022 towards sample allocation for Announcement of Opportunity [2]. Within this work, basic properties of return samples, for both the aggregate and individually picked-up grains, are acquired using microscopy, weighing, and visible/near-infrared spectroscopy and imaging analyzer. One of the methods is near-infrared hyperspectral microscopy by MicrOmega, developed at IAS (Orsay, France) [3].

MicrOmega is installed in a class 1000 clean room, in contact with a sapphire viewport window of a nitrogen-purged clean chamber. By distant monochromatic light illumination of MicrOmega, it enables non-destructive ultraclean analysis without exposure of the samples to the atmosphere and protecting them from contamination such as water and human-derived organics. MicrOmega has a 5x5 mm Field of View (FOV) and 250x256 pixels with a resolution of 22.5 $\mu\text{m}/\text{pixel}$, and generates a hyperspectral (x, y, λ) cube within the 0.99 to 3.65 μm wavelength range. The performance above can mark the presence of absorption bands suggestive of hydrous minerals at 1.4, 1.9, and 2.7-3.0 μm , and of organics and carbonates at 3.4 μm . Also, its FOV can cover the entire body of a single grain, most of which are about a few mm in size, and the image resolution allows to distinguish interstitial materials such as meteoritic inclusions more than 50-100 μm in diameter.

In the production of data for the catalog, it is important to be careful about the shape-dependent signals of grains. The image often shows strong specular reflection and/or the shadow effect at a certain angle due to the instrument's light illumination incidence angle: 35 degrees. Therefore, for the catalog, two monochromatic images with different angles are generated for each single grain to show the effect of angular dependence. In addition, since the FOV usually includes signal from the sapphire sample dish where the grain sits, we extract the average spectra of the grain area only. Furthermore, if there are areas that show distinctive signatures different from most of the others, specific ROIs are also extracted. The database will contain images showing the ROIs and their spectral data, with comments on the inclusions and minerals they may imply.

In this presentation, we will introduce the MicrOmega data acquisition and data processing, including approaches in the presence of angle-dependent effects and sorting strategies for the curatorial initial description, and the characteristics of typical samples based on results obtained so far for each individual grain.

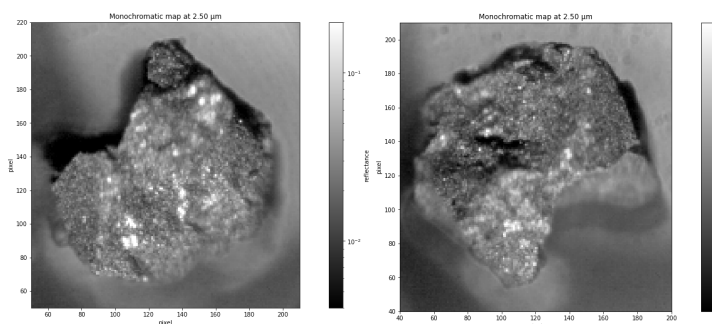


Figure 1. (a) Monochromatic image of A0015 grain at 2.50 μm at 0 deg, and (b) at 180 deg, showing angular dependence on the reflectance.

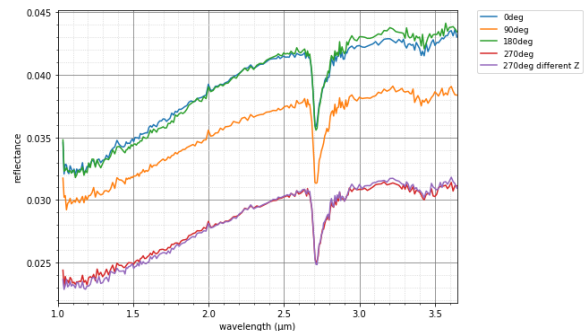


Figure 2. Average reflectance of A0015 at different angles and focal positions.

References: [1] Yada et al. submitted to Nature Astron., [2] Nishimura M. et al. (2021), Astromaterials Data Management in the Era of Sample-Return Missions Community Workshop, Abstract, [3] Pilorget et al. submitted to Nature Astron.

Comparison of ion- and laser-weathered spectra of olivines and pyroxenes

K. Chrbolková^{1,2,3}, R. Brunetto⁴, J. Ďurech², T. Kohout^{1,3}, K. Mizohata⁵, P. Malý⁶, V. Dědič⁷, C. Lantz⁴, A. Penttilä⁸, F. Trojánek⁶, and A. Maturilli⁹

¹*Department of Geosciences and Geography, University of Helsinki, Gustaf Hällströmin katu 2, 00560 Helsinki, Finland*
(katerina.chrbolkova@helsinki.fi)

²*Astronomical Institute of Charles University, V Holešovičkách 2, 18000 Prague 8, Czech Republic*

³*Institute of Geology, The Czech Academy of Sciences, Rozvojová 269, 16500 Prague 6, Czech Republic*

⁴*Université Paris-Saclay, CNRS, Institut d'Astrophysique Spatiale, 91405 Orsay, France*

⁵*Department of Physics, Faculty of Science, University of Helsinki, Pietari Kalmin katu 2, 00560 Helsinki, Finland*

⁶*Department of Chemical Physics and Optics, Faculty of Mathematics and Physics, Charles University, Ke Karlovu 3, 12116 Prague, Czech Republic*

⁷*Institute of Physics, Faculty of Mathematics and Physics, Charles University, Ke Karlovu 5, 12116 Prague, Czech Republic*

⁸*Department of Physics, Faculty of Science, University of Helsinki, Gustaf Hällströmin katu 2, 00560 Helsinki, Finland*

⁹*Institute of Planetary Research, DLR German Aerospace Centre, Rutherfordstrasse 2, 12489 Berlin, Germany*

Introduction: Irradiation by solar wind ions and impacts of micrometeoroids are the leading processes that weather surfaces of airless planetary bodies in the solar system. As a result, key diagnostic features of their spectra get altered. The most prominent changes in the silicate-rich bodies in the visible (VIS) and near-infrared (NIR) wavelengths are increase in the spectral slope, reduction of the albedo, and flattening of the mineral absorption bands (see, for example, [1]).

Our laboratory experiments aimed at understanding what are the similarities and differences between the effect of the solar wind ions and micrometeoroid impacts on the final spectra of the silicate-rich bodies.

Methods: We have used two different terrestrial minerals, olivine and pyroxene, which we ground, dry-sieved, and pressed into pellets.

Hydrogen (H) irradiations proceeded at the Accelerator Laboratory of the University of Helsinki, using 5 keV ions with varying fluences from 10^{14} to 10^{18} ions/cm². Helium and argon irradiations were done using the INGMAR set-up (IAS-CSNSM, Orsay) with 20 and 40 keV ions and with fluences from 10^{15} to 10^{17} ions/cm².

Individual 100-fs laser pulses were shot into a square grid on the pellets' surface to simulate the micrometeoroid impacts (as in [2]) in the laboratories at Charles University. Various densities of the pulses per cm² simulated different weathering stages.

Subsequent spectral measurements covered wavelengths from 0.54 to 13 μ m, i.e. VIS to mid-infrared wavelengths. After the measurements, we evaluated the evolution of the spectral parameters estimated using the Modified Gaussian Model [3, 4].

Results: We found that the variation of the spectra in the VIS range was similar for H+- and laser-irradiated samples, but we have identified a difference in the NIR wavelength range. Laser irradiation caused greater changes in NIR than any of the ions we used, see Fig. 1. The reason for such difference in behaviour may be that the penetration depth of the laser pulses is much larger than in the case of the ions. The relative contribution of the irradiated material in the spectra is then smaller in the ion case than in the laser case.

Otherwise, we found that the original mineralogy of the surface is the leading factor influencing the evolution of the spectral parameters. While olivine and pyroxene showed albedo variations of a similar order, the evolution of pyroxene's spectral slope was negligible when compared to olivine. This has implications for olivine-pyroxene mixtures and their evolution. E.g. in the case of asteroid (433) Eros, the variation of the spectral slope is minor, but other spectral parameters show some variation. As the surface of Eros is old, we hypothesise that spectral slope changes induced by olivine alteration already saturated and the leading source of the spectral variation is pyroxene, which does not show large variations in the slope. In contrast asteroid (25143) Itokawa is younger and thus still shows variations in the spectral slope as it has not saturated yet.

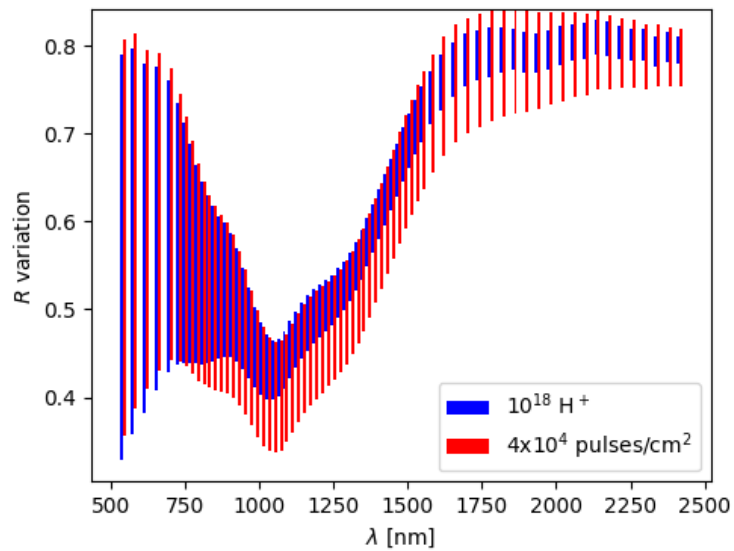


Figure 1. Spectral differences caused by laser and hydrogen ion (H⁺) irradiation. Each bar connects at the upper end the reflectance, R , of the fresh material and at the lower end R of the material weathered to the level marked in the legend.

References

- [1] Hapke, B. 2001, *J. Geophys. Res.*, 106, 10039
- [2] Fazio, A., Harries, D., Matthäus, G., et al. 2018, *Icarus*, 299, 240
- [3] Sunshine, J. M., Pieters, C. M., & Pratt, S. F. 1990, *J. Geophys. Res.*, 95, 6955
- [4] Sunshine, J. M., Pieters, C. M., Pratt, S. F., & McNaron-Brown, K. S. 1999, in *Lunar and Planetary Inst. Technical Report*, Vol. 30, Lunar and Planetary Science Conference, 1306

Solid Materials of Mineral and Rock on the Solar System: X-ray Unit and Mixed Status

Yasunori Miura¹ and Toshio Kato²

¹*Faculty of Science, Yamaguchi University, Yoshida, Yamaguchi, Yamaguchi, JAPAN*

²*Department of Earth System Sciences, Faculty of Science, Yamaguchi University, Yoshida, Yamaguchi, Yamaguchi, JAPAN*

Introduction: Solid materials of all celestial bodies on the Solar System (with technical limits of whole observation and collection by man-made satellites) should be *defined clearly* as main purpose of this paper based on academic data of those solids from the Earth's definition relatively.

Academic definition: All *mineral crystals* on Earth are defined with *X-ray determination* (as arrangement of 0.1nm unit) and *chemical composition* (as stoichiometric compound) with its occurrence on the academic material database (as *Earth's mineral*), where *the rock* is composed on many mineral crystals or mineral with mixed irregular solids (with light or heavy elements) usually. This *Earth's definition* is easily applied to investigate and determination to unknown samples including extraterrestrial samples on Earth and visiting collections on the Moon (and Mars and Asteroids *etc.*). However, basic definition of *solid samples on extraterrestrial sources* is not enough to be defined (especially on its developed status as the Celestial bodies) as shown in Table 1.

New concept of the Solar System's material: Solid bodies of the Solar System have been accepted mainly from their movements from *the geo-centered theory* to the *Helio-centered theory* through many astrophysical investigators based on the Moon and nearest planetary *tracking data*. Therefore, we should investigate by solid *material database* (rock and/or mineral crystal) of *each Celestial body*. This is main reason why a) mineral spices are completely different with the water-planet Earth (three systems of rock, ocean water and atmosphere as the mineral differentiation) and other Celestial bodies (mainly rock and/or atmosphere systems as different generation of mineral and rock compared with the planet Earth), b) previous collected extraterrestrial rocks (without chondrules or not) shows different evolution of glass and mineral, c) final mineral grains (soils, carbonates and silica) of the Earth's sedimentary process cannot be obtained clearly on extraterrestrial samples so far, and d) various mineral deposits of light element of carbon (from extreme to lower conditions) are obtained from macroscopic to microscopically as shown in Table 1.

Table 1. Different concepts of the Solar System's materials discussed in this study.

Celestial body	Mineral crystal	Rock
1) Earth (water-planet)	X-ray atomic structure & stoichiometric chemistry	Its mixed texture (with glass etc.)
2) The Moon	Shocked reformed minerals	Amorphous or mixed minerals
3) Mars	Mainly shocked minerals (with fluid products)	Basaltic evolved rocks (with glasses)
4) Asteroids	Mainly shocked minerals (with reacted vapors)	Shocked chondritic/growth grains

Existence of fluid-related grains: Carbon-bearing grains show only *light element* to exist all phase states from solid to liquid to vapor condition with various compositions, texture and atomic structure. Therefore, it is *significant indicator* to detect its formed process with or without fluid on *water-planet Earth* (to form final *global carbonate minerals* and its rocks), the Moon (to form *global carbon distribution* rich in fine regolith soils on surface), Mars (to form *global carbon-rich grains* and deposits) and Asteroids (*carbon-rich in fine regolith* grains and/or *carbon-bearing grains* and rocks) as shown in Table 2.

Discussion: Earth's minerals formed as large mineral crystals are defined by atomic structure and chemistry based on X-ray analysis and EPMA-A TEM/SEM microanalyses in laboratory on Earth. On the other hand, extraterrestrial samples of the Moon, Mars and Asteroids have no large crystal of mineral grains (due to no global water system on these bodies). Therefore, Earth's mineral crystal cannot be obtained at any other planets and Asteroids without the global water system. Remote-sensing detectors by the IR and Visible wavelengths are mainly instant data obtained from mainly molecular data (atom-atom distances) which are different with Earth's mineral definition. This suggests that extraterrestrial mineral rocks (or rocky minerals) are considered to be *imperfect solids* compared with Earth-type mineral crystal, which means that *main X-ray peaks* of crystal planes (hkl) are mainly formed during the developed processes with short extreme condition of simple or multiple impact heating and cooling processes on the extraterrestrial bodies. In short, all celestial bodies at the Solar System are

completely different on its process and fluid contribution for rocky mineral or mineral rock formation (including the Hayabusa samples), which means that solid bodies of the Solar System might be the *Helio-centered theory-type* material rocks which are not used by the Earth-type mineral rocks to all other extraterrestrial bodies (not as the Earth (geo)-centered materials as used in the astronomical scale previously).

Table 2. Carbon-bearing and/or -rich grains and/or rocks of the Solar System's materials discussed in this study.

Celestial body	Carbon-bearing and/or -rich grains and/or rocks
1) Earth (water-planet)	Final global carbonate minerals and rocks and life/plant solidified rocks (shungite <i>etc.</i>)
2) The Moon	Global carbon distribution rich in fine regolith soils on surface (with shocked grains)
3) Mars	Global carbon-rich grains and deposits (with shocked grains)
4) Asteroids	Fine carbon-rich regolith grains and/or carbon-bearing grains and its rocks

Summary: The following data are summarized in this study. 1) Solid materials of all Celestial bodies on the Solar System are discussed on the solid data from the *Earth's definition* relatively to the extraterrestrial Celestial bodies. 2) All mineral crystals on Earth are defined with X-ray determination and chemical composition with its occurrence on the material database, though basic definition of extraterrestrial sample is not enough to be defined from *less crystalline* rocks. 3) The Earth's minerals show absolutely *huge numbers* of mineral species, *well differentiated* minerals, *various Earth's sedimentary* process, and *various mineral* deposits of *carbon-bearing* grains. 4) Carbon-bearing grains show various grains, texture and compounds which are indicators of the detailed *formation process* on each Celestial body including the Hayabusa samples. 5) The material data of the samples might indicate that all material data of mineral and rock are different from the Celestial bodies of the Solar System.

References:

- Cresswell R., Beukens R., Rucklidge J. and Miura Y., Distinguishing spallogenic from non-spallogenic carbon in chondrites using gas and temperature separations. Nuclear Instruments and Methods in Physics Research Section B (NIM-B) (Elsevier Science, North-Holland), 92, 505-509, 1994.
- Kato T. and Miura Y., The crystal structures of Jarosite and svanbergite. Mineralogical Journal, 8, 419-430, 1977.
- Miura Y., Comparative consideration of Earth's mineral from three major events: Solid formation of other Celestial bodies, JAMS-2021 (Hiroshima Univ.), R5-01, 2021.
- Miura Y., Carbon and carbon dioxides gas fixing by dynamic processes, Publication of JP5958889B2 (Active to 2028), 2016.
- Miura Y., Complex texture and structure of shocked quartz mineral with graphite grain., Acta Cryst., 64, 55, 2008.
- Miura Y., Material evidence for compositional change of dusts by collision applied to the Solar System's formation and the Asteroid belt. The ASP Conf. Series, 63, 286-288, 1994.
- Miura Y. and Kato T., Shock waves in cosmic space and planetary materials. American Institute of Physics (AIP) Conf. Proc., 283 (Earth and Space Science Information Systems), 488-492, 1993.
- Miura Y., Accelerator mass spectrometry facilities in Japan. The Future of AMS Requirements in Canada (NSERC), 1, 45, 1991.
- Miura Y. and Tomisaka T., Composition and structural substitution of meteoritic plagioclases. Mem. Natl Inst. Polar Res., Spec. Issue (NIPR, Tokyo), 35, 210-225, 1984.
- Miura Y., Computer simulation of anomalous composition of Mg-Fe plagioclase in meteorite. Mem. Natl Inst. Polar Res., Spec. Issue (NIPR, Tokyo), 35, 226-242, 1984.
- Smith D.G.W., Miura Y. and Launspach S., Fe, Ni and Co variations in the metals of some Antarctic chondrites. Earth and Planetary Science Letters, 120, 487-498, 1993.

Model of Material Characteristics of Carbonaceous Meteorites from Texture of Carbon-Bearing Grains

Yasunori Miura

Faculty of Science, Yamaguchi University, Yoshida, Yamaguchi, Yamaguchi, JAPAN

Introduction: Carbonaceous meteorites are unique meteorites in the extraterrestrial rocks. In this study author reports proposed model of previous unknown characteristics of *hard samples with voids, carbon-bearing texture, Ca-Al-rich grains* (with H, C, S) and detailed model of *carbon-bearing grains* in the carbonaceous meteorite which are applied to the Hayabusa samples as the present purpose here.

Characteristics of Carbonaceous chondrite: Carbonaceous chondrites contain usually Ca and C elements (with Mg, Na ions and H₂O molecules), where these ions can form molecular *gel (polymer)* and *amorphous* (poorly crystallized Embryo-type of *carbonates* (calcite and aragonite in mineral crystal). This suggests that extraterrestrial Celestial body is started as 1) *Ordinary chondrite-type micrograins* and *intercluster pores* (as less 2nm) followed *gel pores* (2 to 20nm in size) without carbonated calcium silicate matrixes, and 2) *Carbonaceous chondrite-type micrograins* show Ca-modified silica *gel clusters* mixed with *amorphous calcium carbonates (ACC)* with pores (4 to 10nm) as shown in Table 1. This model can be explain why the meteorite shows *porous rocks* and *harder rock* (than normal porous crystalline rocks with light weight). These gel to amorphous grain can be formed in present laboratory and industrial application as *Ca-Al-rich grains* (with H, C, S) as low *carbon binders*. This is just by accident in natural meteorite field academically because author has been investigated carbon origin and its application in science filed (including the AMS carbon dating projects) used in terrestrial age of the Antarctic meteorites (also in the Apollo samples as its carbon origins), and recent project of carbon and *carbon dioxides gas fixing* by dynamic processes (as the public University project). If it can be confirmed in science filed, then we can apply that *carbonaceous meteorites* (and Moon rocks) has similar texture to fix carbon (or carbon dioxides) by its sources and development of its *extraterrestrial rocks* (model of grains of ions-gel polymer-amorphouse calcium carbonates as shown in Table 1, followed clear calcite crystal as in water planet Earth finally). This can be applied it also to decrease the *climate warning* scientifically and inductrially (as well-known Japanese scientist indicated by calculated estimates from global environmental data). The paper is dicussed it as material data with proposed model in the Hayabusa Symposium in Tokyo.

Table 1. Proposed model of micro-grains with pores from of the Solar System.

Meteorite variety	Micro-structure
1) Ordinary chondrite	Micro-grains and inter-cluster pores (as less 2nm), gel pores (2 ~ 20nm in size) (less carbonated calcium silicate matrixes)
2) Carbonaceous chondrite	Micro-grains with Ca-modified silica gel clusters mixed with amorphous calcium carbonates (ACC) with pores (4 to 10nm)

Summary: Author proposes model of hard samples with voids, carbon-bearing texture, Ca-Al-rich grains (with H, C, S) and carbon-bearing grains in the carbonaceous meteorite (also including the Hayabusa samples).

References:

Miura Y., Comparative consideration of Earth's mineral from three major events: Solid formation of other Celestial bodies, JAMS-2021 (Hiroshima Univ.), R5-01, 2021.

Miura Y., Carbon and carbon dioxides gas fixing by dynamic processes, Publication of JP5958889B2 (Active to 2028), 2016.

Miura Y. and Tanosaki T., Characterization of products from the nuclear and fire-electric facilities (in Japanese), University Report (Yamaguchi, Japan), 1-64, 2009.

Miura Y. , Material evidence for compositional change of dusts by collision applied to the Solar System's formation and the Asteroid belt. The ASP Conf. Series, 63, 286-288, 1994.

Miura Y. and Kato T., Shock waves in cosmic space and planetary materials. American Institute of Physics (AIP) Conf. Proc., 283 (Earth and Space Science Information Systems), 488-492, 1993.

Smith D.G.W., Miura Y. and Launspach S., Fe, Ni and Co variations in the metals of some Antarctic chondrites. Earth and Planetary Science Letters, 120, 487-498, 1993.

Miura Y., Computer simulation of anomalous composition of Mg-Fe plagioclase in meteorite. Mem. Natl Inst. Polar Res., Spec. Issue (NIPR, Tokyo), 35, 210-242, 1984.

Neural network for classification of asteroid spectra

David Korda¹, Antti Penttilä², Arto Klami³, and Tomáš Kohout^{1,4}

¹Department of Geosciences and Geography, University of Helsinki, Finland

²Department of Physics, University of Helsinki, Finland

³Department of Computer Science, University of Helsinki, Finland

⁴Institute of Geology, Czech Academy of Sciences, Czech Republic

Introduction

Asteroid mineral composition is important parameter in planetary science, planetary defence, and in-space resource utilisation. Currently-used methods provide us mainly quantitative information about the asteroid composition. The methods are based on empirical relations between spectral parameters (band areas, positions, depths), or on spectral unmixing, and are highly sensitive to quality and consistency of input reflectance spectra. We test artificial neural networks as a tool which can infer mineral composition directly from the reflectance values.

Methods

Artificial neural networks are used in tasks which are very difficult to define with exact mathematics. A sensitivity of the networks to quality of input data (e.g., absolute reflectance values or variations in spectral slope) can be partially suppressed. The networks are made of layers of neurons. Each neuron in a layer is non-linearly connected with neurons in the previous and following layers. The non-linearity and complexity of neural network enable them to solve various tasks.

We use neural network for computing of mineral composition of the most common silicates presented in meteorites (olivine, orthopyroxene, clinopyroxene, and plagioclase). Our neural network composed of the input layer with reflectance values, one ‘intermediate’ layer (hidden layer), and the output layer. The outputs are modal composition of the minerals and their chemical composition represented with end-members.

Data

We utilised measured reflectance spectra from the Relab database^[1]. We are motivated by the ASPECT instrument (part of Hera/Milany CubSat) which will carry-out observations in visible and near-infrared part of spectra. For this reason, we chose spectra which cover interval between 350 nm and 2550 nm with the resolution 15 nm or better.

Results

Olivine and orthopyroxene are the most common minerals in ordinary chondrites. Therefore, we firstly applied the neural network on a set of olivine and pyroxene spectra.

¹<http://www.planetary.brown.edu/relabdata/>

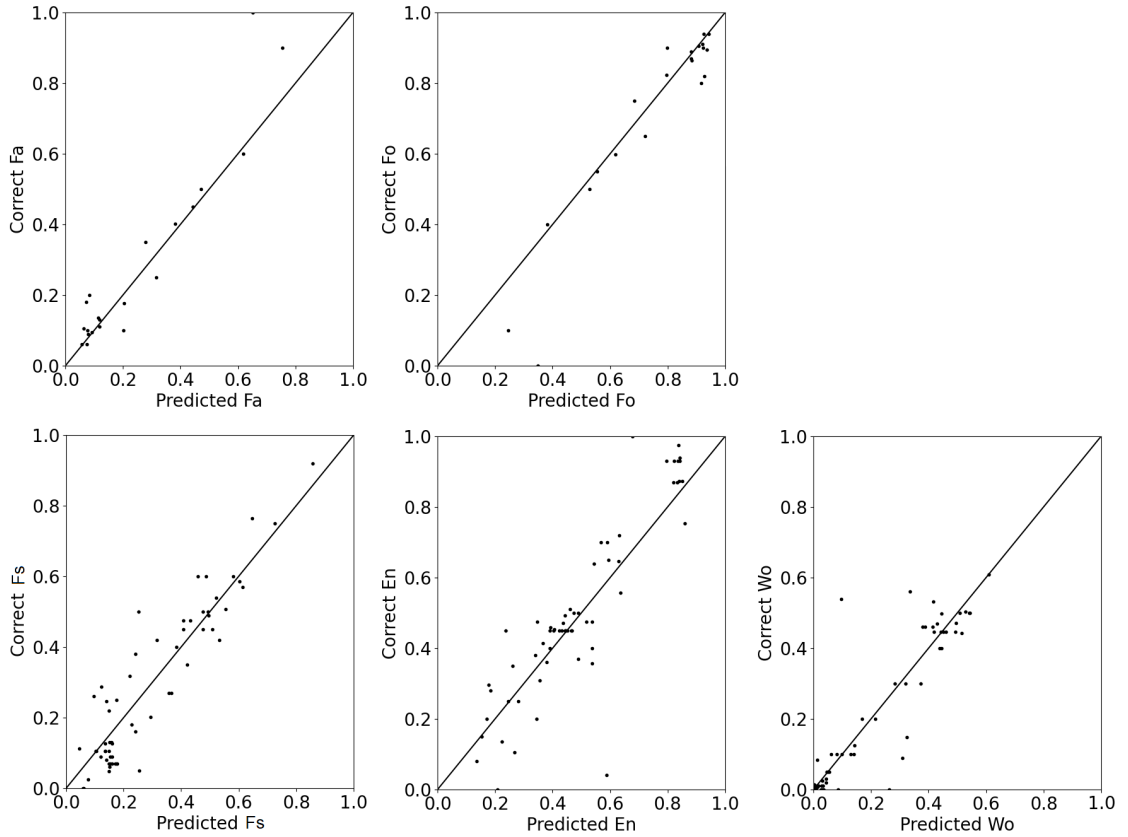


Figure 1: Results of chemical composition. Top row: olivine. Bottom row: pyroxene.

The neural network contained only one hidden layer with 30 neurons. The outputs were volume fractions of the minerals and their chemical composition. We trained the network on about 80% of the whole dataset and used the remaining 20% to test the accuracy of the predictions. The results obtained from the 20% are shown in Fig. 1. The vertical axes show the correct (previously published) values while the horizontal axes the values predicted by the neural network. In the top row, there are iron and magnesium composition in olivine. In the bottom row, there are iron, magnesium, and calcium composition in pyroxene.

Discussion

Except a few outlier, the predicted composition is usually within about 10% from the actual composition. The outliers might be a consequence of a limited training dataset or ambiguously determined actual composition. In the near future, the predictive capability of the network will be improved via optimisation of its architecture and due to increase number of training samples. In the next step, we will train the network on synthetic spectra of olivine, orthopyroxene, and plagioclase and evaluate the network on real ordinary chondrites.

Assessment of organic, inorganic and microbial contamination in the facilities of the Extraterrestrial Sample Curation Center of JAXA

*Yuya Hitomi¹, Toru Yada², Aiko Nakato², Miwa Yoshitake^{1,3}, Kana Nagashima², Haruna Sugahara², Shino Suzuki², Masahiro Nishimura², Kazuya Kumagai¹, Masanao Abe², Tatsuaki Okada², Shogo Tachibana^{2,4}, and Tomohiro Usui²

¹Marine Works Japan Ltd., Yokosuka, Kanagawa 237-0063, Japan, ²Institute of Space and Astronautical Science (ISAS), Japan Aerospace Exploration Agency, Sagami-hara, Kanagawa 252-5210 Japan, ³Japan Patent Office, Chiyoda-ku, Tokyo 100-8915, Japan, ⁴UTOPS, Grad. Sch. Sci., Univ. Tokyo, Tokyo 113-0033, Japan.

The Extraterrestrial Sample Curation Center of JAXA (ESCuC) have received samples from S-type near-Earth asteroid 25143 Itokawa returned by Hayabusa and C-type near-Earth asteroid 162173 Ryugu by Hayabusa2 [1, 2]. The samples have been taken out from sample containers, investigated in a non-destructive way, and stored in high vacuum and purified nitrogen circulating clean chambers installed in ISO Class 6 clean rooms in the ESCuC. A series of cleaning procedures for tools, jigs, and sample storage/transport containers has been established for the usage in the clean chambers to avoid potential contamination of samples [3].

Along with the contamination control, it is also important to keep monitoring the cleanliness of clean rooms and clean chambers. For instance, several biotic amino acids were once detected from contamination coupons set inside the clean chamber for Itokawa grains [4], of which contamination level was similar to that reported at the curation facility at NASA Johnson Space Center [5, 6]. In recent years, contamination of organics has been assessed regularly through exposure of wafers for 15-20 hours in the clean rooms and clean chambers. The regular assessment has found that the clean rooms is kept at the ISO-SCC Class -8 level and the clean chambers at the ISO-SCC Class -9 for organics. Regular contamination assessment of metallic elements has shown that both clean rooms and clean chambers maintain the level of ISO-SCC Class -10 or higher for all measured elements although elements contained in equipments and tools, such as Fe, Cu, Ni, Cr, Al, Zn, Mn, and Co, were often detected at a higher level in the clean chambers than in the cleanrooms. The contamination levels of Na and K, both of which are good indicators of contamination from human beings, are low enough to be at the ISO-SCC class -11 level for both clean chambers and cleanrooms. In addition to organic and inorganic monitoring, assessment of microbial contamination level is scheduled for the cleanrooms and clean chambers in this fiscal year.

References

[1] Yada T. et al. (2014) *Meteoritics Planet. Sci.* 49, 135-153. [2] Yada, T. et al. (2021) LPSC 52, #2008. [3] Yoshitake M. et al. (2021) JAXA-RR-20-004E, 1-30. [4] Sugahara H. et al. (2018) *Earth Planets Space* 70, 194. [5] Dworkin et al. (2018) OSIRIS-REx contamination control strategy and implementation. *Space Sci Rev* 214:9. [6] McLain et al. (2015) Contamination Knowledge Report JSC Curation Cabinets, personal communication.